NUCLEAR SAFETY

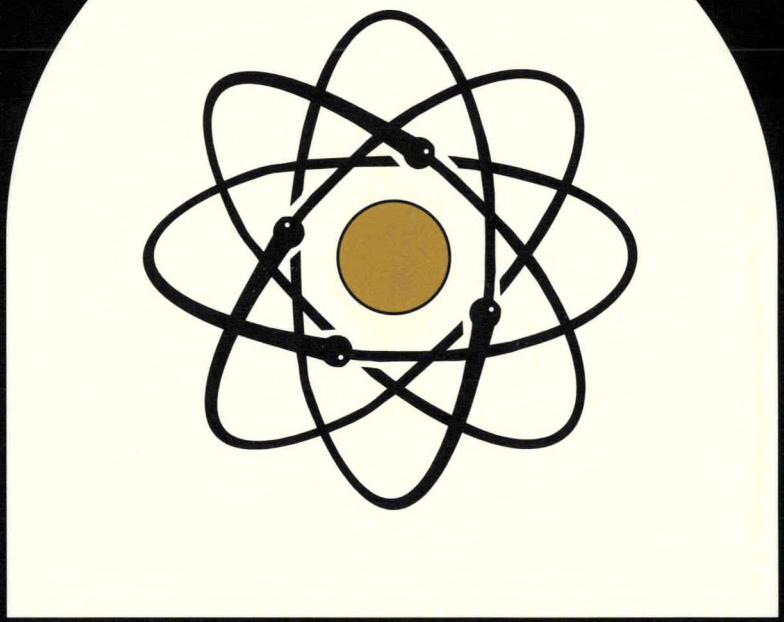

TECHNICAL PROGRESS JOURNAL

VOL. 35 – NO. 2 JULY – DEC 1994

The Operational Performance Technology Section

The Operational Performance Technology (OPT) Section at Oak Ridge National Laboratory (ORNL) conducts analyses, assessments, and evaluations of facility operations for commercial nuclear power plants in support of the Nuclear Regulatory Commission (NRC) operations. OPT activities involve many aspects of facility performance and safety.

OPT was formed in 1991 by combining ORNL's Nuclear Operations Analysis Center with its Performance Assurance Project Office. This organization combined ORNL's operational performance technology activities for the NRC, DOE, and other sponsors aligning resources and expertise in such areas as:

- event assessments
- performance indicators
- data systems development
- trends and patterns analyses
- technical standards
- safety notices

OPT has developed and designed a number of major data bases which it operates and maintains for NRC and DOE. The Sequence Coding and Search System (SCSS) data base collects diverse and complex information on events reported through NRC's Licensee Event Report (LER) System.

OPT has been integrally involved in the development and analysis of performance indicators (PIs) for both the NRC and DOE. OPT is responsible for compiling and analyzing PI data for DOE facilities for submission to the Secretary of Energy.

OPT pioneered the use of probabilistic risk assessment (PRA) techniques to quantify the significance of nuclear reactor events considered to be precursors to potential severe core damage accidents. These precursor events form a unique data base of significant events, instances of multiple losses of redundancy, and infrequent core damage initiators. Identification of these events is important in recognizing significant weaknesses in design and operations, for trends analysis concerning industry performance and the impact of regulatory actions, and for PRA-related information.

OPT has the lead responsibility in support of DOE for the implementation and conduct of DOE's Technical Standards Program to facilitate the consistent application and development of standards across the DOE complex.

OPT is responsible for the preparation and publication of this award-winning journal, *Nuclear Safety,* now in its 35th year of publication sponsored by NRC. Direct all inquiries to Operational Performance Technology Section, Oak Ridge National Laboratory, P.O. Box 2009, Oak Ridge, TN 37831-8065. Telephone (615) 574-0394 Fax: (615) 574-0382.

A semiannual Technical Progress Journal prepared for the U.S. Nuclear Regulatory Commission by the Operational Performance Technology Section at Oak Ridge National Laboratory

Published by the
Office of Scientific and Technical Information
U.S. Department of Energy

NUCLEAR SAFETY

Vol. 35, No. 2 **July–December 1994**

TPJ-NS-35-No. 2
DE94018605

NUSAAZ 35(2), 1994
ISSN: 0029-5604

GENERAL SAFETY CONSIDERATIONS

179 Consideration of Postaccident Consequences in the Determination of Safety Objectives for Future Nuclear Power Plants in France *D. Quéniart, A. Sugier, and J. Lochard*

ACCIDENT ANALYSIS

187 Nuclear Safety Research: The Phebus FP Severe Accident Experimental Program *P. von der Hardt, A. V. Jones, C. Lecomte, and A. Tattegrain*

205 Containment Performance Analysis of the Advanced Neutron Source Reactor at the Oak Ridge National Laboratory *S. H. Kim, R. P. Taleyarkhan, and V. Georgevich*

213 Assessment of Fission Product Deposits in the Reactor Coolant System: The DEVAP Program *G. Le Marois and M. Megnin*

222 Erratum to "A Review of the Available Information on the Triggering Stage of a Steam Explosion," Vol. 35, No. 1

CONTROL AND INSTRUMENTATION

223 Effects of Normal Aging on Calibration and Response Time of Nuclear Plant Resistance Temperature Detectors and Pressure Sensors *H. M. Hashemian*

DESIGN FEATURES

235 Defense in Depth Against the Hydrogen Risk—A European Research Program *F. Fineschi*

ENVIRONMENTAL EFFECTS

246 Technical Note: A Preliminary Analysis of the Risks to Hong Kong Resulting from Potential Accidents of Daya Bay Nuclear Power Plant *Z. Shi and X. Wei*

OPERATING EXPERIENCES

253 Reactor Shutdown Experience *Compiled by J. W. Cletcher*

SPECIAL SECTION ON TMI-2 VESSEL INVESTIGATION PROJECT

256 Three Mile Island—New Findings 15 Years After the Accident *A. M. Rubin and E. Beckjord*

269 Relocation of Molten Material to the TMI-2 Lower Head *J. R. Wolf, D. W. Akers, and L. A. Neimark*

280 Insight Into the TMI-2 Core Material Relocation Through Examination of Instrument Tube Nozzles *L. A. Neimark*

288 Physical and Radiochemical Examinations of Debris from the TMI-2 Lower Head *D. W. Akers and B. K. Schuetz*

301 Results of Metallographic Examinations and Mechanical Tests of Pressure Vessel Samples from the TMI-2 Lower Head *D. R. Diercks and G. E. Korth*

313 Margin-to-Failure Calculations for the TMI-2 Vessel *J. Rempe, L. Stickler, S. Chàvez, G. Thinnes, R. Witt, and M. Corradini*

U.S. NUCLEAR REGULATORY COMMISSION INFORMATION AND ANALYSES

328 1993 Accident Sequence Precursor (ASP) Program Results *L. N. Vanden Heuvel, J. W. Cletcher, D. A. Copinger, J. W. Minarick, B. W. Dolan, and P. D. O'Reilley*

RECENT DEVELOPMENTS

339 Reports, Standards, and Safety Guides *D. S. Queener*

345 Proposed Rule Changes as of June 30, 1994

ANNOUNCEMENTS

234 Thirty-First Annual Meeting of the National Council on Radiation Protection and Measurements

356 1995 International Incineration Conference

358 Fifth International Controls and Instrumentation Conference

359 ANS International Topical Meeting on Safety of Operating Reactors

359 Fifth International Conference on Nuclear Criticality Safety

360 International Conference on Probabilistic Safety Assessment Methodology and Applications

351 The Authors

357 Reviewers of *Nuclear Safety*, Vol. 35

Nuclear Safety is a journal that covers significant issues in the field of nuclear safety.

Its primary scope is safety in the design, construction, operation, and decommissioning of nuclear power reactors worldwide and the research and analysis activities that promote this goal, but it also encompasses the safety aspects of the entire nuclear fuel cycle, including fuel fabrication, spent-fuel processing and handling, and nuclear waste disposal, the handling of fissionable materials and radioisotopes, and the environmental effects of all these activities.

Qualified authors are invited to submit articles; manuscripts undergo peer review for accuracy, pertinence, and completeness. Revisions or additions may be proposed on the basis of the results of the review process. Articles should aim at 20 to 30 double-spaced typed pages (including figures, tables, and references). Send inquiries or 3 copies of manuscripts (with the draftsman's original line drawings plus 2 copies and with black-and-white glossy prints of photographs plus 2 copies) to E. G. Silver, Oak Ridge National Laboratory, P. O. Box 2009, Oak Ridge, TN 37831-8065.

The material carried in *Nuclear Safety* is prepared at the Oak Ridge National Laboratory's Operational Performance Technology Section, which is responsible for the contents. *Nuclear Safety* is funded by the U.S. Nuclear Regulatory Commission's Office of Nuclear Regulatory Research. Editing, composition, makeup, and printing functions are performed by the DOE Office of Scientific and Technical Information (OSTI). Sale and distribution are by the U.S. Government Printing Office; see the back cover for information on subscriptions, postage, and remittance.

EDITORIAL

Three-Mile Island Still has Lessons to Teach

It is hard to overestimate the impact that the 1979 accident at Three-Mile Island (TMI) Unit 2 had on the subsequent history of nuclear power in the United States and, indeed, worldwide. This event massively altered the public's conception of the risks of nuclear energy, although not always in directions consonant with the actual facts. It also impacted the nuclear community both in opening up entirely new lines of research and development on the basis of the lessons learned and in modifying the regulatory perspectives and approaches. Qualification of safety-related components and equipment for service in high-temperature–high-moisture environments such as might exist in a containment building during an accident was required, TMI-related retrofits of existing power plants were mandated and performed, and strenuous efforts were made to focus on the consequences of small-break loss-of-coolant accidents whose potential significance had not previously been fully appreciated.

It is, I think, no exaggeration to say that the TMI event was, in some ways, a very dark cloud with a very bright silver lining. The dark cloud, of course, is the fact that the accident cost a great deal of money; frightened millions of people to the point where, although there were essentially no demonstrable health impacts on anyone, their confidence in the assurances given by the technical experts that nuclear energy was "safe" was severely shaken; and fueled and energized the organized anti-nuclear movement.

The silver lining consists of the immense stimulus to additional safety-related research and calculation, the recognition of many of the oversimplistic assumptions that had underlain safety analysis before TMI, and the concentrated research on the damaged TMI reactor itself, which has led to greatly improved understanding of severe-accident core behavior and, in general, the response to many nuclear reactor systems, components, and materials to the extreme conditions that accompany a nuclear core-damage event.

This perception of the advances in safety spurred by the TMI accident was well explained by E. Beckjord, Director of NRC's Office of Nuclear Regulatory Research at the 22nd Water Reactor Safety Information Meeting on October 26, 1994, in a talk titled "Prospects for Nuclear Safety Research," in which he said, in part:

> The Three Mile Island Unit 2 accident raised major concerns about nuclear reactor safety in this country and abroad, and led to a widespread review of plant performance and safety requirements by NRC. As a result there were many improvements made to emergency safety systems, control rooms and instrumentation, and operator qualifications and training. There is no question that plant safety has improved as a consequence.
>
> Plant owners/operators have made safety improvements. One example is the reduction of the number of automatic reactor trips. They accomplished this by systematic review of plant conditions at the time of the trip, determination of the root cause, and, if the trip was not needed for safety, correction so that the condition will not reoccur. Unnecessary trips are a challenge to safety systems, and reducing unnecessary challenges is a safety improvement.
>
> Reactor safety research conducted by the NRC has also made important contributions to safety over the same period of time. There is, however, no simple measure, such as a numerical performance indicator, to show the improvement. Nevertheless it is possible to explain causes of safety improvement in meaningful terms.

One of the outcomes of the research on the TMI-2 accident and its consequences is featured in this issue of *Nuclear Safety.* Almost half of this issue is devoted to a set of six connected papers that discuss the results of the long-term investigation on the TMI-2 reactor pressure vessel and its contents during and after the accident. In view of the many concerns for the possibility of a "China Syndrome," in which the vessel bottom head fails in the course of a core

(Continues on inside back cover.)

General Safety Considerations

Edited by G. T. Mays

Consideration of Postaccident Consequences in the Determination of Safety Objectives for Future Nuclear Power Plants in France

By D. Quéniart,[a] A. Sugier,[a] and J. Lochard[b]

Abstract: *The design of a new generation of nuclear power units, the construction of which could begin around the year 2000, is currently under investigation in France. The various partners involved have agreed on the need for a significant improvement in the safety of the units of this new generation compared with the units presently in operation or under construction. Releases associated with possible severe accidents involving reactor core meltdown, which could lead to radiological consequences for the public and the environment, are, of course, a major concern. These consequences must be mitigated to be deemed acceptable, considering their probabilities. This article presents a study conducted by the Protection and Nuclear Safety Institute with the collaboration of the Nuclear Protection Evaluation Center to elaborate on this concept of acceptability in which the Soviet populations' reactions after the Chernobyl accidents were used as a reference. This approach allowed definition of the order of magnitude to be sought for the "maximum conceivable release" to serve as a reference for establishing safety objectives to be set for the design of future reactors.*

The French nuclear power program is based on the design, construction, and operation of a standardized series of identical units, the only differences relating to particularities of the sites chosen. After the two units of the Fessenheim plant and the four units of the Bugey plant, two series of 900-MW(e) units (a total of 28 units) were built and commissioned during the 1980s and two series of 1300-MW(e) units (a total of 20 units) were built and commissioned during the last 10 years. Moreover, four units of the N4 generation [1400 MW(e)] are under construction at the Chooz and Civaux sites. All these units are pressurized-water reactors (PWRs) derived from the type initially developed by Westinghouse.

After the N4 generation, the basic design of which dates back to the mid-1980s and which will certainly not consist of more than about ten units, the issue of designing a new generation of nuclear power plants arises with a view to begin renewing the oldest existing units. On the basis of industrial strategy considerations, the ambition is to start construction of the first units around the year 2000.

A key element in this strategy is the setting of safety objectives to support the design of this new generation of reactors. In this perspective, substantial agreement exists among the various partners involved—the utility, the vendor, and the safety authorities—to further improve the general safety performances of the future reactors and particularly to try to significantly reduce radioactive releases in the event of severe accidents with core meltdown. This last concern largely results from the lessons learned from the Chernobyl accident, which revealed the potential for severe social disruptions related to postaccident conditions resulting from a large-scale and heavy land contamination.

[a]Protection and Nuclear Safety Institute, CEA-CE/FAR, B.P. No. 6, 92265 Fontenay-Aux-Roses, Cedex, France.

[b]Nuclear Protection Evaluation Centre, Route du Panorama, B.P. No. 6, 92263 Fontenay-Aux-Roses, Cedex, France.

This article presents the main outcomes of a study conducted at the Protection and Nuclear Safety Institute (IPSN), which is the technical support organization of the French Safety Authorities, to elaborate safety objectives for the future generation of nuclear power plants to be constructed by the turn of the century, taking into account postaccident considerations. This study was done in collaboration with the Nuclear Protection Evaluation Center (CEPN), which analyzed the situation prevailing in the late 1980s in the now ex-Soviet Republics affected by the Chernobyl accident.

After a brief presentation of the general orientation adopted for future reactors in France, this article describes how "source terms" have been defined to qualify different classes of radioactive release in the event of an accident. The following sections outline how postaccident considerations have led to a reassessment of these "source terms" from the perspective of reducing the off-site consequences of potential accidents associated with future reactors. In conclusion, the new safety objectives that are going to be integrated in the design process of the European Pressurized-Water Reactor (EPR) project are presented.

THE NEXT GENERATION OF FRENCH REACTORS

Beyond its direct radiological consequences, the Chernobyl accident had a significant influence in Western countries on the evolution of ideas regarding the safety of nuclear installations as well as the use of this type of installation. The political leaders of some countries have thus been induced to call into question the construction projects of nuclear power plants, to postpone the execution of nuclear projects, and even to decide against putting plants under construction into service. At the same time, the vendors concerned were driven to consider the design of new products, with essential preoccupation about obtaining public acceptance, which led them to emphasize the safety features of these products.

To date, three main ways of reactor development are followed by vendors:

1. The development of "evolutionary" reactors, directly derived from the reactors in service or under construction, with a unit electrical power output of the order of 1300 to 1400 MW(e).

2. The development of "passive" reactors, making extensive use of the design of reactors in service or under construction, but using means of controlling accident situations that do not require off-site power supplies. The unit electrical power output of known projects of this type is around 600 MW(e).

3. The development of "revolutionary" reactors, with a totally new design and a unit electrical power output of the order of 200 to 600 MW(e) for known projects, in which priority is given to a simple and convincing demonstration of their safety.

In the French context mentioned previously, the choice of the "evolutionary" way is the subject of a broad consensus among the operator (Électricité de France), the vendor [FRAMATOME, or the joint venture Nuclear Power International (NPI)], and the safety organizations.[1] Note that this choice was largely determined by the objective of starting to build the new generation of units around the year 2000 and that any other way would assume a more cautious industrial approach. From the safety viewpoint, the adopted strategy presents interesting advantages because it makes possible benefits from both the experience acquired by the construction and operation of existing units and the results of the many in-depth safety studies conducted for these plants. But the "evolutionary" way must also enable an acceptable safety level to be obtained. Here again there is a broad consensus in France that a significant improvement is necessary comparatively to the units in operation or under construction. A number of reasons argue for such a significant improvement, but the fundamental reason is linked to the Chernobyl accident, which has brought to light the difficulties of managing a severe accident situation not only in the short term but also, and above all, in the long term because of the possible radioactive contamination of the environment and food chain.

THE SOURCE-TERM CONCEPT

The design of the French nuclear power units in operation or under construction is such that, for a conventional list of accident situations extending to the total and sudden rupture of a large pipe of the primary circuit, the outside radiological consequences would remain low in terms of public exposures by irradiation or inhalation of radioactive substances. This does not exclude, of course, the possibility, as the result of the combination of more or less complex failures, of more severe accidents with reactor core meltdown. If the improvements brought to the various series of units are taken into account, even retroactively for the oldest units, the probabilistic safety assessments (PSAs) show that the total predicted

frequency of core meltdown of a PWR of the type built and operated in France is of the order of 10^{-5} per year, a value that is consistent with the results of PSAs conducted in other countries.[2,3]

As far as the consequences of severe out-of-design accidents are concerned, they can be assessed according to the behavior of the containment after reactor core meltdown. On the basis of the adaptation to the French units of the American risk study known as the Rasmussen Report (or WASH-1400), three general classes of severe accidents with core meltdown were distinguished at the end of the 1970s as a basis for designing the French severe accident policy and making operational decisions:

1. Accidents resulting in "early" failure of the containment, represented by source term Sl.
2. Accidents resulting in "delayed" failure of the containment, at least 24 hours after the beginning of the accident, without filtration of the corresponding releases. These accidents are represented by source term S2.
3. Accidents resulting in "delayed" failure of the containment, at least 24 hours after the beginning of the accident, with releases via a way ensuring some filtration. These accidents are represented by source term S3.

The three basic classes of "source terms" are summarized in Table 1 as percentages of the radioactive inventory released from the reactor core.

In all cases the consequences of the releases are dominated in the short term by iodine and in the long term by cesium. Furthermore, there is, in orders of magnitude, a factor of 10 between source terms Sl and S2 and a factor of 10 between source terms S2 and S3. As a comparison, the Chernobyl accident releases, which amounted to 20 to 50% of iodines and cesiums, are close to the S1 source term. It must be also clearly understood that these source terms have been defined to cover a set of possible scenarios and were not related to precise accident scenarios; for example, the source term S3 includes scenarios with gaseous releases from the containment after the basemat melt through or scenarios with a limited containment bypass.

Table 1 Source Terms[a]

	Sl	S2	S3
Rare gases	80	75	75
Organic iodine	0.6	0.55	0.55
Inorganic iodine	60	2.7	0.3
Cesium	40	5.5	0.35
Strontium	5	0.6	0.04

[a]For a 1400-MW(e) unit, source term S3 includes 13 000 TBq of iodine-131 and 5 000 TBq of cesium-134 + cesium-137 (two-thirds of cesium-134).

The source term S1, resulting from a total and "early" failure of the containment, could result from phenomena like steam explosion or hydrogen detonation. It is considered that such failure of the containment can be excluded due to the characteristics of the large drywell containment used in France. Of course, this opinion has to be supported by ongoing studies, and, if necessary, improvement of the "defense-in-depth" of the plants. In this perspective, improvements have been decided concerning the possibilities of reactivity accidents caused by scenarios with introduction of deborated water in the core.

Other improvements have been brought to French nuclear power units with a view to reducing S2 type releases to S3 type releases as in, for example, the implementation of an "ultimate" procedure to improve the containment function, including the possibility of releases through a sand bed filter completed by a metallic prefilter. These evaluations explain why source term S3 was finally adopted as the "maximum conceivable release" for French nuclear power units in operation or under construction. On this point, note once again that source term S3 does not correspond to a particular scenario but is a reasonable envelope of the releases of various scenarios.

The definition of what could be called reference source terms has a direct impact on accident management procedures. As an illustration, emergency plans are designed to cope, as far as possible, with the consequences of an S3 type release. In a first step it has been demonstrated that, considering the characteristics of French sites, it is possible to implement the measures deemed necessary to protect the population from such a release (evacuation, sheltering) in the short term, with reference to the recommendations proposed by the International Commission on Radiological Protection (ICRP) on intervention levels in its Publication No. 40. This implies the possibility of evacuating the population within a radius of 5 km and of confining the population indoors within a radius of 10 km around each nuclear plant within less than 24 hours.[4]

Further investigations, however, have demonstrated that an S3 type release would raise difficulties in managing the situation on the site of the damaged plant and, above all, in managing globally the long-term consequences related to the exposures of the public as the result of the deposition of radioactive substances and the contamination of food chains. Another difficulty is related to the marketing of contaminated foodstuffs.

After the Chernobyl accident, the Commission of the European Communities set limits of contamination for food marketing. Even if these limits are not supposed to apply for the whole course of an accident situation, and if exceeding the limits would not result in significant radiological consequences, they constitute an inevitable baseline in assessing the potential consequences of severe accidents. Table 2 shows the European marketing limits for foodstuff;[5] it is known that the most significant radioactive substances are iodines and cesium, and, above all, iodine-131 in the short term and cesium-137 in the long term. With an S3 type release, the preceding marketing limits could be exceeded in the short term up to great distances away from the site of the damaged plant (of the order of about 100 km in some meteorological conditions) and over long periods (several years) within less important distances.

THE TOLERABILITY OF POSTACCIDENT SITUATIONS

The general evolution of the situation prevailing in the contaminated areas in Belarus, Russia, and Ukraine during the years following the Chernobyl accident has clearly demonstrated that the societal impacts have largely overwhelmed the radiological and economic consequences.[6] The pre-established radiation protection criteria, as well as those specifically developed in the following years after the accident, have not significantly influenced the social acceptability of the situation. Most countermeasures had a very limited impact on the attitude of the public, and sometimes they even had an adverse effect. This finding led IPSN to initiate, in the early 1990s, a reflection about the living conditions to be accepted in a postaccident situation with the objective of testing the compatibility of the source terms for future plants with these conditions. This approach was developed with the help of the tolerability of risk model.

The Tolerability of Risk Model

The tolerability of risk model is based on three categories of situations: unacceptable, tolerable, and negligible, separated by two boundaries as shown in Fig. 1. These categories can be further subdivided to reflect more complex situations than the one presented in this figure, but the basic structure remains the same. An approach of this type has been, for example, adopted by ICRP in its Publication No. 40 mentioned earlier[4] to set intervention levels in accident situations: above the upper level, remedial actions are practically always justified; below the lower level, actions are considered unjustified; between the two levels, decisions about their implementation are based on the assessment of their effectiveness according to the optimization principle. In the same way, the British Health and Safety Executive published in 1992 "Safety Assessment Principles for Nuclear Plants"[7] with limits beyond which the regulatory unacceptable category is reached and objectives below which the regulatory organization considers that there is no reason for concern. As regard to severe accidents with core meltdown, the Safety Assessment Principles define a limit value of 10^{-5} per year for the calculated global probability of accidents that could result in releases higher than 10 000 TBq of iodine-131 or 200 TBq of cesium-137.

The objective of the study conducted by IPSN with the collaboration of the CEPN aimed, in fact, at expressing the

Table 2 Derived Intervention Levels for Foodstuffs and Animal Feeding (Bq/kg)

	Infant food	Milk products	Other foodstuffs except those of minor importance	Liquids for consumption	Animal feeding (^{134}Cs and ^{137}Cs)	
Strontium isotopes, namely ^{90}Sr	75	125	750	125	Pork	1250
Iodine isotopes, namely, ^{131}I	150	500	2000	500		
Plutonium isotopes and alpha emitters, transplutonium radionuclides, namely ^{239}Pu and ^{241}Am	1	20	80	20	Poultry, lambs, calves	2500
Other nuclides with a radioactive half-life higher than 10 days, namely ^{134}Cs and ^{137}Cs	400	1000	1250	1000	Others	5000

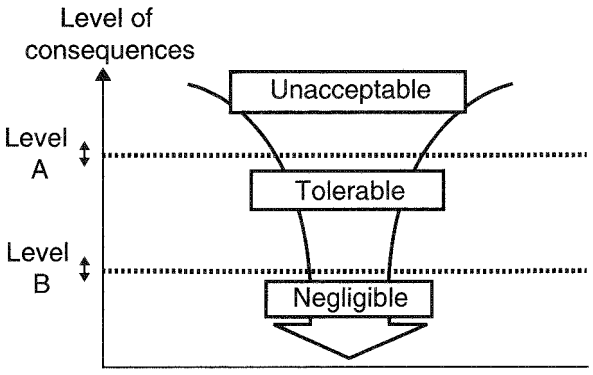

Fig. 1 Tolerability of risk model.

boundary between tolerable and unacceptable, in order of magnitude, with a "source term" for future plants formulated in a simplistic way in the form S3/n (n whole number). The use of such an approach obviously implies that the political leaders and the population do not reject any use of nuclear energy as soon as significant releases of radioactive substances may be involved—in which case the boundary would correspond to an n value unattainable from a technical viewpoint and/or unprovable. On the contrary, it is based on the observation that, in the event of a large-scale industrial accident, the affected populations "accept" greater restraints than those of everyday life for a limited period of time. Thinking was thus focused on the management of a severe accident condition beyond the "reflex" phase during which emergency measures are implemented with a view to returning to "normal life" as quickly as possible.

LESSONS FROM CHERNOBYL

The understanding of the dimensions that have been driving the perception and the acceptability of the postaccident situation in the contaminated areas around Chernobyl was still limited in the early 1990s. Most analysis so far remained at a very general level, and a vague concept such as "radiophobia" was put forward to explain the large gap existing between the real radiological situation and the way this situation was perceived and experienced by the general population over the years. Although limited in scope, the analyses performed by CEPN (1) in the context of the Chernobyl Project conducted by the International Atomic Energy Agency in the late 1980s[8,9] and (2) next in the framework of the CEC–CIS Joint Study project on the development and application of techniques to assist in the establishment of intervention levels for the introduction of countermeasures in the event of an accident[10] have provided useful information for understanding the mechanisms driving the tolerability of the Chernobyl postaccident situation. These investigations have been based on a series of interviews with the inhabitants of the contaminated areas. They allowed delineation of some of the elements that seem to play a significant role.

1. *The focus on contamination.* If the doses received by the public, by external or internal exposure, constitute for experts an indication of the risks associated with an accident situation, the level of contamination of the environment constitutes for the populations the "visible" indication on the subject. The dose calculations involve notions of weighting, depending on organs, and of integration in time over variable periods that are difficult for the general public to understand. The concept of lifetime dose, which has been extensively used in the debate about the potential late effects of radiation, is a good example of such a notion. On the contrary, the level of contamination of the environment appears directly available for measuring and can be easily monitored over time. It is the concrete manifestation of the accident; even if it is, in many cases, not a very accurate indicator of the real risk associated with a situation, it is generally favored to decide on the implementation of countermeasures.

2. *The zoning process.* Implementing countermeasures implies the definition of zones for their application in space and time, which marks the environment and the populations concerned. The indirect effects of the zoning process may be disastrous in terms of human behavior. It induces, for example, a "ghetto" effect for some population groups that are alienated from those living outside the contaminated areas for sanitary or economic reasons. The zoning process induces also a loss of reference to the previous environment, which is a great stress factor.

3. *The focus on time.* The temporal dimension of contamination (the period of cesium-137 is of the order of 30 years) brings questions about the future. The presence of radioactive traces as manifestations of pure duration makes everyone face his own mortality and generates distress. This psychological mechanism also plays a key role in the concern about descendants, which results in a significant overestimation of risks for children. This could explain, for example, why families with young children, even those who were born several years after the Chernobyl accident, apply for rehousing despite the fact that the calculations concerning the exposure of the children show that, in fact, their overall exposure would be very slight.

4. *The reference to the norm.* Although, in accordance with the ICRP Publication 60[11] and in compliance with the optimization principle, the concept of exposure limit does not apply to a de facto situation like that resulting from an accident, the limits set according to the regulations for "normal" conditions constitute an inevitable baseline insofar as, in practice, the populations do not accept the idea of a difference of treatment between the two types of situations. This behavior certainly corresponds to an implicit need to blur any exceptional feature from living conditions so as to feel reassured. This is why, in all the debates about the implementation of countermeasures, and particularly permanent relocation, the reference to values of the order of 1 to 5 mSv per year for individual doses has been systematically pushed forward as a limit of tolerability for living in contaminated areas.

5. *The disruption of social life.* Implementing large-scale countermeasures is also a social destabilization factor because of the population movements (those who are rehoused or who leave their homes voluntarily to escape radioactivity, those who arrive to follow-up the situation and to implement countermeasures. . .); because of the increase in the number of controls of all kinds; and because of imbalances that may arise between population groups or socioprofessional categories.

TOWARD NEW SAFETY OBJECTIVES

The different aspects just described provide only a partial view of the numerous dimensions that are driving the perception and the acceptability of the Chernobyl postaccident situation. Furthermore, the particular sociopolitical and economic context prevailing in the Soviet Union in the late 1980s has also played a key role in the development of the social crisis that characterized the period and is still evident. Even if it may be seen as dangerous to directly transpose the observations from Chernobyl to situations that could happen in Western countries, some general lessons can be learned for the establishment of criteria and countermeasures in the event of an accident.

The following general principles are recommended for the qualification of the boundary between what could be considered as an intolerable situation and what could be seen as a tolerable one.

1. Rehousing people (definitive change of house) appears to be unacceptable.

2. Restraints on the everyday lives of the public in limited numbers may certainly be deemed tolerable over a limited period of about 1 year. Restraints appear unacceptable if they are to be permanent or quasi-permanent over a generation.

3. More generally, changes in the economic activity of a region, limited in space and in time, appear to be tolerable. With regard to crops, for example, the loss of one harvest does not seem to be too disruptive.

4. To be tolerable, the measures taken to monitor the public and the environment have, whatever the case, to be limited in time. The very presence of such measures brings to mind the accident situation and prevents a complete return to "normal life."

On the basis of these orientations concerning the boundary between what is unacceptable and what is tolerable, it is reasonable to consider that the "source term" for the nuclear power units of the new generation should be reduced by one order of magnitude compared with "source term" S3. Calculations have shown that, with an S3/10 type release, without implementing countermeasures, the annual doses received by the members of the public after the first year following the accident would be lower than 1 mSv only beyond about 10 km away from the damaged plant. In the same conditions, the "source term" must be reduced by a value higher than 100 to obtain annual doses at the site boundary that do not exceed 1 mSv by the second year following the accident. In such conditions the reduction by only a factor of 10 could be seen as insufficient. It is clear, however, that the assumption of the absence of implementation of countermeasures is rather pessimistic, and one can reasonably assume that with such measures it would be possible to envisage the consequences of an S3/10 "source term" as manageable.

Finally, these results have confirmed the statement made by the Nuclear Installations Safety Directorate (French Safety Authority) in its orientation letter dated May 29, 1991, concerning future pressurized-water reactors, that "as a tendency, a 'source term' reduced to about a tenth of the S3 baseline 'source term' could be sought."

Further Investigations

As already mentioned, the approach just described is a very rough one. It implies, however, that significant improvement of the containment has to be sought for the new generation units with respect to the various scenarios that may result in an S3 type release. It will then be necessary to go back to the design of the new generation units, to study the development of severe accidents with

core meltdown allowing for the specific characteristics of these units, and to assess the corresponding consequences to decide on the acceptability of their design. This assessment should take into account the uncertainties associated with the results of calculations caused by limited knowledge, imperfections in the calculation tools, and possible variations of parameters. Ideally, these calculations of consequences should use "realistic" values for all parameters, but in practice it may be difficult to determine "realistic" values or even to guarantee the respect of values assumed rather overestimated. Therefore, by means of a series of studies conducted with various values for the parameters and by assessing both the various results and their more or less likely nature, it will be possible to come to a final decision on the acceptability of a given design.

As an example, the integrity of a containment is the subject of both continuous monitoring and periodic testing (leak tightness of the penetrations on the one hand and overall leak tightness on the other hand). These tests as well as, more globally, the experience feedback make it possible to determine "realistic" values for the leak of the containment, but it is not possible to guarantee the permanent respect of such values. At this point IPSN has conducted various complementary simple studies about the leak tightness to be sought for the containment, making a distinction between "direct" leaks to the environment and "collected" leaks, filtrated before being released, as well as considering two types of severe accidents with core meltdown—with or without water spray (water spray makes it possible to reduce the pressure in the containment and to lower the content of aerosols in the containment atmosphere, which results in a reduction of possible releases into the environment). With other assumptions still rather pessimistic, different curves can be plotted, such as that shown in Fig. 2, concerning doses caused by depositions during the second year following the accident without implementing countermeasures. These curves make it possible to quantify the importance, qualitatively evident, of a low rate of "direct" leaks and of water spray in the containment. Other assessment factors, however, are to be considered; for example, is it possible to guarantee a rate of "direct" leaks from the containment as low as 0.01% throughout the life of an installation? Is there a risk with the use of spray in the containment, which is recommended from the viewpoint of radiological consequences according to the preceding criteria, to significantly increase the possibility of a hydrogen explosion that might affect the containment integrity? These various aspects will, of course, be thoroughly discussed in the future.

CONCLUDING REMARKS

Nuclear power installations are too complex and the parameters involved too numerous to enable technical design bases for such installations to be directly derived from individual risk constraints in the sense of ICRP. It must also be understood that setting an objective like S3/10 implies design measures that will probably result in a "maximum conceivable release" lower than S3/10 for iodine-131 and cesium-137, although a complete demonstration of a source term as low as S3/100 could not be rigorously attainable. For the new generation of plants being developed since 1992 within the French–German framework (the EPR project), the French and German safety authorities expressed together such objectives as to "practically eliminate" accident situations that could imply large "early" releases and to improve the containment function so that a low-pressure core-melt accident would necessitate only very limited countermeasures in area and in time; this would be expressed by no permanent relocation, no need for emergency evacuation outside the immediate vicinity of the plant, limited sheltering, and no long-term restriction in consumption of food.[12]

The safety options of the EPR project were sent to the French and German safety authorities during September 1993. They were examined jointly by both countries on the basis of analyses conducted on the French side by the IPSN in connection with its German counterpart, the Gesellschaft für Anlagen-und Reaktorsicherheit (GRS). The EPR project is proposing a "design maximum release" of 2000 TBq of iodine-131 and 100 TBq of cesium-137 corresponding to a reduction factor of the order of 7 for iodine-131 and a reduction factor of about 15 for cesium-137 with previous values. These reductions reflect the special concern about long-term consequences of an accident. The French and German authorities will give their opinion in the future on the compatibility of the technical provisions of the EPR project with their objectives.

ACKNOWLEDGMENTS

The authors are grateful to D. Manesse of IPSN and T. Schneider of CEPN for helpful discussion and advice.

REFERENCES

1. D. Quéniart , *La sûreté des futurs réacteurs en France* (translation: *Safety of Future Reactors in France*), ANP 92 Conference,

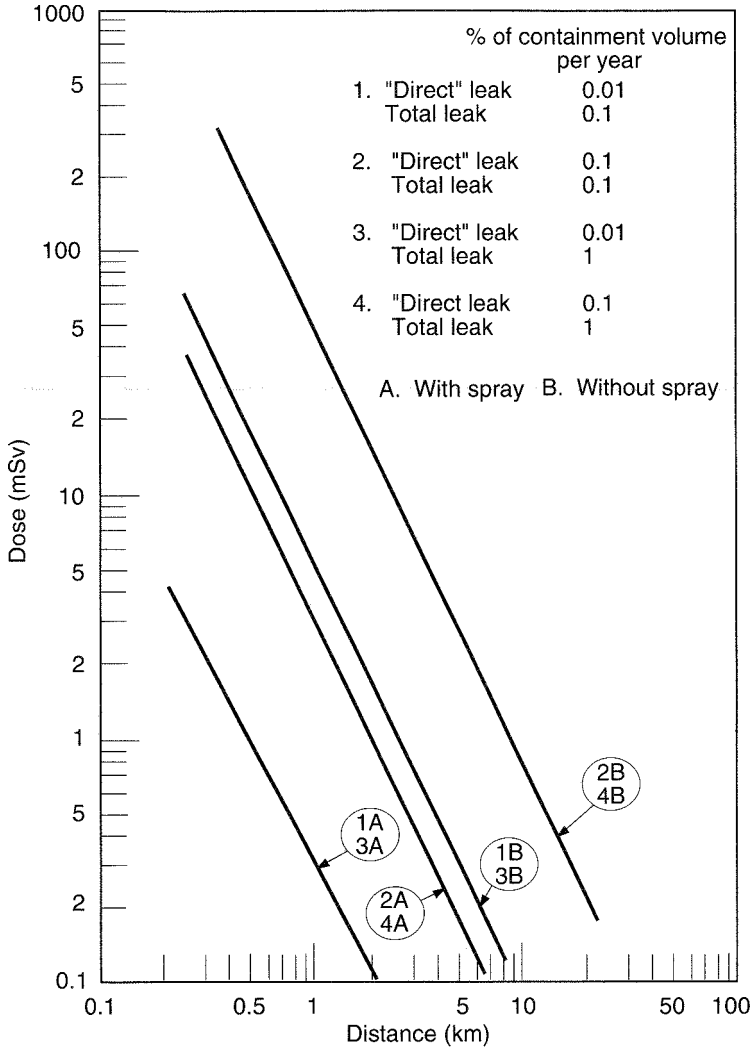

Fig. 2 External dose caused by deposits received during the second year following the accident.

Tokyo, 25–29 October 1992, Report IPSN No. 92/02 (CONF-921003-), 1992.

2. Probability Safety Assessment 900 MW(e) Protection and Nuclear Safety Institute Synthesis Report, April 1990.
3. Probability Safety Assessment 1300 MW(e) Électricité de France Synthesis Report, May 1990.
4. International Commission on Radiological Protection, *Protection of the Public in the Event of Major Radiation Accidents: Principles for Planning*, ICRP Publication 40, 1984.
5. EURATOM Regulations, No. 2218/89, Official Journal of the European Communities, No. L 211, 22, July 1989.
6. J. Lochard and S. Pretre, Intervention After Accident: Understanding the Societal Impact, in *Radiation Protection on the Threshold of the 21st Century, Proceedings of an NEA Workshop, Paris, 11–13 January, 1993*, Report CONF-930181-, pp. 197-209, 1993.
7. Health and Safety Executive, London, *Safety Assessment Principles for Nuclear Plants*, 1992.
8. T. Schneider and J. Lochard, *Réflexions sur l'acceptabilité sociale et conséquences économiques d'un accident nucléaire*, Report CEPN-R-191, April 1992.
9. International Atomic Energy Agency, *The International Chernobyl Project: Technical Report*, 1991.
10. Nuclear Protection Evaluation Center, *Historical Perspectives of the Countermeasures Taken Following the Chernobyl Accident: Reflections on the Concepts and Regulations Adopted in the CIS for Post-Accidental Management*, CEPN Report 225, April 1994.
11. International Commission on Radiological Protection, *1990 Recommendations of the International Commission on Radiological Protection*, ICRP Publication 60, Pergamon Press, 1992.
12. GPR/RSK Proposal for a Common Safety Approach for the Future Pressurized Water Reactors, May 25, 1993.

Accident Analysis

Edited by R. P. Taleyarkhan

Nuclear Safety Research: The Phebus FP Severe Accident Experimental Program

By P. von der Hardt,[a] A. V. Jones,[a] C. Lecomte,[b] and A. Tattegrain[b]

Abstract: *The Phebus FP test reactor at Cadarache, France, has been modified and a new facility built adjacent to it in the scope of a large international severe accident research program. The core, reactor cooling system (RCS), and containment of an accident within a reactor are simulated by appropriate scaled-down experimental components. Test fuel is irradiated in situ and then overheated to melting. Fission products (FPs) and other aerosols are swept through the RCS into the containment by hot steam and hydrogen. Instrumentation and posttest analyses enable physical and chemical phenomena to be studied relative to such factors as fuel dislocation, FP release and transport, and iodine species in the containment. Equipment design and experimental procedures are supported by modeling and code calculations. The results will, in turn, be used for code validation. More than 25 organizations from Europe and overseas contributed to the scientific and technological development of Phebus FP. The first test was carried out between November 1993 and January 1994. Five subsequent experiments will follow at annual intervals.*

Reactor safety analyses performed over the years in a number of countries have identified the possible scenarios for severe accidents in power-generating nuclear plants.[1] In such scenarios, the reactor fuel is damaged and fission products (FPs) are released. Hence, under containment failure conditions, the potential of an FP release into the environment exists. Although the probability of such a severe accident is low, the biological impact to man and the environment may be significant. For this reason, the behavior of FPs during a severe accident has been the subject of numerous theoretical and experimental studies around the world.[2] These studies aim at the determination of the potential source term in the environment—that is, the quantity, composition, and kinetics of radioactive release outside the damaged nuclear plant. This work has resulted, inter alia, in the elaboration of specific computerized tools designed to describe all features of FP behavior during a severe accident, such as ESCADRE[3] in France, ESTER[4] at the Joint Research Centre (JRC) Ispra, the Source Term Code Package (STC)[5] in the United States, and others.

Phebus FP is an integral in-pile experiment for studying, on a reduced scale, FP behavior in a reactor. It makes use of representative spent fuel as a source of real FPs. Its thermal–hydraulic and physical–chemical conditions reproduce representative conditions wherever possible along the path of these FPs.[6]

Main options for the Phebus FP experiments are derived from this strategy:

- Phebus FP has the major aim to quantify relevant phenomena involved in sequences selected for their importance from probabilistic and release level points of view; this approach is preferred to the direct simulation of specific accident sequences.
- Phebus FP is designed as a means to validate computer codes devoted to severe accidents and to derive significant conclusions for the reactor scale.

[a]Commission of the European Communities.
[b]Institut de Protection et de Sûreté Nucléaire.

The Phebus FP bundle inventory is roughly $^{1}/_{5000}$ that of a midlife 900-MW(e) pressurized-water reactor (PWR) core, and for equal FP concentrations in the carrier gas (to induce representative chemistry), the linear dimensions should be scaled down by about a factor of 17. Such scaling obviously would lead to difficulties in reproducing "all" features of any particular accident sequence, such as thermal–hydraulic and physical–chemical conditions in the reactor coolant system (RCS). Efforts have been made to reduce dissimilarities to the extent feasible. Phebus circuit temperatures, for example, of 450 to 1000 K are in the right range, as are atmosphere–structure temperature differences. The average steam, hydrogen, and aerosol concentrations are in the corresponding parametric ranges, as predicted by various codes and detailed in the recently completed Committee on Safety of Nuclear Installations (CSNI) report.[2] The Phebus FP fuel from the BR3 plant in Belgium was manufactured by a commercial supplier rather than on laboratory scale. It is considered to come much closer to power-reactor fuel than rods used earlier in other experiments (such as TREAT STEP, PBF SFD, and HI/VI). Despite its scaling limitations, Phebus FP replicates complex severe reactor accident conditions with better fidelity than any other previous experimental program and also offers unique opportunities for code validation.

OBJECTIVES AND EXPERIMENTAL PROGRAM

Safety Evaluation Needs

Safety analyses performed in the framework of nuclear power-plant severe accident studies have three main goals:

- Prevention
- Mitigation
- Dimensioning and optimization of countermeasures

For the fulfillment of these goals, it is necessary to evaluate the reference source term for emergency plans and to assess the efficiency of preventive and mitigative measures that can be implemented on a plant: operating and emergency procedures and specific hardware (engineered safety features and ultimate devices).

The protection of the population by suitable emergency plans implies that the previously mentioned reference source term for these plans be characterized in terms of activity level and kinetics. In this analysis, the chemistry aspect is essential to determine FP behavior at various points in the plant and to evaluate the radiological impact of potentially large property variations between different species of the same FP.[7]

Code Validation Needs

From the point of view of code validation, the Phebus FP experiments offer a number of novel aspects:

- A source representative as to composition and concentration of FPs, control materials, and structural materials. Hence one can expect representative chemistry—aerosol size distribution and composition, interaction between vapors and aerosols and between vapors and structures—that is difficult if not impossible to obtain with artificial sources or in small-scale experiments.
- Circuit temperatures high enough to be representative of reactor primary system and low-pressure injection system (LPIS) line components. The circuit materials are Inconel and austenitic steel. It is presently thought that there is little difference in the degree of reactivity with regard to FP retention between both materials. The issue, however, is further examined by separate effects tests in Phebus and at Chalk River, Ontario. Components at lower temperatures can be included (e.g., a steam generator tube), which can even be cold enough to induce steam condensation on the walls and onto aerosols.
- A containment vessel with several systems for producing representative thermal–hydraulic conditions, including the sump and wall temperatures and the temperature of surfaces upon which condensation is to take place. Possible multivessel designs exist for later tests.
- Design features of the containment that allow the major features of containment chemistry to be reproduced, including a realistic source, painted surfaces, free or controlled sump pH, and a high radiation level.

Code and model validation requirements that will be met by Phebus FP correspond in the main to these special advantages:

- Data on the release of FPs and other core materials under conditions of advanced degradation (oxidizing or reducing conditions, significant melting of fuel, and oxidized cladding). Data on the release of less-volatile FPs (Ba, Sr, and Ru) are of particular interest both for model validation–improvement and from the point of view of safety analysis.
- With the realistic source and circuit temperatures, data on transport and deposition in circuit components.

Items of particular interest are the role of multicomponent aerosols; vapor–aerosol interaction and revaporization as well as (with realistic source and thermal–hydraulic conditions) the differential depletion of hygroscopic and nonhygroscopic aerosols; and the role of steam condensation on structures in aerosol removal.

• New data on fission-product chemistry and iodine behavior with a range of chemical conditions and in the presence of radiolysis.

Phebus FP Test Matrix

The test matrix has been defined with those basic phenomena in mind for which a representative FP source is essential.[8] These phenomena are encountered in several severe accident scenarios that are important for risk assessment:

• Large-break loss-of-coolant accident (LOCA) (AB sequence)
• Small-break LOCA (SD sequence)
• LPIS-interfacing LOCA (V sequence)
• Transient-initiated accident (TMLB)

They were determined with the use of the results of severe accident computations performed mainly in the frame of "Shared Cost Actions" sponsored by the European Communities, information coming from separate effects experiments, and Phebus FP precalculations.

Presently, three tests are fully defined. Their main objectives are shown on Table 1. Note that "Fuel melting" in the "Fuel bundle" column of Table 1 designates UO_2 melting in addition to possible earlier Zircaloy liquefaction.

Proposals for the remaining three tests include the following:

• Tests at 3.5 MPa rather than 0.4 MPa
• Boiling-water-reactor oriented conditions
• Very high burn-up and/or mixed-oxide fuel
• Melt progression and FP release in a fuel debris bed
• Injection of air rather than steam

Table 1 Phebus FP Test Matrix (Main Objectives of the First Experiments)

		Experimental objectives		
No.	**Test type**	**Fuel bundle**	**Primary circuit**	**Containment vessel**
FPT0	Fresh fuel in oxidizing environment	FP release and speciation from fresh/preconditioned fuel under steam flow during • Heat up • Fuel degradation • Fuel melting (up to 20%) • Cooling down at low steam flow rate	FP retention in the primary circuit of a steam generator without condensation Chemistry of deposits Resuspension scoping study	Aerosol behavior and deposition during FP injection Radiochemistry is iodine in gas and aqueous phase at pH = 5 Iodine partitioning and formation of organic compounds FP reentrainment at slow depressurization
FPT1	Preirradiated fuel in oxidizing environment	As FPT0	As FPT0 Coupons for thermal resuspension	As FPT0, but • pH = 7 with natural evolution • High humidity
FPT2	Preirradiated fuel in reducing environment	As FPT1, under steam starvation conditions Specifically: • Fuel candling and relocation • Cooling down at high steam flow rate	Chemistry of deposits Retention of Inconel and stainless steel Pipe section for thermal resuspension	As FPT1, but • pH = 9 with natural evolution • Intermediate humidity Single droplet spray

FACILITY DESCRIPTION AND EXPERIMENT OPERATION[9,10]

Summary

The Phebus FP program required 5 years and $80 million (U.S.) for design and construction of buildings, reactor components, and experimental equipment.

Reactor Modifications

Phebus, a loop reactor with low-enrichment rod-type driver fuel, had been built in 1979 for short transient fuel tests. The transition toward the FP program with extended reirradiation phases implied the following:

- A new steady-state heat removal plant with heat exchanger, decay tank, and cooling towers.
- An increase of the driver core reactivity by additional fuel elements and a graphite reflector.

The reactor building had to be reinforced at its foundations and its external walls, which is in compliance with recent seismic safety rules.

Experimental Equipment

In-Pile Section (Test Train). A horizontal section on driver core midplane (Fig. 1) shows the 20-rod test fuel bundle surrounded by a ceramic shroud fitted inside the pressure tube. The central position is occupied by a silver–indium–cadmium control rod. The thermal shroud consisted of two concentric, high-density, zirconia tubes in the FPT0 test train, referred to as "the old shroud" in a later section. FPT1 will be fitted with a new porous zirconia shroud and an inner thoria liner.

A remotely operated foot valve below the fuel bundle connects the inner test train volume to the surrounding high-pressure water loop during the fuel reirradiation phase. The valve is closed for the high-temperature transient phase. The upper plenum tube above the fuel bundle acts as a cooling water return pipe during reirradiation. It conducts the hot-steam–hydrogen–FP mixture toward the experimental building during the transient phase. The test fuel is 4.5% enriched UO_2 for the first test and preirradiated fuel for the remaining tests of the program. The irradiated fuel originates from the BR3 plant in Mol, Belgium.

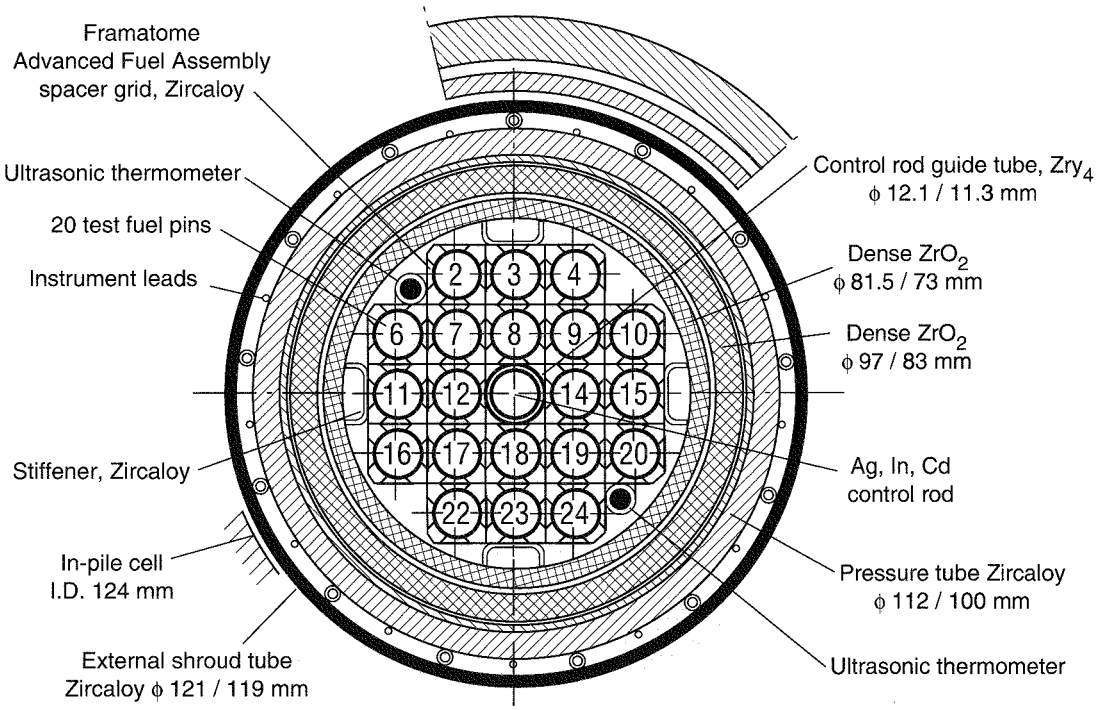

Fig. 1 FPT0 in-pile test section, horizontal section.

Before being shipped to Cadarache, the BR3 fuel pins underwent a lengthy characterization program at JRC, Karlsruhe. The main objectives of these tests were checks on possible deformation and incipient cladding cracks, FP and heavy nuclei distribution, grain size, fuel stoichiometry, and burnup. All pins for Phebus FP were "healthy." In contrast to earlier test fuel from BR3, grain size and oxygen/metal (O/M) ratio correspond to commercial fuel data.

The test train is instrumented with about 70 thermocouples, two ultrasonic thermometers, miniature fission chambers, and a differential pressure transducer. Small bore tubes are provided for the injection of steam and noncondensable gases underneath the test fuel bundle. The test train design described so far refers to the first three or four tests of the test matrix. Design details of the later experiments might be different. The test train sits in a double-walled in-pile cell, a fixed structure in the center of the Phebus reactor core. Together with the double-contained components of the high-pressure water loop, the in-pile cell completes the three-barrier safety design principle as a protection against accidental radioactivity release from the experiment.

Primary Circuit (Simulated RCS). The test train upper plenum and the horizontal line (Fig. 2) are the first components of the primary circuit. Both fulfill the same function during the high-temperature transient; that is, they convey the hot-steam–hydrogen effluents sweeping FPs and other aerosols out of the fuel bundle toward the experimental building. The upper plenum and horizontal line are Inconel-lined, trace heated to 970 K, and instrumented with thermocouples. As mentioned before, both components are part of the high-pressure cooling water circuit during the reirradiation phase.

Inside the experimental building, a branching ("Y") point and two valves separate cooling water and FP circuits (Fig. 3). For safety reasons, all experimental components are housed in a steel caisson, which continues the triple barrier principle mentioned previously. Major components of the primary circuit are two instrumentation groups at points "C" and "G," further described later, and a simulated steam generator. This latter device is operated in a noncondensing mode during the first two tests. For experiments in the later part of the test matrix, the steam generator could be condensing or replaced by a different primary circuit configuration.

Containment Vessel (Figs. 4 and 5). This 10-m^3 cylinder simulates the reactor containment building. Similar to the other experimental components, it is installed inside the safety caisson. Particular design features of the containment vessel are a sump and a group of three condensers in the upper part. They are designed to control steam condensation and to recuperate condensates with entrained FPs for analysis.

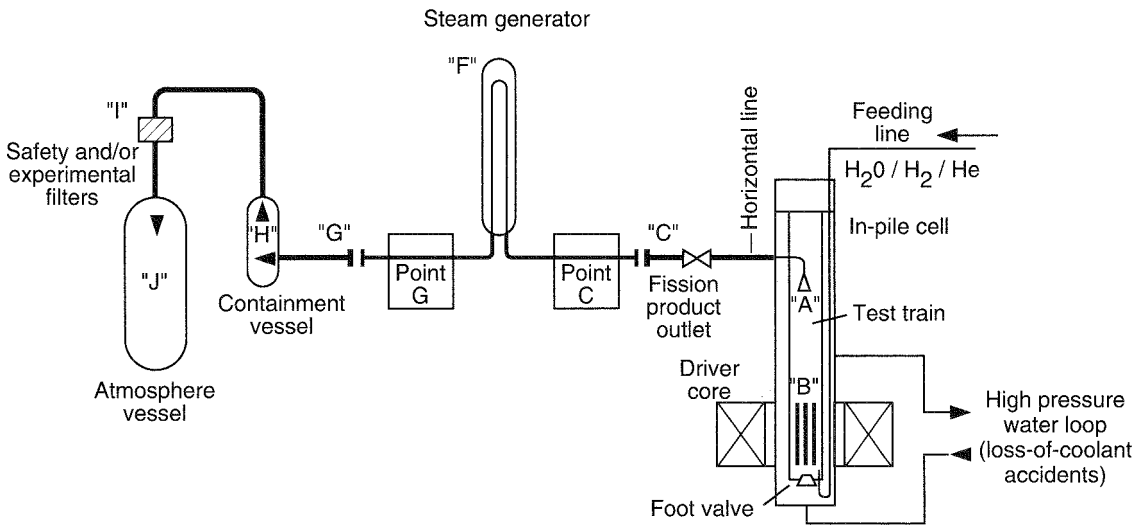

Fig. 2 FPT0 experimental circuit.

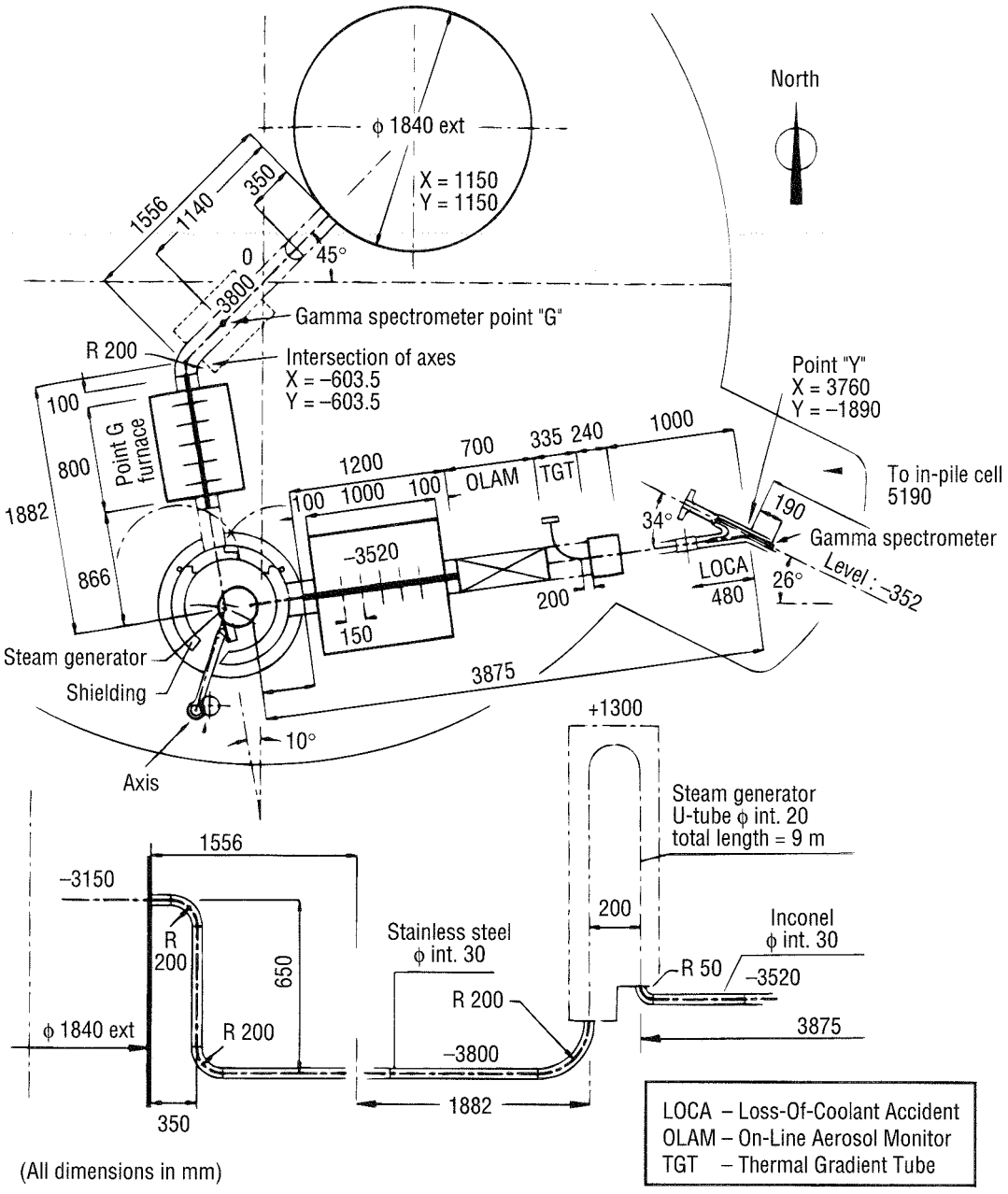

Fig. 3 FPT0 circuit geometry.

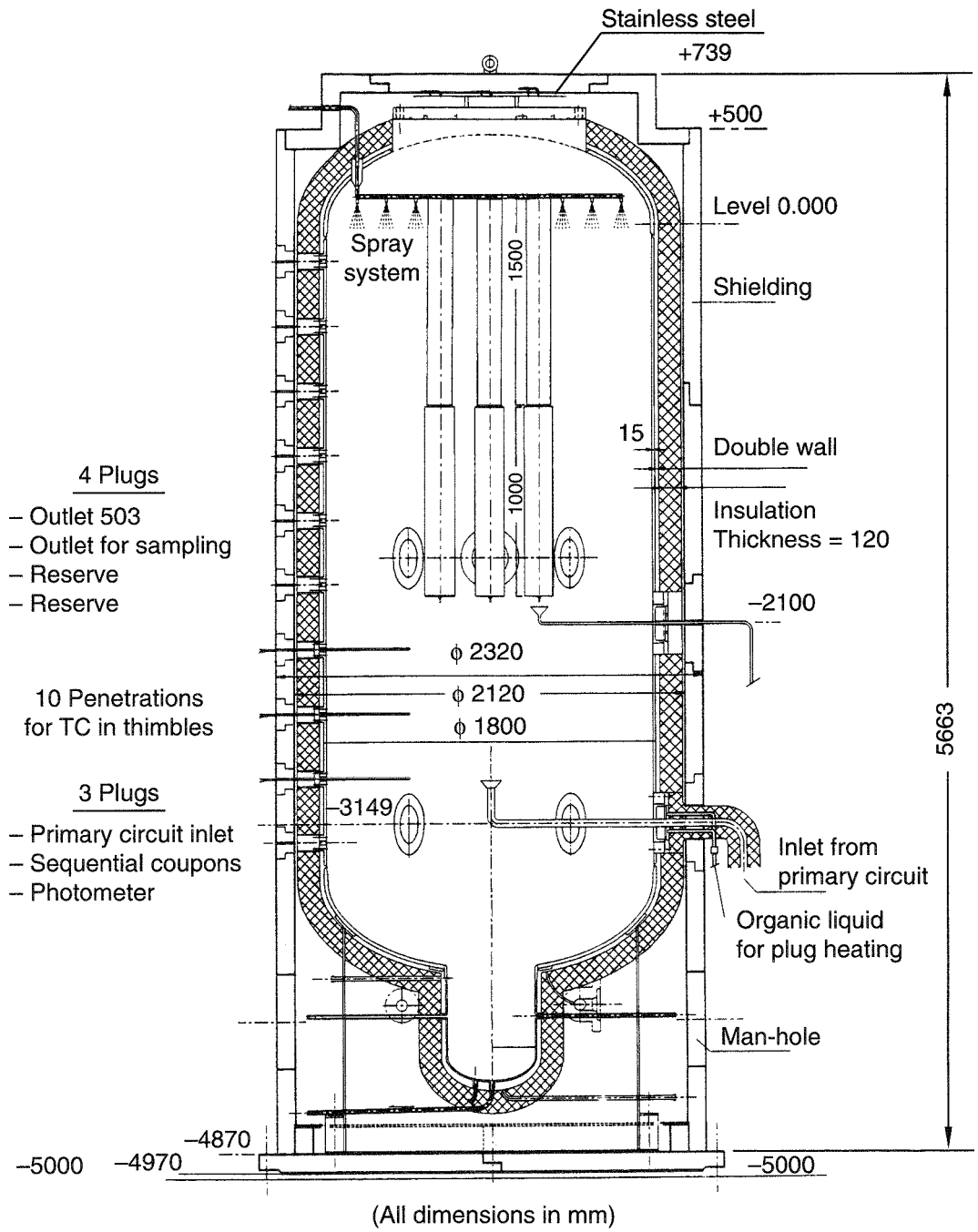

Fig. 4 Phebus FP REPF 502 containment vessel.

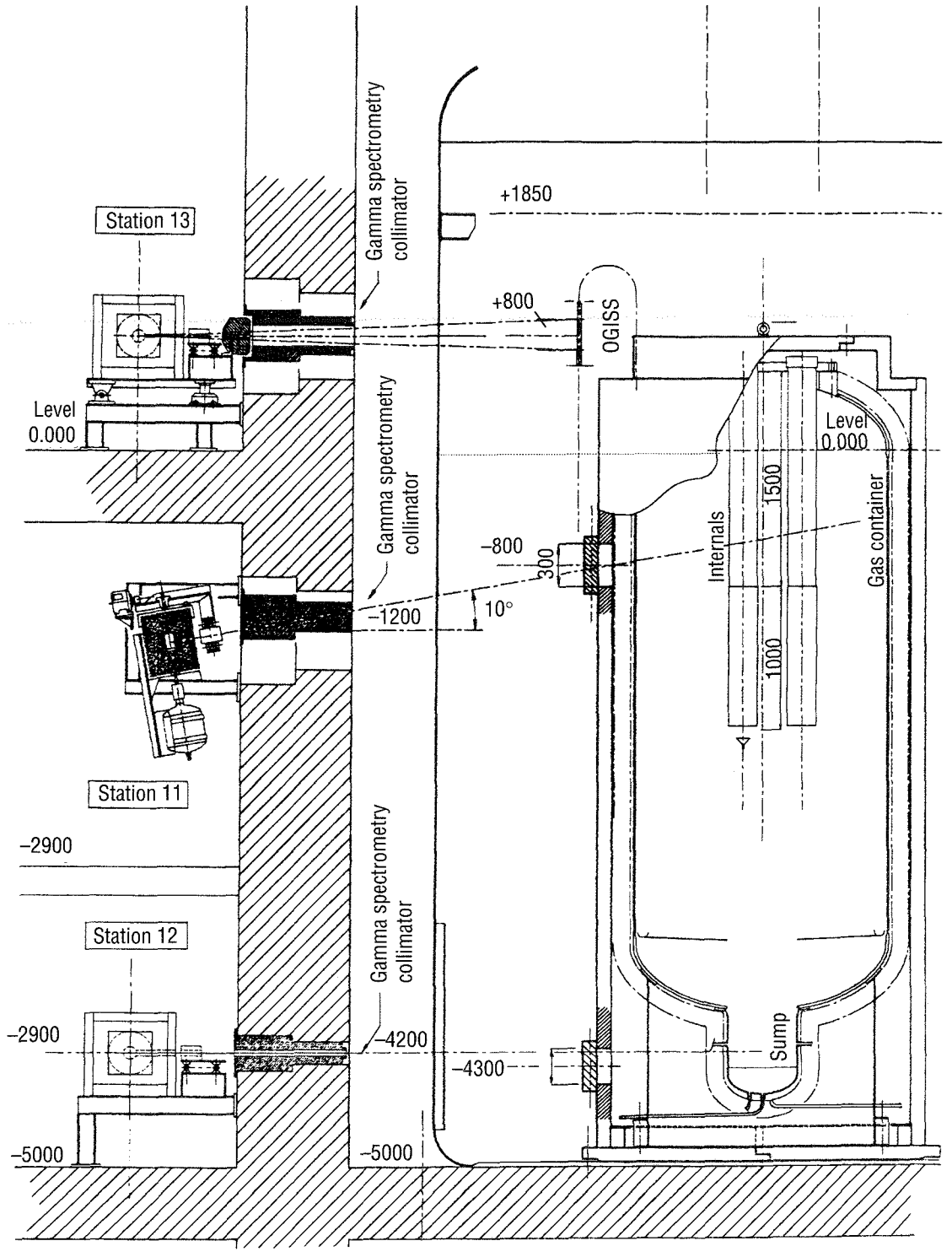

Fig. 5 Gamma spectrometry.

Painted surfaces on the condensers and in the sump support experiments about organic iodine formation during the containment "chemistry" phase. The condensers simulate the cold structures of a reactor building; they limit condensation onto the vessel wall, which could not be quantified accurately.

Experimental Instrumentation[11–14]

A number of methods are used for experimental data acquisition:

- A qualified compilation of as-fabricated component data.
- Characterization of the test fuel.
- Thermal–hydraulic on-line instrumentation, like thermocouples, pressure transducers, and flowmeters.
- FP on-line instrumentation, like gamma spectrometers.
- Sampling instruments, requiring posttest analysis (PTA) of their gaseous, liquid, and/or solid FP contents.
- Postirradiation examination (PIE) of the damaged fuel bundle.

Typical sampling instruments adapted to, or developed for, Phebus FP are inertial impactors, filters and coupons for aerosols, capsules for gas or liquid sampling, and selective iodine speciation samplers.[15] Various primary circuit components, moreover, can be recovered after each test for analysis of FP deposits.

Experimental Sequence

The following test sequence is typical for most of the experiments in the test matrix.

Reirradiation

In this phase the test train is connected to the high-pressure water loop, which cools the test fuel bundle. A representative inventory of medium- and short-lived FPs is generated under the following irradiation conditions:

- Loop pressure and temperature: 2.5 MPa, 360 K
- Phebus driver core power: ~20 MW
- Linear heat generation rate in the test fuel: 150 to 180 W/cm
- Duration of this phase: 9 to 14 days

Intermediate Phase

After reactor scram, the water is eliminated from the test train and horizontal line, the foot valve is closed, and the valve toward the FP circuit is opened. All instruments are made operational and checked.

High-Temperature Experimental Phase

The high-pressure water loop continues to cool the test train outside, whereas steam is injected into its inner volume. The driver core power is raised, which causes the test fuel to heat up to 3000 K, with subsequent fuel degradation and release of FPs and structural materials. Key data of this phase follow for the first test (FPT0):

- Driver core power: up to 10 MW
- Fuel bundle maximum power: 90 kW
- Steam flow rate: 0.5 to 3 g/s
- Total transient time, including plateaus: 18.000 s

The transient is terminated by driver core scram with resulting fast test fuel cooldown. Circuit components and the containment vessel are kept at their specified temperatures during the transient; that is, 970 K into the steam generator and 420 K in the remaining circuit. The vessel walls are maintained at 420 K, the condensers at 400 K, and the sump water at 360 K. All sampling instruments on the experimental primary circuit are operated in sequence, and gamma spectra are taken at close intervals during the transient.

Containment Vessel Experimentation

Test train, horizontal line, and primary circuit are isolated from the containment vessel after the driver core scrammed, backfilled with dry nitrogen, and cooled down. During that time thermal–hydraulic conditions in the isolated vessel remain unchanged for several days. The aerosols will settle quickly, end up in the sump, and generate conditions for radiolysis and iodine volatilization. Liquid- and gaseous-phase samplers are operated during this "chemistry" phase, and the transfer of gamma emitters is followed by spectrometers. At the end of this phase, the vessel is depressurized, backfilled with dry nitrogen, and cooled down. As during the gas sampling operations, all gaseous effluents are directed to the large atmosphere vessel through a condenser and filters.

Posttest Operations

All sampling instruments are recovered by remote handling as soon as the experimental installation is back to atmospheric pressure and room temperature. They are transferred to a hot cell under the FP caisson where first inspections and gamma scans are carried out, beginning with those samplers which have to be scanned for iodine

(see the following section). The remaining circuit components are remotely decontaminated and removed. The caisson should then be accessible for final disassembly and for installation of the equipment for the following test.

Postirradiation Examination and Analyses

After a first selection, specimens are shipped to a number of laboratories for PTA with these objectives:

- An overall FP and other aerosol mass balance.
- Determination of elemental and isotopic composition and of the chemical speciation of the samples.
- Determination of aerosol granulometry and morphology in solid deposits.

The PTA plan has been elaborated together with the participating laboratories, who will use scanning electron microscopy, X-ray diffraction and fluorescence, energy-dispersive X-ray spectroscopy, inductively coupled plasma optical emission spectroscopy, electron microprobe analysis, and wet radiochemistry for the analytical work.[16,17]

The PTA plan includes the horizontal line and the test train upper plenum. The lower part of the test train with the damaged fuel bundle will be examined according to another program, largely based on more traditional destructive fuel PIE techniques. The objectives of PIE are the mapping of fuel debris and corium compounds and the quantification of remaining FPs.

CALCULATIONS

Analytical Work Program

The chief actors in the calculation program are the analytical teams at Commissariat á l'Energie Atomique (CEA) in Cadarache, the JRC Safety Technology Institute, and Phebus program partner organizations. These teams have primary responsibility for providing the technical basis for the various analytical tasks, which are managed by the Analytical Group (Scientific Analysis Working Group, SAWG):

- Propose detailed objectives of each test in line with the orientations of the overall Test Matrix and the geometry and operating conditions recommended to best meet these objectives.
- Achieve a detailed understanding through sensitivity studies of the predicted course of the test and of the effects of uncertainties in physics or data and of possible experimental malfunctions.
- Coordinate, execute, and report on the analysis of each test.

An additional task that the SAWG has found necessary is the formulation and calculation of certain code benchmark problems in which the discrepancies between code predictions appear to be unacceptably great in the context of Phebus test preparation and analysis.

Experiment Precalculations

As mentioned previously, the precalculations help to define the detailed objectives of a test, the experimental geometry, the operating conditions, and guidelines for the calibration and operation of instrumentation. Because test FPT0 is the first in a new facility, its precalculation program has necessarily been extended and is wide ranging.[18]

Bundle Calculations. Calculations confirmed the suitability of the bundle design, with 20 fuel rods and 1 control rod, and the fundamental volumetric or mass scaling factor of 5000 to achieve the correct FP concentrations in the bundle. The calculations stressed the importance of the shroud properties (in particular, thermal conductivity) in determining the peak temperature and axial temperature profile in the bundle and consequently the degradation behavior. The radial temperature profile was nearly flat at high temperatures (100 to 200 K at 3000 K) because of radiation heat transfer. Regardless of the thermal conductivity, the rather severe objective of 20% fuel melting could always be achieved. The main bundle objective for FPT0, however, was significant FP release (that is, about 50% of the volatile species) in oxidizing conditions.

A final series of calculations has been completed to define the neutronic power and the steam flow history to achieve FP release in oxidizing conditions while limiting the flow rate. Figures 6 and 7 give the new boundary conditions and predicted peak fuel temperature at midcore height using various codes.

In parallel with the degradation studies, calculations have been made of the corresponding FP releases. Mechanistic models, such as FUTURE,[19] FREEDOM,[20] and FASTGRASS,[21] give lower releases of the volatile gases (noble gases, cesium, and iodine) than do the rate models like CORSOR, and releases are delayed by 1000 s or more, depending on the details of the transient. For this reason a rather long plateau at high temperature was implemented in FPT0. Note, however, that neither rate models nor detailed models are well validated for trace irradiated fuel.

Circuit Calculations. The bundle transient provides the inputs (steam, hydrogen, and FP flow rates) to the

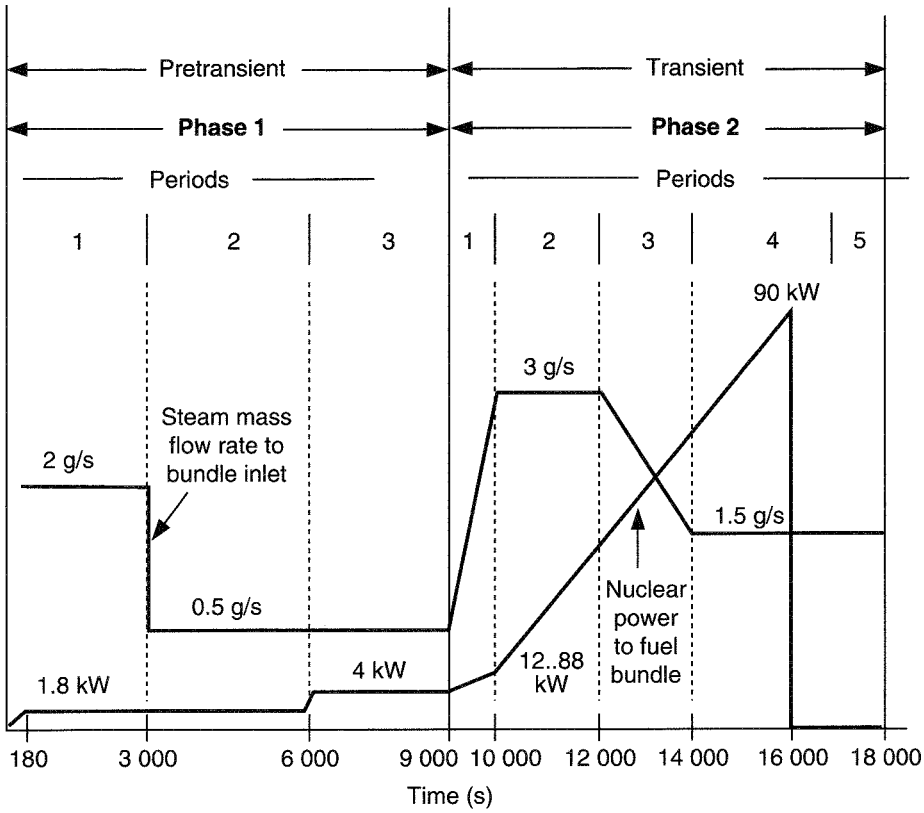

Fig. 6 FPT0 steam flow and neutronic power.

circuit. The chosen steam flow history of Fig. 6 is a compromise between a number of constraints, and its selection has involved a large number of detailed calculations. The detailed analysis of the first experiment will show whether the compromise was correctly chosen.

Beyond the vertical and horizontal lines, the FPT0 circuit includes a steam generator tube. Flow speeds, carrier gas, and FP concentrations in this tube are representative of the reactor case, and the original objectives of FPT0 intended to exploit this fact by studying retention both with a hot secondary side (tube wall at 150 °C) and with a cold secondary side (tube wall at 80 °C). After a series of exploratory calculations, the cold phase was abandoned for FPT0. The thermal–hydraulic conditions of the circuit have become rather simple.

Figures 8 to 10 show the total retention in the various circuit components for cesium, tellurium, and aerosols, as calculated with TRAP-F, RAFT, VICTORIA, and the Japanese code MACRES.[22] Clearly there are significant differences in the details of the predictions (there are differences in the relative importance of the various deposition mechanisms, too), but there is agreement that most

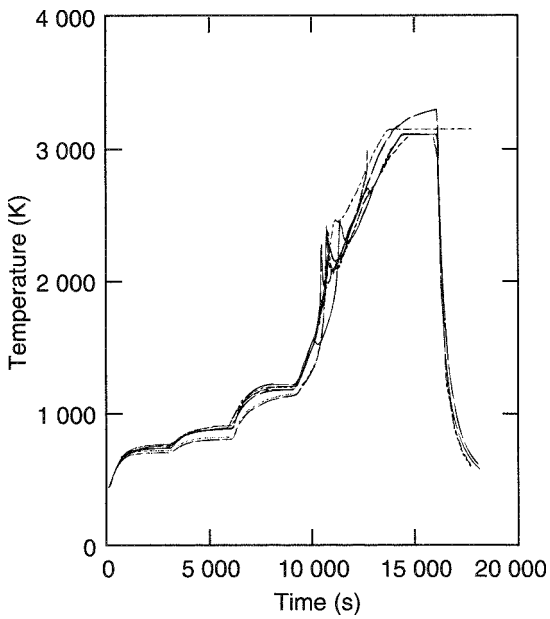

Fig. 7 Predicted fuel temperatures at midcore height using various codes.

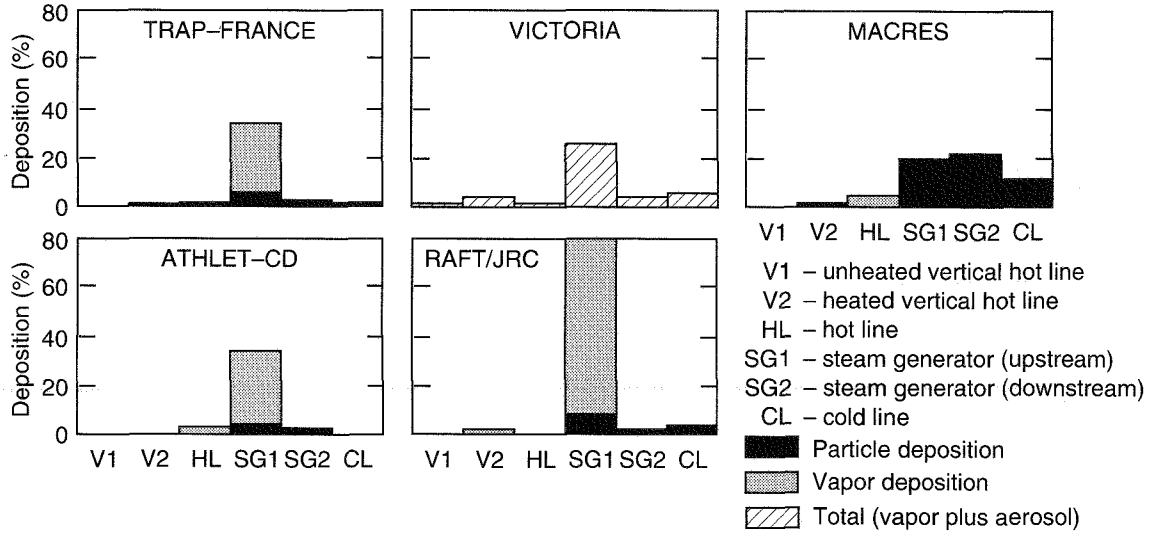

Fig. 8 Predicted cesium retention in FPT0 circuit.

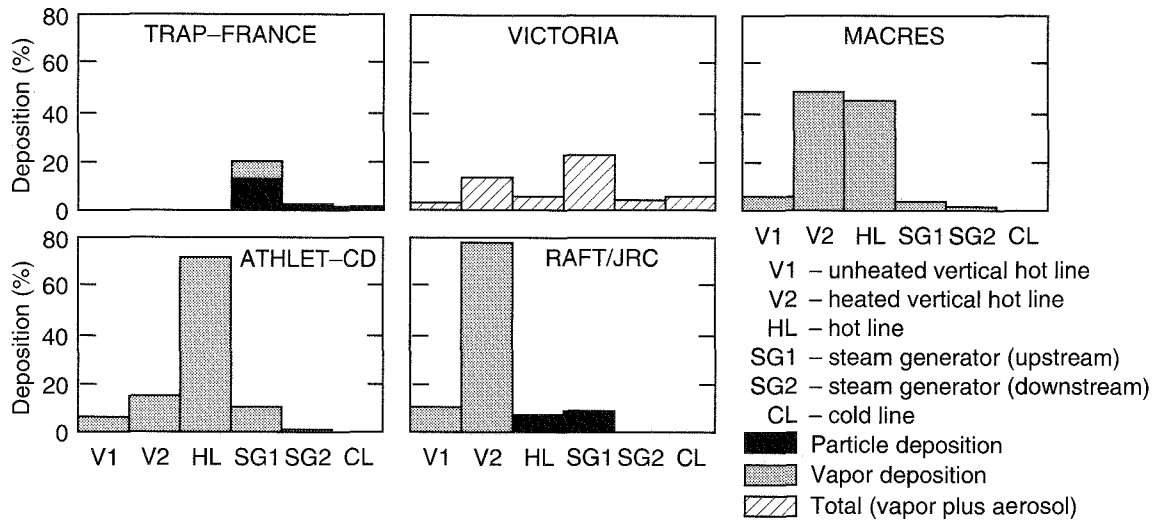

Fig. 9 Predicted tellurium retention in FPT0 circuit.

of the deposition will take place in the rising leg of the steam generator through turbulent impaction and thermophoresis. Impaction in bends is predicted to be an important retention mechanism. Those codes which model it predict significant tellurium retention by chemisorption before the steam generator. The information from the calculations has guided the choice and location of circuit instrumentation and the selection of operating ranges for impactors, other aerosol instruments, and the gamma-scanning devices.

Containment Calculations. As mentioned earlier, the containment vessel has some features absent in reactor containments, notably the condenser structure. Most codes have needed some modification to enable them to treat these features. Nevertheless, participation in the containment calculations has been strong. The original thermal–hydraulic objectives called for high humidity, possibly with bulk condensation. In the first rounds of calculations,[23] the relative humidity was particularly sensitive to the (small) sensible heat component

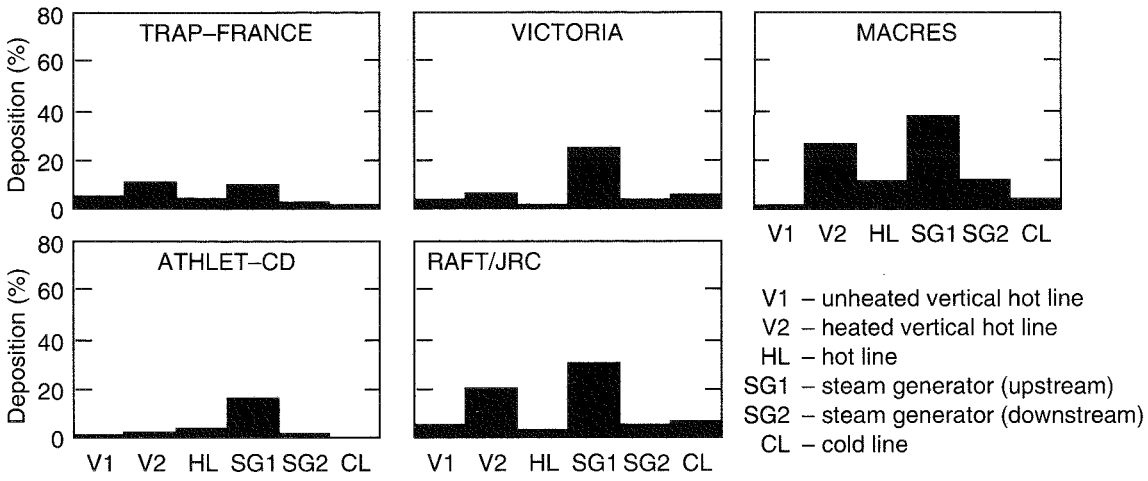

Fig. 10 Predicted aerosol retention in FPT0 circuit.

associated with condensation on the condenser structure, which is not even identified in common correlations.

Therefore the decision was to reduce the target humidity for FPT0 to about 50% (it remains higher for subsequent tests) and to characterize the thermal–hydraulic behavior of the Phebus containment vessel through a series of steam injection tests with the vessel itself together with a smaller existing facility. These tests proceeded in a series of steady states with different condenser temperatures and steam injection rates. The calculation program to prepare them is reported in Ref. 24. Figure 11 displays the predicted relative humidity for FPT0 during the steam injection phase obtained with the CONTAIN code. The code also predicts aerosol removal, primarily by settling and by diffusiophoresis. With the strategy adopted, the removal during the early stages is almost entirely by diffusiophoresis (steam condensation), whereas later on settling predominates. Because of the low humidity, there is no predicted difference in behavior between hygroscopic and nonhygroscopic particles.

In the next phase of the experiment, when the aerosols have largely been removed (after about 10 hours), a washing system transfers all settled particles to the sump. Iodine chemistry calculations have been made by several teams using three codes, both phenomenological and mechanistic. Some results are shown in Fig. 12.

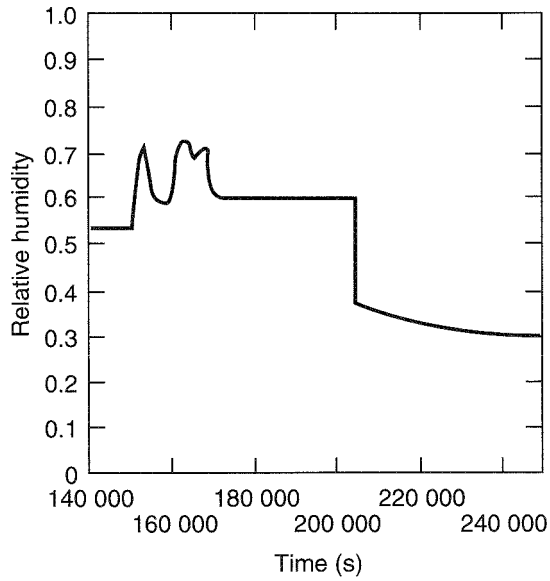

Fig. 11 Calculated relative humidity in FPT0 containment vessel during aerosol deposition and settling.

Sensitivity Calculations

Sensitivity calculations have several purposes:

- To map output parameters as functions of the input parameters in the neighborhood of the desired operating conditions and hence increase understanding of the behavior of the experiment.
- To investigate result dependence on modeling assumptions.
- To help define the operating ranges of instruments.
- To guide the execution of the experiment when incidents such as the failure of circuit heaters or condenser temperature control occur.

Most of the trends observed were obvious, but particularly strong sensitivity has been observed in some cases:

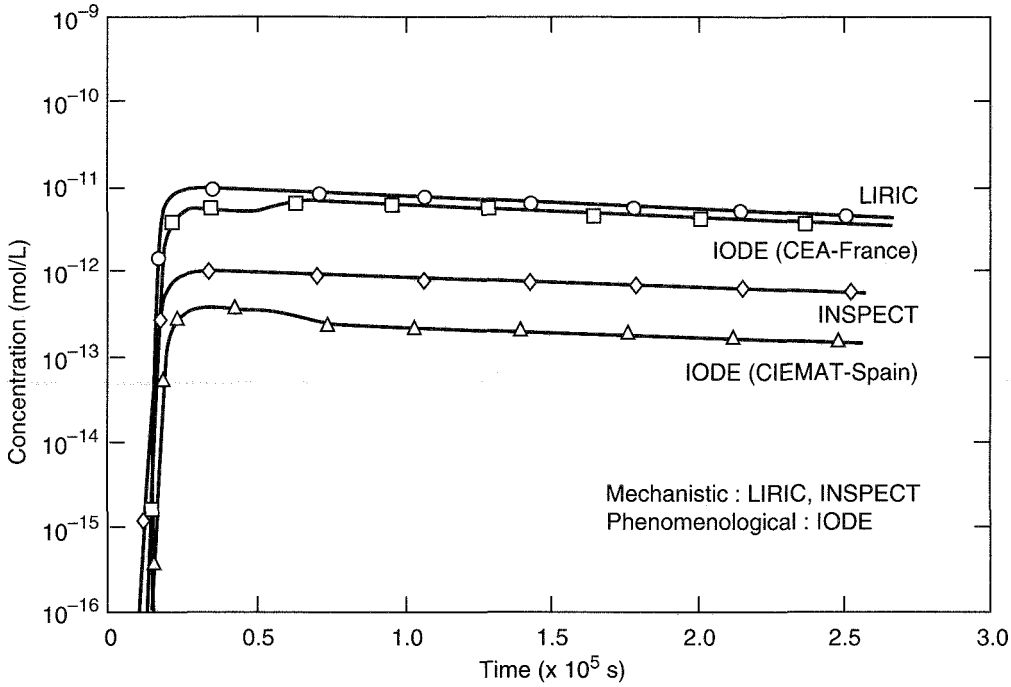

Fig. 12 Predictions for gas-phase concentrations of molecular iodine with various codes (note logarithmic scale).

- Peak fuel temperature on shroud conductivity.
- Hydrogen production rate on degradation models (one- or two-sided oxidation of cladding).
- Low-volatile FP release on model.
- Bundle outlet temperature on degradation model and shroud conductivity.
- Depth of cold trap in the upper plenum on steam flow rate.
- Tellurium transmission on chemisorption model.
- Circuit transmission on vapor condensation on wall vs. condensation on aerosol.
- Relative humidity on condenser temperature and models.
- Iodine in atmosphere on models and on iodine transmission through the circuit.

Benchmarks

Benchmark problems, in which all partners may participate (coordinated by the JRC), are set up when there seems a particular need for intercode comparisons to understand a particular physical problem or to explain wide divergence between model predictions. Some benchmarks of interest are studies of the bundle behavior with the old and new shrouds,[25] studies of circuit transmission, a study of containment thermal–hydraulics for high humidity,[26] and an extensive code comparison exercise concerning iodine chemistry in the Phebus vessel. In each case the process has been an iterative one. A simplified problem is specified, and participants make their calculations. They are urged to use their own judgment for any choices of models and unknown parameters. The results are then compared and presented in synoptic tables and diagrams. The participants meet and review the work and are offered the chance to revise their calculations. They also attempt to explain the differences in predictions. Finally, the best results from all participants are compiled in a report, and some conclusions are drawn bearing on the Phebus tests or on the modeling of the phenomena in such tests. The process is judged to be successful, and more benchmarks are planned, which will be oriented around future Phebus tests and/or the experimental results of FPT0.

SUPPORT PROGRAMS

Scope

As a support to Phebus FP, out-of-pile (separate effects) experiments are required:

- For phenomenological studies and code validation in areas not adequately covered by Phebus FP.

• As direct assistance to preparation, operation, and interpretation of the Phebus FP tests.

Examples are given in the following paragraphs.

FP Release

The HEVA program,[27] which extended from 1983 to 1989, had three main areas of interest:

• FP and structural material release rates.
• Chemical species identification.
• FP aerosol size distribution (as a function of temperature).

The experimental setup was a furnace located in a hot cell; the samples were high-burnup (36 000-MWd/t) fuel pellets with cladding and, in some experiments, control rod material. These pellets were reirradiated for 8 days in the SILOE reactor to have a realistic amount of short-lived FPs and then transferred to the HEVA cell and heated up to 2400 K in a steam or hydrogen gas flow. A large working program is still going on to perform the chemical analysis of numerous samples from the HEVA experiments and to interpret the results.

FP release measurements from BR3 fuel used in Phebus FP are planned at the Battelle Columbus Laboratory and at the Karlsruhe Trans-Uranium Institute, by means of Knudsen cells.

Vapor–Surface Interactions

In the DEVAP experiments,[28] simulated FP vapors deposit on Inconel or stainless steel tubes under different temperature gradients. In a first step, simple compounds (such as CsI and CsOH) have been used. In the current experiments, mixtures of different compounds and the influence of tin aerosols are tested.

Aerosol Studies

A rather large data set is available from earlier experiments using simulated aerosols[29] together with a limited volume of results from in-pile tests. However, specific issues remain to be addressed in support of Phebus FP and for general safety studies.

The TUBA experimental facility[30] consists of a system of steam-generator simulating tubes crossed by a steam–air gas flow; a first section allows preparation of the aerosol injection at a given temperature. In the test section, a cooling circuit creates a temperature gradient between the carrier gas and the walls of the tube; gas and wall temperatures can be controlled up to about 800 K. The test matrix includes the effect of laminar or turbulent flow, the effect of thermal gradient magnitude, and the effect of steam condensation on the walls. Current work includes new experiments under diffusiophoresis conditions (with a variable ratio of steam to noncondensable gases) and interpretation of the test measurements to include improved correlations in the ESCADRE system.

The PITEAS program[30] was initiated around 1984 to measure aerosol behavior in the containment in the presence of steam. The experimental facility is a 3-m^3 vessel with aerosol source and steam moisture control; the wall temperature is also controlled, and the pressure can be monitored up to 5 bars and the temperature up to 140 °C.

THE STORM PROJECT

The Storm project, a new facility at JRC Ispra, is especially designed for investigations into FP resuspension. The first tests are planned for 1994.

Iodine Radiochemistry

The main experimental support for these programs comes from laboratories at Cadarache and at Whiteshell.

The IODE Analytical Experiments (Cadarache) program[31] features small-scale experiments designed to evaluate separately the different mechanisms involved in the chemical transformations and physical transfers of iodine; generally, glass bottles with one or two compartments are used; these bottles can be placed in a radiation generator with an iodine–air–steam flow. Painted, bare steel or concrete plates can be inserted in the bottle.

The Radioiodine Test Facility (RTF)[32] tests at Whiteshell, Manitoba, started in 1993 as a complement to the Cadarache work in the area of iodine partitioning factor measurements under a number of Phebus FP typical conditions. They begin with small capsule tests as benchmarks against Cadarache results before using the larger RTF vessel.

FALCON[33–35]

The FALCON facility at Winfrith, United Kingdom, with its associated analytical laboratories, has been used

in support of Phebus FP since 1988. With the use of simulated FPs or trace-irradiated fuel, FALCON studies aerosol physics, FP chemistry, boric acid problems, instrumental analysis of FP deposits, and specific instrumentation problems.

Technological Tests

Several experimental components were not commercially available and required specific R&D programs:

- The foot valve and the insulating shroud of the in-pile section.
- The 1000 K valve in the primary circuit.
- High-temperature trace heaters.

Most of the development and testing, carried out through industry contracts, is finished. The shroud development for future tests is still ongoing.

Instrumentation

Most of the instruments mentioned earlier required more or less extensive adaptation to the predicted Phebus FP operating conditions. Substantial support has come from CEA/IPSN laboratories (impactors), EG&G Idaho Falls (on-line aerosol monitor), and KfK Karlsruhe (iodine speciation sampler). Several of the more conventional instruments—pressure transducers, flowmeters, and oxygen sensors—did not perform to specifications when tested under Phebus FP conditions and had to be replaced.

ORGANIZATION

Program Management

The program is managed by a Steering Committee (SC) that meets twice a year. The SC receives advice from three working groups (Fig. 13):

- An analytical group (SAWG), assisting in the test matrix definition, preparing the experiments by precalculations, and finally analyzing the results obtained.
- A technical group (TG) that assesses experimental equipment, instrumentation, and operating procedures proposed and analyzes the in-pile performance of equipment, instrumentation, and procedures.
- A restricted financial group controlling the expenditures of the two major program partners according to the contractual definitions.

Between two SC meetings, Phebus FP is managed by a program group that has these mandates:

- Define and schedule the work of the different teams working for the program.
- Prepare and distribute the required information.
- Request SC decisions for matters beyond day-to-day management.
- Prepare the SC meetings, together with the working group chairmen.

International Relations

The CEA and the Commission of the European Communities (CEC) have been major program partners since the signing of the basic contract in July 1988. Organizations from European Economic Community Member States are represented in the SC by JRC but participate directly in the work of the analytical and the technical groups.

Since 1988 several overseas partners joined the program: the U.S. Nuclear Regulatory Commission, the Nuclear Power Engineering Test Center [Ministry of International Trade and Industry (Japan)] and Japan Atomic Energy Research Institute, COG Canada, and the Korean Atomic Energy Research Institute. Their collaboration, particularly in the analytical and technical groups, is encouraged. Assistance in solving numerous technical problems and participation in precalculations and analysis of the experiments safeguard the best possible expertise transfer to the Phebus FP Program.

Proposals concerning the test matrix are accepted and discussed on the working group and SC levels. The current test matrix revision has largely been guided by discussions with all partners.

Status and Planning

After 5 years of design, manufacture, testing, and commissioning and of thorough safety clearance procedures, the first test FPT0 took place between November 1993 and January 1994. The following tests are scheduled in about annual intervals.

THE FIRST PHEBUS FP TEST

Chronology of Events

An extended testing and commissioning period, from September 1992 to October 1993, followed the construction phase. First criticality of the modified reactor was reached in February, and the first rise to full power was in

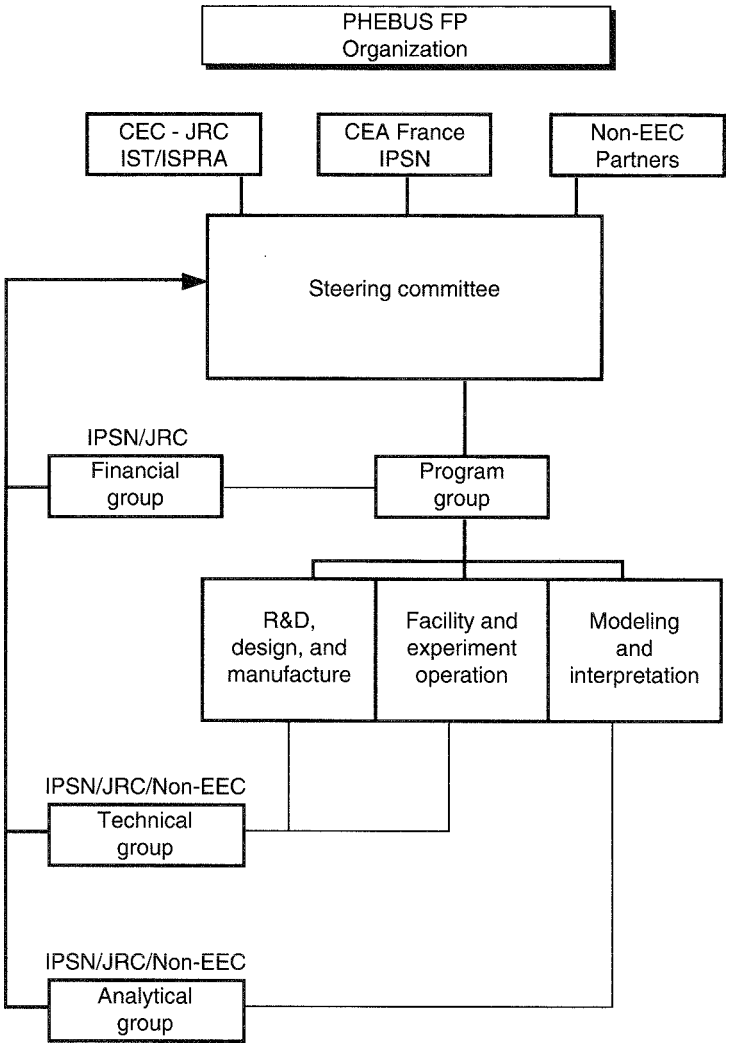

Fig. 13 Phebus FP organization chart.

August 1993. The irradiation device (test train) was loaded in October, and the preirradiation took place at 240-kW bundle power between November 21 and 30, 1993. After a 30-hour shutdown period for Xe-135 override and instrumentation checkout, the high-temperature transient was operated between 10 a.m. and 3 p.m. on Dec. 2, 1993. The subsequent containment period was terminated on December 8, with the transfer of liquid waste toward the storage tanks, followed by depressurization, inert gas filling, and cooling down of the circuits. Recovery, by remote handling, of the FP samplers took place in January and February 1994 together with first checks of the samples taken by gamma spectrometry. Detailed PTAs are scheduled from March to November, and the test train examination (PIE) is scheduled from May to December 1994.

Observations

It appeared, from the in-pile thermocouple readings, that the time–temperature profile predicted (see Fig. 7) could be followed closely. Extrapolations from prefailure thermocouple readings and shroud temperatures indicate that a maximum fuel temperature of 3100 K was reached before test termination. Simultaneous readings on reactor instrumentation and on the on-line aerosol monitor seem to confirm test fuel motion and a burst release. On-line gamma spectrometry showed that at least 50% of the noble gases was released. First inspections of the

sampling instruments confirm significant release of both fission products and other aerosols.

Preliminary Conclusions

The overall performance of the modified reactor and of the new experimental systems during the first test was remarkably trouble-free. The experimental sequence planned, as described earlier, could be reproduced without major problems. All on-line measurements indicate that the two objectives (that is, incipient fuel melting and significant FP release) have been achieved. These conclusions need to be confirmed by the forthcoming posttest analyses.

REFERENCES

1. See, e.g., Nuclear Regulatory Commission, *Reactor Safety Study, An Assessment of Accident Risks in U.S. Commercial Nuclear Power Plants*, Report WASH-1400 (NUREG-75/014), 1975; NUREG-1150; Deutsche Risikostudie Kernkraftwerke; J. Duco et al., at the Seminar on International Approach to Nuclear Reactor Safety, Blackpool, U.K., June 1988; Risico's van de splijtstofcyclus (ECN Petten, Netherlands 1993); similar studies in other countries.
2. See, e.g., A. L. Wright (Ed.), *Primary System Fission Product Release and Transport: A State-of-the-Art Report to the CSNI*, Report OECD/NEA/CSNI, July 1994; W. Schöck et al., *Nucl. Technol.*, 81 (May 1988); I. H. Dunbar et al., *Nucl. Technol.*, 82 (July 1988).
3. C. Renault and A. Mailliat, ESCADRE Mod O and Its Validation, *CSARP Meeting, Bethesda, Md., May 1993.*
4. A. V. Jones and I. M. Shepherd, ESTER, A European Severe Accident Code System, in *Proceedings of the 20th Nuclear Regulatory Commission Water Reactor Safety Information Meeting, Bethesda, Md., October 1992*, Report NUREG/CP-0126-Vol. 2 (CONF-921007-Vol. 2), 1993.
5. J. A. Gieseke et al., *Source Term Code Package: A User's Guide (Mod.1)*, Report NUREG/CR-4587 (BMI-2138), July 1986.
6. I. M. Shepherd and A. G. Markovina (Eds.), *Summary of the Dimensioning Verification Studies of the Phebus FP Experiments*, Report EUR-13906, 1992.
7. R. G. J. Ball et al., *Thermochemical Data Acquisition, Parts I and II*, Report EUR-14004, 1991, and EUR-14844, 1992.
8. A. Arnaud and A. Markovina, Objectives, Test Matrix and Representativity of the Phebus FP Experimental Programme, in *The Phebus Fission Product Project: Presentation of the Experimental Programme and Test Facility*, W. Krischer and M. C. Rubinstein (Eds.), Report EUR-1352 (CONF-9106425), pp. 144-158, 1992.
9. M. Livolant, H. Holtbecker, A. Tattegrain, and A. Meyer-Heine, The Phebus Fission Products: A Severe Accident International Research Program, *Trans. Am. Nucl. Soc.*, 65: 3.C.1-3.C.10 (1992).
10. P. von der Hardt and A. Tattegrain, The Phebus Fission Product Project, *J. Nucl. Mater.*, 188: 115-130 (1992).
11. G. Hampel and G. Poss, *Development of Advanced Instrumentation for the Phebus FP Project—Preliminary Studies*, Report EUR-12396, 1989.
12. G. Hampel, G. Poss, and H. K. Fröhlich, *General and Preliminary Thermohydraulic, Hydrogen, and Aerosol Instrumentation Plan for the Phebus FP Project*, Report EUR-12397, 1989.
13. R. Zeyen and B. Clement, Instrumentation for Integral Severe Accident Simulating Experiments, *CSNI Specialists' Meeting, Cologne, Germany, March 16–18, 1992.*
14. B. Clement et al., Integral Source Term Experiment Phebus FP, with Special Emphasis on In-Pile and Circuit Instrumentation, in *International Conference on Irradiation Technology, Saclay, France, May 20–22, 1992.*
15. R. Zeyen, J. G. Wilhelm, and M. Lucas, The Phebus FP Integral Source Term Experimental Project, with Emphasis on Iodine Selective Filtering, in *Proceedings of the 22nd DOE/NRC Air Cleaning and Treatment Conference, Denver, Colorado, August 24–27, 1992*, Report NUREG/CP-0130-Vol. 1 (CONF-920823-Vol. 1), 1993.
16. A. Tani and P. von der Hardt, *Bibliographic Study for Posttest Analysis of Samples from Fission Product Release Tests*, Report EUR-13804, 1991.
17. B. R. Bowsher and A. L. Nichols, *Review of Analytical Techniques to Determine the Chemical Forms of Vapours and Aerosols Released from Overheated Fuel*, Report EUR-12399, 1989.
18. A. Mailliat, F. Serre, A. V. Jones, and I. Shepherd, The Calculation Programme to Prepare the First Phebus FP Test, in *Proceedings of the 20th Nuclear Regulatory Commission Water Reactor Safety Information Meeting, Bethesda, Md., October 1992*, Report NUREG/CP-0126-Vol. 2 (CONF-921997-Vol. 2), 1993.
19. C. Ronchi and J. van de Laar, *The Fuel Performance Code FUTURE*, Report EUR-11387, 1988.
20. L. D. MacDonald, D. B. Duncan, B. J. Lewis, and F. C. Iglesias, *FREEDOM: A Transient Fission Product Release Model for Radioactive and Stable Species*, Report AECL-9810 (CONF-8809420), May 1989.
21. J. Rest and S. A. Zawadzki, *FASTGRASS: A Mechanistic Model for the Prediction of Xe, I, Cs, Te, Ba, and Sr Release from Nuclear Fuel Under Normal and Severe-Accident Conditions*, Report NUREG/CR-5840 (ANL-92/3), 1992.
22. J. Fermandjian et al., Exploratory Circuit Calculations for the First Test of the Phebus FP Project, in *12th Annual Meeting of the AAAR, Oak Brook, Ill., October 1993.*
23. I. Shepherd et al., Scoping Calculations for the Containment in Phebus FPT 1, in *18th Annual Meeting of the Spanish Nuclear Society, Jerez, Spain, October 1992.*
24. A. V. Jones, I. M. Shepherd, P. von der Hardt, and S. Gaillot, The Quest for Prototypical Conditions in the Phebus FP Containment, in *4th International Conference on Simulation Methods in Nuclear Engineering, Montreal, Quebec, June 2–4, 1993.*
25. I. Shepherd et al., *Phebus FPT0 Benchmark Calculations*, Report EUR-13698, 1991.
26. I. Shepherd et al., *Scoping Calculations to Examine a Strategy for the Thermal–Hydraulic Control of the Phebus FP Containment Vessel During High Humidity Transients*, Report EUR-14984, 1993.
27. G. Le Marois and R. Warlop, Source Term Experiment for Fission Product Transport Assessment: The HEVA Programme,

in *International European Nuclear Society/American Nuclear Society Meeting on Thermal Reactor Safety (NUCSAF 88), Avignon, France, October 1988*, Report CONF-88104-, 1988.
28. G. Le Marois, DEVAP: An Experimental Programme on Fission Product Deposits in the Primary Circuit, in *Third European Severe Accident Chemistry Meeting, Karlsruhe, Germany, June 1992*, C. G. Benson (Ed.), Report EUR-15056, 1993.
29. Paul-Scherrer-Institut (Ed.), *MARVIKEN-V/DEMONA/LACE Workshop, Montreux, Switzerland, June–July 1988.*
30. C. Lecomte and G. Lhiaubet, CEA Analytical Activities: HEVA, PITEAS, Mini-Containments, in *Proceedings of the Seminar Held at the Chateau Cadarache, St. Paul-Lez-durance, France, June 5–7, 1991*, W. Krischer and M. C. Rubinstein (Eds.), Report CONF-9106425 (EUR-1352-EN), 1992.
31. C. Hueber, M. Lucas, and J. Gauvain, Validation of the IODE Code, in *Third CSNI Workshop on Iodine Chemistry, Tokai-mura, Japan, September 1991*, Report JAERI-M-92-012 (CONF-9109373-), 1992.
32. W. C. H. Kupferschmidt et al., *Final Report on the ACE/RTF Experiments*, Report ACE-TR-B 3, 1992.
33. P. Fasoli-Stella and A. Markovina, CEC Support Activities: EC Shared Cost Actions and Others, *Phebus Fission Product Project: Presentation of the Experimental Programme and Test Facility Seminar*, W. Krischer and M. C. Rubinstein (Eds.), Report CONF-9106425- (EUR-1352), 1992.
34. A. M. Beard et al., *Chemistry Studies in Support of Phebus FP: Multicomponent Aerosol Behaviour*, Vols. 1 and 2, Report EUR-14005/1 and 2, 1992.
35. P. J. Bennett and B. R. Bowsher, *Falcon II Seminar, Winfrith Technology Centre, 13–14 March 1991*, Report AEA-RS-5116, May 1991.

Containment Performance Analysis of the Advanced Neutron Source Reactor at the Oak Ridge National Laboratory

By S. H. Kim, R. P. Taleyarkhan, and V. Georgevich[a]

Abstract: *This article discusses salient aspects of methodology, assumptions, and modeling of various features related to the estimation of source terms from two conservatively scoped severe-accident scenarios in the Advanced Neutron Source (ANS) reactor at the Oak Ridge National Laboratory. Various containment configurations are considered for steaming-pool-type accidents and an accident involving molten-core–concrete interaction. Several design features (such as rupture disks) are examined to study containment response during postulated severe accidents. Also, thermal–hydraulic response of the containment and radionuclide transport and retention in the containment are studied. The results are described as transient variations of source terms for each scenario, which are to be used for studying off-site radiological consequences and health effects for these postulated severe accidents. Also highlighted will be a comparison of source terms estimated by two different versions of the MELCOR code.*

[a]Engineering Technology Division, Oak Ridge National Laboratory, Oak Ridge, TN 37831-8057.

The Advanced Neutron Source (ANS), which is to be a multipurpose neutron research center, is currently in the design stage at the Oak Ridge National Laboratory (ORNL). The major purpose of the reactor will be condensed matter physics, materials science, isotope production, and fundamental physics research.[1,2] The ANS is planned to be a 330-MW research reactor that uses U_3Si_2–Al cermet fuel in a plate-type configuration. A defense-in-depth philosophy has been adopted. In response to this commitment, the ANS project management initiated severe-accident analyses and related technology development early in the design phase to aid in designing sufficiently robust containment for retention and controlled release of radionuclides in the event of an accident. It also provides a means for satisfying on- and off-site regulatory requirements, accident-related dose exposures, containment response, and source-term best-estimate analysis for Levels-2 and -3 Probabilistic Risk Analyses (PRAs) that will be produced. Moreover, it will provide the best possible understanding of the ANS under

severe-accident conditions and, consequently, provide insights for development of strategies and design philosophies for accident mitigation, management, and emergency preparedness efforts.[3]

A focused severe-accident study is being conducted to evaluate conservatively scoped source terms to support the ANS Conceptual Safety Analysis Report (CSAR) and to aid in the introduction of built-in design features for mitigation and management controls. This article describes thermal–hydraulic and radionuclide transport modeling aspects along with analyses conducted for deriving source terms in support of the ANS CSAR. An ancillary purpose is to highlight differences in predictions from two different versions of the MELCOR code. Because severe-accident technology for the ANS is in an early stage of development, relevant mechanistic tools have not been developed for evaluating core-melt-progression phenomena. Consequently conservatively scoped scenarios were postulated and analyzed. For initial source-term estimates for the high-consequence, low-probability end of the severe-accident-risk spectrum, early containment failure cases also are evaluated for scenarios analyzed and reported in this article. In addition, containment response for an intact containment configuration is analyzed. Modeling and specific analysis results for two of these scenarios are described.

DESCRIPTION OF ANS SYSTEM DESIGN

The ANS is currently in the conceptual design stage. As such, design features of the containment and reactor systems are evolving on the basis of insights from ongoing studies. Table 1 summarizes the current principal design features of the ANS from a severe-accident perspective compared with those of ORNL's High-Flux Isotope Reactor (HFIR)[4] and a commercial light-water reactor (LWR). Specifically, the ANS reactor will use about 15 kg of highly enriched (i.e., 93% ^{235}U enrichment) uranium silicide fuel in an aluminum matrix with a plate-type geometry and a total core mass of 100 kg. The power density of the ANS will be about 2 to 3 times as high as that of the HFIR and about 50 to 100 times as high as that of a large LWR. Because of such radical differences, high-power-density research reactors may give rise to significantly different severe-accident issues. Such features have led to increased attention being given to phenomenological considerations dealing with steam explosions, recriticality, core–concrete interactions, core-melt progression, and fission-product release. As opposed to power-reactor scenarios, however, overall containment loads from hydrogen generation and deflagration are relatively small for the ANS.

The reactor core is enclosed within a so-called core pressure boundary tube and enveloped in a reflector vessel. This reactor system is immersed in a large pool of water. Experiment and beam rooms for researchers are located on the first and second floors, which are connected to the third-floor high-bay region through a rupture disk. The subpile room housing the control-rod-drive mechanisms also is connected to the third floor through lines with a rupture disk in between. The approximately 95 000-m^3 primary containment of the ANS consists of a 25-mm steel shell housed in an 0.8-m-thick,

Table 1 Severe Accident Characteristics of the ANS[a] and Other Reactor Systems

Parameter	Commercial LWR[b]	HFIR[c]	ANS
Power, MW(t)	2600	85	330
Fuel	UO_2	U_3O_8–Al	U_3Si_2–Al
Enrichment, m/o	2 to 5	93	93
Fuel cladding	Zircaloy	Al	Al
Coolant–moderator	H_2O	H_2O	D_2O
Coolant outlet temperature, °C	318	69	92
Average power density, MW/L	<0.1	1.7	4.5
Clad melting temperature, °C	1850	580	580
Hydrogen generation potential, kg	850	10	12

[a]ANS, Advanced Neutron Source.
[b]LWR, light-water reactor.
[c]HFIR, High-Flux Isotope Reactor.

reinforced concrete secondary containment wall with a 1.5-m gap in between. The targeted design leak rate for the primary containment is 0.5 vol %/day (to the annulus), whereas for the secondary containment, the design leak rate is 10 vol %/day. Annulus flow is exhausted through vapor and aerosol filters. The containment isolation system is designed to initiate closure of isolation valves automatically on lines that penetrate the primary containment wall.

MODELING OF ANS CONTAINMENT THERMAL–HYDRAULICS AND RADIONUCLIDE TRANSPORT

This section describes the accident scenarios postulated in this study, modeling of the ANS containment thermal–hydraulic analysis, and a radionuclide retention and transport study of containment.

Description of Severe-Accident Scenarios

Because the ANS is in the preliminary stage of severe-accident technology development, it has not been possible to develop mechanistic tools for capturing core-melt progression phenomena. Two severe-accident scenarios are postulated for this study with a view toward evaluating conservatively estimated source terms. The first scenario (SC-1) evaluates maximum possible steaming loads and associated radionuclide transport. The second scenario (SC-2) is designed to evaluate maximal containment loads from the release of radionuclide vapors and aerosols and the associated generation of combustible gases.

SC-1: Severe-Accident Steaming Event. The evaluation of loads from steaming events during severe accidents is modeled along the lines of the Nuclear Regulatory Commission's guidance for power reactors[5] and will be called Scenario 1 (SC-1). The core debris for this case is assumed to be confined within a 100-m^3 volume of water. At the beginning of the calculations, a partitioning of fission products is assumed. All noble gases and 50% of the halogen inventory are assumed to escape from the water and move directly into the atmosphere of the primary containment high-bay area. The balance of the radionuclides would remain behind and cause the water to boil. This prescription would be characterized as conservative because no time-span allowance is made for core material degradation, relocation, fission-product release, and possible retention. Also, the prescription does not take into account iodine removal caused by scrubbing as iodine passes through the large reactor pool in the ANS; however, the prescription does represent a conservative guide for evaluating source terms in the absence of mechanistic melt progression analysis and has a long history of similar usage[5] for the power-reactor licensing process. For the maximum possible source-term estimate, failure of both primary and secondary containment is assumed to exist in the third-floor high-bay region as the initial condition (SC-1A). Therefore this failure allows a direct pathway of radionuclides from the high-bay region to the environment. Intact containment is another case of the current study to determine a containment response to maximum steaming load (SC-1B).

SC-2: Molten-Core–Concrete Interaction (MCCI) Event. After more than a decade of research into severe accidents for power reactors, it is now well known that the study of MCCIs represents an important phase of any hypothetical severe accident that results in the relocation of core debris outside the primary system and onto a concrete surface. MCCI events can release large amounts of combustible gases (CO and H_2) as well as considerable quantities of radionuclides in the form of vapors and aerosols. Because of the relatively high power density of the ANS fuel debris, it is postulated that during a core-meltdown accident core debris could ablate penetration seals or other reactor-vessel boundary structures and fall onto the concrete floor of the subpile room. Thereafter core debris would spread, and an MCCI event would begin. The scenario postulated for the current study conservatively assumes that core debris would relocate at 50 s after reactor scram onto a dry concrete floor in the subpile room. Thereafter containment capacity will be challenged from the resulting loads arising from combustible gas deflagration and released radionuclides in addition to other gases produced from MCCI. Additional conservatism is factored into the scenario through the assumption that none of the more than 100 m^3 of heavy water from the primary coolant system would relocate through the same breach (as the core debris) into the subpile room. This assumption may be nonconservative if a recriticality event or steam explosion occurs on the wet floor. As assumed for Scenario 1, both configurations of containment are analyzed for Scenario 2; viz., early containment failure (SC-2A) and the intact containment (SC-2B) case.

MELCOR Modeling of ANS Containment

The MELCOR severe-accident analysis code (Version 1.8.1) was used to develop an overall representation of ANS containment. MELCOR is a fully integrated

computer code that has been developed primarily for power-reactor severe-accident analysis;[6] however, MELCOR cannot model specific ANS core-melt progression phenomena associated with radically different fuel types, power densities, materials, and geometry. Therefore MELCOR was used at this stage primarily for capturing containment transport phenomena. The MELCOR model of ANS containment is represented by 11 control volumes, 15 flow paths, and 21 heat structures (representing walls, ceilings, shells, and miscellaneous structures) of various shapes (Fig. 1). Aerosol and vapor filtration processes also are modeled, as are several complex aerosol and vapor transport phenomena associated with various severe-accident scenarios. Fission-product inventory and its associated decay heat have been calculated with the ORIGEN2 code[7] for the ANS

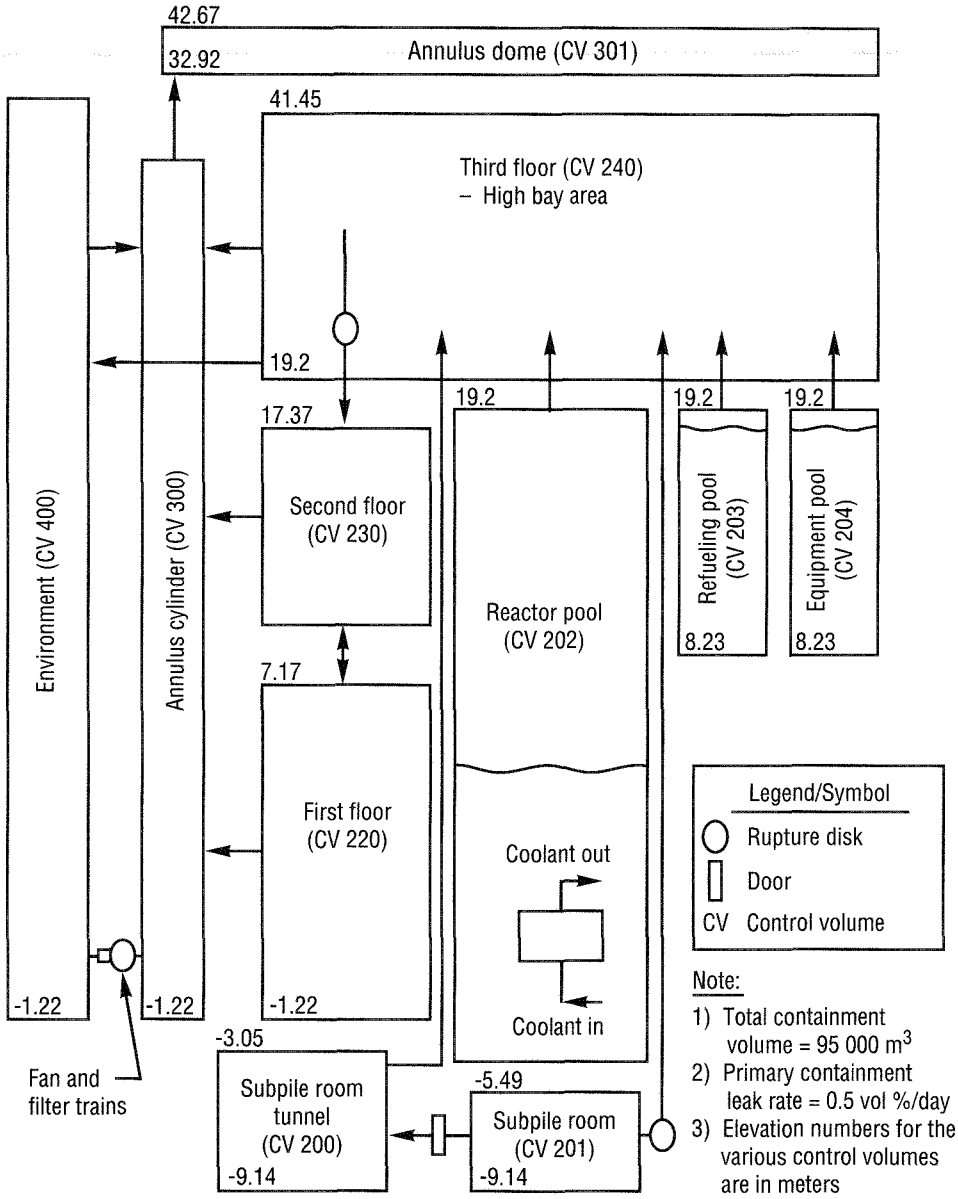

Fig. 1 MELCOR representation of Advanced Neutron Source containment.

core-averaged end of cycle assuming a 17-day core life at an operating power level of 330 MW.

For the steaming pool case (SC-1), all noble gases and 50% of iodine inventory (in vapor form) initially are sourced into the high-bay region at the start of the calculations. As the reactor pool is heated to saturation because of decay heating of the rest of the fission products, cesium and tellurium are assumed to be released at a rate proportional to the steaming rate (with a rate constant of 1). This arbitrary assumption is used to consider possible entrainment of these elements by steam leaving the pool in conjunction with the ancillary assumption that these elements are soluble in steam. Cesium is modeled as being in hydroxide form (i.e., CsOH). The remaining iodine release (i.e., the other 50% not released initially) is modeled mechanistically. The iodine that is vaporized as the pool heats up is assumed to be released from the pool instantaneously without chemical interaction with water. This treatment provides additional conservatism in conjunction with the source-term specification in DOE Report TID-14844.[5] Chemical interactions between radionuclides are neglected, whereas aerosol formation, deposition, and transport are allowed.

For Scenario 1 cases, the assumption is made that, because of some events (e.g., beam-tube rupture), the reactor pool water becomes depleted to the level of the beam tubes. This gives rise to a pool volume of 100 m^3. The use of a pool volume of 100 m^3 instead of a full volume of 600 m^3 is conservative because the depleted pool allows for faster heat-up and less scrubbing of fission products. It is further assumed that pool cooling equipment (for all pools in the high-bay area) does not function.

For the MCCI cases (SC-2), all volatile fission products were sourced into the subpile room atmosphere at the start of evaluations of radionuclide transport. Initially, iodine is specified in vapor form, whereas cesium and tellurium species are specified to be in aerosol form (molecular iodine is assumed for conservatism). The nonvolatile species contribute to the continuation of MCCI and stay in the debris; that is, they are not allowed to volatilize or form aerosols. About 50% of the total core decay power is associated with nonvolatile fission products. For this study, mass and energy of gases generated from the MCCI are obtained through an independent study[8] and then specified through user input.

For modeling cases with containment failure, upon occurrence of a severe accident, a 0.5-m-diameter opening is made available in the high-bay region primary containment shell for release of radionuclides. Such a release can occur either directly to the environment without filtration or to the annulus region housed in the secondary containment. Release to the environment is modeled to occur at ground level. This assumption will lead to a larger source term because the ground level represents maximum pressure difference (driving force for radionuclide release) between inside and outside containment because of the inclusion of density head. Such pathways simulate early containment failure from the possible effect of explosive and/or external events as well as the possibility of failure of isolation valves in ventilation ducts.

The ANS containment (normal and emergency) ventilation flow paths were not modeled or accounted for as being potential radionuclide release pathways. However, the 0.5-m-diameter containment failure path postulated for some cases is based on the assumed failure-to-isolate of one normal containment ventilation line; it also could represent an opening created by missiles or shock waves generated during energetic events such as steam explosions.

The subpile room is modeled as though functioning igniters existed. Therefore, if oxygen is available there, any combustible gases will be allowed to deflagrate (but not to detonate). The basement of the subpile room is modeled as being made of limestone and common sand concrete. The actual material choice for the basemat of the ANS has not been finalized.

Rupture disks are in place (and modeled) to allow passage of materials between the subpile room and the high-bay region and between the high-bay region and the first- and second-floor volumes (where experimentalists are located), respectively. These rupture disks open if a pressure differential of 115 kPa (2 psi) or greater is imposed. The doorway in the subpile room leading to the access tunnel will fail to open if a pressure differential of 136 kPa (5 psi) or greater is imposed to prevent excessive pressure buildup in the subpile room.

The filter trains are modeled to perform conservatively with decontamination factors of 100 for iodine and 200 for aerosols, respectively, without consideration of filter degradation.

RESULTS OF SOURCE-TERM EVALUATION

MELCOR predictions of containment thermal–hydraulic behavior, radionuclide transport, and source terms are presented in this section. Comparisons of the results obtained from new (Version 1.8.1) and old (Version 1.8.0) versions of MELCOR also are described.

Severe-Accident Steaming Event (SC-1)

Key results of interest for the intact containment configuration (SC-1B) are shown in Figs. 2 and 3. Pressurization traces for various regions of containment are shown in Fig. 2. Iodine left in the pool is released into the atmosphere quickly as the pool heats and it develops sufficient vapor pressure. The reactor pool starts steaming at 4 hours, and cesium and tellurium are released at a rate proportional to the steaming rate. As shown in Fig. 2, high-bay volume pressure rises quickly after about 4 hours when pool steaming begins (about 50% of the pool steams during 70 hours). Thereafter rupture disks between the high-bay and experiment areas of the first and second floors provide pressure relief when a pressure difference of 115 kPa (2 psi) is reached. Eventually, the entire containment volume pressure levels off at about 120 kPa because of continuing condensation of steam on various structure surfaces in the containment. A mild atmospheric temperature increase of various containment regions is predicted. Specifically, the atmospheric temperature in the high-bay area rises to 335 K (140 °F), primarily because of steam condensation and radionuclide deposition on various heat structures. During 70 hours of transient duration, about 0.05 kg of radionuclides is predicted to be deposited on the structural surfaces. Deposition seems to keep increasing linearly at about 0.67 g/hour. In the first few hours, revaporization of radionuclides deposited on the structures is predicted when surface temperatures of the structures increase and sufficient vapor pressure of a specific radionuclide element is built up. Fractional radionuclide mass released into the environment is shown in Fig. 3. The figure shows that only about 0.1% of the noble gases and less than 6×10^{-4} % of the halogen inventory is released over 70 hours. About 10^{-5} % of the cesium and tellurium inventory is released in this time frame.

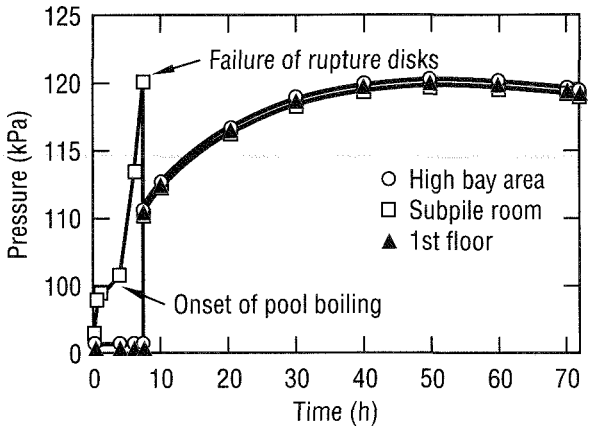

Fig. 2 Variations in containment pressures for steaming pool-type accident with intact containment.

The results of the MELCOR calculations for SC-1A (i.e., steaming pool case with early containment failure) are shown in Fig. 4. In this case, negligible pressurization results in the various control volumes. The rupture disk leading to the first- and second-floor volumes remains intact because the high-bay region pressure does not exceed 115 kPa (2 psi). Characteristics of radionuclide deposition onto heat structures are like those of the intact containment configuration (SC-1B). Because of early

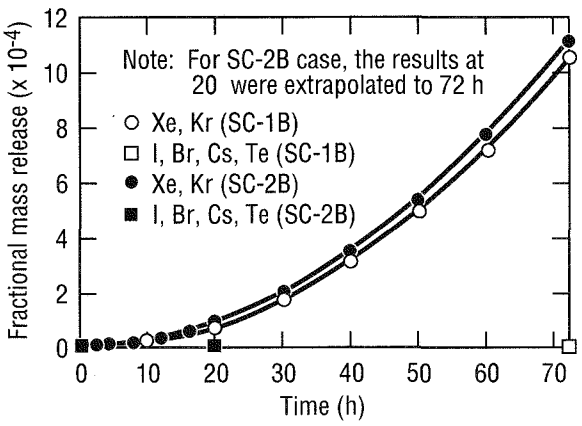

Fig. 3 Fractional radionuclide mass released into environment for intact containment cases.

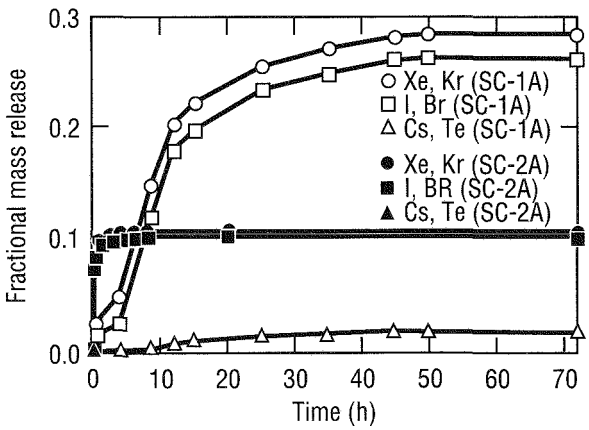

Fig. 4 Fractional radionuclide mass released into environment for early containment failure cases.

containment failure, however, the total amount deposited is about 20% lower than that for SC-1B. The principal difference in results concerns the magnitude of the source term. Figure 4 provides the transient variation of the radionuclides leaving containment (i.e., source term) and entering the environment. A sharp increase in aerosol and vapor mass release to the environment at the onset of steaming and the leveling off characteristic behavior are seen. Approximately 28% of the noble gases, about 26% of the halogen inventory, and about 1.6% of the cesium and tellurium inventories are released into the environment (Fig. 4).

Molten-Core–Concrete Interaction Event (SC-2)

Key results of interest for SC-2B are given in Figs. 3 and 5. As noted in Fig. 5, the subpile room pressure rises rapidly because of the intensity of the MCCI and causes the rupture disk to open and allow passage of radionuclides to the high-bay area. The pressure in the subpile room does not rise high enough to cause the door leading to the subpile room tunnel to fail. A direct pathway exists from the high-bay region to the subpile room tunnel, however, which causes the pressure in the subpile room tunnel to rise concomitantly. The high-bay region pressure does not exceed 115 kPa (2 psi); hence the first- and second-floor volumes are not subject to pressurization and radionuclide transport. The short spike in subpile room pressure lasting a few seconds is caused partly by hydrogen and carbon monoxide deflagration. Afterward, the oxygen content is completely depleted. Because no ventilation flow path is available in the model to bring in a fresh supply of oxygen, hydrogen combustion stops. A very high temperature (i.e., on the order of a few thousand degrees Celsius) can result in the subpile room because of heating from fission products and combustion of H_2 and CO. This high atmospheric temperature may cause penetration or equipment failure and enhance concrete degradation in the subpile room. None of these effects are considered in the current study. After the initial high-temperature rise, subpile room air begins to cool as combustion ceases, and heat-producing radionuclides are transported to the high-bay region, coupled with energy absorption in structure materials. Many radionuclides are deposited on cold structural surfaces in this case. When compared with an equivalent steaming event (SC-1B), about five times as many radionuclides are deposited on heat structures. Figure 3 provides the transient variation of the source term. As shown, about 0.009% of the noble gas inventory, about 4×10^{-5} % of the halogen inventory, about 6×10^{-5} % of the cesium-class inventory, and about 5×10^{-4} % of the tellurium-class inventory are released into the environment over 20 hours. These low source-term values essentially are caused by the leak-tight nature of the intact ANS dual-containment design and by the containment size being large enough to accommodate significant pressure and thermal sources. No radionuclides enter the first- and second-floor areas.

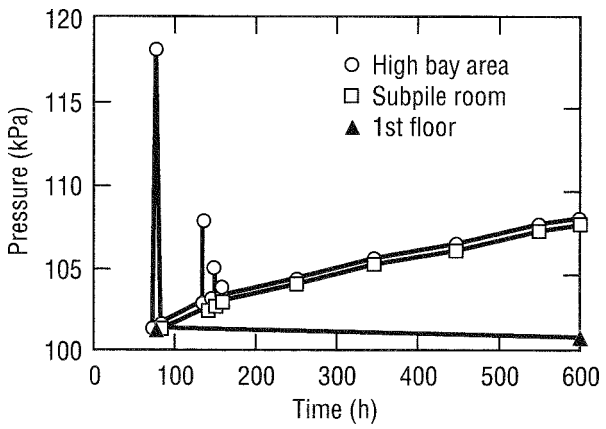

Fig. 5 Variations in containment pressures for molten-core–concrete interaction accident with intact containment.

Results for the MCCI case with early containment failure (SC-2A) are shown in Fig. 4. Variations of important parameters in the subpile room are like those of SC-2B. One major difference, which can be expected, deals with the degree of high-bay region pressurization. A very mild pressurization results in the various control volumes, as seen from the containment failure case of steaming event. The high-bay region pressure is well below 115 kPa (2 psi). Consequently the first- and second-floor areas are not available to receive radionuclide vapors and aerosols. As shown in Fig. 4, about 10.5% of the noble gases, 9.9% of the halogen inventory, and 10% of the cesium and tellurium inventories are released into the environment over 70 hours. For the MCCI case (SC-2), most radionuclide releases occur well within the first hour of the start of MCCI. This contrasts sharply with the steaming pool cases described earlier, in which significant releases to the environment occur only after the reactor pool water starts steaming.

Comparison with MELCOR 1.8.0 Results

This section describes the comparisons of the results predicted by the new version of MELCOR (Version

1.8.1-HN) with those predicted by the old version (Version 1.8.0). In general, the new version's prediction is close to that of the old version when the amount of steam involved in the radionuclide transport and retention process is limited. For the MCCI event (SC-2), results from both versions of MELCOR agree very well because the magnitude of steam content in containment in this case is not significant. In the steaming pool event (SC-1), however, substantial differences are seen, specifically in the transport and retention of radionuclides. At the end of the calculation, a noticeable difference is seen in the amount of iodine source term (26% from the new version vs. 8% from the old version for the early containment failure configuration, SC-1A). This difference in results is caused mainly by an error in the old version associated with evaporation and condensation of fission products on various surfaces; viz., aerosol and heat structures. Therefore caution is advised to users of the MELCOR Version 1.8.0 code for situations involving significant vapor condensation and evaporation phenomena.

CONCLUSIONS

To summarize, this article has provided conservatively scoped estimates for source terms arising from two different severe-accident scenarios for two different containment configurations. In addition, potentially erroneous predictions that can arise when using the MELCOR (Version 1.8.0) code have been highlighted. Caution is advised to users of this MELCOR code version for situations involving significant vapor condensation and evaporation phenomena. Extensive study is ongoing to validate and verify the models used in MELCOR elsewhere. Also, it may be necessary in the future to verify MELCOR applicability to ANS either by using other mechanistic computational tools or by performing experiments. From the standpoint of severity, Scenario 2 (MCCI event) is expected to dominate in terms of health risks (for ANS), primarily because of the rapidity with which source terms are released to the environment.

As a cautionary note, it should be realized that severe accidents coupled with early containment failure in the ANS are very unlikely events. Preliminary PRA scoping studies indicate probability levels of 2.5×10^{-8}/year for Scenario 1 with early containment failure (SC-1A) and about 10^{-8}/year for Scenario 2 with early containment failure (SC-2A). Nevertheless, these calculations provide bounding estimates of health risk arising from hypothetical severe accidents in the ANS as part of the CSAR and provide insights into the development of mitigative features. Health risks from these postulated severe accidents are described in a companion article.[9]

REFERENCES

1. C. D. West, The Advanced Neutron Source: A New Reactor-Based Facility for Neutron Research, *Trans. Am. Nucl. Soc.*, 61: 375-376 (June 1990).
2. C. D. West, *Advanced Neutron Source: Plant Design Requirements*, Report ORNL/TM-11625, Oak Ridge National Laboratory, May 1992.
3. R. P. Taleyarkhan and S. H. Kim, Severe Accident Risk Minimization Studies for the Advanced Neutron Source (ANS) Reactor Plant at the Oak Ridge National Laboratory, in *Proceedings of the Fifth Workshop on Containment Integrity for Nuclear Power Plants, Washington, D.C., May 12–14, 1992*, Report CONF-920541-1, April 1992.
4. F. T. Binford and E. N. Cramer (Eds.), *The High Flux Isotope Reactor, A Functional Description*, Report ORNL-3572 (Rev. 2), Oak Ridge National Laboratory, June 1968.
5. J. J. Dinunno, R. E. Baker, F. D. Anderson, and R. L. Waterfield, *Calculation of Distance Factors for Power and Test Reactor Sites*, DOE Report TID-14844, March 1962.
6. R. M. Summers, R. K. Cole, Jr., E. A. Boucheron, M. K. Carmel, S. E. Dingman, and J. E. Kelly, *MELCOR 1.8.0: A Computer Code for Nuclear Reactor Severe Accident Source Term and Risk Assessment Analyses*, Report NUREG/CR-5531 (SAND-90-0364), January 1991.
7. A. G. Croff, *ORIGEN2—A Revised and Updated Version of the Oak Ridge Isotope Generation and Depletion Code*, Report ORNL-5621, Oak Ridge National Laboratory, July 1980.
8. C. R. Hyman and R. P. Taleyarkhan, *Characterization of Core Debris/Concrete Interactions for the Advanced Neutron Source*, Report ORNL/TM-11761, Oak Ridge National Laboratory, February 1992.
9. R. P. Taleyarkhan, S. H. Kim, and V. Georgevich, Radiological Consequence Analyses Under Severe Accident Conditions for the Advanced Neutron Source Reactor at the Oak Ridge National Laboratory, in *Proceedings of the Probabilistic Safety Assessment International Topical Meeting, Clearwater, Florida, January 27–29, 1993*, Report CONF-930116-12, October 1992.

Assessment of Fission Product Deposits in the Reactor Coolant System: The DEVAP Program

By G. Le Marois and M. Megnin[a]

Abstract: *The aim of the DEVAP Program was to study the deposits of volatile fission products (FPs) in the coolant system of a pressurized-water reactor in case of a severe accident. The deposition rate of major FP components released, such as CsI, CsOH, and Te, can thus be determined. Deposits were made at 920 and 1070 K inside a pipe that simulates the primary circuit: a representative oxide layer on the pipe was obtained by special pretreatment. Posttest chemical speciation and thermodynamic analysis show the following:*

- *A physisorption controlled reaction occurs for CsI and CsOH deposits. A further reaction with the pipe material leads to partial decomposition of the CsI; for CsOH, this reaction is enhanced when the temperature or the surface oxidation increases.*
- *The tellurium deposits depend on nickel surface activity. The deposits thus strongly depend on the state of the oxide layer and on the alloy composition.*

In the event of a serious accident in a pressurized-water-reactor (PWR) core, the fission products (FPs) released from the fuel would be transported through parts of the primary circuit. If significant amounts could be removed in this circuit, however, the radioactive emission would be lowered in the containment and, potentially, in the environment. Existing models predict significant FP retention in the cooling system; however, they are based on analytical studies in which the thermohydraulic conditions and the state of the deposition surface may be far from accident conditions and could thus overestimate the retention level.[1–6]

To provide a realistic data base for computing FP deposition and transport in the primary circuit, the French Institute for Nuclear Protection and Safety (IPSN) launched an experimental program 3 years ago, co-funded by IPSN and the Electricité de France (EDF). This so-called DEVAP program is operated by the Fuel Behavior Studies Branch (SECC) in the Grenoble Nuclear Research Centre [Commissariat à l'Energie Atomique (CEA)-Grenoble].

The operating parameters are defined on the basis of the results of calculations of the most likely accident sequences at low pressure, and the tests focused on the behavior of the predominant chemical forms CsI, CsOH (Ref. 7), and Te of the volatile FPs, which would have the major radiological effects. The overall program includes studies of vapor deposition and condensation and aerosol transport with or without the presence of core materials. CsI, CsOH, and tellurium (Te) stimulants are vaporized and removed under steam and hydrogen inside a 304 stainless steel (304 SS), Inconel 600 or 690, straight pipe, which has the same diameter as a steam generator tube. A representative oxide layer on the pipe is built by means of special pretreatment. The experimental values of the deposition velocity obtained will be taken as an input in the SOPHIE Code, a module of the ESCADRE Code system, which evaluates FP behavior during a severe accident.[8]

Every effort is made to understand and analyze the physical and chemical phenomena occurring during these tests: thermodynamic calculations to predict vapor pressures in the pipe and activities at the surface layer, aerosol sizing measurements, and microanalysis to measure the composition of the oxide layer and the deposits.

The first results, including single simulant tests, are reported in the following sections. The program is continuing toward more realistic conditions with multiple simulant tests. In these tests a mixture of the three simulants is injected with a representative cesium to iodine and tellurium ratio. Structural material aerosols are added to take account for the interactions of the FP with the large surface area of the aerosol cloud.[9]

[a]Commissariat à l'Energie Atomique, DTP/SECC, Centre d'Etudes Nucléaires de Grenoble, 17, rue des Martyrs, 38054 Grenoble Cedex 9, France.

APPARATUS AND ANALYTICAL METHODS

Description of the Loop

Figure 1 shows a diagram of the DEVAP loop used to perform the single simulant tests. It consists of a vertical tube of 20-mm inside diameter surrounded by furnaces and insulating sleeves to provide the following:

- Vaporization of the species from a crucible (at the bottom).
- An isothermal vapor deposition zone (in the middle).
- A thermal gradient zone for vapor condensation (at the top).

The carrier gas, steam and hydrogen, is injected at a constant flow rate of about 500 K at the bottom of the tube. A peristaltic pump provides water supply. The hydrogen flow rate is monitored with a mass flowmeter.

Each species, CsI, CsOH, or Te, is placed in an alumina crucible supported by a rod that can be vertically displaced in the vaporization furnace along the tube centerline to adjust the furnace's temperature (measured by a K thermocouple). This also gives the vapor flow rate of the species: this flow rate is precalculated from the saturation pressure value and the thermohydraulic conditions and adjusted with calibration tests. For given stable temperature and carrier gas flow rates, a constant flow rate of a given species is obtained.

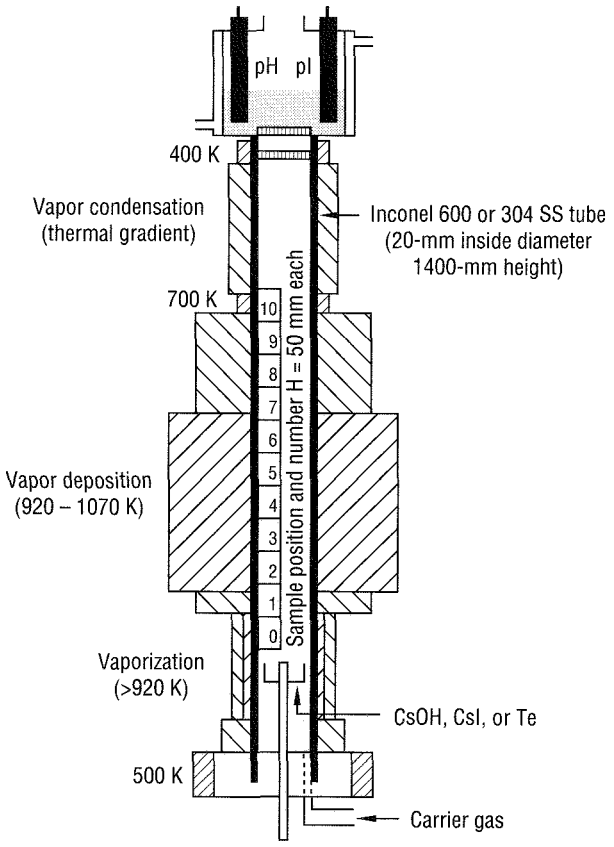

Fig. 1 DEVAP experimental device.

The top of the pipe is closed with a trap comprising, from bottom to top, a heated Inconel filter to recover the aerosols without steam condensation and a second filter acting as the bottom of a small tank filled with water to condense the steam and detect volatile water-soluble species by on-line pH and pI measurements.

Pretreatment of the Pipe

Before the test the tube is isothermally preoxidized in a pressurized-water loop for 45 days at 610 K and 18 MPa. The chemistry of the pressurized water is similar to that in the primary system of a PWR. Corrosion studies show that this treatment gives an oxide layer representative of what is expected of a reactor pipe internal surface after operating for 1 to 3 years. Inner surface analysis of sections of the tube was performed with the use of a scanning electron microscope (SEM) fitted with an energy dispersive spectroscopy (EDS) attachment to determine the elemental composition of either specific areas or individual particles.

Thermal Profile

The temperature profiles of the carrier gas (T gas) and of the tube wall (T tube) along its entire length are established by a calculation fitted to the experimental measurements by thermocouples to link the mass deposition at a given level to the related temperature. Typical profile curves are shown in Fig. 2.

Test Procedure

The procedure is similar for all tests. At the beginning the crucible is placed in the lower cold part of the vaporization furnace. When CsOH is studied, the crucible temperature is increased first under helium to about 600 K, to avoid hydration of the salt, and then under steam and hydrogen. When all temperatures in the loop are at equilibrium, the crucible is raised to its vaporization position and held at that level for a period of 0.5 to 6 hours, depending on the chosen test parameter. The crucible is then pulled down. For one test, the crucible temperature was held for 8 hours to study possible revaporization.

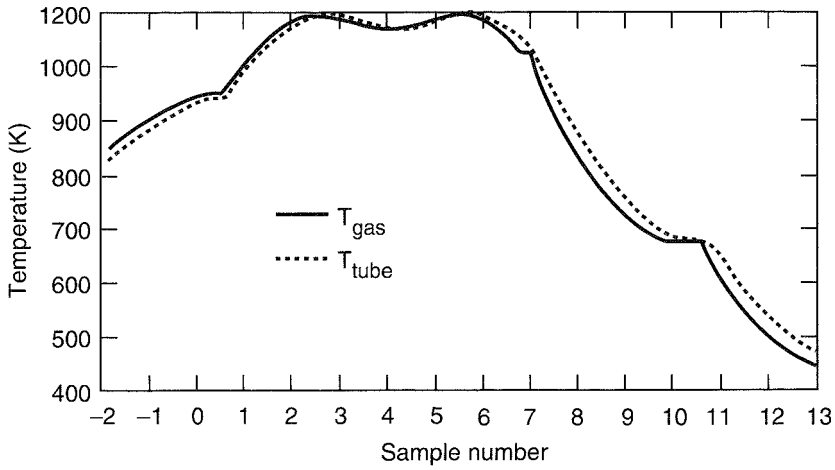

Fig. 2 DEVAP 08-14-20, calculated temperature profile.

Balance and Deposit Distribution

By weighing the crucible before and after the test, the mass of vaporized material for the species can be determined. After the test the tube is cut into 50-mm-long samples (Fig. 1). A short sample of tube, taken from the vapor deposition zone, is kept for further surface analysis. For each sample, progressive dissolution removes first water-soluble deposits and then fixed deposits (by acid etching). The solutions are titrated by ionic chromatography [iodine (I) and cesium (Cs)] and atomic absorption (Te). Dissolution of the deposit on the components of the upper trap completes the analysis, so the ratio of vaporized mass to deposited mass can be established.

Thermodynamic Calculations

Phase studies and thermochemical calculations with the use of the GEMINI code[10] were carried out to assess the chemical reactions of the species with the tube and determine the chemical activity of the different components of the oxidized alloy.

EXPERIMENTAL RESULTS

Surface Tube Examination

Some SEM/EDS examinations were performed on the inner wall of the tubes before and after the tests. During the pretreatment, the alloys are oxidized as would be expected in normal reactor operation. On 304 stainless steel, the outer layer obtained is made of small iron-rich particles, probably composed mainly of Fe_3O_4. The inner layer, an Fe–Cr–O spinel, seems to adhere to the metal. At the surface of the Inconel 600, large iron-rich grains cover the inner Cr_2O_3 oxide. After the tests at high temperature (920 and 1070 K), under steam and hydrogen, the aspect of both alloys changes (see Fig. 3). This change is probably explained by a predictable reduction of magnetite Fe_3O_4 to FeO on the 304 stainless steel surface and precipitation of Cr(Fe,O) at the Inconel surface.

CsI Study

Seven tests were carried out. The operating parameters (see Table 1) are the nature of the tube (304 stainless steel or Inconel 600), the temperature of the vapor deposition zone (920 and 1070 K), and the duration (0.5 to 6 hours).

Thermodynamic equilibrium calculations, using the GEMINI Code, took into account the following species: (Cs)g, (I)g, (CsI)c, (CsI)g, (Cs_2I_2)g, (CsOH)c, (CsOH)g, $(Cs_2O_2H_2)$g, HI, H_2, and H_2O. It was thus possible to determine the condensation temperature of the vaporized salt. A typical distribution of iodine in the loop is shown in Fig. 4.

In the vapor deposition zones, CsI deposition represents only about 0.5% of the vaporized mass. This result, also observed by several authors,[2,5,11] is attributed to the high stability of the CsI molecule in the range of temperatures between 920 and 1070 K and consequently to a weak affinity with the oxide of iron, nickel, and chromium.

In the test conditions of this study, only silicon can react with CsI at the metal–oxide interface to give cesium–silicate and HI; however, because of the low level of deposition, no evidence of this assumption was obtained. The cesium reacts preferentially with the tube,

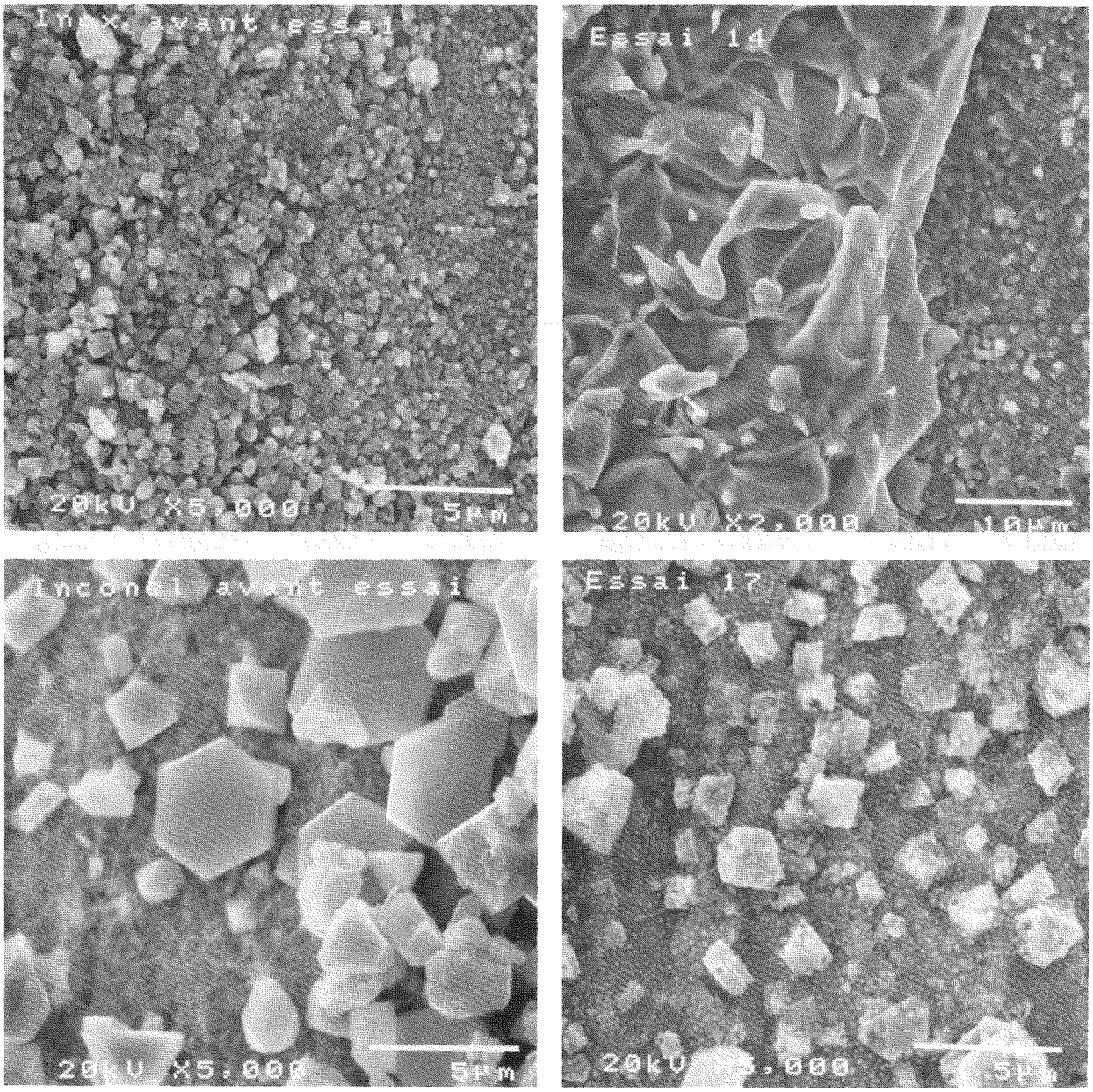

Fig. 3 Scanning electron microscope observation of preoxidized tube before and after DEVAP tests. (top) 304 stainless steel before and after DEVAP 14 test (tellurium at 800 °C for 0.5 hour) and (bottom) Inconel 600 before and after DEVAP 17 test (CsI at 650 °C for 6 hours).

Table 1 Operating Parameters

Test	Carrier gas	Tube	T deposit, K	Duration, hours	Flow rate, $kg \cdot s^{-1}$	Concentration, $kg \cdot m^{-3}$	T_{sat}, K
			CsI				
DEVAP 02	H_2O	304 SS	920	2.8	9.40×10^{-9}	3.15×10^{-4}	868
DEVAP 03	H_2O/H_2	Inc 600	920	3.16	9.74×10^{-9}	2.77×10^{-4}	863
DEVAP 06	H_2O/H_2	Inc 600	920	3	1.87×10^{-8}	5.30×10^{-4}	885
DEVAP 07	H_2O/H_2	Inc 600	920	0.5	1.83×10^{-8}	5.20×10^{-4}	884
DEVAP 08	H_2O/H_2	Inc 600	1070	3	1.19×10^{-8}	2.96×10^{-4}	865
DEVAP 17	H_2O/H_2	Inc 600	920	6	1.64×10^{-8}	4.73×10^{-4}	882
DEVAP18	H_2O/H_2	Inc 600	920	1.5	1.53×10^{-8}	4.40×10^{-4}	880
			CsOH				
DEVAP 04	H_2O/H_2	304 SS	920	3	1.81×10^{-9}	5.62×10^{-5}	600
DEVAP 11	H_2O/H_2	304 SS	920	0.5	3.00×10^{-9}	9.30×10^{-5}	620
DEVAP 12	H_2O/H_2	Inc 600	920	0.5	1.22×10^{-9}	3.78×10^{-5}	587
DEVAP 15	H_2O/H_2	304 SS	920	3	2.92×10^{-9}	9.04×10^{-5}	617
DEVAP 16	H_2O/H_2	304 SS	920	3 + 8[a]	9.54×10^{-9}	2.96×10^{-5}	580
DEVAP 20	H_2O/H_2	304 SS	1070	3	1.30×10^{-9}	3.09×10^{-5}	582
			Te				
DEVAP 05	H_2O/H_2	304 SS	920	3	8.92×10^{-9}	3.19×10^{-4}	701
DEVAP 09	H_2O/H_2	304 SS	920	0.5	1.31×10^{-8}	3.77×10^{-4}	704
DEVAP 10	Argon	304 SS	920	3	5.83×10^{-9}	1.68×10^{-4}	683
DEVAP 13	H_2O/H_2	Inc 600	920	0.5	1.31×10^{-8}	3.76×10^{-4}	704
DEVAP 14	H_2O/H_2	304 SS	1070	0.5	1.34×10^{-8}	3.32×10^{-4}	703

[a]Revaporization.

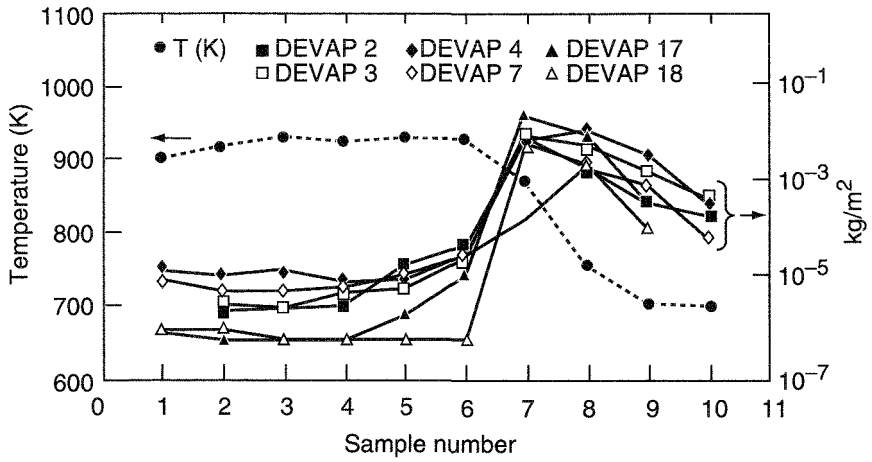

Fig. 4 Distribution profile for iodine.

as indicated by an I/Cs ratio less than 1 in the vapor deposition zone (Fig. 5). This ratio tends to decrease with time. If decomposition of CsI occurs by reaction with silicon at the metal–oxide interface, since diffusion of the CsI molecule is not possible because of its size, the gradual change in the oxide layer structure during the test could help the CsI transfer and explain the increase in molecule decomposition with time. In the upper part of the tube, the high level of CsI deposition is probably due to vapor condensation of the salt because it occurs when

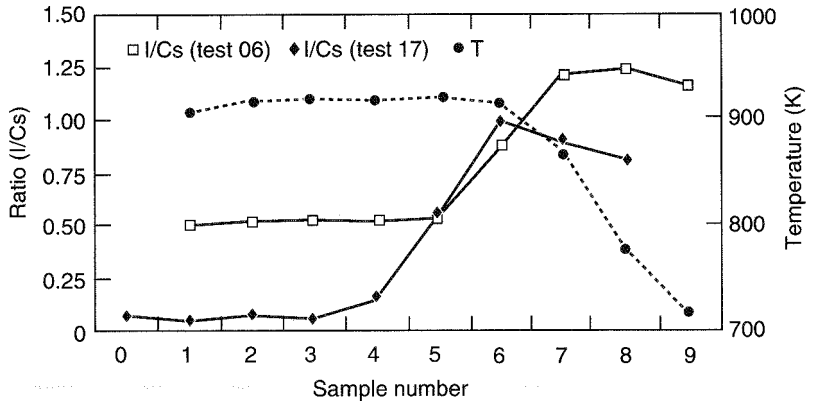

Fig. 5 Iodine/cesium ratio profile.

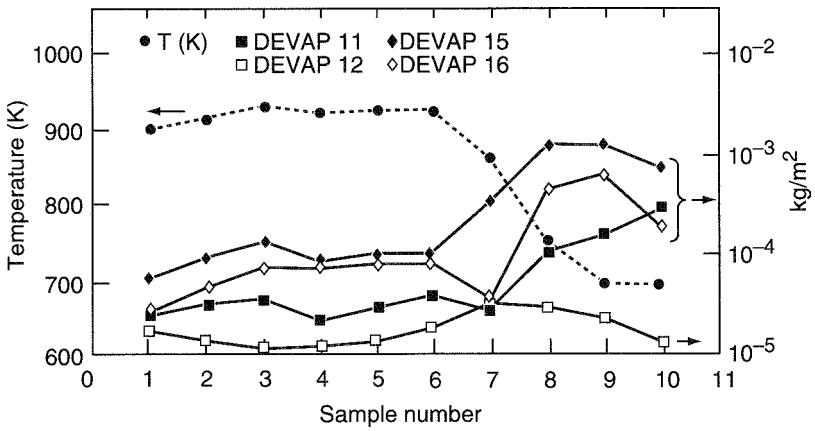

Fig. 6 Distribution profile for CsOH.

the temperature is lower than T_{sat} (882 K in the DEVAP 17 conditions).

CsOH Study

Six tests were carried out with the use of the same operating parameters as those for CsI (Table 1). So that the change in deposition in postaccident conditions could be studied, test 16, after 3 hours of CsOH vaporization, was extended for 8 hours without vaporization, whereas the other parameters (carrier gas flow rate and tube temperature) were kept the same. More than 10% of the CsOH vaporized mass is deposited as vapors in the isothermic zone. Figure 6 shows that the cesium distribution is more regular than that obtained during the previous CsI tests.

The nature of the tube, the time (0.5 to 3 hours), and the temperature (920 and 1070 K) of the deposition zone have negligible effects on the total deposition velocity (about 3×10^{-4} m · s^{-1}). This result, significantly different from other studies,[3,5,6] is probably caused by the preoxidation of the tube, which lowered its chemical reactivity with the CsOH molecule, and the CsOH vapor deposition is probably governed by physical mechanisms. Progressive dissolution of the deposit gives a finer analysis. It shows that cesium is present in both water-soluble and water-insoluble (or fixed) forms.

An Arrhenius plot of the deposition velocity as a function of temperature (see the section on Numerical Analysis and Fig. 7) highlighted two different mechanisms for these two forms:

- The proportion of water-soluble form increases when the temperature decreases. This indicates a highly probable physisorption phenomenon. Greater water-soluble

deposits are found, probably because of the more ionic nature of the CsOH molecule compared with that of CsI.

• The rate of fixed cesium increases with temperature. Diffusion of cesium through the oxide layer is thermally activated. It can then react with the silicium. Comparison with the CsI deposit found in the previous tests shows that the fraction of dissociated CsI according to

$$CsI + H_2O = CsOH + HI \quad (1)$$

is equivalent to the ratio of their deposition velocity v(CsI) / v(CsOH). This seems to indicate that the CsOH content controls the cesium deposition.

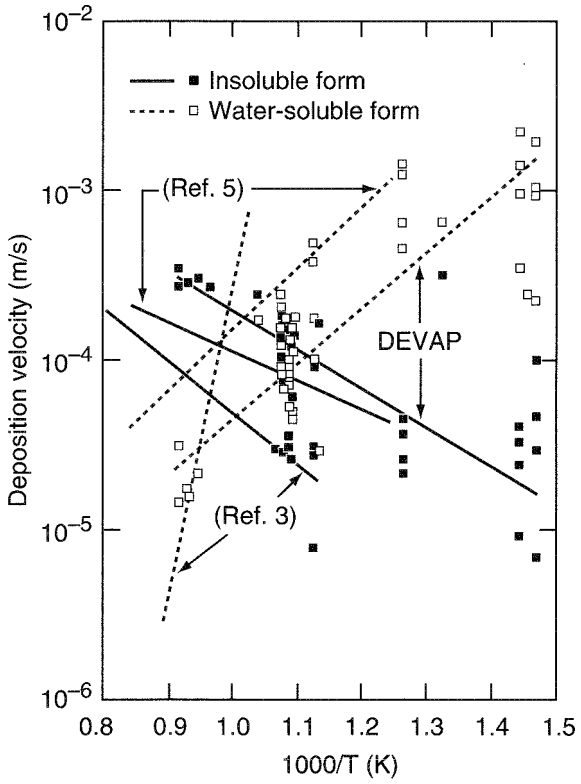

Fig. 7 An Arrhenius plot of velocity for the deposition of CsOH vapor.

Cesium tends to be more fixed when the temperature plateau duration increases, even when the CsOH vaporization is stopped (DEVAP 16). This seems to indicate that the cesium adsorbed at the surface diffuses slowly through the oxide layer instead of being vaporized.

Previous experiments carried out by Elrick et al.[3] give slightly lower fixed deposition: the author indicates that oxidation of the tube increases the silicon content at the metal–oxide interface and consequently the rate of cesium deposition. In the present work silicon segregation during preoxidation probably becomes greater compared with the test sequence and may explain this result.

Tellurium Study

Five tests were performed (Table 1). Condensation temperature calculations take into account (Te)c, (Te)g, (Te_2)g, (H_2Te)g, (TeOH)g , H_2, and H_2O. In the present tests the main gaseous species is thought to be Te_2.

The level and distribution of tellurium deposits are comparable with those of CsOH (Fig. 8). Calculated velocities indicate that tellurium vapor deposition depends on both the nature of the alloy and the temperature. Deposits on Inconel 600 are higher than on 304 stainless

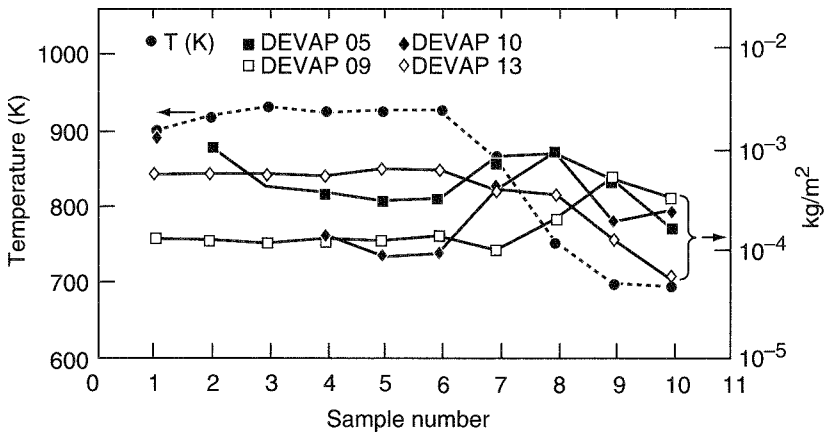

Fig. 8 Distribution profile for tellurium.

steel at 920 K. At 1070 K, no tellurium deposition was observed on stainless steel. Furthermore, tellurium is detected by SEM/EDS examination of the inner surface of the steel tubes after a test performed at 920 K. At 1070 K, the observed lack of tellurium may be a consequence of its lower reactivity with the tube: when the tube is highly oxidized, only a reaction between tellurium and nickel is foreseen according to the equilibrium:

$$0.55 \cdot Te_2 + Ni = Ni\,Te_{1.1} \qquad (2)$$

The stability of this compound depends on the partial pressure of vapor of tellurium, which can be deduced from the following:

$$0.55 \cdot \ln P_{Te_2} = \frac{\Delta G}{RT} - \ln \frac{a_{Ni}}{a_{NiTe_{1.1}}} \qquad (3)$$

where ΔG is free enthalpy of the reaction[4] and a is activity.

Data for nickel activity (a_{Ni}) were estimated from a GEMINI calculation for the two alloys, as given in the following table:

	a_{Ni}	
	920 K	**1070 K**
304 SS	0.0632	0.0563
Inconel 600	0.6094	0.5774

When a high segregation of the Ni $Te_{1.1}$ compound (a = 1) was assumed, the partial pressure of Te_2 was calculated from Eq. 3 (Fig. 9). The upper stability limit of the compound for DEVAP tests 09 and 14, performed using 304 stainless steel at 920 K and 1070 K, respectively, was deduced: the theoretical limit (≅ 990 K) is intermediate between the two temperatures. This could explain why no deposit was found at 1070 K and leads to the possibility of considering that the tellurium deposition limit depends on its partial pressure in the carrier gas. Higher activity of nickel at the surface of the Inconel 600 could also explain the greater affinity of the tellurium for this alloy. Because the reacting nickel is mainly located at the metal–oxide interface, the tellurium reaction is limited by its diffusion through the oxide layer.

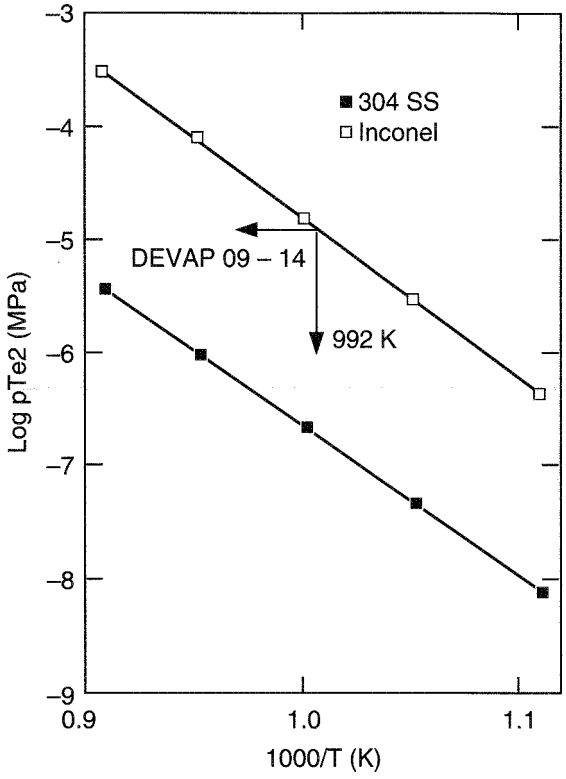

Fig. 9 Partial pressure of Te_2 in equilibrium with Ni $Te_{1.1}$ at the surface of preoxidized 304 stainless steel and Inconel 600.

pH Values

Under CsI conditions, the pH decreases slightly to about 5. When CsOH is vaporized, it increases rapidly to about 9 to 10 and remains constant. In both cases it seems to have been buffered by the metallic hydroxides released from the tube.

NUMERICAL ANALYSIS

The deposition velocity, v, is a first-order rate constant defined as the ratio of the rate of deposition of the species (dM_d/dt) to the concentration C in the gas phase and to the surface area S:

$$v = \frac{1}{C} \cdot \frac{d^2Md}{dS \cdot dt} \qquad (4)$$

This is the form used in the codes (TRAPF and SOPHIE) to model the deposition. Calculation of the ith piece and of a given species is made using the following equation:

$$v_i = \frac{Md_i \cdot D_g}{S_i \left(M_v - \sum_{j=1}^{i-1} Md_j - Md_i / 2 \right)} \quad (5)$$

where D_g is the carrier gas flow rate ($m^3 \cdot s^{-1}$), M_v is the vaporized mass of the species (kg), and v($m \cdot s^{-1}$) is either the vapor deposition or the vapor condensation. Fitted data and recommended values for the SOPHIE code are given here.

CsI

The velocity ranges between 2 and 10×10^{-6} $m \cdot s^{-1}$. Because these values are very low, it is recommended that 0 be put in the code.

CsOH

The deposition was correlated with Arrhenius-type expressions for the two different forms:

$$v\left(m \cdot s^{-1}\right) = \begin{cases} 2.14 \times 10^{-8} \exp\left(+7586/T\right) & \text{for the water-soluble form} \\ 3.73 \times 10^{-2} \exp\left(-5245/T\right) & \text{for the fixed form} \end{cases}$$

In the temperature range studied, this gives for the total CsOH deposit a velocity of around 3×10^{-4} $m \cdot s^{-1}$, which is the recommended value for the code. When these data are compared with data from previous experiments (Fig. 7), there are some slight differences: the current studies show higher velocities for the water-insoluble fraction and lower velocities for the water-soluble component. These results are explained by the different chemical activities of the tube.

Tellurium

The nature of the surface and the tellurium pressure must be taken into account. The model proposed to be introduced in the code depends on both parameters.

On 304 stainless steel:

$$v = 10^{-4} \text{ m} \cdot \text{s}^{-1} \text{ for } T_K < \frac{14167}{9.341 - \log\ p\text{Te}_2\ (\text{MPa})}$$

On Inconel 600:

$$v = 10^{-3} \text{ m} \cdot \text{s}^{-1} \text{ for } T_K < \frac{13379}{6.740 - \log\ p\text{Te}_2\ (\text{MPa})}$$

Above those temperatures, $v = 0$. Previous studies using nonoxidized alloy or alloys preoxidized at high temperature (giving probably a more porous oxide layer) show higher deposition velocities (10^{-2} to 10^{-3} m/s),[4,11] probably because of higher metallic activity at the surface.

SUMMARY AND CONCLUSIONS

From the DEVAP tests concerning the deposits on 304 stainless steel and Inconel 600, CsOH, CsI, and Te vapor deposition velocities under PWR accident conditions can be indicated in the temperature range 900 to 1100 K. A pipe, with the geometry of a steam generator tube and a representative oxide layer, was used for the test. The major observations and analyses from these tests are as follows:

1. The CsI vapor deposit is very weak. At the surface, decomposition of the molecule is observed, enhanced by the temperature level and the duration.

2. CsOH deposits are in two forms: one readily dissolves in water; the second is a water-insoluble (fixed) deposit. Physisorption of the salt at the tube surface, followed by diffusion through the oxide layer and reaction with the silicon at the metal–oxide interface, could explain this result. As a consequence, the amount of chemically reacted cesium increases with time and temperature when the adsorbed part decreases but remains predominant at low temperature.

3. The smaller amount of tellurium deposition than that of previous studies is probably the result of preoxidation of the tubes in conditions of an operating reactor. In addition, the present assessments of tellurium deposition are generally overestimated. The extent of the reaction appears to be related to the nickel activity at the surface and to the tellurium partial pressure in the carrier gas because the most likely compound formed is $Ni\ Te_{1.1}$.

In the most complex environment of a reactor under accident conditions, reactions among these three elements and others can occur and modify their deposition. For more realistic tests, the plan is to continue to progressively vaporize these species together and then in the presence of core materials, vapors, or aerosols (Sn, Ag–In–Cd control rod elements). This approach is also expected to provide a better understanding of fission-product deposition and transport in the primary circuit.

REFERENCES

1. D. J. Wren, *Kinetics of Iodine and Cesium Reactions in the Candu Reactor Primary Heat Transport System Under Accident Conditions,* Report AECL-T181, 1983.
2. R. A. Sallach, R. M. Elrick, S. C. Douglas, and A. L. Ouellette, *Reactions Between Some Cesium–Iodine Compounds and the Reactor Materials 304 Stainless Steel, Inconel 600, and Silver, Volume II. Cesium Iodine Reactions,* NRC Report NUREG/CR-3197/2 of 3 (SAND 83-0395), U.S. Nuclear Regulatory Commission, August 1986.
3. R. M. Elrick, R. A. Sallach, A. L. Ouellette, and S. C. Douglas, *Reaction Between Some Cesium–Iodine Compounds and the Reactor Materials 304 Stainless Steel, Inconel 600 and Silver, Volume I. Cesium Hydroxide Reactions,* Report NUREG/CR-3197/1 of 3 (SAND 83-0395), U.S. Nuclear Regulatory Commission, June 1984.
4. R. A. Sallach, C. J. Greenholt, and A. R. Taig, *Chemical Interactions of Tellurium Vapors with Reactor Materials,* Report NUREG/CR-2921 (SAND 82-1145), U.S. Nuclear Regulatory Commission, March 1984.
5. B. R. Bowsher, S. Dickinson, and A. L. Nichols, *High Temperature Studies of Simulant Fission Products. Part I: Vapor Deposition and Interaction of Caesium Iodide, Caesium Hydroxide and Tellurium with Stainless Steel,* AEEW-R 1697 (July 1983). *Part III: Temperature Dependent Interaction of Caesium Hydroxide Vapor with 304 Stainless Steel,* Report AEEW-R 1863, April 1990.
6. D. A. Powers and R. M. Elrick, Interaction of Radionuclide Vapors with Surfaces During Transport Through the Reactor Coolant System, in *Workshop on Chemical Processes and Related Products in Severe Reactor Accidents, National Research Council, Captiva, Fla., December 10, 1987,* p. 3.
7. J. L. Collins et al., Fission Product Iodine and Cesium Release Behavior Under Light Water Reactor Accident Conditions, *Nucl. Technol.,* 81:78-94 (April 1988).
8. J. Dufresne et al., Presentation of the ESCADRE System, Together with a Practical Application, in *International Symposium on Severe Accidents in Nuclear Power Plants, Sorrento, Italy, 21–25 March, 1988.*
9. R. D. Spence and A. L. Wright, The Importance of Fission Product/Aerosol Interactions in Reactor Accident Calculations, *Nucl. Technol.,* 77: 150-160 (May 1987).
10. B. Cheynet et al., GEMINI: Gibbs Energy Minimizer Codes for Complex Equilibria Determination, *CALPHAD XXI,* 16(4): 339 (1992).
11. I. Johnson, M. K. Farahat, J. L. Settle, J. D. Arntzen, and C. E. Johnson, *Downstream Behavior of Volatile Iodine, Cesium and Tellurium Fission Products,* Report NP-6182 (Project 2136-1, Final Report), Electric Power Research Institute, January 1989.

ERRATUM

On page 55 of Issue 35(1) of *Nuclear Safety,* the acknowledgments statement attached to the paper, "A Review of the Available Information on the Triggering Stage of a Steam Explosion," by D. F. Fletcher, was inadvertently printed incompletely. The section should read:

> "This work was partially funded by Nuclear Electric plc. The author would like to thank Nigel Buttery and Brian Turland for helpful comments on a draft and the Australian Nuclear Science and Technology Organisation (ANSTO) for the use of its library."

Control and Instrumentation

Edited by R. C. Kryter and C. R. Brittain

Effects of Normal Aging on Calibration and Response Time of Nuclear Plant Resistance Temperature Detectors and Pressure Sensors

H. M. Hashemian[a]

Abstract: *Resistance temperature detectors (RTDs) and pressure, level, and flow transmitters provide a majority of the vital signals for the control and safety of nuclear power plants. Therefore it is crucial to ensure that the performance of these sensors is maintained at an acceptable level while a plant is operating. Because aging can potentially cause performance degradation in RTDs and pressure transmitters, the U.S. Nuclear Regulatory Commission has sponsored several research projects to study the aging characteristics of these sensors and to see that the nuclear industry follows adequate test methods and test frequencies to ensure safety. The details of these projects are summarized in this article.*

This article presents the key results of four experimental research projects conducted for the U.S. Nuclear Regulatory Commission (NRC) on the aging of safety system resistance temperature detectors (RTDs) and pressure transmitters in nuclear power plants. Each project was conducted in two phases. A Phase I feasibility study was followed by a comprehensive research and development (R&D) effort in Phase II. The results of these projects have been published in the following NRC reports:[1–4]

1. NUREG/CR-4928, *Degradation of Nuclear Plant Temperature Sensors,* June 1987.
2. NUREG/CR-5560, *Aging of Nuclear Plant Resistance Temperature Detectors,* June 1990.
3. NUREG/CR-5383, *Effect of Aging on Response Time of Nuclear Plant Pressure Sensors,* June 1989.
4. NUREG/CR-5851, *Long Term Performance and Aging Characteristics of Nuclear Plant Pressure Transmitters,* March 1993.

The overall purpose of these projects has been to determine if the current nuclear industry practice of response time testing and calibration performed once every fuel cycle (typically 18 to 24 months) is adequate for the management of aging of the safety-related RTDs and pressure transmitters. In addition, the response time and calibration test methods for RTDs and pressure transmitters were evaluated and validated as necessary.

The projects summarized in this article were performed under a special U.S. Government program that promotes the commercialization of federally funded R&D efforts. As such, commercial testing services and integrated equipment and procedures were developed during the course of these projects to provide the nuclear industry with a reliable means of testing for any aging degradation that may occur in the RTDs or pressure transmitters.

AGING CHARACTERISTICS OF RTDs

Definition of Performance

The performance of an RTD is characterized by its accuracy and response time. Accuracy is a measure of

[a]Analysis and Measurement Services Corporation, AMS 9111 Cross Park Drive, Knoxville, TN 37923.

how well the RTD may indicate a static temperature, and response time defines how quickly the RTD may detect a temperature change. The accuracy and response time of RTDs are generally independent.

The deterioration of accuracy is called calibration drift or calibration shift, and the deterioration of response time is called response time degradation. Accuracy can be restored by recalibration if the RTD is stable, but response time is an intrinsic characteristic that cannot be altered once the RTD is manufactured. In the case of thermowell-mounted RTDs, however, response time degradation caused by movements of the RTD in its thermowell can sometimes be reversed.

Definition of Aging

The term *aging* used in this article refers to decalibration or response time degradation of RTDs with time in normal environments and under normal operating conditions in the primary coolant system of pressurized-water reactors (PWRs). Table 1 summarizes these conditions.

Table 1 Normal Aging Conditions for Primary Coolant RTDs in PWRs

Temperature range	300 to 320 °C
Temperature cycling conditions	Shutdowns, start-ups, plant trips
Temperature fluctuations	±0.5 °C
Containment temperature range	50 to 60 °C
Storage temperature	Ambient temperature (approx. 20 °C)
Containment humidity range	10 to 90%
Vibration sources	Flow-induced vibration of nearby machinery
Sources of mechanical shock	Shock in shipping, handling, installation, and plant trips

The definition of aging mentioned previously is based on the NRC's definition of aging, which is "the cumulative degradation that occurs with the passage of time in a component, system, or structure which can, if unchecked, lead to loss of function and impairment of safety."[5]

Because the performance of RTDs is periodically tested, the degradation is not allowed to accumulate through recalibration or replacement of the RTD, cleaning of the thermowell, or readjustment of the RTD in the thermowell. Therefore the word *cumulative* was deleted in our definition. Furthermore, we concentrated on the aging that occurs in an 18-month period, the length of a typical PWR fuel cycle, and the period of time between periodic response time and cross-calibration tests currently performed in nuclear power plants.

Effects of Aging on Performance

Normal aging of RTDs occurs from long-term exposure to any combination of heat, humidity, vibration, temperature cycling, and mechanical shock. Nuclear radiation can also affect RTD performance, but this was not studied to limit the project scope and concentrate on aging effects that are believed to have major impacts. Since primary coolant RTDs are remote from the reactor core, they are normally unaffected by nuclear radiation, except for gamma, which may cause degradation in the insulation and other RTD materials.

Effects of Aging on Calibration

A significant calibration shift should not occur in an RTD so long as the sensing element is not stressed or contaminated after calibration and the insulation material is kept in place and dry. Any new stress, contamination, or metallurgical changes in the sensing element or moisture in the insulation material can cause a calibration shift.

Stress results from any combination of heat, vibration, temperature cycling, and mechanical shock. The effect of temperature is the most important because the RTD materials have different thermal expansion coefficients, which cause the element to experience stress whenever the temperature changes. The resistance of the sensing element increases with tension stresses and decreases with compression stresses. For small temperature variations, the stress reverses itself, but for large ones, the effect is not reversible except by annealing. Chemical contamination and oxidation of the sensing element result from long-term exposure to high temperatures. To avoid oxidation, RTDs may be built with a reducing atmosphere in the sheath. However, this leads to contamination because of migration of metal ions from the sheath to the sensing element at temperatures above 500 °C.

The insulation resistance of an RTD decreases as moisture enters the sheath. The electrical resistance of an RTD is a parallel combination of two resistances: the sensing element and the insulation resistance (Fig. 1). The insulation resistance is normally high compared with that of the sensing element and has a negligible effect on resistance measurement. However, with moisture the insulation resistance decreases and causes the RTD to

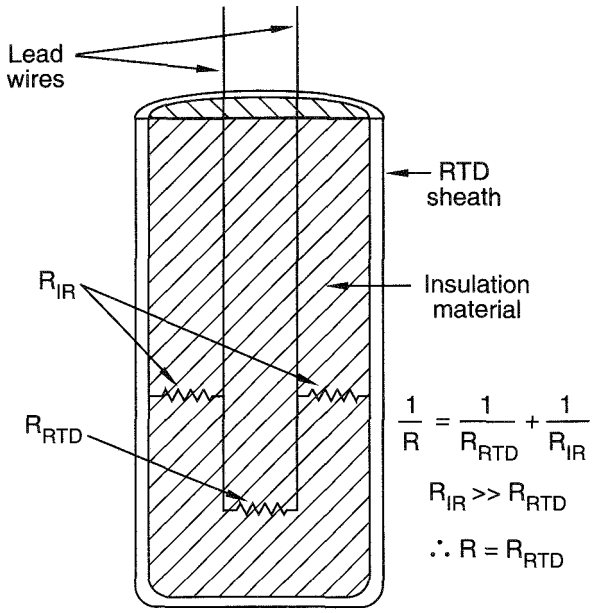

Fig. 1 Electrical resistances of an RTD.

indicate a lower temperature than normal. Moisture can also cause high-frequency noise at the output of the RTD.

At high temperatures moisture in the RTD is not normally a major concern because water vapor is likely to diffuse out of the RTD. However, because the insulation resistance significantly decreases at high temperatures, any remaining moisture in the RTD may have a significant impact on the insulation resistance value.

Effects of Aging on Response Time

The RTD/thermowell response time usually depends on such parameters as the average density, specific heat, geometry, film heat-transfer coefficient, and the thermal conductivities of the materials inside the assembly. Over time, such aging effects as high temperature, vibration, and thermal cycling will cause these parameters to change and thereby influence the heat-transfer characteristics; for example, high temperature, thermal cycling, and vibration of the insulation material can cause embrittlement and formation of cracks, which will affect the RTD thermal conductivities. The heat-transfer conditions at the thermowell surface will change with time because of crud deposit and corrosion. If moisture enters the RTD, the response time may decrease at the cost of a calibration shift. Although improvement in response time with age is possible, an RTD whose response time continues to decrease with age could be suffering from degradation of insulation resistance.

A major cause of response time degradation in nuclear plant RTDs is changes that can occur in the RTD/thermowell interface in thermowell-mounted RTDs. Experience shows that air gaps in the RTD/thermowell interface play a major role in controlling the overall response time of the RTD (Fig. 2). Changes as small as a few hundredths of a millimeter in the size of the air gap caused by vibration, shock, and other mechanical effects during plant operation, installation, handling, or dimensional tolerances will significantly change the response time. If the RTD is spring-loaded into the thermowell, mechanical effects may change the insertion length or the contact pressure, increase the size of the air gap in the thermowell, and result in a response time increase.

Aging Test Results

The first step in performing the RTD aging project was to set up a laboratory with calibration and aging equipment and to obtain nuclear-grade RTDs. The project was started with 51 nuclear-grade and 17 commercial-grade RTDs. The commercial-grade RTDs were included for comparison purposes. Of the 51 nuclear-grade RTDs, 21 were dual element, which provided a total of 72 independent RTD elements. These RTDs were used in one or more of the five aging categories: thermal aging, vibration aging, humidity aging, thermal cycling, and

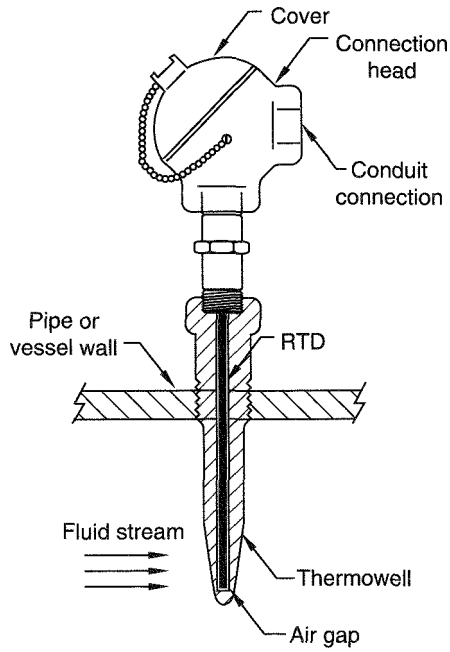

Fig. 2 A typical RTD in thermowell installation.

high-temperature testing. The project focused on the effects of aging on RTD calibration more so than RTD response time. As such, the results presented here concentrate on the effects of aging on calibration. When the conclusions of the RTD aging project are presented, however, the response time issue is included.

Next, a computer-based automatic calibration and monitoring system and procedure were developed. The RTDs were calibrated and placed in two furnaces at approximately 320 °C, the primary coolant temperature in most PWRs. The RTDs were monitored in the furnaces with a computer scanning system, which measured and stored their loop resistance, insulation resistance, open circuit voltage, and lead wire resistance. These measurements helped identify and characterize the failures when they occurred. Once every 1 or 2 months, the RTDs were removed from the furnaces and calibrated to quantify any drift. The thermal aging process was continued for 18 months, which is equivalent to a typical PWR fuel cycle. Of 30 RTD elements tested for thermal aging, 2 failed early in the program, 6 showed drift in the range of 0.6 to 3.0 °C, but the remaining 22 drifted less than 0.2 °C over the entire thermal aging period. The average positive and negative drifts of the unfailed RTDs as a function of calibration interval are in Fig. 3. Each calibration interval corresponds to 1 to 2 months. The results show that after an apparent burn-in period, which lasted until the fifth calibration or approximately 9 months into the aging process, the RTDs stabilized in a drift band of ±0.2 °C at about 320 °C. The accuracy of this drift band and other drift results presented in this article is about ±10%.

Note that the results in Fig. 3 and the remaining sections of this article are presented in terms of an average drift band rather than a drift rate because the calibration changes as a function of time were random and not systematic and we could not therefore arrive at a drift rate.

The RTDs were then stored at room temperature, pressure, and humidity and periodically tested for shelf-life drift. The results showed that the RTDs are not immune to degradation during storage (Ref. 2, Sec. 14.2). This problem can be resolved if the RTDs are recalibrated shortly before they are installed in the plant.

The aging of the RTDs was continued to identify the effects of vibration, humidity, mechanical shock, high temperature, and thermal cycling. These effects could not be combined and were performed individually, one group of RTDs at a time. These tests resulted in three more failures but did not increase the average drift of the RTDs beyond that of thermal aging. The results are summarized in Fig. 4 along with the duration of each test. Although the duration of the tests other than thermal aging was short, a thorough analysis of the data indicated that the drifts would probably plateau at the average values shown in Fig. 4. Furthermore, the aging effects were determined to be interactive rather than accumulative, and if the aging effects had been combined in a single test, the results would not have exceeded the drift bands shown in Fig. 4.

In addition, a number of RTDs removed from operating nuclear power plants after 2 to 5 years of service were tested to determine the drift of naturally aged RTDs. The results are shown in Fig. 5. The drift results are mostly within ±0.2 °C, which is consistent with the laboratory

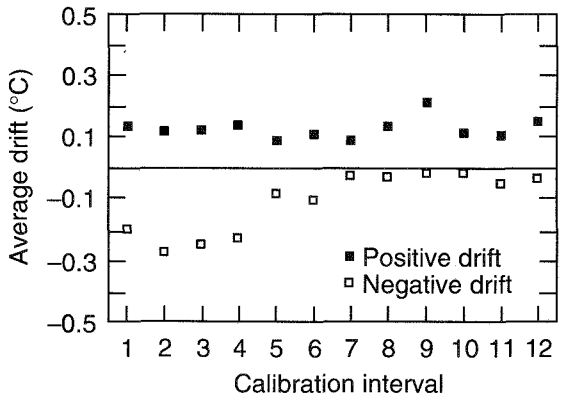

Fig. 3 Average drift of the test RTDs as a function of time in the aging furnace.

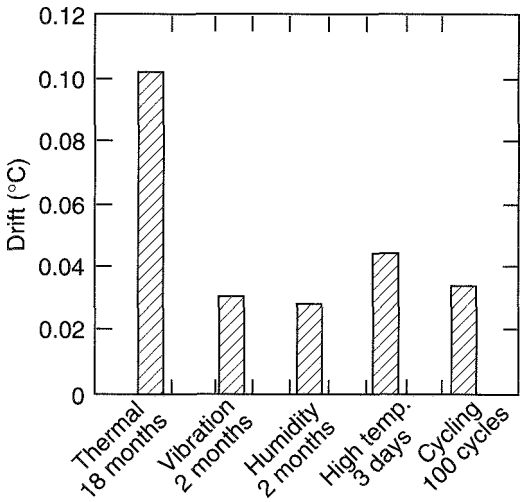

Fig. 4 Summary of aging test results.

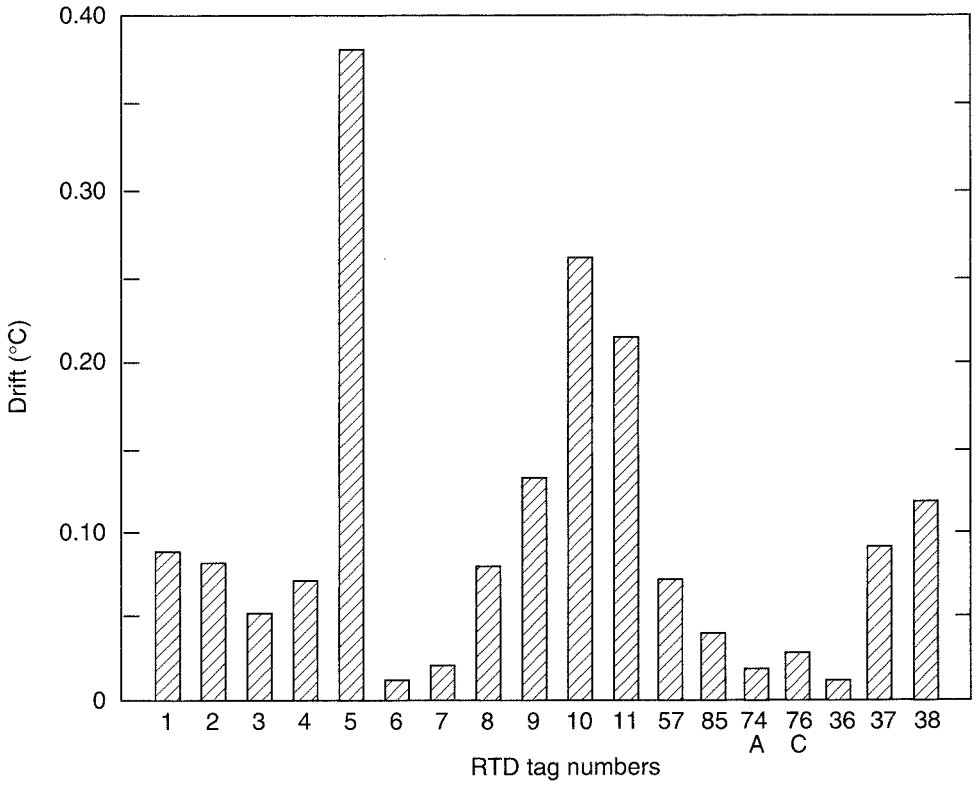

Fig. 5 Drift of naturally aged RTDs.

aging test results. The results presented in this section are for a limited number of RTDs, and the effect of nuclear radiation was not studied. As such, one must keep these points in mind when evaluating the conclusions of this article.

Testing Intervals and Replacement Schedules

The current industry practice for verifying adequate RTD accuracy and response time is to perform on-line cross calibration and response time testing at least once every fuel cycle. In light of the results generated in the aging project discussed here and elsewhere, this practice is reasonable unless plant-specific problems require more frequent testing or the RTDs are suspected of deficiencies in design, fabrication, or installation. In one plant, for example, a small margin between the required response time and the nominal response time of primary coolant RTDs, in addition to a history of response time problems caused by degradation of a thermal compound used in the thermowell, required periodic response time testing to be performed once every 1 or 2 months. Reference 6 provides more information about the response time characteristics of nuclear plant RTDs.

The data available on both drift and response time degradation of RTDs, including those discussed here, are so random that a reliable rate of change for either calibration or response time of RTDs cannot be established. Therefore RTD replacement schedules should be based on performance problems identified during the periodic in-plant tests; for example, an RTD that consistently shows measurable monotonic drift in either positive or negative directions should be replaced. Any RTD that has suffered a shift of more than 1 °C should be replaced. Any major change or consistent increases in response time of well-type RTDs should be followed by an attempt to clean and reseat the RTD in the cleaned thermowell. This may or may not resolve the problem. If not, the RTD and sometimes even the thermowell may have to be replaced. Any direct immersion RTD that has an unacceptable response time should be replaced because there is no other way to restore the response time of direct immersion RTDs.

Those RTDs which consistently pass response time and calibration testing can be kept and used in the plant for their manufacturer-specified design life. The typical

design life of nuclear-grade RTDs is 10 to 40 years, depending on the type of sensor and conditions of use.

Conclusions on Aging of RTDs

Aging affects the calibration and response time of RTDs, even at normal operating conditions. However, periodic tests performed once every fuel cycle can generally manage the aging.

If an RTD has been in storage for more than 2 years, it should be recalibrated before it is installed in the plant. The same argument applies to RTDs that have been inactive, such as those installed in a nonoperating plant for a period of more than 2 years. The stability of these RTDs may improve if they are first annealed and then calibrated.

The drift of nuclear-grade RTDs was found to generally lie in a ±0.2 °C band. A drift band is used instead of a drift rate because the drift of RTDs does not occur in a monotonic fashion to provide a unique value for calibration changes as a function of time. The accuracy of the drift band stated here is ±10%.

AGING CHARACTERISTICS OF PRESSURE TRANSMITTERS

Aging degradation may occur in a pressure transmitter when the material in the transmitter is exposed to a stress for a period of time. Typical aging mechanisms that can cause a material's mechanical strength or physical properties to degrade include thermal, mechanical, or electrical fatigue; wear; corrosion; erosion; embrittlement; diffusion; chemical reaction; cracking or fracture; and surface contamination. These degradations may result from exposure to any combination of the following stressors: heat, humidity, vibration, radiation, mechanical shock, thermal shock, temperature cycling, pressure cycling, testing, and electromagnetic interferences.

Examples of how aging stressors may affect the integrity of a pressure transmitter during a period of normal plant operation are:

• *Radiation.* Ionizing radiation plays a role in aging of equipment that is in the reactor containment. Such materials as organic fluids, elastomers, and plastics that are used in the construction of some transmitters are especially susceptible to radiation damage. Radiation can cause the embrittlement and cracking of seals, especially in the presence of heat; increase the viscosity of fill fluids; and affect the transmitter's electronics, especially the integrated circuit components.

• *Temperature.* Temperature is one of the dominant stressors in pressure transmitters. Temperature predominantly affects the transmitter's electronics. The ambient temperature in the reactor containment is about 120 °F ± 20 °F (about 50 °C ± 10 °C) during normal operating conditions. Long-term exposure to such temperatures is detrimental to the life of the transmitter. Temperature also affects other stressors. Detrimental effects of humidity, for example, are often increased at higher temperatures because of higher diffusion rates.

• *Pressure.* Pressure transmitters are continuously exposed to small pressure fluctuations during normal operation and large pressure surges during reactor trips and other events. Water hammer, for example, is a well-known phenomenon in nuclear power plants that can degrade the performance of pressure transmitters. Other pressure-induced degradations occur during calibration and maintenance, when transmitters are inadvertently overpressurized or cycled with pressures that are above or below their normal range. Cyclic pressures accelerate the normal wear and loosening of parts in the mechanical systems of transmitters.

• *Humidity.* Humidity affects the operation of a transmitter's electronics and can cause corrosion in other parts of a transmitter. Moisture sources and sinks exist within the transmitter and are therefore unavoidable. The humidity levels inside reactor containment are in the range of 10 to 100%. The higher humidities result from leaking valve seals or broken water or steam lines. Some moisture will leak into transmitters because the organic polymer seals used in most transmitters cannot provide perfect sealing under long-term exposure to the temperatures that exist around pressure transmitters. A significant degrading effect of humidity is short circuits in the transmitter electronics. In addition, moisture weakens the dielectric strength of insulators.

• *Vibration.* Vibration generated by nearby machinery during plant operation is transmitted to pressure transmitters through the building structure. The vibration of concern in this aging project was not that of seismic events, which are addressed during the qualification of pressure transmitters. Normal vibration can produce mechanical fatigue and loosen or disintegrate the transmitter components.

• *Maintenance.* An example of a maintenance-induced problem that occasionally occurs in pressure transmitters is with test pressures that are inadvertently applied to the wrong side of the transmitter during calibration activities. Another example is when isolation and equalizing valves are not manipulated in the correct

sequence to prevent exposure of the transmitter to sudden changes in pressure. Furthermore, excessive calibration and other maintenance activities can contribute to the wear and tear of transmitter components; for example, calibration potentiometers and other components on circuit cards may wear out after a few years of service because of periodic calibrations.

Effects of Aging on Calibration and Response Time

The stresses experienced by nuclear plant pressure transmitters during a long period of normal plant operation can cause performance degradation in the mechanical and electronic components of the transmitter and result in steady-state (calibration) and dynamic (response time) performance problems. A few examples of potential effects of some of the most dominant stressors are listed in Table 2 and discussed in the following text.

Effects of Aging on Mechanical Components

Some examples of the mechanical components of pressure transmitters susceptible to aging degradation during normal operation are:

• *Permanent deformation of sensing elements caused by pressure surges during reactor trips and*

Table 2 Examples of Aging Effects That Can Cause Performance Degradation in Pressure Transmitters

	Degradation	Potential cause	Predominantly affected performance		
			Calibration	Response time	Total failure
1.	Partial or total loss of fill fluid	• Manufacturing flaws • High pressure	✓	✓	✓
2.	Degradation of fill fluid	• Viscosity changes caused by radiation and heat		✓	
3.	Wear, friction, and sticking of mechanical linkages (especially in force-balance transmitters)	• Pressure fluctuations and surges • Corrosion and oxidation		✓	
4.	Failure of seals allowing moisture into transmitter electronics	• Embrittlement and cracking of seals caused by radiation and heat	✓		✓
5.	Leakage of process fluid into cell fluid resulting in temperature changes in sensor, viscosity changes in fill fluid, etc.	• Failure of seals • Manufacturing flaws • Rupture of sensing elements	✓	✓	✓
6.	Deformation of sensing element resulting in changes in stiffness	• Pressure cycling • Overpressurization • Vibration	✓	✓	
7.	Changes in values of electronic components	• Heat, radiation, humidity • Changes in power supply voltages • Maintenance	✓	✓	
8.	Changes in spring constants of bellows and diaphragms	• Mechanical fatigue • Pressure cycling	✓	✓	
9.	Blockage of holes in ceramic inserts in sensing modules (Rosemount transmitters) or crimped capillaries	• Normal aging • Manufacturing flaws • Mishandling		✓	
10.	Drift of damping resistors	• Thermal fatigue • Radiation effects • Vibration		✓	
11.	Failure of transmitter electronics	• Normal aging			✓

maintenance. This will affect both the calibration and response time of pressure transmitters.

• *Failure of the bellows.* Bellows can rupture and cause leaks, which produce false pressure indications or total failure of transmitters.

• *Degradation or leakage of the fill fluid.* The fill fluid (usually oil) in pressure transmitters can suffer degradation because of radiation and heat or may leak out. If the degradation affects fluid properties, changes in response time will result. Changes in both response time and calibration may accompany any leakage of the fill fluid.

• *Degradation of the diaphragm as the result of work hardening.* Work hardening may cause cracks in the diaphragm and change its stiffness. This will result in response time changes and can also affect the transmitter calibration.

• *Friction in mechanical linkages as the result of corrosion.* Corrosion can cause response time degradation and may also affect the transmitter calibration.

• *Failure of seals.* Seals can harden or crack and thus allow moisture to leak into the transmitters and affect the transmitter calibration.

• *Loosening of mechanical components in force-balance transmitters.* This loosening is due to pressure fluctuations, surges, and mechanical vibration and can result in calibration and response time problems.

• *Blockages in capillary tubes and other passageways.* These blockages restrict the flow of fill fluid in oil-filled systems.

Effects of Aging on Electronics

The electronic components of pressure transmitters include numerous resistors, capacitors, diodes, and integrated circuits that are used for signal conversion, signal conditioning, and linearization of the transmitter's output. In some transmitters, 10 to 20 resistors are used to maintain the linearity of the transmitter output in addition to resistors and capacitors to control the transmitter "zero" and "span." Almost all these components are affected by long-term exposure to temperature, humidity, and radiation. Any significant change in the value of electronic components can cause calibration shifts and, in some cases, response time changes.

Aging Test Results

The effects of normal aging on the performance of representative nuclear plant pressure transmitters were studied in a series of laboratory measurements. The transmitters were first calibrated, response time was tested, and then they were aged in simulated plant conditions for as long as 1 year. Following this aging, the calibration and response time tests were repeated, and the results were compared with the original unaged test results to determine if significant changes or failures had occurred because of the aging. The results of the aging tests are presented here in terms of aging effects on complete transmitter assemblies.

The project involved 57 pressure transmitters representing 8 manufacturers. The aging processes included heat and humidity levels corresponding to normal operating conditions of nuclear power plants, heat and humidity simulating the extremes of normal conditions, normal vibration, pressure cycling, and overpressurization. The aging tests conducted in this project focused on determining gross malfunctions, more so than identifying small changes or verifying the manufacturer's specifications. The goal was to determine if testing frequencies of once every fuel cycle or every 18 to 24 months that the nuclear power industry currently employs are justified.

Because the project focused on determining gross and unusual transmitter behavior, instead of presenting the results in terms of numerical changes in zero, span, and response time of the transmitters, we used the following qualitative criteria to present the results:

1. For the steady-state results, the transmitter instabilities or their deviations from a reference transmitter or a normal value were categorized as high, medium, or low, corresponding, respectively, to gross malfunction or failure, degraded but acceptable performance, and readily acceptable performance.

2. For the response time results, the degradations were categorized again as high, medium, or low, corresponding, respectively, to an increase in response time of more than 50%, 20 to 50%, or less than 20%. The response times of nuclear plant pressure transmitters are usually very small (30 to 300 ms). Therefore increases of up to 50% may correspond to a very small change in the sensor response time. In addition, the inherent repeatability problems with response time testing of pressure transmitters usually make it impractical to distinguish differences of less than 20% for those transmitters which have a small response time.

The aging test results are summarized in Table 3 in terms of the aging conditions, the aging periods, and percentages of transmitters that were affected, were not affected, or failed because of aging. The results in the last six columns in Table 3 were averaged as shown in the

Table 3 Summary of Aging Test Results

	Aging stressor	Duration, months	Aging conditions	Number of transmitters involved	Aging test results: Effect on calibration: Not affected	Effect on calibration: Moderately affected	Effect on calibration: Failed	Effect on response time: Not affected	Effect on response time: Moderately affected	Effect on response time: Failed
1.	Normal heat and humidity	6 to 12	110 °F, 65% RH	23	61%	35%	4%	87%	4%	9%
2.	Extremes of normal heat and humidity	3	150 °F, 90% RH	11	73%	18%	9%	64%	27%	9%
3.	Vibration	2	3 mils at 20 Hz	7	0	100%	0	57%	43%	0
4.	Pressure cycling	2	50% of span: 100K to 500K cycles	8	63%	37%	0	100%	0	0
5.	Overpressurization	0.5	1000 psi	8	75%	25%	0	100%	0	0
6.	Phase I results	See Ref. 3		17	59%	23%	18%	88%	12%	0
Average results of all laboratory aging tests performed in this project										
	Straight average				55	40	5	83	14	3
	Weighted average				58	35	7	84	12	4

results section at the bottom of the table. Both straight and weighted averages were calculated. The straight averages use the sum of the percentages in each column divided by six. The weighted averages are calculated as follows: multiply the percentages by the corresponding number of transmitters, add the results for each column, and divide the sum by 74. Note that some transmitters were exposed to more than one stressor (i.e., the total number of transmitters involved was less than 74). The results in Table 3 also include those of the Phase I project performed on 17 pressure transmitters, as documented in Ref. 3.

The results in terms of weighted averages are shown in Fig. 6. Overall, 5 to 7% of the transmitters failed from a calibration standpoint during various aging tests throughout the project, 35 to 40% were affected by aging but not severely, and 55 to 58% were not affected by aging at all. The effects of aging on response time were even less than the effects on calibration. Less than 5% failed from a response time standpoint, 12 to 14% were moderately affected, and 83 to 84% were unaffected. Although the number of transmitters and the duration of the aging tests were limited and no radiation effects were included, the results obtained here are consistent with the experience of the nuclear power industry. The experience of the nuclear power industry is documented in Sec. 13 of Ref. 4 in terms of a search of the Licensee Event Report (LER) data base, a search of the Nuclear Plant Reliability Data System (NPRDS) data base, and a survey of the instrumentation and control personnel in 24 nuclear power plant units.

Aging of Pressure Sensing Lines

A potential problem with the performance of pressure sensing systems that was examined in this project is the effect of sensing line blockages on response because of a gradual buildup of boron, crud, and other particles in the reactor water. Figure 7 shows how sensing line blockages may affect the response times of some of the most widely used pressure transmitters in the nuclear power industry. These results are from laboratory tests that used two different snubbers to simulate blockages. Note that, because of a difference in the design of the two snubbers, the response time results for the same percentage of blockage are different for the two snubbers. More specifically, snubber No. 1 has a piston that slides in and out in order to dampen the pressure fluctuations, whereas snubber No. 2 only simulates a local reduction in the sensing line diameter.

The effects of sensing line blockages on the response time of pressure sensing systems depend predominantly on the compliance of the transmitter. *Compliance* is defined as the change in the volume of the sensing chamber per unit of applied pressure. If the transmitter has a large compliance value, then its response time will be greatly affected by any blockage in the sensing line that can restrict the flow of fluid to the transmitter.

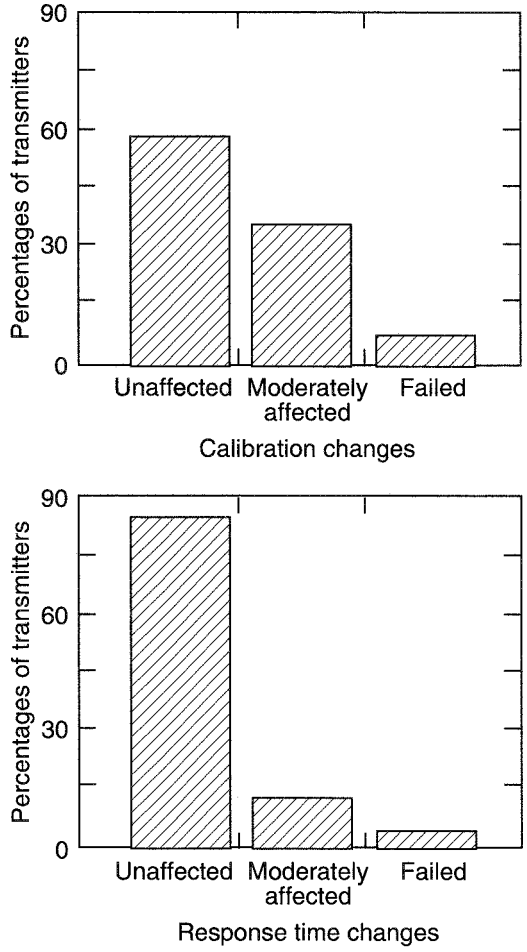

Fig. 6 Overall results of aging effects on transmitter calibration and response time.

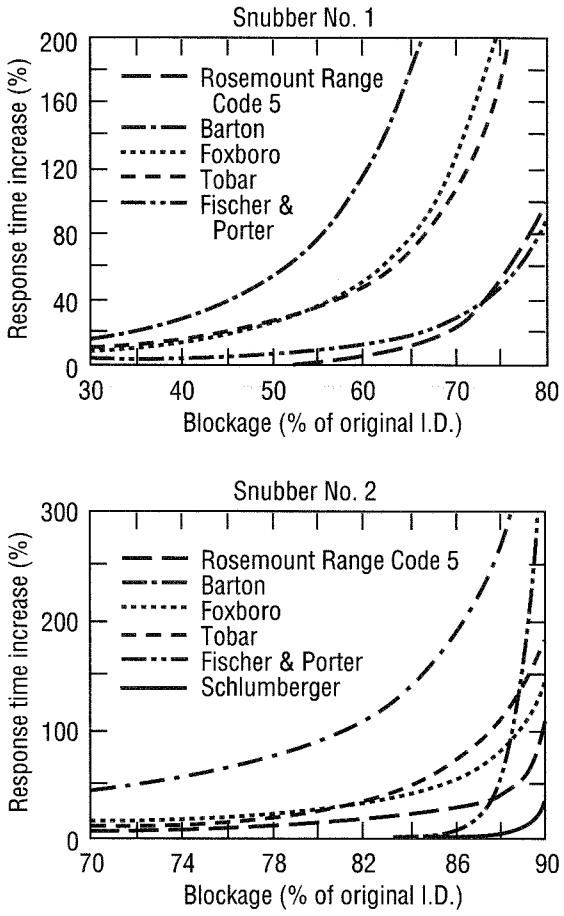

Fig. 7 Percent increase in response time as a function of sensing line blockages simulated by the use of two different snubbers in sensing lines.

Otherwise, sensing line blockages are not a major concern unless they are advanced to more than 90% of the original diameter of the sensing line. A comprehensive overview of the effects of sensing lines on the response time of pressure transmitters appears in Sec. 8 of Ref. 4.

Conclusions on Aging of Pressure Transmitters

The aging test results presented in earlier sections of this article show that the calibration and response time of pressure sensing systems in nuclear power plants are subject to degradation from normal aging and must therefore be tested periodically to ensure acceptable performance. The questions are, How often shall the transmitters be tested or replaced, and what is the useful life of the transmitters? Those questions are addressed next.

Testing Intervals

Typical nuclear industry practices for the management of aging degradation of pressure sensing systems are as follows:

- Calibrate all safety-related transmitters once every fuel cycle.
- Conduct a response time test on the transmitters in one safety-related channel once every fuel cycle.
- Blow down or purge the sensing lines as needed if there is reason to believe that blockages are present.

Discussions of whether the previous practices are adequate for aging management of pressure transmitters are provided in the following text.

Transmitter Calibration Intervals

The calibrations of about 60% of the transmitters investigated in various aspects of the project reported herein were found to be unaffected by normal aging. Of the remaining 40%, about 5% drifted out of tolerance, and the rest were only moderately affected by the aging tests, so their calibrations were still acceptable. Other aging data included searches of the LER and NPRDS data bases, which showed about 1 to 3% calibration failures in a typical fuel cycle of 2 years, and a survey of the nuclear industry, which showed that, although up to about 20% of pressure, level, and flow transmitters experience some drift, less than 5% actually drift out of tolerance and require a new calibration.[4] With this information, we concluded that the current calibration interval of once every fuel cycle is sufficient for the management of the effects of aging on calibration of pressure transmitters.

Response Time Testing Intervals

According to the results shown in Table 3, aging produced less degradation in the response times of pressure transmitters than in their calibrations. The response times of 84% of the transmitters tested in this study were unaffected by aging. Of the remaining 16% that suffered response time degradation, only about 4% failed from a response time standpoint. Furthermore, the search of the LER and NPRDS data bases did not show much evidence of response time degradation except in the case of the oil loss problem in some models of Rosemount transmitters. The results of the survey of the nuclear power industry indicate that response time problems are not prevalent and pressure transmitters are only rarely replaced because of response time failures. On the basis of this information, response time testing intervals of once every fuel cycle are conservative.

Replacement Schedules and Useful Life of Pressure Transmitters

The useful life of pressure transmitters depends on the conditions in which they are used. Transmitter manufacturers usually provide the useful life of their transmitters as a function of environmental conditions, especially temperature. On the basis of typical life vs. temperature data published by manufacturers, the useful life of most pressure transmitters used in typical nuclear plant operating environments varies between 10 and 20 years.

The life of the electronics in pressure transmitters is the dominating factor in determining how long a transmitter may be used in a plant. In most cases, a transmitter can be rejuvenated by replacement of its electronics.

The test results in this project suggest that, in light of the regular testing and maintenance activities in nuclear power plants, pressure transmitters can be used safely for as long as specified by the manufacturer provided that the transmitter has not shown sustained drift, response time degradation, or other problems.

CONCLUSIONS

The key results of two experimental research projects on long-term performance and aging characteristics of nuclear plant RTDs and pressure transmitters were presented in this article. These studies were performed on a limited number of sensors from each of the most commonly used manufacturers of nuclear grade RTDs and pressure transmitters. The results of these studies along with the historical data from nuclear power plants and the experience of the nuclear power industry indicate that, although aging can result in performance degradation in RTDs and pressure transmitters, the problem is readily manageable by calibration tests and response time measurements performed once every fuel cycle (18 to 24 months).

New methods have been developed and validated in the past 5 years for in situ testing of calibration and response time testing of RTDs and pressure transmitters as installed in nuclear power plants under operating conditions. These methods are described in Ref. 7. They can be used for the management of aging of the sensors without the need to remove them from service.

REFERENCES

1. H. M. Hashemian, K. M. Petersen, T. W. Kerlin, R. L. Anderson, and K. E. Holbert, *Degradation of Nuclear Plant Temperature Sensors*, Report NUREG/CR-4928, June 1987.
2. H. M. Hashemian, D. D. Beverly, D. W. Mitchell, and K. M. Petersen, *Aging of Nuclear Plant Resistance Temperature Detectors*, Report NUREG/CR-5560, June 1990.
3. H. M. Hashemian, K. M. Petersen, R. E. Fain, and J. J. Gingrich, *Effect of Aging on Response Time of Nuclear Plant Pressure Sensors*, Report NUREG/CR-5383, June 1989.
4. H. M. Hashemian, D. W. Mitchell, R. E. Fain, and K. M. Petersen, *Long Term Performance and Aging Characteristics of Nuclear Plant Pressure Transmitters*, Report NUREG/CR-5851, March 1993.

5. U.S. Nuclear Regulatory Commission, *Nuclear Plant Aging Research (NPAR) Program Plan*, Report NUREG-1144, July 1985.
6. H. M. Hashemian, T. W. Kerlin, and E. M. Katz, Experience with RTD Response Time Testing in Nuclear Power Plants, in *Proceedings of the Industrial Temperature Measurement Symposium, Knoxville, Tennessee, September 1984*, Report CONF-8409109-, pp. 14.01-14.23, 1985.
7. J. L. Riner, In-Situ Testing of Industrial Sensors, *Control Engineering*, 38(15): 175-176 (November 1991).

Design Features

Edited by D. B. Trauger

Defense in Depth Against the Hydrogen Risk—A European Research Program

By F. Fineschi[a]

Abstract. *The Commission of European Communities is promoting study and research on the hydrogen risk in water-cooled nuclear power plants. This activity, known as the Hydrogen Project, involves many organizations from several European countries. Coordinating such a multipartner contract means ensuring that the project is dealt with consistently by following some general safety principles and a homogeneous view of the various aspects of the problem. This article presents the coordinator's opinion on a strategy to assess hydrogen risks, to investigate and understand the related phenomena, and to provide mitigative measures. Research and study can thus be harmonized into a single consistent program, and suggestions for future activities can be made in a logical framework.*

In water-cooled nuclear reactors, hydrogen may be generated during a severe accident, and a fast combustion may occur when hydrogen comes into contact with the oxygen of the containment atmosphere. Although the likelihood of a severe accident is very low in a nuclear power plant, the hydrogen problem is important in safety analysis because deflagrations or detonations may jeopardize the containment's integrity and cause the release of fission products from the failed containment.

The severity of the hydrogen problem varies from plant to plant. It is dependent on many design features, such as size and strength of the containment, the material from which it is constructed, and the layout.

[a]Professor of Nuclear Plant Control and Operation, Università di Pisa—Dipartimento di costruzioni meccaniche e nucleari, via Diotisalvi 2, 56126 Pisa, Italy.

Research is being carried out all over the world to learn about hydrogen mixing and combustion mechanisms and to set up measures that can prevent or mitigate the consequences of hydrogen explosions. The European Union (EU) is partially funding a Reinforced Concerted Action (RCA) involving several European organizations within the Third Framework Program. The first contracts started on December 1, 1992, and the last will end on June 30, 1995.

Nine organizations from five countries cooperated in the Hydrogen Project, coordinated by Professor Fabio Fineschi of the University of Pisa, Italy:

- Forschungszentrum Jülich (KfA), Germany, Institut für Sicherheitsforschung und Reaktortechnik (ISR)
- Framatome, France (associated contractor of Siemens)
- Gesellschaft für Reaktorsicherheit (GRS), Germany
- Kernforschungszentrum Karlsruhe (KfK), Germany, Institut für Neutronenphysik und Reaktortechnik (INR), Institut für Reaktorsicherheit (IRS)
- National Nuclear Corporation (NNC), England
- Siemens AG KWU, Germany
- Technische Universität Munchen, Germany, Lehrstuhl für Reaktordynamik und Reaktorsicherheit
- Università degli Studi di Pisa, Italy, Dipartimento di costruzioni meccaniche e nucleari
- Universitad Politécnica de Madrid, Spain, Escuela Técnica Superior de Ingenieros Industriales

The organizations proposed some research to the Commission of European Communities (CEC) from

studies they conducted in the hydrogen field with results they were ready to share with other partners. The coordinator of the project then suggested possible modifications to the proposals to make the work more efficient and useful for all the countries involved. On the basis of the coordinator's advice, the CEC decided which proposals were worth financing and how much the CEC should fund.

The coordinator outlined the program to make it consistent with a strategy against the hydrogen risk, a strategy based on the defense-in-depth principles of safety.[1] This outline naturally reflects the coordinator's experience acquired in years of study and research in this field and in many international meetings. The following are personal opinions that in no way bind CEC or the countries and organizations involved.

The CEC contract keeps to generalities rather than specifics on modeling or experimental tests to allow the contractors to fit their tools and procedures to the results obtained during the work in progress. In addition, CEC funds cover only a minor part of the program costs; thus the contract cannot impose too restrictive clauses on the contractors.

The main aspects of the hydrogen problem in nuclear reactor containments must be briefly recalled, without any pretension of thoroughness, to explain the logic and the objectives of the CEC program.

THE HYDROGEN PROBLEM

During an accident in a water-cooled nuclear reactor, hydrogen is chiefly produced by metal–water reactions at high temperatures but also by core–concrete interaction, radiolysis, and corrosion. Hydrogen and steam are released into the safety containment. The timing and magnitude of the hydrogen generation (or generation of other combustible or inert gases, e.g., CO and CO_2) affect the gas chemical composition inside the containment (in particular, the H_2 concentration) and, as a consequence, the combustion risks. Hydrogen generation is not treated by the Hydrogen Project, however, because it is related to phenomena studied by other RCA projects.

The hydrogen–air–steam mixture in the containment is flammable when it is able to sustain the propagation of a combustion that has been initiated at a point by an adequate energy source (a spark is enough). For this to happen, the following conditions must be met:

1. The production rate of energy and free radicals by combustion must be sufficiently high (i.e., the gaseous mixture must be sufficiently reactive).

2. The mechanisms of free radical and energy transfer from the reaction zone must be so efficient that they can cause the ignition of the adjacent unburned gas layer.

The reaction front (flame), which separates the still cold unburned gas from the hot burned gas, advances in the gas as a wave. The speed of the flame increases in proportion to the increase in the production rate and the transfer rate of free radicals and energy toward the unburned gas.

The transfer of heat and radicals to solid or liquid surfaces becomes particularly high when the flame comes into contact with them and may cause the elimination of part of the energy and the free radicals needed for the flame to spread. This might prevent or interrupt the combustion process if the mixture is not sufficiently reactive because it is not near enough to the stoichiometric composition or because it has been diluted too much with inert gas. The heat capacity of the inert gas reduces the increase in temperature and thus the reaction rate.

The limit volumetric concentrations for which a flame can propagate in a hydrogen–air–steam mixture are called flammability limits: 4 to 5% for hydrogen if the mixture is lean in fuel and 5 to 6% for oxygen if the mixture is rich. The geometry of the containment and the temperature and the pressure of the mixture before combustion have little influence on them, at least within certain limits (up to 450 K and 5 bar).

Two different flame propagation mechanisms are theoretically possible for any flammable mixture:

- *Deflagration:* the flame has a subsonic speed, and the energy is fundamentally transferred from the flame to the unburned gas as heat. If the flame advances slowly (a few meters per second) in a closed vessel, the pressure rises uniformly according to the global energy balance.
- *Detonation:* the flame speed is greater than the sonic speed (thousands of meters per second) in the unburned gas, and the energy is transferred as work energy by the shock wave that accompanies the combustion wave.

In reality, many intermediate flame speeds are possible and may be accompanied by shock waves of different strengths.

When the chemical composition of the mixture is close to the flammability limits, there is virtually no chance of a detonation, and in a closed vessel the theoretical, adiabatic, and complete combustion overpressure is not very high (it is proportional to the molar density of the deficiency reactant) and causes static loading on the containment structure. Furthermore, in a real "slow" (or "weak") deflagration, the overpressure is further reduced for the following reasons:

• The low burning velocity gives enough time for part of the gas energy to be transferred to the containment walls during the flame propagation.

• The flame may quench when it comes into contact with solid or liquid surfaces before the reaction has involved the whole volume of the containment and thereby prevent the combustion from being completed.

• The speed with which the burned gas, which has a lower density than the unburned gas, moves upward because of gravity, may be, for not very reactive mixtures, greater than the flame speed; thus downward flame propagation may be made impossible.

When the reactivity of the mixture increases, so do the flame speed and the maximum pressure. The combustion tends to become more adiabatic and complete because the time available for the heat transfer to the walls decreases and the flame propagation becomes more isotropic. Similar effects to those of an increase in mixture reactivity are due to the increase in turbulence caused by fans, by obstacles to the expanding gas flow, and by strong jets of hot burned gas into the unburned gas. In fact, the area of the interfacial surface between the burned and unburned gas increases because the reaction front folds, and both heat and mass can be transferred also by eddy diffusion.

When turbulence increases the flame speed, the velocity of the unburned gas in front of the combustion wave increases, so that turbulence increases more and more. This positive feedback creates accelerating flames, and shock waves and dynamic loads (explosion) result. So deflagrations can become strong, or even a deflagration–detonation transition (DDT) may occur. In these cases the strengths of the shock waves may become very dangerous for the integrity of the containment and safety-related equipment.

For slow deflagrations, the overpressures between communicating compartments depend on the balance of the expanding rate of the burned volume and the gas flow rate through the communication openings. Shock waves, on the other hand, cannot be affected by openings because their speed is higher than the speed of sound, and in front of them the unburned gas is not moved by an expanding burned gas.

DEFENSE IN DEPTH AGAINST HYDROGEN

A strategy for dealing with hydrogen risks should be based on three main rules according to the defense-in-depth principles:

1. Hydrogen–oxygen mixtures must be avoided in the reactor containment.

2. If hydrogen and oxygen are in the containment, combustion must be avoided.

3. If combustion is possible, then strong explosions must be avoided.

Today the theoretically possible fourth rule—"If strong explosions are possible, containment structures and safety-related equipment must withstand the related dynamic loads"—is not considered by the Hydrogen Project, even for containments of new design. In fact, designing against strong explosions would be very difficult and unreliable if it were "realistic"; but the containment system would be too expensive if designing were "conservative." For this reason the final objective is to avoid strong dynamic loads, and the research on the possible methods of designing the containment structures against dynamic loads is a matter for another RCA, the Containment Project.

The measures against the hydrogen risks will be briefly described here without scientific and technical details with the only aim to explain the strategy and the logic and objectives of the Hydrogen Project program. It is up to each country, and not to the EU, to decide the measures that are practicable for technology and safety and are the best for its plants. The Hydrogen Project is cooperating with the International Atomic Energy Agency (IAEA) to publish a document, "Hydrogen Mitigation in Water-Cooled Power Reactors," in which all mitigation measures will be thoroughly described and compared.

Prevention of Hydrogen–Oxygen Mixtures

Hydrogen–oxygen mixtures could be avoided inside the containment through the application of one or more of the following measures:

• Preventing accidents and excessive overheating of fuel cladding.

• Using materials that cannot be oxidized by steam at high temperatures.

• Preaccident inerting (i.e., replacing air with nitrogen during normal operation).

• Postaccident inerting with an early venting (i.e., replacing air with nitrogen or CO_2 just at the beginning of the accident while radioactivity is still negligible inside the containment).

Some measures related to the first level of defense are not always suitable or successful because, for example, the following are not possible:

• To exclude all possibilities of accidents or overheating.

• To find materials for the core internals that are absolutely inoxidizable by steam at high temperatures.

• To preinert large containments where air breathability must be assured because equipment must be serviced frequently.

• To eliminate generation of hydrogen and oxygen by radiolysis.

Moreover, with reference to postinerting with early venting, we do not know as yet the answers to some questions:

• What are the appropriate criteria for the operator to initiate early venting?

• Can early venting definitely be stopped before reaching dangerous radioactivity levels?

• Can a fast injection of liquid nitrogen or CO_2 at a very low temperature generate such efficient stratification effects that air is totally replaced during the short period of the early venting?

• Can the very low temperature of the inert gas jeopardize safety-related equipment?

For these reasons, a second level of defense is necessary.

Prevention of Combustion

Combustion cannot propagate if at least one of the two reactants is below its flammability limit.

The second level of defense tries to maintain the containment atmosphere nonflammable through the following:

• Mixing hydrogen with a large amount of air.

• Recombining hydrogen (or oxygen in inerted containments) with thermal or catalytic devices.

• Injecting inert gas to dilute hydrogen ("dilution") or oxygen ("postinerting") below their respective flammability limits.

Mixing can be achieved by natural mechanisms (convection and diffusion) and/or engineered systems (dampers, high point vents, sprays, fans, coolers, ventilation systems, and passive recombiners). Mixing (together with recombiners for the long-term control of the radiolytic hydrogen) can only prevent deflagration if the amount of hydrogen is small (such as in a design-basis accident) and the containment is large. Mixing processes provide the context for the action of all mitigation measures, however, and an analysis of mixing processes is a key aspect in the hydrogen problem.

The new passive catalytic recombiners that are currently being marketed seem to be able to cope with higher generation rates of hydrogen than the old active thermal recombiners because more units can be installed at the same cost and in the same space. Therefore they can also prevent flammability in some less severe accidents if the hydrogen generation rate is not too high when the hydrogen concentration is close to the "lean" flammability limit. Recombining is also needed in inerted containments to eliminate hydrogen before venting.

If the injection of inert gas is not enough to keep the mixture nonflammable, the consequent deflagration may cause a higher final pressure because the initial pressure is higher.

Among these combustion preventive measures, only postinerting (+ recombiners) could theoretically solve the hydrogen problem in any accident, but its adequacy in terms of the safety requirements has yet to be proven because it brings venting forward and may jeopardize safety-related equipment if the temperature of the CO_2 is too low. Halogenated carbon–hydrogen compounds (Halons) would have the best inerting characteristics, but Halons destroy ozone and cannot be produced anymore; moreover, their corrosive properties would be dangerous for safety-related equipment.

A preventive partial preinerting, which means an oxygen dilution above the breathability limit or preinerting of some parts of the containment, could minimize the postinerting disadvantages. It is difficult to ensure breathability everywhere, however, because of inert gas pocketing, or to isolate parts of the containment.

Reliable values of the flammability limits for hydrogen–air–steam mixtures are available only for temperatures of 473 K or lower.[2] Autoignition temperatures, flammability limits, and diffusion flame stability of H_2–CO–air mixtures diluted with steam and CO_2 need to be established at elevated temperatures.[3] Very high temperatures could be in cavity because of core–concrete interaction or in the vicinity of the hydrogen–steam release point from the primary system or in other zones because of direct containment heating.

For all these reasons, a third level of defense is necessary except in inerted containments.

Prevention of Explosion

If the gas mixture composition approaches the stoichiometric H_2/O_2 ratio and there is not enough inert gas for the mixture to be nonflammable, a possible propagating flame front can accelerate so that dynamic loads can add to the static loading caused by the combustion overpressure.

All measures that reduce the volumetric concentrations of the reactants (dilution, recombining, etc.) are also

useful for avoiding explosions, but the fastest method to eliminate hydrogen is a deliberate deflagration as soon as the mixture becomes flammable so that the static overpressure and the likelihood of accelerated flames are as low as possible (weak deflagration). The burning rate of a deflagration is always higher than the generation rate of hydrogen, even if the deflagration is "slow." Active (glow and spark plugs) and/or passive (catalytic) ignitors can be put in several locations inside the containment if structures are sufficiently strong and safety-related equipment is fireproof.

The location of the ignitors is a critical parameter for burning all hydrogen that is flammable at the ignition instant, for preventing flame acceleration, and for avoiding pockets of very reactive gas and standing flames near important pieces of equipment or structures.

Ignitors do not increase the likelihood of deflagration because in a flammable gas mixture sooner or later an ignition will happen as the result of more or less natural sources. However, ignitors do increase the likelihood that a possible deflagration is weak. For this reason, a deliberate ignition system cannot worsen the accident development, and it can be automatically started up.

The success of deliberate ignition cannot be assured in all situations, however, even if the ignitors have been correctly placed in the containment. These are the main uncertainties:

- Deliberate ignition could increase the likelihood of simultaneous ignitions in two or more points in the containment. Turbulence generated by one flame could, theoretically, accelerate another flame that is simultaneously propagating and facilitate a deflagration–detonation transition. This phenomenon has never been observed in experiments (tests were made in vessels with volumes up to 3×10^3 m^3).
- The ignitors located in the vicinity of a pipe rupture could be damaged by missiles and fail to function. Hence hydrogen could be ignited only if it has spread to ignitors that have been installed at more remote locations. This would result in a flame propagating from lean mixtures into areas with richer mixtures. Flame front acceleration together with local turbulence may increase the potential for local detonations.
- The gas mixture may be initially inerted by steam and may later burn when the mixture composition is near the "rich" flammability limit where the deflagration overpressure and likelihood of explosion are higher than near the "lean" flammability limit. In this case, the pressure might be higher than the failure pressure of the containment.
- High temperatures could increase the likelihood of explosion near the flammability limits as well.
- It may be difficult to predict the consequences of an explosion on a complex structure or piece of equipment.

Moreover, some time must pass before the gas mixture becomes flammable and the deliberate ignition system can intervene. In other words, if deliberate ignition is the only measure against hydrogen, in a less severe accident there would not be safety intervention until the accident has degenerated.

For all these reasons, an ignition system can be a good third level of defense after combustion preventive measures have been taken (e.g., recombiners); however, if possible, ignitors should not be the only mitigation measure.

Recombiners can increase the chances of success of deliberate ignition by reducing the number and size of possible pockets of more reactive mixtures.

Another measure against DDT is the injection of CO_2. We can estimate how much CO_2 has to be injected on the basis of experimental tests carried out in small volumes, but we do not know whether scaling effects could modify these data in large containment volumes.[4,5]

MITIGATION ASPECTS FOR NEW PLANT DESIGN

For the elimination of all hydrogen problems, water should not be in the reactor core, either as a moderator or as a coolant, in normal and accidental conditions. Another radical solution is to have a containment without air (preinerted), but only boiling-water reactors (of the water-cooled reactors) are compact enough to be contained by small containments where no equipment needs servicing. What type of reactor to install depends on weighing many other advantages and disadvantages; thus the hydrogen problem may also exist for new plants.

Preventive and Mitigative Methods

Future plants will have novel designs for reactor core cooling to prevent or limit degraded core accidents and hydrogen generation. Severe accidents will, in any case, always be taken into account in plant safety analysis, even if there is less chance of their happening.

The practicability of new alloy compositions that cannot be oxidized fast by high-temperature steam still needs to be proven. The volumes of the new containments cannot be so large and mixing so effective that hydrogen will remain below its flammability limit even if multiple

modular reactors are located inside one containment alone. Ignition sources cannot be eliminated with certainty because of the very small energy that can ignite a flammable hydrogen–air mixture.

The mitigation measures discussed in the previous chapters are also valid and sufficient for new plants. Their capacity and/or reliability may increase in the future, particularly with catalytic recombiners. Today other ideas would not seem practicable.

Containment Design

The greatest chance for the new plants is a containment design such that the structure strength, the compartment geometry, and the equipment layout are consistent with the mitigation measures adopted.

The geometry and layout might allow us to make a better prediction of mixing to locate correctly recombiners, ignitors, or nozzles for inert gas injection.

The geometry and layout could also reduce the likelihood of flame acceleration and the onset of detonation:

- Volumes with one dimension (i.e., the dimension along the possible path of the expanding unburned gases) much greater than the other ones should be avoided.
- The openings between compartments should be large and not obstructed by equipment and grids.
- Ignitors should be located near the openings to avoid jet ignition.
- Large amounts of venting transverse to the flame path hinder flame acceleration.
- Obstacles should not be closely and regularly spaced.
- Deadening materials or structures could cover the walls.

The structures should withstand the pressure caused by postinerting or the combustion of all the hydrogen that can accumulate inside the containment compatibly with the mitigation systems installed. In both cases the maximum pressure is higher when the temperature of the containment atmosphere is higher. The new containment should have very effective systems to remove heat and to reduce the temperature needed to transfer the power generated inside the containment; this does not, however, include the power of a possible deflagration, which is obviously too high.

Metal foil inserts are now used in some applications (e.g., some aircraft fuel tanks and flammable liquid storage tanks) to absorb combustion energy and thereby limit flame speeds and pressures. The feasibility of deploying some types of flexible metal ribbons–foil arrays or other materials, such as ceramic fiber or mineral wool blankets, from the ceiling of a containment (including large internal compartments) during a severe accident might be discussed in the future, but the sensitivity of hydrogen toward flame acceleration by obstacles is greater than other combustible gases.

New filtered venting schemes seem more promising for providing an early venting with postinerting than for mitigating deflagration overpressures. Venting is ineffective against detonation, however.

THE CEC HYDROGEN PROJECT

The objectives of the present RCA program of the CEC on hydrogen are to assess the present knowledge of hydrogen-related phenomena in water-cooled nuclear reactors, to improve modeling techniques, and to investigate measures to reduce the risks resulting from hydrogen. Progress in calculating the amounts of hydrogen produced during an accident has been entrusted to other RCA projects.

Table 1 shows a summary of the present and future activities of the Hydrogen Project and the organizations involved.

State of the Art

Present knowledge on hydrogen problems is being critically assessed to produce a framework within which key uncertainties affecting hydrogen problems in nuclear power reactors can be addressed.

The 1991 CEC–IAEA state-of-the-art report[6] concerning hydrogen distribution and combustion phenomena is being reviewed. Moreover, a document on mitigation is being written jointly with IAEA.

In the meantime, information and bibliography on the most recent work in this field can be found in several papers and reports.[4,7–12]

Study and Research

The hydrogen project expects to provide a more reliable background of knowledge to assess the adequacy of mitigation measures in avoiding a global strong deflagration or detonation through

- Hydrogen dilution: natural and engineered mixing, preinerting, and postinerting.
- Hydrogen removal: recombiners and ignitors.

The flammability of a gas mixture and the burning rate of a flame depend on the chemical composition of the gas mixture. Hence knowledge of the distribution of hydrogen, oxygen, steam, and other inert gases in the

Table 1 1993–1995 Program of the CEC Hydrogen Project

Objects	Current program 1993–1994 (organizations)	Refueling program 1994–1995 (organizations)
DISTRIBUTION PREDICTION (natural mixing)	• State-of-the-art report (SOAR) [NNC] • Validation of "lumped parameter" codes on the basis of Battelle Containment Model (BCM) and HDR tests (NNC, Siemens) • Validation of a "field" code on the basis of BCM tests (Framatome)	• Validation of "lumped parameter" codes on the basis of NUPEC tests (NNC) • Calculations of H_2 stratification in the upper dome of a real containment with a "field" code (Framatome) • Validation of a 3-D code on the basis of BCM, HDR, Phoebus tests (KfK)
COMBUSTION PREDICTION	• SOAR (University of Pisa, GRS)	
Slow deflagrations	• Development and validation of a code for semiempirical evaluations of burning rates in vented compartments (University of Pisa) • Postcalculations of BCM tests with available deflagration models (Siemens)	• Semiempirical evaluations of burning rates on the basis of tests in a vented glass vessel (University of Pisa) • Development of new, more accurate, models for simulating deflagrations in multi-compartment containments with "lumped parameter" codes (Siemens)
Fast deflagrations		• Development of 3-D codes to evaluate fast deflagrations in complex geometries (KfK) • Experiments in small and large scales for code validation (KfK)
DDT		• SOAR, test analysis, scaling analysis, modeling, software development (KfA) • Experimental evaluation of the "minimum energy" to start detonation (KfK)
MITIGATION	• SOAR (GRS, University of Pisa, Siemens)	
Inerting	• Analytical simulations of postinerting in large containments (University of Munich) • Evaluation of inerting procedures in containments with a new design (University of Pisa)	• Probabilistic sensitivity analysis of postinerting simulations (University of Madrid)
Recombining and deliberate ignition		• Development, installation, and application of ignitor and recombiner models in "lumped parameter" codes (Siemens, University of Pisa)
PROBABILISTIC RISK ASSESSMENT		• Development and application of a general methodology for the assessment of the H_2 risk and the effectiveness of mitigation measures (NNC, Siemens)

containment volume is essential to make reliable predictions about the damaging effects of combustion.

Damage may increase if the combustion wave propagates in a nonuniform medium toward more reactive zones or if it meets obstacles, openings between compartments, or turbulent eddies generated by fans or venting systems.

Distribution and combustion models will be developed according to their complexity (lumped parameter codes, field codes, and 3-D codes) and degree of advancement and will be validated with distribution and combustion tests from the Battelle Containment Model (BCM), Germany's Heissdampfreaktor (HDR), and the Nuclear Power Engineering Test Center (NUPEC).

By comparing the outputs of different codes and the available experimental data,[13–16] we can identify the following:

• The areas of study that are crucial for predicting hydrogen distribution and combustion.

• The factors that appear to influence code accuracy (e.g., the estimates of buoyancy, heat transfer, and burning rate).

• The degree of accuracy needed for each area.
• The test and validation processes needed to improve the predictive capabilities.

An ad hoc code, NEVE, is being developed to assess the burning rate of slow vented deflagration tests; the code will be validated with tests carried out in the glass vessel of a small-scale facility, VIEW.[17–19]

Theoretical and experimental activities will be carried out on fast deflagration and DDT:

• Codes will be developed to simulate turbulent reactive flow and strong gas dynamic wave processes in complex geometries and to describe flame acceleration mechanisms on the basis of small-scale experimental observations. The effects of hydrogen concentration, obstacles, and the position of the ignitors will also be investigated with large-scale experiments of fast deflagrations.
• The DDT mechanisms will be studied through a review of analytical models and experiments, scaling analysis, and proposals for fundamental and semiempirical models. Small-scale tests will be carried out to identify what circumstances can turn a fast deflagration into a stable detonation.

The consequences of the dynamic loads on structures are being evaluated in another project, the Containment Project.

Calculations of the injection flow rates and of the total amounts of inerting gases (nitrogen and carbon dioxide) will show which quantities are sufficient to inert large full-pressure containments or containments with a new design (parameters: uniform or nonuniform gas distribution, steam concentration, etc.). The postinerting effects will be investigated in connection with the distribution of gas composition, pressure, and temperature (parameters: different locations and numbers of the injection points, injection flow rates, etc.). Various postinerting systems and procedures will be compared by taking into account the ultimate pressure of the containment, the injection temperature, chemical corrosion, and the safety characteristics, whether active or passive. Possible signals that can be used to start postinerting will be investigated to assess the usefulness and feasibility of combining postinerting with recombiners to control oxygen generated by radiolysis. The advantages and disadvantages will be further assessed by simulating postinerting transients, followed by a sensitivity analysis with advanced Monte Carlo sampling techniques, to verify the effects of uncertainties in parameters and properties on the results obtained from the simulation code.

The recombining effects on the distribution of the gas concentrations, on the pressure, and on the temperature in accidental conditions will be further investigated, taking into account the experimental tests. Also, the capacity of the recombiner is affected by mixing as the result of the buoyancy forces caused by recombining itself. The available data[20–24] are being reviewed and analyzed about the startup times and the steady-state recombining rates as well as the stability and the reliability of the present catalytic and thermal recombiners for forced flow and/or natural convection.[19] The combination of recombiners with other prevention and mitigation systems (inert gas injection and ignitors) will also be investigated.

A general probabilistic methodology to combine experimental data, computer-generated results, and expert judgment will be applied to the complex phenomena associated with the production, distribution, combustion, and mitigation of hydrogen. As an example, the hydrogen risk will be assessed with this method in a particular nuclear plant.

Earlier sections have described the many uncertainties associated with the prediction of hydrogen behavior in nuclear reactor containments. For this reason, the question of whether a probabilistic approach would be a useful method for addressing the hydrogen problem will be investigated.

INTERFACES WITH OTHER RCA PROJECTS

In addition to the Hydrogen Project (H_2), there are seven other RCA Projects on Fission Reactor Safety of the Third Framework Program:

• Core Degradation (CORE)
• Reactor Pressure Vessel (RPV)
• Molten Fuel–Coolant Interaction (MFCI)
• Molten Core–Coolant Interaction (MCCI)
• Source Term (ST)
• Containment (CONT)
• Accident Management Support (AMS)

Table 2 shows the possible exchanges of information among the various groups.

Hydrogen Generation

The timing and magnitude of the hydrogen generation (or generation of other combustible or inert gases, e.g., CO and CO_2) affect the gas chemical composition inside the containment (in particular, the hydrogen concentration) and, as a consequence, the combustion risks. Nevertheless, hydrogen generation is not treated by the Hydrogen

Table 2 Synoptic Table of Interactions Between H_2 and Other CEC Projects (symbols: gives to ↑, wishes to receive from ↓)

Projects		Hydrogen
CORE	↑	H_2 production rate by metal–water reactions
MCCI	↑	H_2 production rate by a core–concrete interaction
ST	↑	H_2 production rate by radiolysis + gas distribution models + aerosol concentration and size + radioactive field
	↓	Gas distribution models + deflagration overpressure and overtemperature + data on H_2 mitigation systems affecting the radioactive release from the containment
CONT	↑	Heat transfer coefficients
	↓	Deflagration overpressure and overtemperature + detonation possibility
AMS	↑	Reliability of thermodynamic measurements inside the containment

Project because it is related to phenomena studied by other projects: the CORE Project—steam oxidation of core materials before, during, and after core material relocation, reflooding, and quenching; and the MCCI Project—reduction of the steam mixed with molten fuel and structure materials during a possible molten corium–concrete interaction.

The contribution of radiolysis to hydrogen generation is not significant when the accident is very severe and the containment is not inerted. The evaluation of the oxygen (more than the hydrogen) generated by radiolysis may be important in the future if postinerting proves to be suitable for the largest containments as well. In any case the results of the ST Project will be essential to assess the radiolysis generation rate of hydrogen and oxygen.

Hydrogen Distribution and Heat Transfer Assessment

Thermal–hydraulics is another parameter that affects the distribution of combustible and inert gases in the containment as well as the distribution of radioactive substances, pressure, and temperature. Therefore, in this field, the Hydrogen Project has the same interest as the CONT Project (and perhaps the ST Project), and contact between the people involved will be organized.

Prevention and Mitigation of Hydrogen Combustion and Explosion

The gas injected into the containment, to prevent any hydrogen combustion with a postaccident inerting system, can have chemical effects on the fission-product behavior. Moreover, postinerting could bring forward containment venting and the release of radioactive substances into the environment. For these reasons the final assessment on postinerting should be made after a discussion with the members of the ST Group.

The startup of some systems to prevent or mitigate hydrogen combustion or explosions, such as postinerting or deliberate ignition, may be more or less appropriate according to how the accident evolves. The views of the AMS Project on the capacity of having at any time a correct picture of the thermodynamic conditions inside the containment (the pressure and chemical composition of the gas mixture are particularly important) might be crucial for accepting or rejecting these systems.

Hydrogen Deflagrations and DDT

The ST Project will analyze the hydrogen combustion effects on the fission-product behavior. In the future the Hydrogen Group should reconsider the effects of the aerosol and the radiation field on the ignition, gas flammability, and flame propagation according to the assessment of the ST Group on the concentration, size, and properties of the radioactive substances in the containment.

The Hydrogen Group will attempt to identify the conditions for DDT and to provide a methodology to assess the probability of a hydrogen detonation in a nuclear reactor containment with and without mitigation measures. Moreover, the shock waves generated by a fast deflagration in a complex multicompartment geometry and with a possible nonuniform gas distribution could be very different from a steady detonation wave as well as the loads on the equipment and the containment building. A future collaboration with the CONT Project might be necessary.

SUGGESTIONS AND CONCLUSIONS

The current RCA program on hydrogen will probably not give a final answer to the many questions the partners face. At the end of the contracts (June 1995) we will know the results and, consequently, the questions that should still be investigated.

The Hydrogen Project does not in any case deal with all hydrogen problems. We have already spoken about the still partially unknown effects of carbon monoxide and carbon dioxide, particularly at high temperatures, on flammability limits, detonation onset, and flame stability of hydrogen–air–steam mixtures; however, the most important objective of future work should be to identify reliable scaling techniques to relate small-scale test results with effects occurring at realistic dimensions.

Many phenomena and mitigation devices concerning hydrogen are affected by scaling problems:

• *Mixing and all mitigation features*—All processes expected within the containment during hydrogen-dominated situations are affected by the spatiotemporal distribution of the composition of the mixture. In present containments, mixing depends on natural convection within large complicated compartments with different distributions of structures, obstacles, heat sources, and sinks. Similarities between an experimental test arrangement and the containment compartment to which the test results should be extrapolated must be discussed to verify the reliability of the code validation process carried out on the basis of those experimental tests.

• *Recombiners*—The present evaluations of the recombination rate of passive recombiners are based on experimental data of decreases in hydrogen concentration obtained during recombiner operation in relatively small volumes.[19,21,22] The mixture composition was uniform in the test vessels because of the convective flow generated by the recombiner itself. In larger volumes, the recombiner might not be able to ensure a perfect mixing, and its actual capability might be different from the present semiempirical assessment.

• *Ignitors*—Experience shows that effects of partially confined deflagrations and explosions in terms of flame speeds and overpressures are always reduced at smaller scales. Nevertheless, geometrically scaled down experiments are obviously necessary because of their lower costs and environmental impact. A CEC-sponsored project[25] was completed recently in which eight institutions from five different European countries cooperated to increase the understanding of the vapor cloud explosion mechanism. One objective was to validate scaling theories. Although hydrogen was not one of the gases tested, the results could also be interesting for the Hydrogen Project.

• *Ignitors and dilution with inert gas*—The possibility of DDT, with or without dilution by CO_2, has not as yet been modeled, but the chances of DDT have been proven to increase with scale.

Although many aspects of hydrogen-related phenomena remain to be studied, we can already see the possibility of a hydrogen control in which heavy explosions could certainly be avoided by combining different mitigation measures. The characteristics of a measure can be used for balancing the disadvantages or the uncertainties of another measure, for example: mixing plus ignitors, recombiners plus ignitors, and recombiners plus dilution. Study and research would be useful for evaluating the best design, number, and location of these devices rather than finding new but potentially impractical measures.

REFERENCES

1. F. Fineschi, A Strategy for Dealing with Risks Due to Hydrogen Explosions in the Containments of Pressurized-Water Reactors of Russian Design (WWERs), *Nucl. Saf.*, 32(3): 380-387 (July–September 1991).
2. D. W. Stamps and M. Berman, *A Critical Review of High-Temperature Hydrogen Combustion in Reactor Safety Applications*, Report SAND88-0680C (CONF-881014-8), 1988.
3. D. W. Stamps, P. R. Worthington, and C. C. Wong, Uncertainties in Hydrogen Combustion for Nuclear Reactor Safety, in *Third International Seminar on Containment of Nuclear Reactors, Los Angeles, California*, Report SAND89-1854C (CONF-8908127-1), 1989.
4. OECD-NEA State-of-the-Art Report, *Flame Acceleration and Transition to Detonation in Hydrogen/Air/Diluent Mixtures*, Report NEA/CSNI/R(92)3, 1992.
5. W. P. M. Mercx, Post-Accident Dilution of the Containment Atmosphere as a Potential Hydrogen Explosion Mitigation Technique, TNO Prins Maurits Lab., Hydrogen Workshop, Apeldoorn, The Netherlands, Nov. 10–11, 1993.
6. Commission of European Communities, *Hydrogen in Water Cooled Nuclear Power Reactors*, CEC Report EUR 14037, 1991.
7. E. Della Loggia (Ed.), *Proceedings of the International Conference of CEC, IAEA, KIAE on Hydrogen Behaviour and Mitigation in Water-Cooled NPPs, Brussels, 4–8 March 1991*, Report EUR 14039 EN, The European Union, 1992.
8. S. B. Dorofeev, A. S. Kochurko, and B. B. Chaivanov, Evaluation of the Hydrogen Explosion Hazard, in *Eighteenth Water Reactor Safety Information Meeting*, Report NUREG/CP-0114-Vol. 2 (CONF-9010185-Vol. 2), pp. 327–342, April 1991.
9. R. K. Kumar and G. W. Koroll, Hydrogen Combustion Mitigation Concepts for Nuclear Reactor Containment Buildings, *Nucl. Saf.*, 33(3): 398-414 (July–September 1992).
10. *Hydrogen Management Techniques in Containment*, OECD-NEA Report NEA/CSNI/R(93)2, Restricted, 1993.
11. M. G. Plys, Hydrogen Production and Combustion in Severe Reactor Accidents: An Integral Assessment Perspective, *Nucl. Technol.*, 101(3): 400-410 (March 1993).
12. S. R. Tieszen, Effect of Initial Conditions on Combustion Generated Loads, *Nucl. Eng. Des.*, 140(1): 81-94 (1993).
13. L. Wolf, H. Holzbauer, and T. Cron, Detailed Assessment of the HDR–Hydrogen Mixing Experiments E11, in *Proceedings of the International Conference on New Trends in Nuclear System*

Thermohydraulics, Pisa, Italy, May 30–June 2, 1994, Vol. 2, pp. 91–103.

14. L. Wolf et al., Detailed Assessment of the HDR–Hydrogen Deflagration Experiments E12, in *Proceedings of the International Conference on New Trends in Nuclear System Thermohydraulics, Pisa, Italy, May 30–June 2, 1994*, Vol. 2, pp. 105–116.
15. R. Reinders, F. Timmermann, and S. Bode, Numerical Simulation of Hydrogen Deflagration in Containments, in *Proceedings of the International Conference on New Trends in Nuclear System Thermohydraulics, Pisa, Italy, May 30–June 2, 1994*, Vol. 2, pp. 117–124.
16. M. Heitsch, A Model of Vented Hydrogen Deflagrations in a Containment, in *Proceedings of the International Conference on New Trends in Nuclear System Thermohydraulics, Pisa, Italy, May 30–June 2, 1994*, Vol. 2, pp. 133–142.
17. M. N. Carcassi and F. Fineschi, A Theoretical and Experimental Study on the Hydrogen Vented Deflagration, *Nucl. Eng. Des.*, 145(3): 355-364 (1993).
18. M. Carcassi, F. Fineschi, and S. Lanza, Flame Propagation in Hydrogen–Air Mixtures in Partially Confined Environments, in *Proceedings of the International Conference on New Trends in Nuclear System Thermohydraulics, Pisa, Italy, May 30–June 2, 1994*, Vol. 2, pp. 125–132.
19. F. Fineschi, M. Bazzichi, and M. Carcassi, A Study on the Hydrogen Recombination Rates of Catalytic Recombiners and Deliberate Ignition, in *International Conference on Containment Design and Operation, Toronto, Canada, 18–22 October, 1994.*
20. R. Heck, W. Heinrich, and V. Scholten, *Igniters and Recombiners for Hydrogen Reduction Following Severe Accidents*, Service Report No. 14, Siemens, September 1991.
21. R. Heck and A. Hill, A Two-Pronged Approach to Hydrogen Reduction, *Nucl. Eng. Int.*, 37 (456): 21-28 (July 1992).
22. Electric Power Research Institute, *Qualification of Passive Autocatalytic Recombiners for Combustible Gas Control in ALWR Containments*, 1993.
23. U. Wolff, Control of Hydrogen Concentration in Reactor Containment Buildings by Using Passive Catalytic Recombiners, in *ASME/JSME International Conference on Nuclear Engineering*, Vol. 1, Report CONF-930352-, pp. 435–438, American Society of Mechanical Engineers, 1993.
24. K. Fisher, Qualification of a Passive Catalytic Module for Hydrogen Mitigation, in *Proceedings of the International Conference on New Trends in Nuclear System Thermohydraulics, Pisa, Italy, May 30–June 2, 1994*, Vol. 2, pp. 143–146.
25. CEC Project MERGE, *Modelling and Experimental Research into Gas Explosions*, Contract STEP-CT-0111, 1993.

Environmental Effects

Edited by B. Berven

Technical Note: A Preliminary Analysis of the Risks to Hong Kong Resulting from Potential Accidents at Daya Bay Nuclear Power Plant

By Z. Shi and X. Wei[a]

Abstract: *This article presents a preliminary assessment of the risks to Hong Kong resulting from potential accidents at Daya Bay Nuclear Power Plant using the computer code CRACTH. WASH-1400 accident source terms and hourly directional weather data for the Daya Bay site were used as the basis for this assessment. This study shows that, because of the distance separating the power plant from Hong Kong, both the social and individual risks from nuclear plant accidents are very small compared with other nonnuclear risks in the city. The results presented in this article indicate that, even under the assumption of no early and delayed evacuations, the risks of early and latent health effects are very low in relation to the safety goals of the U.S. Nuclear Regulatory Commission.*

Since the accident at Chernobyl Nuclear Power Plant, more and more people have paid attention to the Daya Bay Nuclear Power Station in Hong Kong because they are concerned with the risk and environmental effects from the nuclear plant. With the use of the program CRACTH,[1,2] we have assessed additional risks to Hong Kong from potential accidents at the Daya Bay Nuclear Power Plant. Our findings are based on WASH-1400[3] source terms and 1-year hourly meteorological data for the Daya Bay site. We calculated the radiological consequences and risks from the Daya Bay Nuclear Power Plant and provided some appropriate protective measures for an emergency plan.

CODE AND MODELS OF ACCIDENT CONSEQUENCE CALCULATION

The code CRACTH is used in the accident consequence analysis of the Daya Bay Nuclear Power Plant. The schematic outline of the CRAC2 model is shown in Fig. 1. The calculation steps follow according to the source terms and the meteorological data of Daya Bay site; the atmospheric dispersion and deposition of the radioactive material are calculated by a Gaussian-plume formulation and the well-known Pasquill–Gifford parameterization of atmospheric dispersion. The movement of the material as it disperses downwind of the plant, the deposition of the radioactive material onto the ground and food, and the radiation doses to citizens are calculated. Several different emergency response measures are also taken into account to decrease radiation doses. The health effects and the economic effects are calculated on the basis of dose–response relationship, population distribution, and all costs. From the calculation, we can see the following results: (1) the atmospheric concentration distribution of radioactive material; (2) radiation doses on citizens (early exposure and chronic exposure); (3) such health effects as early fatalities and early injuries, latent cancer fatalities, and thyroid nodules; and

[a]Institute of Nuclear Energy Technology, Tsinghua University, Beijing 100084, People's Republic of China.

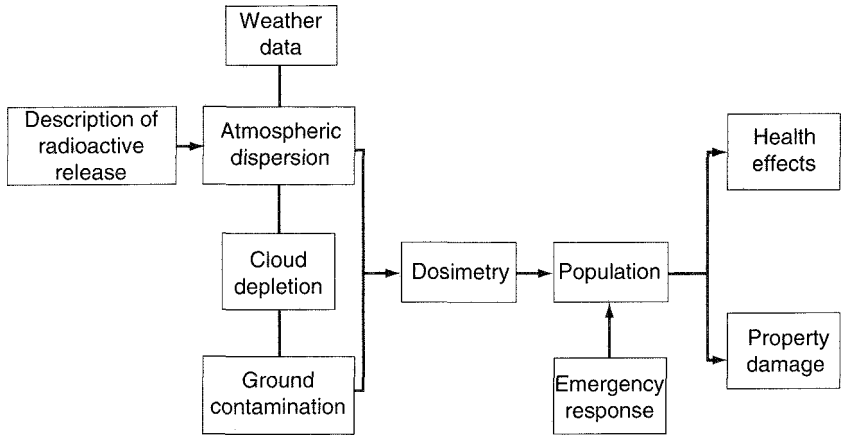

Fig. 1 Schematic outline of the CRAC2 model.

(4) area, population, and economic costs involved in emergency measures.

SELECTION OF MODELS AND PARAMETERS

Source Terms

The source terms are the most important and sensitive parameters affecting accident consequences. The pressurized-water reactor's (PWR's) ten accident release types in the Reactor Safety Study[1] (RSS) PWR IA–PWR 9 are used for the following reasons:

- The RSS results are often thought of as conservative (at least before the Chernobyl accident); they are the upper limit of accident source terms.
- RSS source terms are the main foundation of the U.S. Emergency Planning Criterion.[4]

Since RSS was published in 1975, many probabilistic risk assessments (PRAs) for nuclear power plants have indicated that the RSS source-term calculation predicts the pressure resistance of containment excessively low. The deposit of fission products in the primary loop system and containment is not fully taken into account, so the RSS's release amount is too high.[4] Furthermore, according to the accident series analysis results of Framatone 900-MW(e) Standard Plant and PWR design differences analysis of France[5] and NUREG-1206 by the U.S. Nuclear Regulatory Commission (NRC),[6] the severe accident frequency of Guangdong Nuclear Power Plant (imported from France) will be too small compared with that of the RSS. The frequency of external events (such as earthquake, flood, typhoon, plane crash, etc.) leading to core meltdown is not taken into account in the source terms.

When the total radioactive source is used, the thermal power of the PWR is 2905 MW. The dimensions of the containment are 39 by 57 m.

Atmospheric Dispersion and Weather

The deposition velocity is generally assumed to be zero for noble gases, 10^{-2} m/s for iodine, and 10^{-3} m/s for other isotopes.

The weather sequence sampling method used is the stratified sampling method, which ensures a complete coverage of diurnal, seasonal, and dry cycles without the statistical noise of methods that use random sampling. The sampling method is important because it greatly reduces the variability observed with any of these three techniques (including random sampling, stratified random sampling, and stratified sampling), and it can also reduce the calculation time.[7] In the calculation, the effects of topography and oceanography on the atmospheric dispersion have not been taken into account. According to other studies,[8,9] these factors have very little influence on the results.

Dose

The model and parameters of code CRAC2 are used here, and the food-chain pathway is not considered. Because almost all foods (but not the drinking water) used in Hong Kong are imported from Guangdong province and other regions or countries,[10] the food-chain pathway will not greatly impact the risk.

Population

With the use of the Hong Kong population (within 85 km) number in 1985 and the estimated population number in 1992 and 2000, the population in different directions and different distances is calculated for the year 2000. In 1985, the population in Hong Kong was 5.44 million.

Emergency Plan

Three types of protective measures are incorporated into the emergency response model of CRAC2. These measures include evacuation (early and delayed), sheltering, and early relocation. Other protective measures include long-term mitigative actions and acute mitigative actions. According to emergency planning for the accidents at Chernobyl[11] and Three Mile Island,[12] within several hours of accidental radioactive material release, it is difficult to determine and predict the scale and actual consequence, so it is unrealistic to decide whether to evacuate nearby residents. In fact, not early evacuation but delayed evacuation occurred in the Chernobyl accident. The French and U.S. emergency planning zone sizes, the 30-km distance between Hong Kong and the Daya Bay nuclear power plant, the complicated terrain around the plant site, and the changeable wind direction (these are harmful for evacuation) are taken into account in the emergency plan model for this paper. Therefore the sheltering measure, not early evacuation, is considered in the analysis. This method is simple: residents stay at home with doors and windows closed. According to Chernobyl survey data, the shielding factor used is 0.33. Delayed evacuation is not used in the calculation, but the result of the delayed evacuation plan is compared with the results of other plans. Delayed evacuation means that, when the radiation exposure of ground deposition to an individual exceeds 0.50 Sv whole body within 7 days, the evacuation must be put into effect within 24 hours. When the ground exposure to the individual exceeds 0.1 Sv whole body within 30 years, it is imperative to decontaminate land and property. The maximum decontamination factor is 10.

Health Effects

The health effects model and parameters of acute fatalities and acute injuries are similar to those in the code CRAC2. The linear nonthreshold model is used for the latent health effects. That particular model is normally thought to be the upper limit of radiation danger prediction. Because of limited data, the economic costs are not calculated in the analysis.

RESULTS AND DISCUSSION

Individual Risks

The expected risk values of individual acute fatality, acute injury, and latent fatal cancer with respect to distance from the Daya Bay Nuclear Power Plant are plotted in Fig. 2. The risk values of acute fatality and injury in the diagram are the average ones for Hong Kong directions (the two directions are southwest and west-southwest from the plant). The risk values of latent fatal cancer are the average ones for 16 wind directions. Figure 2 shows that the risk values are far below the Probabilistic Safety Criterion (PSC) for latent fatal cancers and acute individual fatalities. The individual risk values with respect to distance are shown in Table 1. The risk values of individual acute fatality with respect to distance decrease rapidly. The risk value is below 10^{-11}

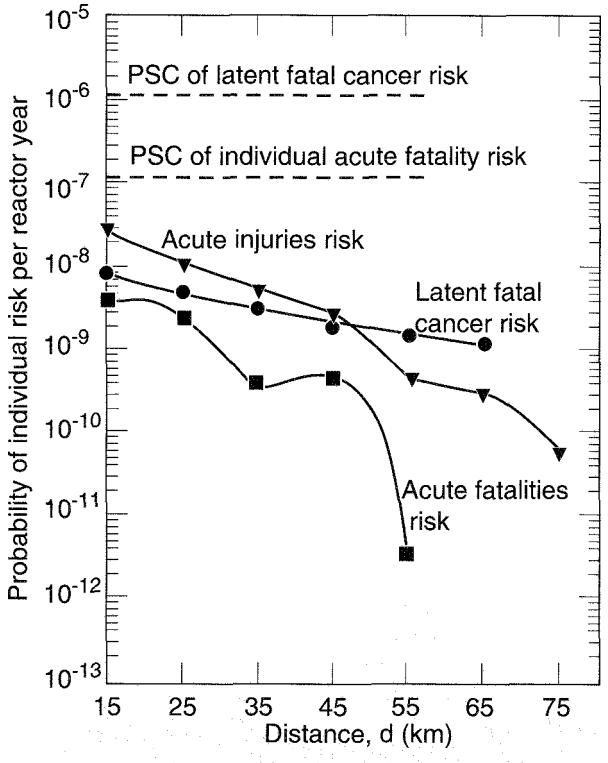

Fig. 2 Expected values of individual risks with respect to distance.

Table 1 Expected Values of Individual Risk (per reactor year)[a]

Distance, km	Acute fatalities	Acute injuries	Latent cancer fatalities
15	4.25×10^{-9}	2.90×10^{-8}	1.00×10^{-8}
25	2.60×10^{-9}	1.17×10^{-8}	5.34×10^{-9}
35	4.50×10^{-10}	5.35×10^{-9}	3.40×10^{-9}
45	5.35×10^{-10}	2.85×10^{-9}	2.24×10^{-9}
55	3.65×10^{-12}	4.55×10^{-10}	1.60×10^{-9}
65	0.0	3.65×10^{-10}	1.32×10^{-9}
77.5	0.0	6.55×10^{-11}	

[a]Emergency measure adopts sheltering within 85 km. No early and delayed evacuation.

per reactor year in the center of downtown Hong Kong (50 km from the plant).

Social Risks and Their Frequency Distributions

The average social risks and their frequency distributions to Hong Kong arising from the nuclear power-plant accidents are shown in Table 2. The social risk values associated with delayed evacuation are also included for comparison with other results. The percentages of the risk values for different release categories to the average social risk values are shown in Table 3. According to the table, the release categories from PWR 4 to PWR 9 produce no acute health effects. The release categories PWR 1, PWR 2, and PWR 3 are commensurate with the Chernobyl accident release or a more serious incident; their occurrence frequencies are expected to be 1.3×10^{-5} per reactor year, according to the RSS.

Individual Whole-Body Dose and Frequency Distribution

The acute individual whole-body dose with respect to distance and frequency distribution is calculated by code CRACTH in Fig. 3. As shown in Fig. 3, when the whole-body dose exceeds 0.5, 1.0, and 2.0 Sv, the frequency with respect to increasing distance obviously drops.

Effect of Delayed Evacuation to Risk

The results of whether to adopt delayed evacuation are shown in Table 2. The influence of delayed evacuation on latent health effects is slight but clear in regard to a decrease in early fatalities.

Assessment of Risk

For an assessment of the risks, the PSC is needed; moreover, the nonnuclear individual and social risks of

Table 2 Expected Values of Social Risk to Hong Kong

Accident consequences	Expected values: No evacuation	Expected values: Delayed evacuation
Social Risk (per reactor year)		
Acute fatalities	1.77×10^{-3}	9.98×10^{-6}
Acute injuries	9.41×10^{-3}	1.58×10^{-3}
Whole-body dose >0. 5 Sv	5.24×10^{-2}	1.05×10^{-2}
Latent cancer fatalities	1.31×10^{-2}	1.30×10^{-2}
Thyroid nodules	4.86×10^{-2}	4.85×10^{-2}
Frequency Distribution		
Acute fatalities		
>1	4.06×10^{-8}	1.12×10^{-8}
$>10^3$	2.03×10^{-8}	1.47×10^{-9}
$>10^5$	5.94×10^{-10}	0
Acute injuries		
>l	3.42×10^{-7}	1.49×10^{-7}
$>10^3$	1.15×10^{-7}	3.94×10^{-8}
$>10^6$	1.79×10^{-9}	2.17×10^{-11}
Number of people >1	4.01×10^{-7}	2.39×10^{-7}
Whole-body dose $>10^3$	1.94×10^{-7}	1.02×10^{-7}
Exceeds 0.5 Sv $>10^6$	1.43×10^{-8}	2.37×10^{-9}

Table 3 Percentage of the Risk Values for Different Release Categories to the Average Social Risk Values[a]

	Social risk				
Release category	Acute fatality	Acute injury	Whole-body dose > 0.5 Sv	Latent fatal cancer	Thyroid nodule
PWR 1A	21.2	12.6	11.2	16.9	7.3
PWR 1B	30.3	9.2	9.3	9.2	4.7
PWR 2	48.1	52.3	52.1	28.0	48.7
PWR 3	0.6	25.8	27.5	40.5	29.4
PWR 4	0	0	0	1.8	5.7
PWR 5	0	0	0	0.9	2.5
PWR 6	0	0	0	0.9	1.0
PWR 7	0	0	0	0	0.2
PWR 8	0	0	0	2.4	1.4
PWR 9	0	0	0	0	0

[a]The unit of social risk in the table is average number of people per reactor year.

Hong Kong are compared with those of the PSC. "Safety Goals for the Operation of Nuclear Power Plants,"[13] issued by the U.S. Nuclear Regulatory Commission after Chernobyl, is used here.

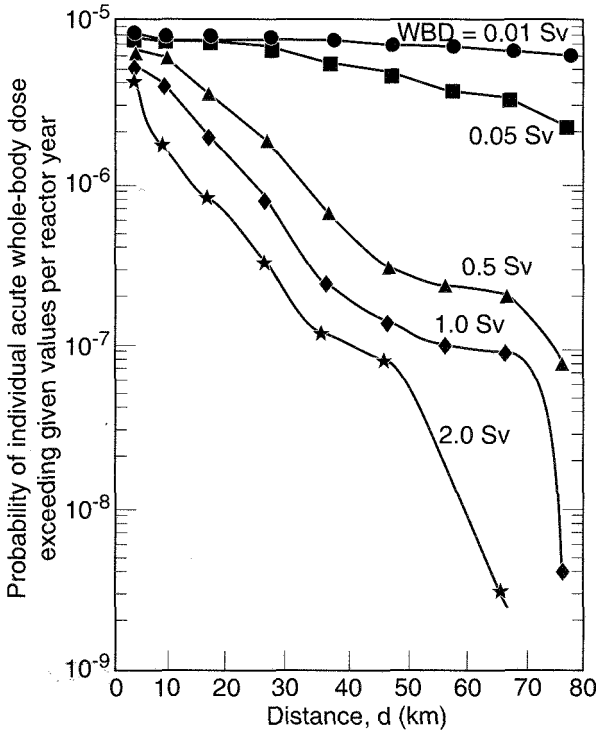

Fig. 3 Frequency of individual acute whole-body dose (WBD) exceeding given value with respect to distance.

Safety Goals of U.S. Nuclear Power-Plant Operations

The safety goals include quantitative and qualitative values as well as the average general frequency demands of large amounts of radioactive release from a severe accident at a nuclear power plant. The objectives of the safety goals for the operation of nuclear power plants are to be used in determining achievement of the goals. For an average individual in the vicinity of a nuclear power plant, the risk of prompt fatalities that might result from reactor accidents should not exceed 0.1% of the sum of prompt fatality risks resulting from other accidents to which members of the U.S. population are generally exposed. For the population in the area near a nuclear power plant, the risk of cancer fatalities that might result from the operation of the plant should not exceed 0.1% of the sum of cancer fatality risks resulting from all other causes. Because of the distance between Hong Kong and the Daya Nuclear Power Station, the radiation effects to the Hong Kong region only are analyzed. The acute individual fatalities risk at the nearest distance from the plant (15 km) is compared with the fatal cancer risk (social risk) of all Hong Kong.

Statistics of Accident Deaths and Fatal Cancer Rates During Several Years in Hong Kong

The average death rates per year for accidents and fatal cancers in Hong Kong during 1975 and 1985 are shown in Table 4.[10] Table 5 shows the individual risk

Table 4 Nonnuclear Death Rate Statistics for Hong Kong

Year	Unexpected death rate	Fatal cancer rate
1971	2.398×10^{-4}	1.098×10^{-3}
1973	2.898×10^{-4}	1.057×10^{-3}
1975	1.781×10^{-4}	1.165×10^{-3}
1977	2.176×10^{-4}	1.238×10^{-3}
1979	2.586×10^{-4}	1.266×10^{-3}
1981	2.126×10^{-4}	1.278×10^{-3}
1983	1.767×10^{-4}	1.333×10^{-3}
1985	1.353×10^{-4}	1.370×10^{-3}
Average	2.133×10^{-4}	1.226×10^{-3}

Table 5 Comparison of Nuclear and Nonnuclear Risks Per Year for Hong Kong

Risk type	Individual acute fatalities	Fatal cancer
Nonnuclear risk in 1985	1.35×10^{-4}	7431
Nuclear risk from Daya Bay Nuclear Power Plant	8.5×10^{-9}	2.62×10^{-2}
Nuclear risk/Nonnuclear risk	6.29×10^{-5}	3.52×10^{-6}

(death rate per year) and social risk (average number of deaths per year) arising from potential accidents of two reactor units at the Daya Bay Nuclear Power Plant compared with the nonnuclear death rate in 1985 of Hong Kong. As shown in Fig. 2 and Table 5, the risks to Hong Kong arising from the potential accidents of the Daya Bay Nuclear Power Plant are far below those of the PSC, and a large safety margin exists.

CONCLUSIONS

1. Because of the 45-km distance between the Daya Bay Nuclear Power Plant and Hong Kong's urban district boundary, so long as the containment system is reliable, even if a core meltdown accident occurs, there will be no acute health effects or nonrandom radiation effects to Hong Kong residents. According to an RSS conservative prediction, the frequency of the core meltdown accident for a PWR is about 6×10^{-5}.

2. When a core meltdown accident and containment failure happen simultaneously, leading to the release of a large amount of radioactivity into the environment, the incident will produce definite harmful effects to Hong Kong; however, the possibility of this kind of accident is remote. According to an RSS conservative prediction, the frequency of it is about 1×10^{-5}.

3. The calculation shows that, in a low-frequency severe accident in which a core meltdown and containment failure happen at the same time, severe results will probably occur only in the most unfavorable weather conditions. The frequency of this kind of weather condition is only about 1×10^{-3} per year, so the possibility of serious harmful effects to Hong Kong is even more remote.

4. If the design, construction, and operation of the Daya Bay Nuclear Power Plant are in accordance with the international nuclear safety criterion and if the frequency of a large amount of radioactive release into the environment rising from the severe nuclear accident is lower than 1×10^{-5}, then the residents near the nuclear power plant need only to stay home with doors and windows closed and do not need to follow procedures for early evacuation and delayed evacuation. The health effect risks compared with the nonnuclear risks to Hong Kong are very small. According to the United States "Safety Goals of Nuclear Power Plant Operation," the risks arising from plant accidents are acceptable and within a large safety margin.

5. In light of the international emergency plans of nuclear power stations (such as those of the United States and France) and the preceding results, early evacuation does not need to be considered in the emergency plan for Hong Kong. Despite the conservative source terms in the calculation and the failure to consider the urban characteristics of models and parameters for radioactive material deposition in the rain (such as substantial radioactive dust deposits on the roof in the rain, the shielding function of buildings to ground radioactive material, etc.), the average social risk values are still very small. Therefore early evacuation as an emergency plan is unnecessary.

These results are initial analyses. The risks arising from the food-chain pathway, the effects of accident frequency arising from outside events, and the influence of atmospheric dispersion caused by terrain and sea are not taken into account. All the source terms and several important models are conservative; therefore the actual risk values will be much lower than expected in the calculation.

REFERENCES

1. L. T. Ritchie et al., *CRAC2 Model Description,* Report NUREG/CR-2552 (SAND--82-0342), 1984.
2. Zhongqi Shi, in *Proceedings of the Seminar on the Nuclear Power Plant Site Selecting and Environment,* pp. 301-318, 1987 (in Chinese).
3. U.S. Nuclear Regulatory Commission, *Reactor Safety Study*, Report WASH-1400, 1975.
4. *ANS Report of the Special Committee on Source Terms*, 1984.
5. J. Des Deserts and J. C. Peyran, *Adaptation of WASH-1400 Results to the Framatone 900 MWe Standard Plant and Comparison with a Risk Criterion*, 1980.
6. U.S. Nuclear Regulatory Commission, *Analysis of French (Paluel) Pressurized Water Reactor Design Differences Compared to Current U.S. PWR Designs,* Report NUREG-1206, 1986.
7. Xingli Wei, *A Preliminary Assessment of the Risks to Hong Kong and Guangdong Province (Within 80 km from the Site), Posed by the Proposed Nuclear Plant at Daya Bay*, 1988 (in Chinese).
8. D. C. Aldrich et al., in *Topical Meeting on Probabilistic Risk Assessment*, pp. 778-787, 1981.
9. I. Cook and L. Allen, Report AERE G-3786, 1986.
10. *The Main Statistical Data: 1970–1985, Statistical Bureau of Shenzhen City*, 1986.
11. USSR State Committee on the Utilization of Atomic Energy, *The Accident at Chernobyl Nuclear Power Plant and Its Consequences*, 1986.
12. *The Report on the U.S. Three-Mile-Island Accident*, 1980.
13. *Fed. Regist.*, 51 (162): 30028–30033 (1986).

Operating Experiences

Edited by G. A. Murphy

Reactor Shutdown Experience

Compiled by J. W. Cletcher[a]

This section presents a regular report of summary statistics relating to recent reactor shutdown experience. The information includes both numbers of events and rates of occurrence. It was compiled from data about operating events entered into the SCSS data system by the Nuclear Operations Analysis Center at the Oak Ridge National Laboratory and covers the six-month period of January 1 to June 30, 1994. Cumulative information, starting from May 1, 1984, is also shown. Updates on shutdown events included in earlier reports are excluded.

Table 1 lists information on shutdowns as a function of reactor power at the time of the shutdown for both boiling-water reactors (BWRs) and pressurized-water reactors (PWRs). Only reactors in commercial operation at the start of the reporting period (January 1, 1993) are included. The second column for each reactor type shows the annualized shutdown rate for the reporting period. The third and fourth columns list cumulative data (numbers and rates) starting as of May 1, 1984.

Table 1 Reactor Shutdowns by Reactor Type and Percent Power at Shutdown[a] (Period Covered is the First Half of 1994)

	BWRs (37)				PWRs (76)			
Reactor power (P), %	Number	Shutdown rate (annualized for period)	Cumulative number	Cumulative shutdown rate per reactor year[b]	Number	Shutdown rate (annualized for period)	Cumulative number	Cumulative shutdown rate per reactor year[c]
0	5	0.27	664	1.86	6	0.16	456	0.64
$0 < P \leq 10$	2	0.11	129	0.36	2	0.05	165	0.23
$10 < P \leq 40$	1	0.05	159	0.44	5	0.13	316	0.44
$40 < P \leq 70$	3	0.16	150	0.42	6	0.16	174	0.24
$70 < P \leq 99$	8	0.44	364	1.02	7	0.19	507	0.71
$99 < P \leq 100$	9	0.49	463	1.29	23	0.61	1131	1.59
Total	28	1.53	1929	5.39	49	1.30	2749	3.87

[a]Data include shutdowns for all reactors of the designated type while in commercial service during all or part of the period covered. The cumulative data are based on the experience while in commercial service since the starting date of Jan. 1, 1984, through the end of the reporting period; it includes the commercial service of reactors now permanently or indefinitely shut down.

[a]Based on cumulative BWR operating experience of 357.79 reactor years.

[c]Based on cumulative PWR operating experience of 710.53 reactor years.

[a]Oak Ridge National Laboratory.

Table 2 shows data on shutdowns by shutdown type: *Shutdowns required by Technical Specifications* are automatic scrams under circumstances where such a shutdown was required; *Intentional or required manual reactor protection system actuations* are manual shutdowns in which the operators, for reasons that appeared valid to them, took manual actions to actuate features of the reactor protection system; *Required automatic reactor protection system actuations* are actuations that the human operators did not initiate but that were needed; *Unintentional or unrequired manual reactor protection system actuations* are essentially operator errors in which the human operators took action not really called for; and *Unintentional or unrequired automatic reactor protection system actuations* are instrumentation and control failures in which uncalled-for protective actuations occurred. Only reactors in commercial operation are included. The second column for each type of reactor shows the annualized rate of shutdowns for the reporting period. Cumulative information is shown in the third and fourth columns for each reactor type.

Table 3 lists information about shutdowns by reactor age category, both total numbers and rates in that category; it also shows cumulative results. Note that the age groups are not cohorts; rather reactors move into and out of the specified age groups as they age. The reactor age as used in this table is the number of full years between the start of commercial operation and the beginning of the reporting period (January 1, 1994, for this issue). The first line of this table gives the information for reactors licensed for full power but not yet in commercial operation on that date.

Table 2 Reactor Shutdowns by Reactor Type and Shutdown Type[a] (Period Covered is the First Half of 1994)

	BWRs (37)				PWRs (76)			
Shutdown (SD) type	Number	Shutdown rate (annualized for period)	Cumulative number	Cumulative shutdown rate per reactor year[b]	Number	Shutdown rate (annualized for period)	Cumulative number	Cumulative shutdown rate per reactor year[c]
SDs required by Technical Specifications	2	0.11	249	0.70	10	0.27	398	0.56
Intentional or required manual reactor protection system actuations	6	0.33	188	0.53	10	0.27	358	0.50
Required automatic reactor protection system actuations	13	0.71	903	2.52	27	0.72	1548	2.18
Unintentional or unrequired manual reactor protection system actuations	0	0.00	9	0.03	0	0.00	19	0.03
Unintentional or unrequired automatic reactor protection system actuations	7	0.38	580	1.62	2	0.05	426	0.60
Total	28	1.53	1929	5.39	49	1.30	2749	3.87

[a]Data include shutdowns for all reactors of the designated type while in commercial service during all or part of the period covered. The cumulative data are based on the experience while in commercial service since the starting date of Jan. 1, 1984, through the end of the reporting period; it includes the commercial service of reactors now permanently or indefinitely shut down.

[b]Based on cumulative BWR operating experience of 357.79 reactor years.

[c]Based on cumulative PWR operating experience of 710.53 reactor years.

Table 3 Reactor Shutdowns by Reactor Type and Reactor Age[a] (Period Covered is the First Half of 1994)

Years in commercial operation (C.O.)	BWRs (37)						PWRs (76)					
	Exposure during the period (in reactor years)	Number		Shutdown rate (annualized for the period)	Cumulative number	Cumulative shutdown rate per reactor year	Exposure during the period (in reactor years)	Number		Shutdown rate (annualized for the period)	Cumulative number	Cumulative shutdown rate per reactor year
		Reactors	Shutdowns					Reactors	Shutdowns			
Not in C.O.[b]	0.496	1	0	0.00	330	22.79	0.000	0	0	0.00	336	34.24
First year of C.O.	0.000	0	0	0.00	121	9.00	0.496	1	2	4.04	280	9.96
Second through fourth year of C.O.	0.019	1	0	0.00	264	6.29	0.991	2	2	2.02	526	5.59
Fifth through seventh year of C.O.	2.459	5	2	0.81	178	4.40	4.709	10	7	1.49	317	3.27
Eighth through tenth year of C.O.	3.469	7	6	1.73	201	5.31	6.105	15	5	0.82	367	3.73
Eleventh through thirteenth year of C.O.	0.991	2	1	1.01	271	5.74	4.548	10	3	0.66	496	4.26
Fourteenth through sixteenth year of C.O.	0.496	1	1	2.02	396	6.20	2.409	5	2	0.83	364	3.24
Seventeenth through nineteenth year of C.O.	2.724	7	1	0.37	280	4.65	5.662	13	12	2.12	252	2.66
Twentieth through twenty-second year of C.O.	4.709	10	9	1.91	154	4.63	9.273	20	9	0.97	94	2.10
Twenty-third through twenty-fifth year of C.O.	2.973	6	7	2.35	47	3.57	1.982	4	5	2.52	28	2.02
Twenty-sixth through twenty-eighth year of C.O.	0.000	0	0	0.00	8	2.67	0.991	2	2	2.02	16	2.67
Twenty-ninth through thirty-first year of C.O.	0.238	1	1	4.20	9	3.00	0.000	0	0	0.00	5	1.67
Thirty-second through ninety-ninth year of C.O.	0.257	1	0	0.00	0	0.00	0.496	1	0	0.00	0	0.00
Total	18.831		28	1.49	2259	6.07	37.662		49	1.30	3081	4.28

[a]Age is defined to be the time (in years) from the start of commercial operation to the time of the shutdown event, except for the first line, which lists reactors not yet in commercial service (see b below).
[b]This category includes reactors licensed for full-power operation but not yet commercial. During this reporting period reactors in this category included 1 BWR (Shoreham) and no PWRs.

Special Section on TMI-2 Vessel Investigation Project

Edited by D. B. Trauger

Three Mile Island—New Findings 15 Years After the Accident

By A. M. Rubin and E. Beckjord[a]

Abstract: *On March 28, 1979, the Three Mile Island Unit 2 (TMI-2) nuclear power plant underwent a prolonged small-break loss-of-coolant accident, compounded by human errors and equipment failures, that resulted in severe damage to the reactor core. The accident, the most severe that has occurred in a commercial pressurized-water reactor, resulted in a partial melting of the reactor core and significant release of fission products from the fuel into the reactor vessel and the containment building. The progression of the TMI-2 accident was mitigated by the injection of emergency cooling water.*

A great deal has been learned about the TMI-2 accident since it occurred 15 years ago. Much of our knowledge about the accident has evolved over time as cleanup, defueling, examinations inside the reactor vessel, and analyses have been completed. In October 1993 a 5-year major research project on the damaged reactor, called the TMI-2 Vessel Investigation Project (VIP), was completed. This article summarizes the views of the accident over the past 15 years, what we have learned from the VIP, and the broad significance of these findings. In particular, the VIP has added significant insights about the TMI-2 accident in the areas of reactor vessel integrity and issues related to accident management.

By the time the Kemeny Commission released its report to President Carter in October 1979 the circumstances that led to the accident, the course of events, and the actions taken by plant operators were clear for the plant systems for which measurements and records were available: these were the systems outside containment and inside to a lesser extent. As an observer attempted to focus attention on the reactor coolant system and the reactor vessel, clarity vanished, and he or she could only attempt to speculate on events and final conditions by inferring from external measurements and judgment. An article published in the *Spectrum* of the Institute of Electrical and Electronics Engineers (IEEE) gives an excellent account of the widely held view in the months after the accident: " . . . .This was because most of the core damage was to the cladding, which primarily yields noble gases. Iodine is released by damage to the fuel pellets, and this damage was minimal at Three Mile Island."[1]

The article identified the 100-minute mark after the main feedwater pumps tripped, which was the start of the accident, as the point of time before which there was the possibility of recovery to prevent a severe accident and after which core damage was unavoidable. Notice especially, too, the statement that most of the damage was to the clad, and the fuel pellets themselves experienced minimal damage. Four years passed before the error of this latter view came to light. This change in view is marked in a second *Spectrum* article: "What is now known is that most of the 177 fuel assemblies . . . were nearly completely destroyed in the upper quarter of the reactor core. What exists now is a void measuring 9.3 cubic meters. . . . Other material from the core void is believed to be at the bottom of the reactor vessel."[2] The suggestion that "resolidified mass from the molten

[a]Office of Nuclear Regulatory Research, U.S. Nuclear Regulatory Commission, Washington, DC 20555.

material could exist below the cavity in the core" represents a drastic change in the view of the accident in comparison with the October 1979 IEEE *Spectrum* article.

By 1987 the Three Mile Island (TMI) research had advanced considerably, and the investigators had developed a much better understanding of the accident sequence on the basis of the location and condition of core materials, fragments, and once-molten core materials that had resolidified. On the basis of this research, knowledge of the end-state condition of the TMI-2 reactor vessel and core is shown in Fig. 1. A central cavity existed in the upper portion of the core approximately 1.5 m above a loose debris bed. A previously molten region that was contained by partly or fully metallic crust layers was found below the loose debris layer. Overall, at least 45% (62 metric tons) of the core had melted. Video examinations also indicated that approximately 19 000 kg (19 metric tons) of molten material had relocated onto the lower head of the reactor vessel.

Information presented in a paper entitled "A Scenario of the Three Mile Island Unit 2 Accident"[3] describes the accident in seven periods: (1) the first 100 minutes of the loss-of-coolant accident, (2) initial core heat-up, (3) formation of the upper core debris bed, (4) growth of a pool of molten core material, (5) injection of emergency core coolant system water, (6) failure of the crust supporting the molten pool and flow of molten material to the bottom of the vessel, and (7) finally quenching and cooling of the lower debris bed and eventual stabilization of conditions.

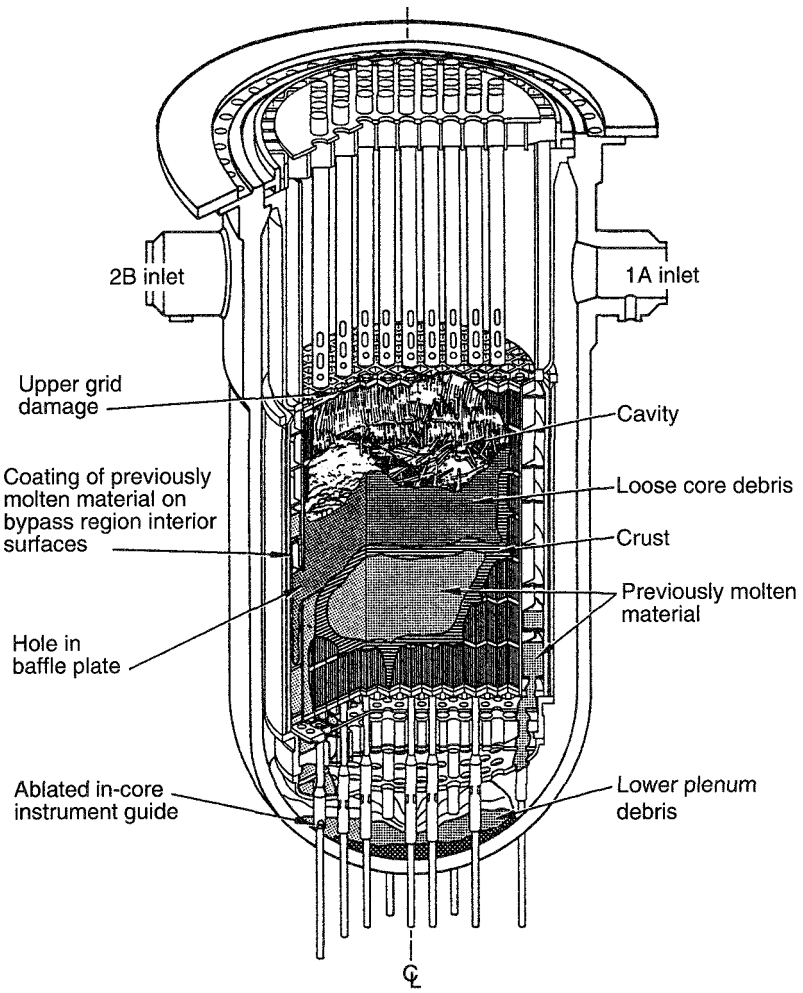

Fig. 1 TMI-2 reactor vessel end-state configuration.

The change indicated in the 1987–1989 views, compared with the views of 1984, is in the condition of the vessel, with the suggestion of "possible thermal ablation of the reactor vessel lower head." At the same time, the scenario confirms the view of the first 100 minutes of the accident that was presented in the 1979 *Spectrum* article. So the 1979 view of the first 100 minutes has stood the test of time, whereas the view of what subsequently took place within the vessel has changed drastically.

It is interesting to reflect on the long time (i.e., 8 to 10 years) that it took to develop the final view of the TMI core conditions. Did the initial erroneous view extend the time required to obtain the facts? Probably not. The long lead time required to develop the means of discovery and solve myriad technical problems associated with the removal of reactor internals, core, and fuel debris under difficult working conditions played the major role in extending the effort.

INITIATION OF THE TMI-2 VESSEL INVESTIGATION PROJECT

As researchers gained more information in the early and mid-1980s concerning the extent of damage to the TMI-2 reactor, they realized that cleanup of the reactor would take several years and would require the cooperation of both private industry and government agencies. As a result, an organization named GEND, which included General Public Utilities Nuclear Corporation (GPUN), the Electric Power Research Institute (EPRI), the U.S. Nuclear Regulatory Commission (NRC), and the U.S. Department of Energy (DOE), was formed. GEND gave technical and financial assistance to the owner of the TMI-2 reactor, GPUN was responsible for ongoing plant cleanup operations, and DOE was responsible for providing transportation and interim storage of the core until permanent disposition was decided. DOE also supported an extensive research program, the TMI-2 Accident Evaluation Program (AEP), to develop a consistent understanding of the accident. The primary objective of the DOE AEP was to develop an understanding of (1) core damage progression in the upper core region, (2) the heat-up and the formation and growth of the molten central region of the core, (3) the relocation of approximately 19 metric tons of debris to the lower head, and (4) the release of fission products to the reactor vessel and the containment.

The AEP was focused primarily on core damage progression and the mechanisms that controlled fission-product behavior. Observations made during the latter portions of the defueling effort, however, indicated that the accident progressed even further than was envisioned when the AEP was established. Molten core materials were found to have moved laterally through the east-side core baffle and former plates and into the core bypass region between the core-former wall and the core barrel. Visual observation also indicated the presence of a large hole approximately 0.6 m wide and 1.5 m high extending across the lower portion of three core-former plates. The 1.9-cm-thick core-former plates and sections of three 3.2-cm-thick horizontal baffle plates were melted in this region. Molten material from the core region flowed through this hole and into the upper core support assembly. Loose debris was found in the area behind the baffle plates and extended completely around the core region. It was estimated that 4200 kg of core debris was in the upper core support region. Closed-circuit television pictures indicated evidence of thermal damage to instrument structures in the lower plenum and around flow holes in the elliptical flow distributor.

The principal conclusions from the DOE program were that the TMI-2 core damage progression involved the formation of a large consolidated mass of core material surrounded by supporting crusts, the failure of the supporting crusts, and finally, the long-term cooling of a large volume of molten core material. The TMI-2 accident demonstrated that, at least for one severe accident scenario, the accident can be terminated and confined to the reactor pressure vessel by cooling water before the lower head fails. However, there was no quantitative information that could be used to determine how close the vessel was to failure.

In October 1987 the NRC proposed that a joint international cooperative program be formed that would be sponsored by the Nuclear Energy Agency of the Organization for Economic Cooperation and Development (NEA-OECD). This program would conduct further investigations of potential damage to the TMI-2 reactor vessel lower head from the relocation of molten fuel to that region. A steering committee was established to determine if there were sufficient interest from the OECD member countries to warrant formation of such a program. The OECD efforts led to issuing the "Agreement to Investigate the Three Mile Island-2 Reactor Pressure Vessel" in June 1988. Signatories to the project, commonly called the Vessel Investigation Project (VIP), included Belgium, Finland, France, Germany, Italy, Japan, Spain, Sweden, Switzerland, the United Kingdom, and the United States.

As described in the formal project agreement, the objectives of the VIP were to do the following: Jointly carry out a study to evaluate the potential modes of failure and the margin to failure of the TMI-2 reactor vessel during the TMI-2 accident. The conditions and properties of material extracted from the lower head of the TMI-2 pressure vessel will be investigated to determine the extent of damage to the lower head by chemical and thermal attack, the thermal input to the vessel, and the margin of structural integrity that remained during the accident.[4]

The examinations performed under the VIP went beyond the work that had been performed during the previous TMI-2 examinations. Specifically, the VIP plan was to obtain and examine samples of the lower-head steel, instrument penetrations, and previously molten debris that was attached to the lower head and use this information to estimate the vessel margin to failure. The schedule for the VIP was determined by the tasks required for fuel removal, the development of the cutting tools to remove lower-head samples, the laboratory metallurgical work, and finally the study and analyses of results. It took nearly 5 years to carry out the project, during which time nearly all the objectives were accomplished.

PROJECT ORGANIZATION

The management and organization of the VIP were defined in the 1988 formal agreement that established the project. Overall control and direction of the VIP were vested in a Management Board that consisted of one member designated by each of the signatories. The primary function of the Management Board was to approve the overall VIP work scope and budget, including the allocation of tasks among the signatories.

A Program Review Group was also formed that consisted of one member designated by each signatory. The primary function of the Program Review Group was to act as the technical advisor to the Management Board for both ongoing activities and future work. The Program Review Group was also chartered to provide technical advice and recommendations to the VIP operating agent, NRC, which was responsible for implementing project objectives in accordance with the project agreement and directions from the Management Board.

MAJOR PROJECT ELEMENTS

The VIP objectives were realized through a combination of several major activities that included extraction of vessel steel, nozzle, and guide tube samples from the lower-head region; examinations of the extracted material; and analyses to determine the structural integrity that remained in the vessel. Various project members examined the steel samples, along with the nozzles, guide tubes, and previously molten debris that were found in the lower-head region to determine the condition and properties of the samples and the extent of damage to the lower head during the accident. The results of these examinations were used to assist in quantifying potential reactor vessel failure modes, to estimate the vessel steel temperatures in the lower head during the accident, and to develop physical and mechanical property data to support the analysis effort. In the area of analysis, scoping calculations and sensitivity studies were performed in an effort to quantify the margin to failure for different reactor failure modes and to identify which modes had the smallest margin to failure during the accident.

The significant conclusions and accomplishments of each of the major project elements are discussed in the following text. Additional details on each of the major VIP elements and project results and conclusions are provided in a series of reports that were issued under the VIP.[5–12]

SAMPLE ACQUISITION

One of the major accomplishments of the VIP, accounting for approximately one-half of the total cost of $9 million, was the recovery of samples from the TMI-2 vessel lower head. This task, which was performed under the direction of MPR Associates, Inc., required careful planning because only a 30-day window was available at the site to set up the equipment and remove the samples. Specialized extraction tools had to be developed and tested before the actual sample removal.

One of the unique challenges in removing the samples was that the reactor vessel could not be breached or significantly weakened. Also, work had to be performed on a shielded platform mounted 40 feet above the lower head while samples that were covered by highly borated water were extracted. Because this was a first-of-a-kind process and the available time was limited, the exact number of samples removed could not be predicted in advance. It was hoped that 8 to 20 samples could be obtained. Despite extensive mock-up testing of the cutting tools, which used an electrical discharge metal disintegration process for cutting, a number of unexpected problems arose during the first half of the time for

working in the reactor vessel, and no samples were taken during that time. The effort was very successful in the last half of the window, however, and 15 vessel steel samples, 14 nozzles, and 2 guide tubes were removed from the vessel in February 1990. The location of these samples is shown in Fig. 2. The prism-shaped vessel steel samples extended approximately half way through the 13.7-cm-thick reactor vessel wall.

GPU Nuclear provided access to the reactor during this window at its cost, and the VIP paid only the incremental cost of sample cutting and removal. An extension of the 30-day window would have added greatly to the cost of the project and was not financially possible for the VIP.

VESSEL STEEL EXAMINATIONS

Argonne National Laboratory (ANL) in the United States coordinated the metallographic examinations and mechanical property tests of the vessel steel samples. All the lower-head steel samples were visually examined, decontaminated, sectioned, and sent to eight of the VIP member countries for testing. The participants that examined the vessel steel samples were Belgium, Italy, Finland, France, Germany, Spain, the United Kingdom, and, in the United States, ANL and Idaho National Engineering Laboratory (INEL). Examinations performed by the project participants included tensile, creep, and Charpy V-notch impact tests, microhardness measurements, micro and macro photography, and chemical composition. The primary purpose of these tests was to determine the mechanical properties of the lower-head steels over the temperature range experienced during the accident. Optical metallography and hardness tests were performed to evaluate the microstructure to estimate the maximum temperature of various portions of the lower head reached during the accident.

The results of the wide range of inspections, mechanical property determinations, and metallographic examinations of the lower-head vessel samples revealed several important and previously unknown facts relating to the degree of thermal attack on the lower head. Overall, these examinations revealed that a localized hot spot formed in an elliptical region on the lower head that was approximately 1 m by 0.8 m, as shown in Fig. 3. The hot spot was in the area where visual observations made during the defueling process indicated that the most severe nozzle damage had occurred. Metallographic examinations of samples taken from this region indicated that the inner surface of the vessel steel reached temperatures between 1075 and 1100 °C during the accident. At this

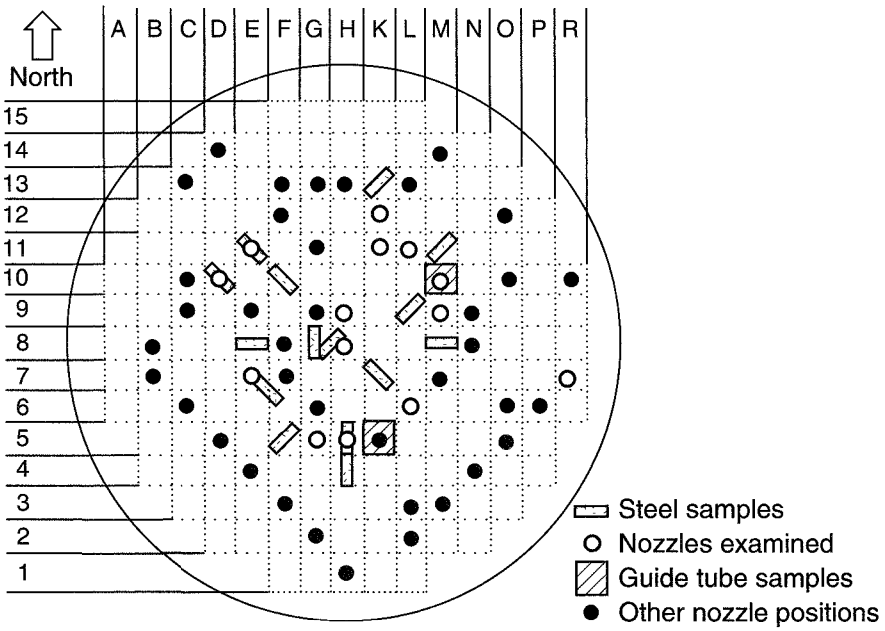

Fig. 2 Location of lower-head steel, nozzle, and guide tube samples.

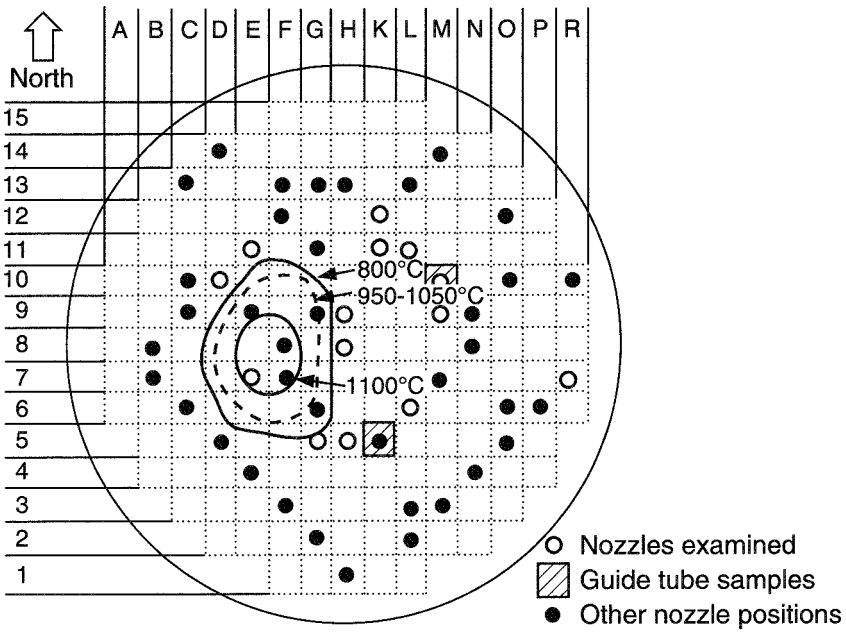

Fig. 3 Lower-head hot spot location.

location, temperatures 0.45 cm into the vessel wall were estimated to be 100 ± 50 °C lower than the peak vessel inner surface temperature.

By comparing results of the TMI-2 lower-head sample examinations with results from metallurgical examinations of heat-treated samples from an equivalent ("archive") steel from the Midland reactor, the vessel steel temperatures, time at temperature, and cooling rate were estimated. Standards with known thermal histories were prepared from the Midland archive material and later from actual as-fabricated TMI-2 material. The standards provided a means for comparing a similar material with a known thermal history to TMI-2 material with an unknown thermal history. As the standards were prepared and examined, various metallurgical observations revealed a stepwise process that could be used in determining thermal histories of the TMI-2 samples. G. Korth[6] constructed a diagram (shown in Fig. 4) that illustrates the metallurgical changes with time and temperature of the Midland and TMI-2 lower head A 533 B steel with a 308L stainless weld clad. Because the vessel was stress-relieved at 607 °C after the weld clad was added, no thermal effects from the accident could be detected at or below this temperature, and therefore the diagram shows only metallurgical observations for temperatures above this point. The lowest temperature indicator, above the stress relief temperature, was the ferrite–austenite transformation, which starts at 727 °C and is complete by about 830 °C. Variations in the typical as-fabricated hardness profile were evident when this temperature threshold was exceeded. The next indicator is the dissolution or dissipation of a dark feathery band at the interfact between the base metal and the stainless steel clad; this occurs between 800 and 925 °C, depending on the time. The next indicator of increasing temperature is the appearance of small equiaxed grains, which formed in the A 533 B steel adjacent to the interface at temperatures between 850 and 900 °C and disappeared between 1025 and 1100 °C as they were consumed by grain growth in the low-alloy steel. Grain growth in the A 533 B steel becomes significant above approximately 950 to 1075 °C, depending on the time involved. The highest temperature indicator shown on the diagram is the change in morphology of the δ-ferrite islands in the stainless steel cladding. In the approximate range of 975 to 1000 °C at 100 minutes or 1100 to 1125 °C at 10 minutes, the δ-ferrite islands begin to lose their slender branch-like morphology and become spherical. Additional details on how these indicators were used to estimate the TMI-2 vessel steel sample temperatures are provided in Ref. 6.

Temperatures in the hot spot were considerably higher than those in the surrounding region of the lower head.

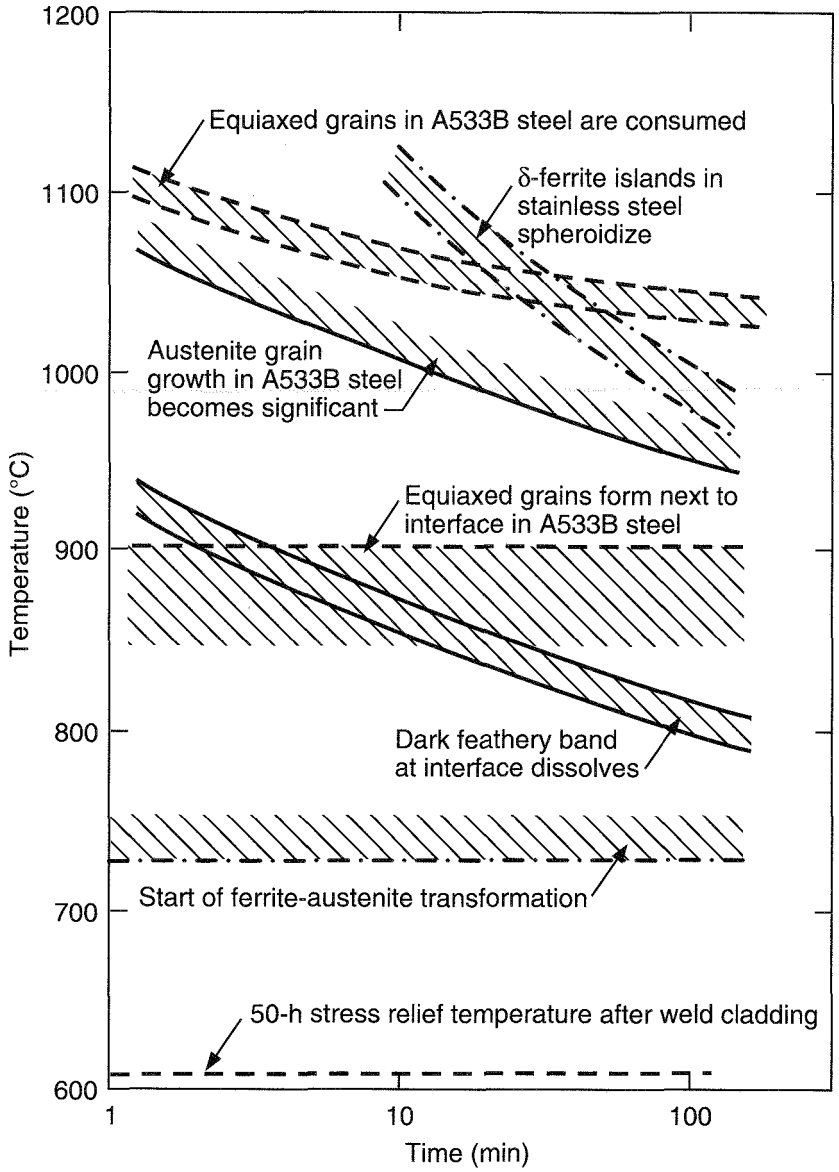

Fig. 4 Diagram of time–temperature observations of A 533 B pressure vessel steel clad with type 308L stainless steel.

Generally, the vessel temperature away from the hot spot did not exceed the 727 °C ferrite–austenite transformation temperature for the A 533 B pressure vessel steel. The results of metallographic and hardness examinations could determine whether the 727 °C transition temperature in the steel was exceeded. However, because microstructural and associated hardness changes in the steel do not occur below 727 °C, it was not possible to estimate how far below 727 °C the vessel steel temperature was away from the hot spot. Therefore there is a large uncertainty in the actual vessel steel temperature away from the hot spot. The temperature of the vessel inner surface in this region during the accident could have ranged from a minimum of 327 °C (normal plant operating conditions) to a maximum of 727 °C.

The hardness profiles of most of the TMI-2 samples had the typical characteristic profile of as-fabricated material, as shown in the shaded band in Fig. 5; but

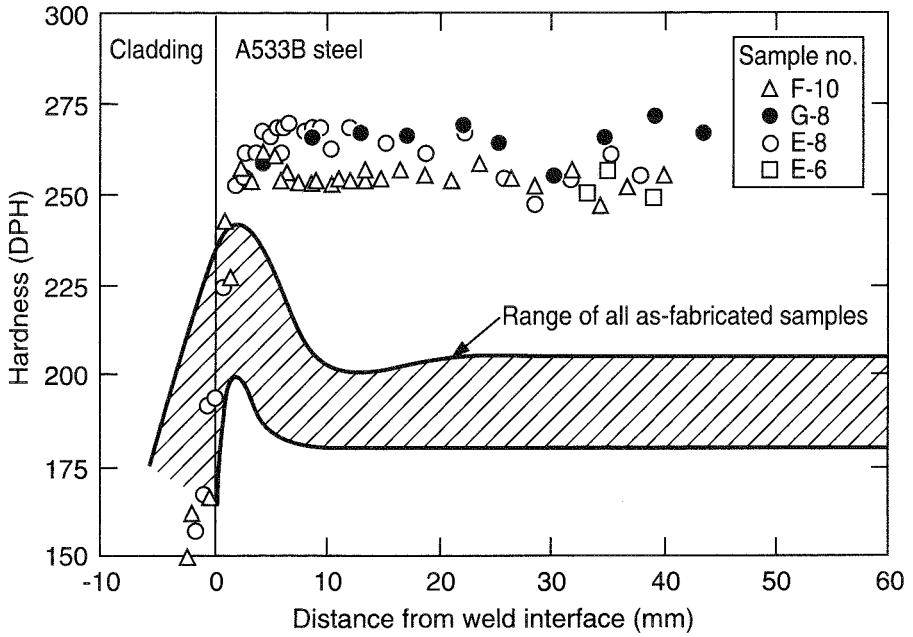

Fig. 5 Hardness profiles of samples F-10, G-8, E-8, and E-6 compared to the as-fabricated samples.

the hardness profiles from sample locations E-6, E-8, F-10, and G-8 (see Fig. 2) were markedly different from all other samples, as shown in this figure. In these four samples the characteristic hardness profile through the heat-affected zone near the clad weld interface had risen sharply to much higher levels and was then sustained throughout the full sample depth. Heat-affected bands from the weld cladding were not evident in these four samples but were completely eliminated by the thermal effects of the accident. Two other samples (H-8 and F-5) also showed anomalies in the hardness profiles. Results of these hardness profile measurements indicated which samples exceeded the 727 °C transformation temperature.

The steel examinations were also able to provide data on the cooling rate of the lower-head hot spot. Microstructural and hardness observations in the as-received state for two samples in the hot spot reflected the austenitizing heat treatment and the subsequent relatively rapid cooling of this material during the accident. Cooling rates were estimated to have been in the range of 10 to 100 °C/min through the transformation temperature. It was also determined that samples in the hot spot may have remained at their peak temperature for as long as 30 minutes before being cooled.

Mechanical property tests performed on the TMI-2 vessel steel samples produced a wealth of high-temperature mechanical property data. Results of these tests, along with observations of the samples, provided information on the postaccident condition of the lower head as well as input to the margin-to-failure analysis. Creep tests performed at 600 to 700 °C indicated no significant differences in behavior between samples that exceeded a maximum temperature of 727 °C and those which did not. Tensile tests for specimens that exceeded 727 °C showed significantly higher strengths at room temperature and at 600 °C when compared with those which did not exceed 727 °C. The tensile tests at lower test temperatures further confirmed the hardness measurements, which showed that the material from the hot spot had been austenitized and subsequently cooled rapidly.

During the sample removal effort, tears or cracks were found in the cladding of the vessel around three nozzles. ANL analyzed vessel steel samples containing these cracks and found that the cracks penetrated only superficially into the base metal. The cracks were attributed to hot tearing of the cladding caused by differential thermal expansion between the stainless steel cladding and the carbon steel vessel that occurred during vessel cooling. Furthermore, the presence of control assembly material (Zr, Ag, Cd, and In) within the cladding tears and intergranularly on the surface of some sample locations indicated that a layer of debris containing metallic material was already present on the lower head when the

major relocation of ceramic molten core material to the lower head took place at 224 minutes after the initial reactor scram.

NOZZLE EXAMINATIONS

Fourteen nozzles and two guide tube specimens were extracted from the vessel by being cut off as close to the lower head as possible. Four nozzles in the hot spot region were melted off almost flush with the vessel and could not be removed. The damage states of the nozzles and guide tubes and their location with respect to the hot spot are shown in Fig. 6.

The nozzles and guide tubes were removed and shipped to INEL; six were then shipped to ANL for examination. Examinations included micro and macro photography, optical metallography, scanning electron microscope measurements, gamma scanning, melt penetration measurements, and microhardness. There were two primary purposes for these examinations. First, these examinations would help to determine the extent of nozzle degradation to evaluate the thermal challenge to the lower head. Second, they would provide information on the movement of molten core material onto and across the lower head during the relocation. Portions from selected INEL nozzles and guide tubes were later sent to CEA Saclay, France, where similar examinations were performed.

Examinations performed on the nozzles and guide tubes, conducted primarily at ANL, provided insights

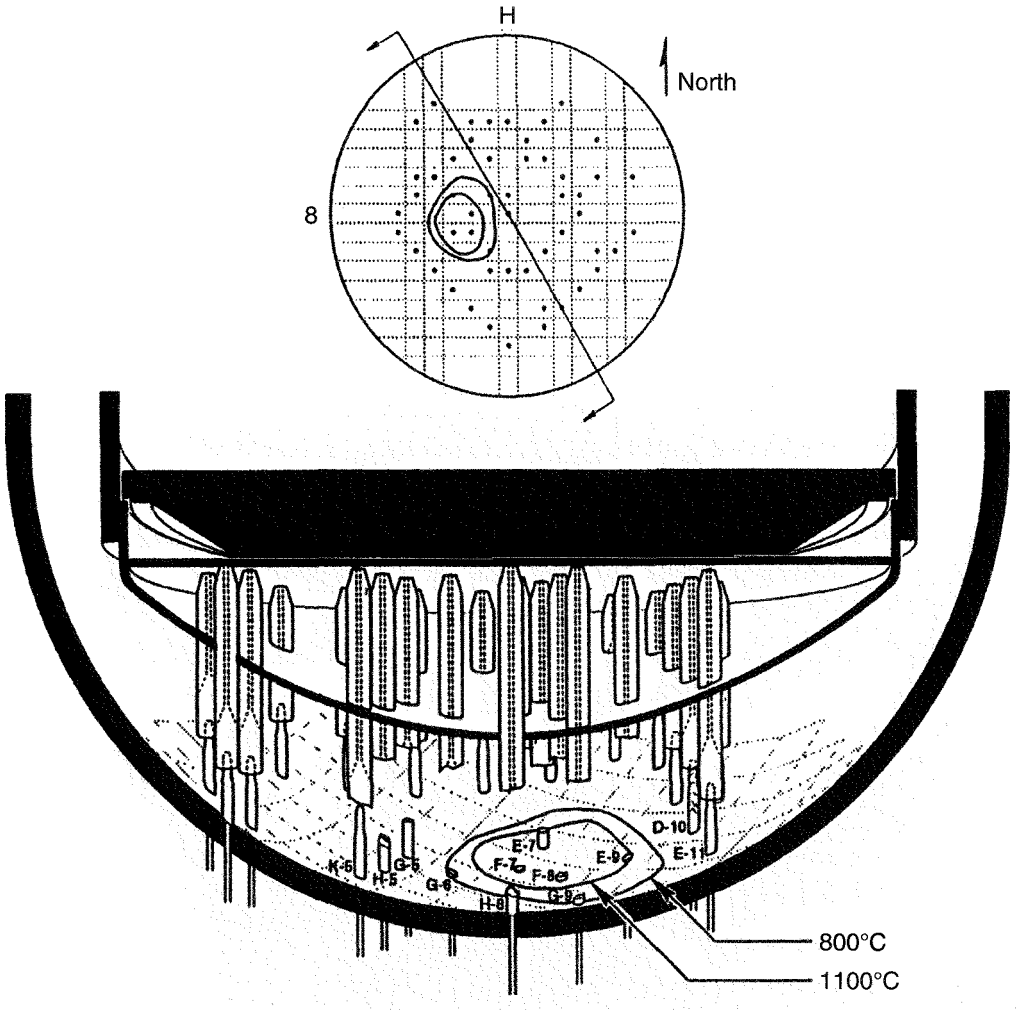

Fig. 6 TMI-2 lower head, southwest section.

into the accident progression. Damage to several nozzles indicated that their end-state condition was caused by molten core material coming in contact with the nozzles at an elevation ranging from 140 to 270 mm above the lower head. Surface scale found on the nozzles below their melt-off points suggested that this molten material flowed on top of a crust of preexisting solidified debris that had been cooled below its solidus temperature.

During the examinations it was estimated that nozzle temperatures varied widely as a function of location and elevation above the lower head. They ranged from 1415 °C, which is the Inconel 600 nozzle's liquidus temperature, to 1000 °C at elevations of 140 and 64 mm above the lower head, respectively. The penetration of debris downward into the nozzles was probably influenced by the temperature of the molten material at the time of entry, debris composition (and hence its fluidity), and the temperature of the nozzle itself. Temperature was found to greatly affect the solidification of molten debris and also the degree of interaction between the debris and the nozzle.

Examination results also indicated the presence of Zr and Ag–Cd on nozzle surfaces, which interacted with the material. The presence of this material indicated that control-rod material had relocated before the primary fuel relocation. The early movement of control material to the lower head was substantiated by the presence of control assembly material found in the cladding tears. However, it was not possible to determine the quantity of these materials that had relocated.

COMPANION SAMPLE EXAMINATIONS

The debris samples examined as part of the VIP were known as companion samples because they came from the hard layer that was in contact with the lower head. Hence they were "companions" to the lower-head steel samples. Results of the companion sample examinations were used to determine the debris composition and to estimate the lower-head decay heat load. During the defueling process, it was discovered that the hard layer was indeed extremely hard and had to be broken into pieces for removal. However, there was virtually no adherence of the material to the lower head itself. Because the hard layer had to be broken into pieces during sample acquisition, information on the sample location was limited to identifying the quadrant from which the sample was obtained.

The primary constituents of the companion samples were uranium, zirconium, and oxygen $(U, Zr)O_2$ with only small percentages (<1 wt%) of other structural material, such as Fe, Ni, and Cr. Control-rod materials such as Ag, In, and Cd were present in low (<0.5 wt%) concentrations. The average sample debris density was 8.4 ± 0.6 g/cm^3 with an average porosity of $18 \pm 11\%$. Overall, the examinations indicated that the companion samples were relatively homogeneous with small variations in composition and density.

On the basis of the debris composition, it is quite probable that the molten material reached temperatures greater than 2600 °C in the central core region before relocation. The temperature of the debris when it reached the lower head is not known. However, the material reached the lower head in a molten state, and results of the examinations suggest that portions of the debris cooled slowly over many hours.

Radiochemical examinations indicated that the primary radionuclides retained in the debris bed were medium and low volatile constituents. Almost all the radiocesium, radioiodine, and radioactive noble gases volatilized from the molten core before it relocated to the lower head. Knowledge of the retained fission products is critical to estimating the debris decay heat and the resulting heat load on the lower head. Decay heat calculations indicated an overall heat load of $0.13 \pm 20\%$ W/g of debris when the relocation occurred at 224 minutes after scram and $0.096 \pm 20\%$ W/g at 600 minutes after scram. At the time of relocation, the total decay heat load was approximately 2.47 MW for the estimated 19 000 kg of material that relocated to the lower head.

The average burnup of the TMI-2 core at the time of the accident was relatively low. If the accident had occurred with the core near its end of life, the debris would have had a higher decay heat load. Although more volatile fission products would be retained in higher burnup fuel, calculations indicate that the decay heat for relocated fuel from a full burnup core would increase by less than 20% above that for the TMI-2 accident for the time period of concern (i.e., the first 16 hours after reactor scram).[11] Such a change in decay heat level would not have significantly altered the results of the margin-to-failure analysis or the conclusions of the VIP.

MARGIN-TO-FAILURE ANALYSIS

The final element of the VIP, the margin-to-failure analysis, was performed to investigate mechanisms that could potentially threaten the integrity of the reactor

vessel and to help improve understanding of events that occurred during the accident. Analyses addressed mechanisms that could result in lower-head penetration tube and vessel failures. Specific failure modes examined were instrument tube rupture, tube ejection, localized vessel failure, and global vessel failure.

Margin-to-failure calculations relied upon three major sources of VIP examination data: (1) nozzle examination data for characterizing melt composition and penetration distances within instrument tubes; (2) companion sample examination data for characterizing debris properties (e.g., decay heat and material composition); and (3) vessel steel examination data for characterizing peak vessel temperatures, duration of peak temperatures, and vessel cooling rate.

The margin-to-failure analyses provided significant insights into potential failure mechanisms of the TMI-2 lower head. Results of these calculations eliminated tube rupture and tube ejection as potential failure mechanisms during the accident. Melt penetration results indicated that ceramic melt did not penetrate below the lower head, which effectively eliminated ex-vessel tube rupture as a failure mechanism. Analyses also indicated that the instrument tube weld would remain intact even if the peak reactor coolant system (RCS) pressure were conservatively assumed to occur at the same time the hot spot formed. As a result, tube ejection was also eliminated as a potential failure mechanism.

Calculations indicated that the magnitude and duration of hot spot temperatures estimated in TMI-2 vessel examinations could not have been caused by an impinging jet. Rather, hot spot temperatures were due to a sustained heat load from debris on the lower head.

Because of insufficient available data, it was not possible to come up with a best-estimate quantification of the margin to failure for global or local creep rupture of the lower head. Such failures would be associated with high temperatures on the lower head coincident with high reactor coolant system pressure. However, an extensive series of analyses and calculations was performed[10] with the best available information to try to scope the issue as described in the following text.

The potential for the vessel to experience a global failure was evaluated for temperature distributions obtained from thermal analyses with best-estimate and lower-bound input assumptions for such parameters as debris decay heat, outer vessel heat-transfer coefficient, and the debris-to-gap heat-transfer resistance. Calculations for both of these cases indicated that global failure caused by creep rupture was predicted to occur within the first 2 hours after debris relocation because of the sustained high vessel temperatures when the RCS was repressurized. This rise in RCS pressure occurred when the plant operators closed the block valve for the power-operated relief valve at 320 minutes after reactor scram.

Localized vessel failure analyses indicated that it is possible to withstand the 1100 °C hot spot temperatures for the 30-minute time period inferred from the vessel steel examinations provided that the rest of the vessel (i.e., outside the area of the hot spot) remained relatively cool. Localized calculations also indicated that the predicted time to vessel failure was reduced when a localized hot spot was superimposed on the calculated best-estimate background temperature (i.e., outside the hot spot).

Taken together, the localized and global vessel failure calculations indicated that the background vessel steel temperature behavior, which greatly depends on the heat load from the relocated debris in the lower head, was key to predicting failure from either of these mechanisms. Cool background vessel temperatures can potentially reduce structural damage and preclude global vessel failure even at high pressure and in the presence of a localized hot spot.

Thermal and structural analysis results were dominated by input assumptions on the basis of companion sample examination data, which suggested that the debris experienced relatively slow cooling over a period of many hours. However, differences between these analysis results and data from the vessel steel examinations indicated that the entire lower head cooled within the first 2 hours after debris relocation. An energy balance that considered coolant mass flows entering and exiting the vessel supported the hypothesis that the debris cooled in the time period between relocation and vessel repressurization.

Although there are insufficient data to quantitatively determine the exact mechanisms that caused this cooling, scoping calculations were performed to investigate possible mechanisms that could provide this cooling. In these analyses it was assumed that the simultaneous presence of cracks and gaps within the debris provided multiple pathways for steam release (e.g., water may travel down along the gap and boil up through cracks). Results of these calculations indicated that a minimal volume of cooling channels within the debris and a minimal size gap between the debris and the vessel could supply the cooling needed to obtain vessel temperatures and cooling rates determined in metallurgical examinations. Such cooling is not currently modeled in severe

accident computer codes. Also, there are uncertainties in models that estimate the cooling of debris as it breaks up and relocates to the lower plenum through water. Some questions also remain regarding the best failure criterion to be used for predicting vessel failure. However, the uncertainties in the amount of debris cooling on the lower head appear to be more significant for quantifying the margin to failure of TMI-2 vessel than either the vessel failure criterion or cooling of debris as it relocates to the lower plenum. Because of these uncertainties, results of the margin-to-failure analysis should be viewed as providing insights into areas such as identifying the failure mode with the smallest margin during the TMI-2 event and emphasizing areas in which additional research may be needed in severe accident analysis.

CONCLUSIONS

Through the efforts of the VIP signatories who supported the project, numerous significant contributions were made that dramatically increased both the understanding of the extent of damage to the vessel lower head and the margin of structural integrity that remained in the vessel during the TMI-2 accident. The principal results and conclusions from this project are summarized below.

- Vessel steel examinations indicated that a localized hot spot developed in an elliptical region approximately 1 m by 0.8 m. In this region, the maximum temperature of the ferritic steel base metal near the interface with the stainless steel cladding was approximately 1100 °C. The steel may have remained at this temperature for as long as 30 minutes before cooling occurred. Temperatures 0.45 cm into the 13.7-cm-thick wall were estimated to be 100 ± 50 °C lower than the peak surface temperatures. Away from the vicinity of the hot spot, lower-head temperatures did not exceed the 727 °C transformation temperature.
- Nozzle examinations and postaccident visual examinations indicated that the major lower-head relocation flow path for molten material was from the northeast and southeast quadrants of the vessel lower head toward the hot spot location in the western sector.
- Large margins to failure existed throughout the TMI-2 accident for the failure mechanisms of tube rupture and tube ejection. In fact, calculational results indicated that tube rupture and ejection can essentially be eliminated as potential failure mechanisms.
- Analyses results indicated that a localized effect, such as a hot spot, can shorten the overall vessel failure times caused by creep rupture. However, by itself it is unlikely to cause vessel failure for the temperatures and pressures that occurred in the vessel during the TMI-2 accident.
- Without modeling-enhanced cooling of the debris and lower head, the margin-to-failure scoping calculations indicated that lower-head temperature distribution based upon data from companion sample examination data would have resulted in vessel failure when the reactor system was repressurized by plant operators at about 300 minutes after reactor scram.
- Even though a definitive scenario describing the movement of molten debris and the formation of a localized hot spot cannot be determined, considerable evidence indicates that a debris layer containing both ceramic and metallic material insulated the lower head. The hot spot formed in a location where this layer had insufficient thickness to effectively insulate the lower head from the molten flow.

SIGNIFICANCE OF THE VIP FINDINGS

One of the most important implications of the VIP conclusions relates to accident management. The TMI-2 accident began with the main feedwater pumps' trip, an anticipated event. It was compounded by closure of the auxiliary feedwater system block valves, a human procedural error, and by the failure of the pressurizer relief electromatic valve to close after the proper relief of excessive primary system pressure, an electromechanical fault. The operator action of reducing the high-pressure safety injection system flow turned the event in a very serious direction. The operator had erroneously interpreted the indication of rising pressurizer water level to mean that the reactor coolant system was nearly filled with water, whereas in actual fact it was becoming a saturated system with steam formation caused by the loss of primary coolant. The operators failed to regain control of events in the first 100-minute period short of severe damage, which was the first opportunity for accident management. However, the operators were successful in discovering and opening the auxiliary feedwater system block valves early in this period, a necessary condition for final stabilization and recovery. In the intervening period of time since the TMI-2 accident, the total set of actions carried out to improve the interface between control room person and machine, to increase emergency safety system reliability, to develop emergency symptom-oriented procedures, and to improve reactor

operator training makes a repetition of such a failure very unlikely.

In the subsequent severe accident phase of TMI-2, the operators, though halting and inexperienced in an unknown field of reactor operations, were finally successful in stabilization and recovery. They isolated the stuck-open pressurizer relief valve and reactivated the high-pressure safety injection pumps, which were also necessary conditions, and thus enabled restoration of cooling water and heat removal in the primary system. This was the second and more difficult opportunity for accident management. The operators had cooling water and emergency power and pumps at their disposal, and they used them. The core was not cooled immediately when cooling water flow was restored. A crust surrounded the molten ceramic pool and prevented water from penetrating and cooling the material. The ceramic pool and surrounding crust continued to grow for about 25 minutes after high-pressure injection cooling water flow was restored until the crust broke through at its side at 224 minutes into the accident. The molten core material subsequently cooled after flowing to the vessel lower head. The experience at TMI-2 thus validates the importance of accident management and perseverance in a strategy of delivering cooling water. But it is also now clear as a result of the VIP that the reactor vessel provided a previously unrecognized defense in depth for a severe accident that was, of course, essential to success.

To pursue this point further, the VIP has also shown that global creep failure of the reactor vessel could occur under conditions of high vessel temperature and high pressure. Therefore accident management procedures should recognize the following: (1) the importance of cooling water not only for the reactor core but also for limiting the reactor vessel wall temperature and (2) the need for controlling pressure to avoid vessel creep failure. There should be here a word of caution about energetic fuel–coolant interactions (FCI) that could challenge pressure vessel integrity. We know that such an interaction did not occur at TMI-2 (Ref. 3), but some work on FCIs indicates an increased potential for triggering an FCI at low pressure.[13] Nevertheless, most experts today believe that depressurization should take priority over the FCI concerns. Work separate from the TMI-2 VIP is under way to address remaining questions about energetic FCIs.

As a follow-up to the TMI-2 VIP, additional research can confirm the conditions under which reactor vessel integrity is likely to be maintained during a severe accident. The cooling of the external reactor vessel, by flooding the cavity surrounding the lower part of the reactor vessel, could reduce the potential for reactor vessel failure. Analysis of the effects of ex-vessel cooling or plant-specific design features, such as vessel support structures or insulation that could restrict the flow of coolant or steam around the lower head, were not part of the VIP. However, several logical follow-on programs to the VIP, both internationally and at NRC, are currently under way or are in the planning stages to address reactor vessel failure issues. Additional research could also improve the understanding and quantification of the cooling of debris by water on the lower head.

The participants among the NEA-OECD countries examined the evidence, analyzed it, and reached conclusions about the accident as far as was possible. The international support and cooperation among the project participants, both technical and financial, helped make the TMI-2 VIP a success. For example, independent examinations of the vessel steel samples at laboratories around the world corroborated the estimated steel temperatures in the hot spot, which added credibility to the findings and conclusions of this project. Analysis of the accident shows that the TMI-2 reactor vessel was more robust than experts believed 15 years ago when the accident occurred and that this fact has broad implications for the accident management and safety of light-water reactors.

REFERENCES

1. *Spectrum*, 16 (11): 33 (November 1979).
2. *Spectrum*, 21 (4): 27 (April 1984).
3. J. M. Broughton, P. Kuan, D. A. Petti, and E. L. Tolman, A Scenario of the Three Mile Island Unit 2 Accident, *Nucl. Technol.*, 87 (1): 34-53 (August 1989).
4. *Agreement on the OECD Project to Investigate the Three Mile Island-2 Pressure Vessel*, OECD Document EN/S/1480, July 1988.
5. *Removal of Test Specimens from the TMI-2 Reactor Vessel Bottom Head, Project Summary*, Phase 4 Status Report MPR-1195, October 1, 1990.
6. G. E. Korth, *Metallographic and Hardness Examinations of TMI-2 Lower Pressure Vessel Head Samples*, Report NUREG/CR-6194 (EGG-2731), March 1994.
7. D. W. Akers, S. M. Jensen, and B. K. Schuetz, *Examination of Relocated Fuel Debris Adjacent to the Lower Head of the TMI-2 Reactor Vessel*, Report NUREG/CR-6195 (EGG-2732), March 1994.
8. L. A. Neimark, T. L. Shearer, A. Purohit, and A. G. Hins, *TMI-2 Instrument Nozzle Examinations at Argonne National Laboratory*, Report NUREG/CR-6185 (ANL-94/5), March 1994.
9. D. R. Diercks and L. A. Neimark, *Results of Mechanical Tests and Supplementary Microstructural Examinations of the TMI-2*

Lower Head Samples, Report NUREG/CR-6187 (ANL-94/8), April 1994.
10. L. A. Stickler et al., *Calculations to Estimate the Margin to Failure in the TMI-2 Vessel*, Report NUREG/CR-6196 (EGG-2733), March 1994.
11. J. R. Wolf et al., *TMI-2 Vessel Investigation Project Integration Report*, Report NUREG/CR-6197 (EGG-2734), March 1994.
12. D. W. Akers and B. K. Schuetz, *TMI-2 Nozzle Examinations Performed at the Idaho National Engineering Laboratory*, Report NUREG/CR-6198 (EGG-2735), March 1994.
13. N. Yamano, J. Sugimoto, Y. Maruyama, and K. Soda, Studies on Fuel–Coolant Interactions During Core Melt Accident of Nuclear Power Plants, in *Proceedings of the CSNI Specialists Meeting on Fuel-Coolant Interactions*, Report NUREG/CP-0127 [NEA/CSNI/R-(93)8] (CONF-930157-), pp. 271-281, March 1994.

Relocation of Molten Material to the TMI-2 Lower Head[a]

By J. R. Wolf,[b] D. W. Akers,[b] and L. A. Neimark[c]

Abstract: *This article presents one possible scenario describing the relocation of debris to the lower head of the Three Mile Island Nuclear Station Unit 2 (TMI-2) reactor vessel and is based on available plant instrumentation records and postaccident examination results. The scenario presented here is not the only potential debris relocation scenario, but it is consistent with information obtained from plant data, Vessel Investigation Project examinations, analysis efforts, and other TMI-2 programs. This scenario addresses debris relocation events chronologically and assesses factors that may have contributed to the end-state condition of the lower head, the damage to the structures in the lower part of the reactor vessel, and the debris on the lower head. Included is the initial movement of molten material from the core, through the reactor vessel core support assembly to the lower internals, and finally onto the lower head.*

INITIAL EVENTS

The initial event that affected the relocation scenario was the melting of control and fuel rods that occurred between 100 and 174 minutes when the upper half of the core was uncovered.[1] During this period, fuel-rod cladding, control-rod cladding, and metal melted and drained down through the uncovered core and thus left intact fuel-pellet stacks and rubble. The cladding material flowed down through the core to form a metallic crust 10 to 15 cm thick at the lower core region.[2] This lower bound was at the water level near the lowest grid spacer and approximately 20 cm from the bottom end of the fuel rods. The water level was approximately 2 m above the lower head, which was the lowest level during the entire accident.

At 174 minutes, the 2B coolant pump was activated for 19 minutes. However, significant flow through the core lasted only for about 15 seconds before the reactor coolant system repressurized. This repressurization was due to Zircaloy oxidation and steam formation in the upper core debris bed, which was caused by injection of relatively cool water by the 2B pump. Jets of steam from this event caused damage to the southern and northern portions of the upper fuel assembly grid and transported debris to the top of the upper plenum,[3,4] onto lead-screw surfaces,[5,6] and onto several other horizontal surfaces in the reactor vessel.[7] Examinations of the upper core debris indicated that the control-rod materials (Ag–In–Cd) were concentrated in particles smaller than 1 mm and would thus be susceptible to transport as a hydrosol.

As discussed in Ref. 6, the overall upper core debris region was composed of about 27 000 kg of material. Between 3 and 10% of this debris was less than 1 mm in diameter. Because particles less than 1 mm may be

[a]This work was supported by the U.S. Nuclear Regulatory Commission in conjunction with the Organization for Economic Cooperation and Development, through DOE Contract DE-AC07-76IDO1570.

[b]Idaho National Engineering Laboratory, EG&G Idaho, Inc., P.O. Box 1625, Idaho Falls, ID 83415-3840.

[c]Argonne National Laboratory, 9700 South Cass Avenue, Argonne, IL 60439.

transportable as a hydrosol, quantities of loose debris from both control and fuel rods either settled directly in the lower part of the reactor vessel during quiescent periods or were transported through the reactor coolant loop by the 2B pump transient and settled in areas such as the lower head, where there was relatively low flow. Therefore, finding intergranular Ag–In–Cd in the surfaces of several nozzles and in the vessel cladding cracks should not be unexpected. Unfortunately, the amount of such material and the depth of the deposition layer on the lower head cannot be definitely determined.

RELOCATION TO THE LOWER HEAD

Between 224 and 226 minutes, several almost simultaneous events indicated that a major change in core configuration occurred and molten material relocated to the lower head in one continuous flow. The count rate of the neutron source-range monitor located on the outside of the reactor vessel increased sharply. Also, the simultaneous alarm of in-core self-powered neutron detectors (SPNDs) at all levels on the same instrument stalk suggested that a common point of damage occurred. The molten material in the lower head heated the instrument nozzles sufficiently to produce thermoelectric currents in the SPNDs, which caused the instruments to set off an alarm. Examination of the alarm data[8] indicated that the first alarms were for SPND stalks in instrument tubes on the east side of the lower vessel and then propagated to the center. Postaccident measurements of in-core thermocouple loop resistance, as discussed in Ref. 8, indicated that new thermocouple junctions were formed in the lower head as the leads were melted by high temperatures caused by the relocated fuel. The new junctions also resulted in alarms of several of the in-core thermocouples. The alarms followed a sequence similar to the SPNDs. A primary system pressure pulse (2 MPa) also occurred during this time period. These data indicate the time when the relocation occurred and that it initiated in the eastern part of the core and lower head.

Movement of Molten Material Through the Vessel

Postaccident examinations of the eastern half of the core region and lower vessel internals confirmed plant instrumentation data and showed that relocation of the fuel debris to the lower head occurred in the eastern half of the vessel. Overall, about 19 metric tonnes of material reached the lower head. As discussed in Sec. 5, the relocated material was primarily a $(U,Zr)O_2$ ceramic. Visual examinations of this part of the vessel during defueling indicated that the primary path through the vessel was through a hole melted in the R6 vertical core-former wall and then downward through the horizontal baffle plates. Figure 1 shows a cross section of the reactor

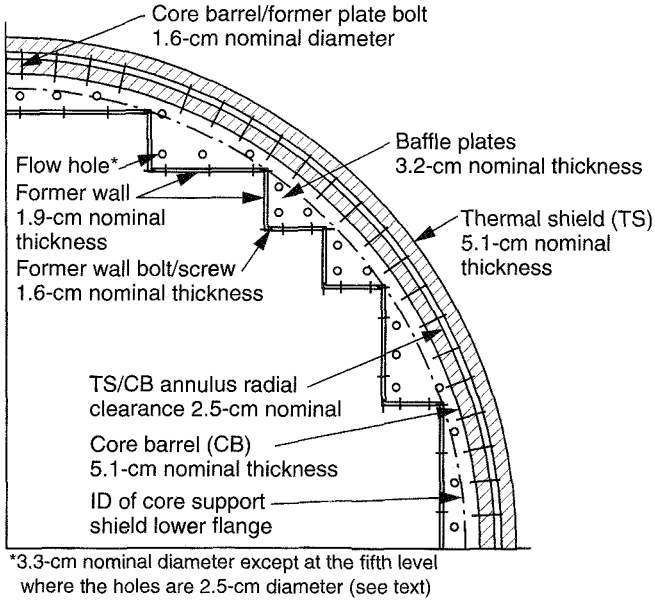

Fig. 1 Reactor vessel internal structure.

vessel internal structure. Fuel melt was found in the P-5 and R-6 assemblies near the bottom of the fuel assemblies, which indicated that some liquefied fuel had drained into these assemblies and solidified during the relocation. Because no flow path was found through these assemblies to the lower head, however, the principal relocation path was identified as being through the damaged core former at the R-6/P-5 core locations. Three holes in the core-former wall were identified. Dimensions of the holes through the former wall ranged from 23×3 cm to 20×7 cm.[9,10] The damage to the core-former wall was approximately 140 cm from the bottom of the core, or a little below the midpoint of the reactor core. The damage location is indicated in Fig. 2.

Movement of Molten Debris Through the Core Support Assembly

At the bottom of the vertical core-former plates, the molten material melted back into the lower core support assembly (CSA). Visual observations indicate a massive hole and damage in the bottom on the vertical core-former wall located at core grid locations R-6, R-7, P-4, and P-5.

It is very difficult to trace the exact path the molten material took as it moved through the CSA structures. The flow movement scenario presented here is based on evidence derived from the assumption that the presence of flow holes plugged with solidified material indicates that molten material flowed through these holes or adjacent holes during the relocation. Once a hole was plugged with solidified material, any subsequent material that flowed in that area was most likely diverted by the plug and flowed downward through an adjacent hole.

The CSA geometry consists of a number of plates and forging, as shown in Fig. 3. Once in the CSA, the majority of the molten material continued to flow down through the structures on the eastern periphery in the R-6/7 and P-4/5 areas. However, visual examinations indicated that some of the molten material was found to have flowed around the perimeter of the CSA structures as it penetrated downward toward the lower head. Figure 4 shows the location of solidified material at several locations in the flow holes of the lower grid, the area between the lower grid and the flow distributor plate, and between the flow distributor plate and the grid forging. The presence of solidified material is assumed to indicate that molten material flowed through or adjacent to these locations.

Molten Debris Movement on the Elliptical Flow Distributor

On the basis of the locations of solidified material in the CSA as shown in Fig. 4, it is postulated that the molten material flowed onto the elliptical flow distributor

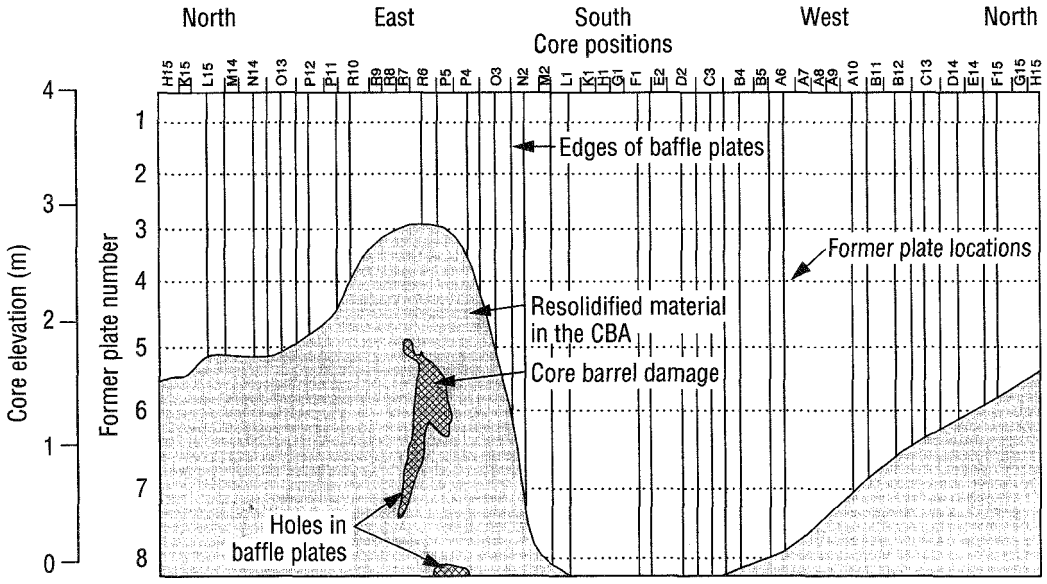

Fig. 2—Fuel debris profile inside core former (laid flat). CBA is core barrel assembly.

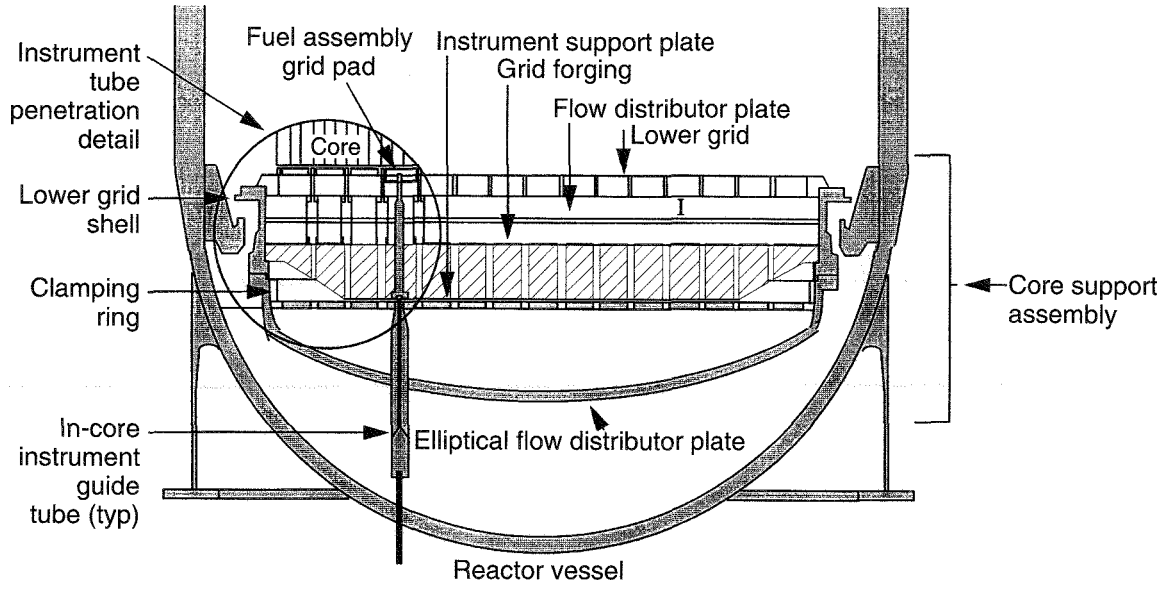

Fig. 3—TMI-2 core support assembly.

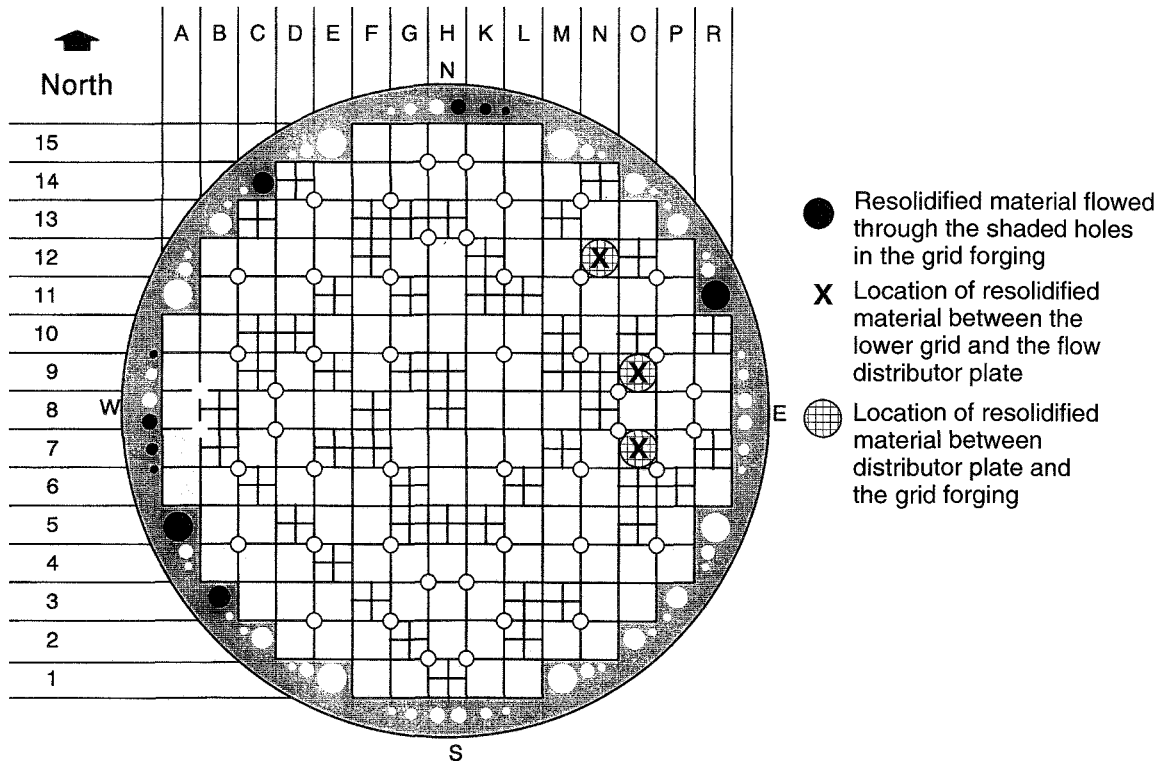

Fig. 4—Solidified material in core support assembly.

(EFD) from the same areas where plugged flow holes existed in the CSA. Figure 5 indicates the locations in the EFD where solidified material was observed in or above a flow hole.[11,12] As shown in the figure, these locations are in general agreement with the locations in Fig. 4, where solidified material was observed in the CSA. As shown in Figs. 4 and 5, many of the plugged flow holes line up quite well, which indicates that the flow moved vertically downward and covered much of the periphery of the CSA structure as it followed the flow hole alignment pattern onto the EFD; for example, the plugged holes near locations H-15, K-15, and L-15 shown in Fig. 4 are near plugged locations H-15, K-15, and K-14 shown in Fig. 5. Also, the plugged holes in location C-14 shown in Fig. 4 are near the plugged holes in locations D-13 and D-14 shown in Fig. 5.

The minimal amount of damage on the EFD suggests that the first material that reached the EFD, and subsequently the lower head, was probably relatively cool. The exact temperature depends on both the amount of heat given up by the molten flow before it reached the EFD and the exact composition of the molten flow. As the flow moved downward toward the EFD and eventually the lower head, heat was lost to the melting of core-former structures and to water that filled the lower plenum region. If lower temperature phases were present in the molten material, especially in the initial portion of the flow that would tend to incorporate melted structural material, it would be possible for this material to be mobile at temperatures below the solidus temperature of $(U,Zr)O_2$. Microstructural and microchemical examinations of portions of the loose debris that were removed from the lower head before the Vessel Investigation Project (VIP)[13,14] indicate that eutectic structures present in grain boundary phases could have had a solidus temperature that was considerably lower than that of the bulk $(U,Zr)O_2$ material. This low melting point compared with that of the bulk material suggests that the grain boundaries may have remained liquid after the grains themselves had solidified. This would have allowed

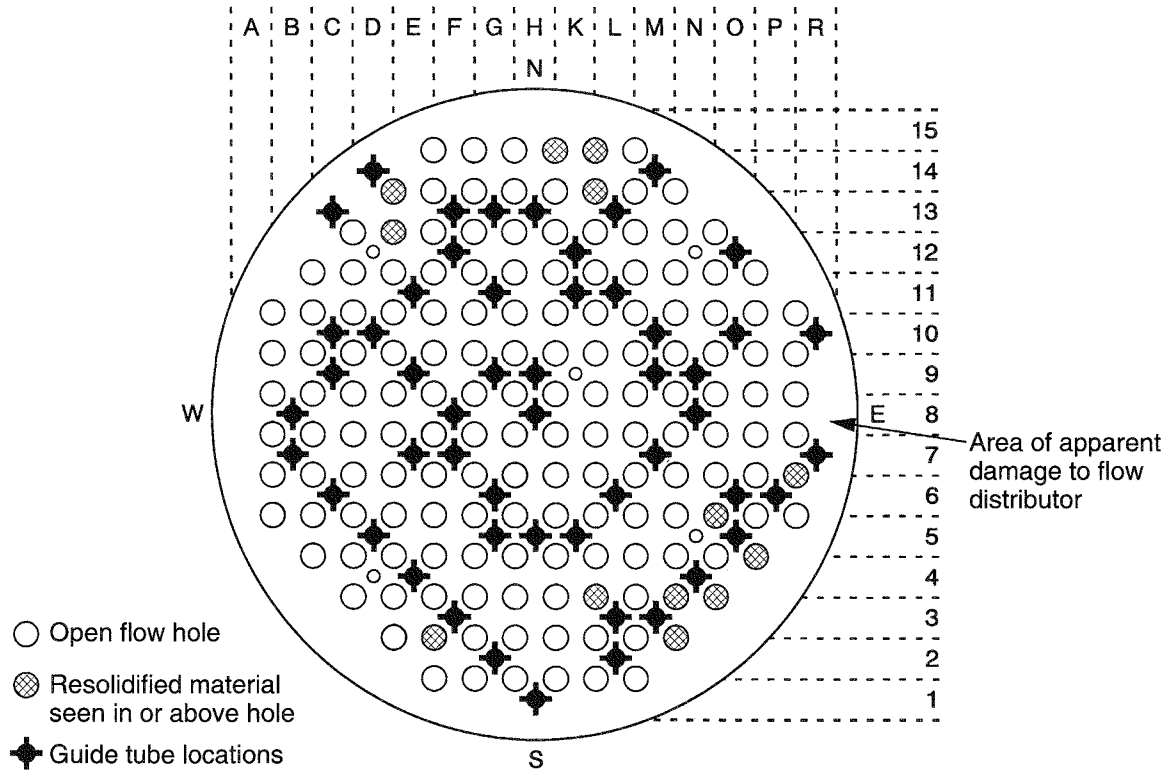

Fig. 5. Solidified material in the elliptical flow distributor.

portions of the molten relocation flow to remain mobile at temperatures below the bulk $(U,Zr)O_2$ solidus temperature.

Some of the molten material solidified on the EFD and formed plugs in the flow holes at locations shown in Fig. 5. The subsequent flow of material was probably diverted by the plugged holes and dropped onto the lower head from several different locations around the periphery of the EFD.

Movement of Molten Debris on the Lower Head

One of the most puzzling questions of the VIP has been why the molten material that relocated to the lower head did not do more damage to the vessel itself and why some nozzles were completely buried in solidified debris but showed absolutely no damage while others were almost totally destroyed. It is postulated that, when the initial portion of the continuous relocation flow reached the lower head, the combination of the heat sink provided by the nozzles and the vessel lower head itself, along with insufficient thermal energy in the molten flow, cooled and rapidly froze the initial portion of molten material that reached the lower head. This made it possible for the rapid formation of a thick ceramic crust regardless of the temperature of the molten material. The rapid buildup of this crust resulted in the formation of an insulating ceramic layer that covered much of the lower head and also formed around many nozzles. Wherever the lower head and nozzles were covered by this insulating debris layer, they were protected from thermal damage.

As the initially cooler material fell onto the lower head from several different locations around the periphery of the EFD, the material effectively formed a cup-shaped basal crust structure that served to insulate the lower-head structures in these areas. Then hotter material flowed downward across the top of this basal crust and caused the nozzle damage pattern shown in Fig. 6. The pattern of nozzle damage indicates that multiple flow paths existed, and the movement of molten material onto and across the lower head was not one massive unified flow.

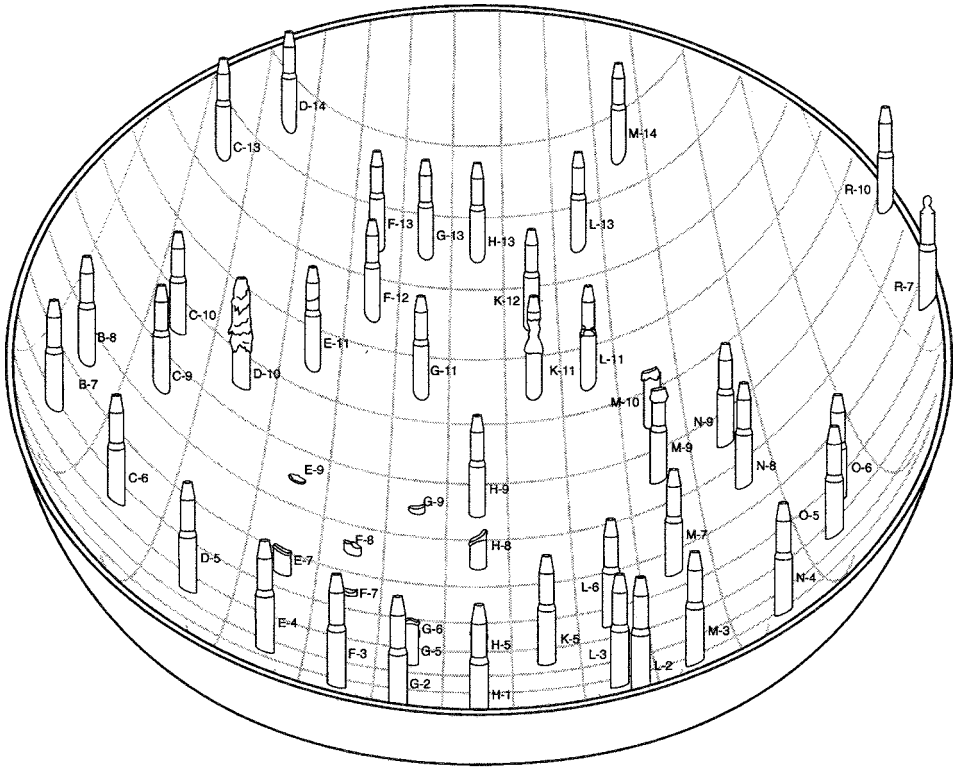

Fig. 6—Nozzle damage profile.

The pattern of nozzle degradation observed at elevated levels for several nozzles is shown in Fig. 6 and indicates the extent of the insulating ceramic debris layer that formed in the lower head and protected many of the nozzles and the lower head from extensive thermal damage. As the flow moved on top of the initial insulating debris layer, newly exposed molten fuel came in contact with the nozzles at elevated levels. These nozzles were melted at an elevation that is thought to be representative of the bottom of the molten fuel flow. Since the molten material flowed on top of the initial debris layer, this height is also representative of the thickness of insulating material that protected the lower head and the lower portions of many nozzles. As an example, examinations showed that the nozzle damage at M-9 was at about 25 cm above the lower head, and the damage to H-5 was about 15 cm above the head. Damage to nozzles around the M-9 and H-5 core locations, which have damage at elevations above the base of the nozzles, suggests that the insulating layer was about 25 cm thick at the M-9 location and 15 cm thick at H-5.

As the hotter molten material flowed across the top of the insulating ceramic debris layer, the cup-shaped structure that had initially formed on the lower head began to be filled. In the end, this resulted in what is known as the hard debris layer, which is shown in Fig. 7.[15] The debris depths shown in this figure were determined from mechanical probing of the hard layer during the defueling operation.

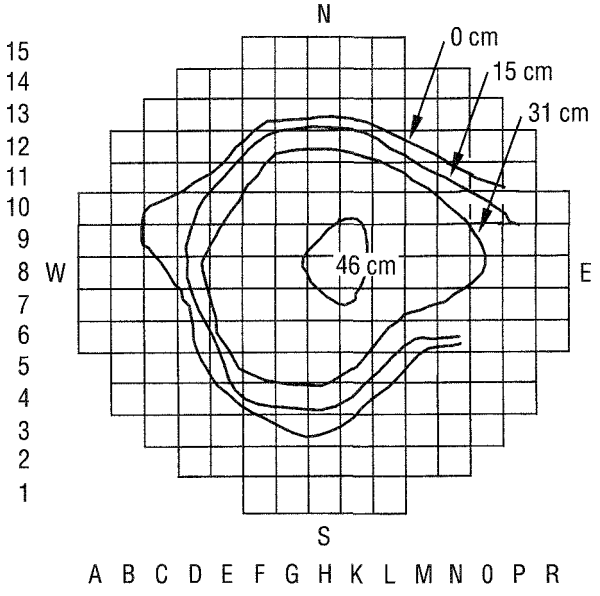

Fig. 7 Hard-layer debris depth. (Contour lines represent incremental increases. The outside line is equal to a depth of 0 cm and the inside is equal to a depth of 46 cm.)

The last material to flow onto the lower head was what is known as the loose debris layer. The depths of the loose debris layer are shown in Fig. 8 and were determined before the defueling effort began.[16,17] The depths were determined by probing examinations and by analysis of videotapes taken of the lower-head debris. Figures 9, 10, and 11 show cross sections of the thickness of the hard debris layer at several representative locations. As shown in these figures, relatively steep cliff-like areas occur along the periphery of the debris bed, and both full-length and damaged nozzles are embedded in the debris.

Formation of the Hot Spot

In addition to damaging the nozzles on the lower head, the flow of the hotter molten material may have also resulted in the formation of the localized lower-head hot spot. It is postulated that, as the hotter material flowed down the sides of the cup-like shape that was formed by the initial insulating crust toward the bottom of the vessel, the insulating layer crust became progressively thinner. Eventually, the flow of hotter material reached an area where the basal crust thickness was insufficient to adequately insulate the lower head, and a localized hot spot formed. The location of the hot spot on the lower head is shown in Fig. 12.

The hypothesis that the hot spot occurred beneath a crust that was of insufficient initial thickness to protect the lower head is consistent with the observation that the deepest debris was found in other locations of the vessel rather than over the hot spot. A progressively thinner crust was also indicated by data from the nozzle examinations, which showed that more of the nozzle length was melted in the vicinity of the hot spot. The region where the most severe nozzle damage occurred was consistent with the location of the hot spot and indicated that the insulating layer was thinnest in this area.

COOLING OF THE LOWER HEAD

Metallurgical examinations conducted as part of the VIP indicated that at the hot spot location the lower head was heated to peak temperatures of approximately 1100 °C and indicated that the temperature was maintained at that level for approximately 30 minutes before cooling rapidly (50 °C/min).[18]

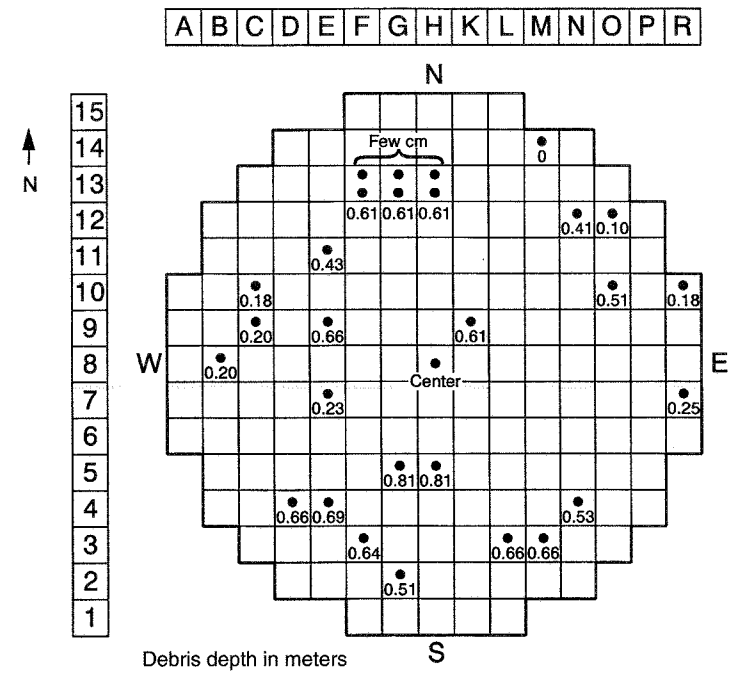

Fig. 8 End state hard- and loose-layer debris configuration.

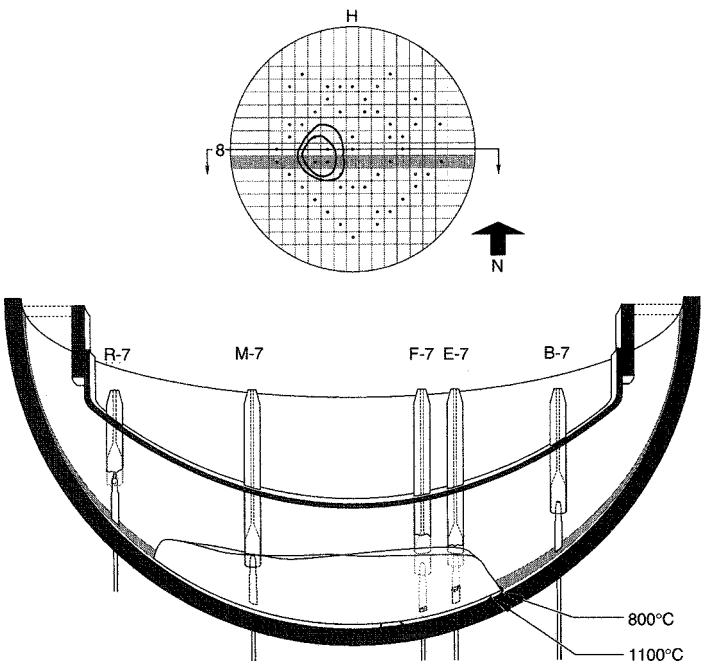

Fig. 9 TMI-2 lower-head cross section of hard debris, row 7.

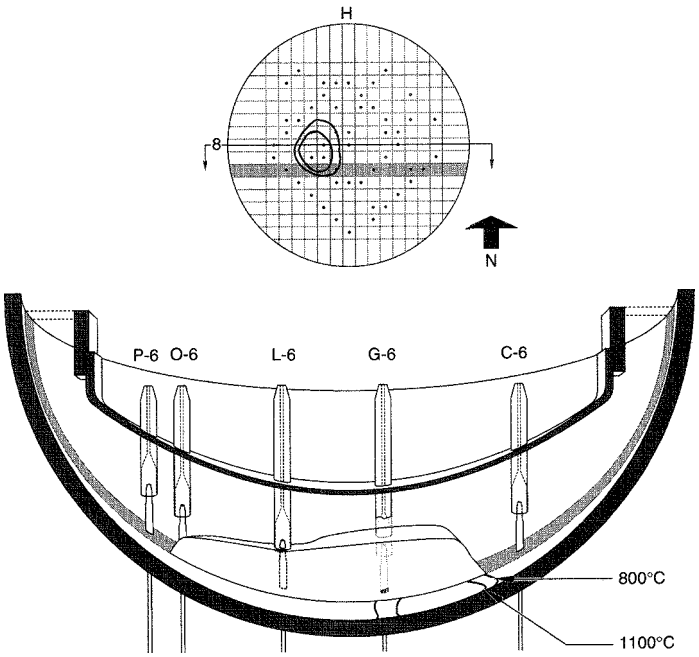

Fig. 10 TMI-2 lower-head cross section of hard debris, row 6.

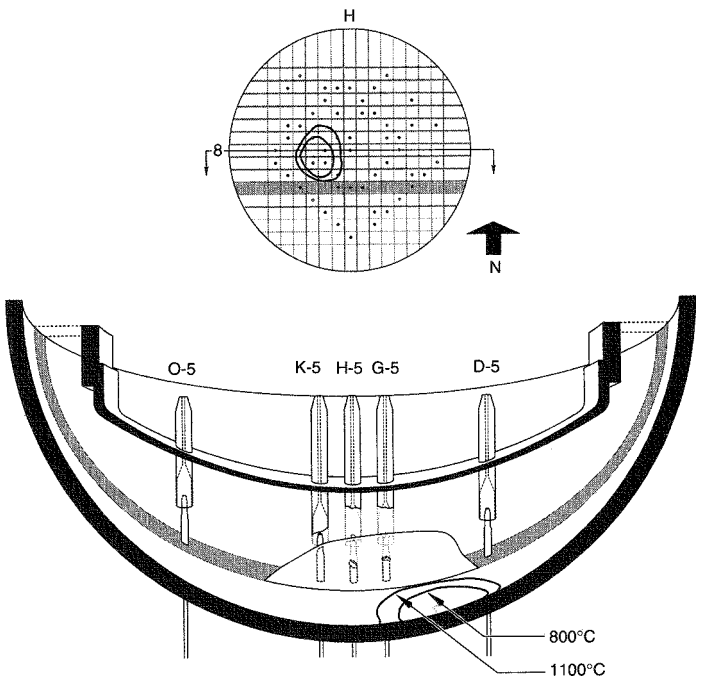

Fig. 11 TMI-2 lower-head cross section of hard debris, row 5.

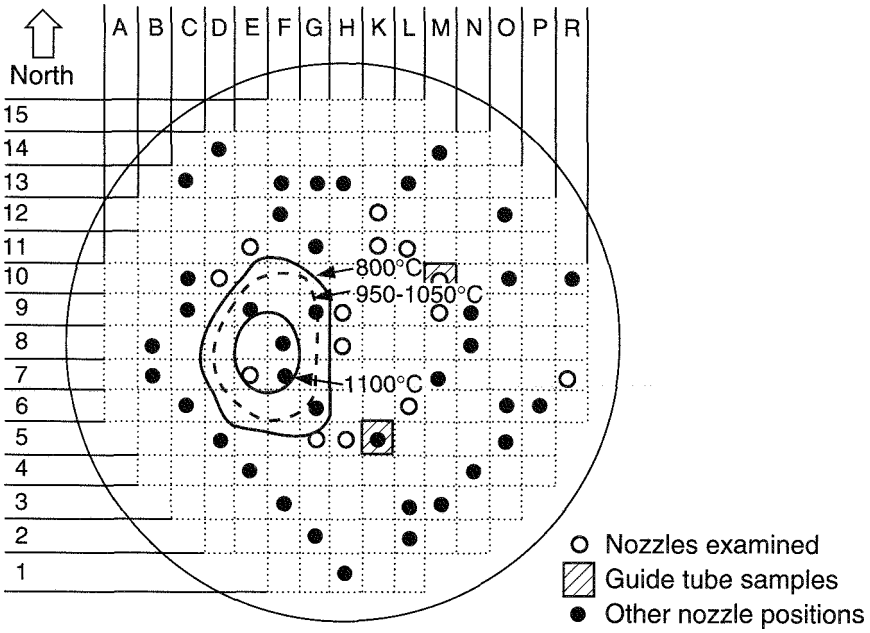

Fig. 12 Lower-head hot spot and nozzle–guide tube locations.

The mechanism responsible for the postulated rapid cooling of the lower head after 30 minutes has not been adequately explained. One proposed mechanism for this rapid cooling is the presence of interconnected flow channels within the debris and between the vessel and the debris layer. A considerable period of time (up to 30 minutes) would be required to adequately cool the peripheral portions of the debris before water could penetrate to the hot spot location. Upon penetration of water through gaps between the debris and the vessel wall, the vessel steel could have cooled rapidly, as indicated by the metallurgical examinations.

RELOCATION SCENARIO CONCLUSIONS

A scenario has been postulated on the basis of available plant instrumentation records and postaccident examination results. Although it is recognized that this scenario is not the only potential relocation scenario, it is consistent with information from plant data, VIP examinations, and analysis efforts. Key points of the scenario discussed in this section are:

- Relocating molten fuel flowed down through the core support assembly and onto the elliptical flow distributor plate.
- The initial molten fuel flow plugged holes around the periphery of the elliptical flow distributor plate and thus caused molten material to relocate from this plate to the lower head at several locations.
- The initial molten debris on the lower head cooled rapidly and formed an insulating layer of variable thickness that protected the lower head and many of the nozzles from damage.
- The pattern of molten material deposition on the lower head resulted in most of the vessels being insulated and protected from thermal damage. In the area just to the west of center (E-7, E-8, and F-8), however, the insulating layer was not sufficiently thick to protect the lower head, and thus a localized hot spot was produced.
- Effects, such as porosity in the insulating debris bed and cracking that occurred as the basal crust was formed, allowed water to penetrate into the debris bed to maintain some cooling.
- The hot spot remained hot for 30 minutes until water penetrated to the lower head between the crust and the vessel wall and caused rapid cooling of the vessel steel.

REFERENCES

1. J. M. Broughton, P. Kuan, D. A. Petti, and E. L. Tolman, A Scenario of the Three Mile Island Unit 2 Accident, *Nucl. Technol.*, 87(1): 34-53 (August 1989).

2. D. W. Akers and R. K. McCardell, Core Materials Inventory and Behavior, *Nucl. Technol.*, 87(1): 214-223 (August 1989).
3. EG&G Idaho, Inc., *Quick Look Inspection: Report on the Insertion of a Camera Into the TMI-2 Reactor Vessel Through a Leadscrew Opening*, Report GEND-030, Vols. 1 and 2, March/April 1983.
4. M. L. Russell, *TMI-2 Core Cavity Sides and Floor Examinations*, Report GEND-INF-074, EG&G Idaho, Inc., December 1985 and January 1986.
5. K. Vinjamuri, D. W. Akers, and R. R. Hobbins, *Examination of H8 and B8 Leadscrews from Three Mile Island Unit 2*, Report GEND-INF-052, EG&G Idaho, Inc., September 1985.
6. D. W. Akers, E. R. Carlson, B. A. Cook, S. A. Ploger, and J. O. Carlson, *TMI-2 Core Debris Grab Samples—Examination and Analysis*, Report GEND-INF-075, EG&G Idaho, Inc., September 1986.
7. V. R. Fricke, *Quick-Look Inspection Results*, GPU Technical Report TPO/TMI-026, Rev. 0, December 1982.
8. P. Kuan, *Core Relocation in the TMI-2 Accident*, Report EGG-TMI-7402, November 1986.
9. S. Bokharee, *Fuel Debris in Region Between Core Former Baffle Plates and Core Barrel*, TMI-2 Technical Bulletin TB 87-9, May 12, 1987.
10. S. Bokharee, *Fuel Debris in Region Between Core Former Baffle Plates and Core Barrel*, TMI-2 Technical Bulletin TB 87-9, Rev. 1, July 9, 1987.
11. GPU Nuclear, Inc., Color Inspection of E/SE Core Former Region After Defueling Former Plates 6, 7, 8, LGRS, VHS video, October 26, 1987.
12. G. R. Eidam, E. L. Tolman, J. M. Broughton, R. K. McCardell, and W. R. Stratton, TMI-2 Defueling Conditions and Summary of Research Findings, in *Proceedings of the International Symposium on Severe Accidents in Nuclear Power Plants, Sorrento, Italy, March 21–25, 1988*, Report CONF-880309-6, 1988.
13. P. Hofmann, S. J. L. Hagen, G. Schanz, and A. Skokan, Reactor Core Material Interactions at Very High Temperatures, *Nucl. Technol.*, 87(1): 146-186 (August 1989).
14. R. V. Strain, L. A. Neimark, and J. E. Sanacki, Fuel Relocation Mechanisms Based on Microstructures of Debris, *Nucl. Technol.*, 87(1): 187-190 (August 1989).
15. V. R. Fricke, *Reactor Lower Head Video Inspection—Phase II*, TMI-2 Technical Bulletin TB-86-3, January 8, 1986.
16. J. Adams and R. Smith, *TMI-2 Lower Plenum Video Data Summary*, Report EGG-TMI-7429, July 1987.
17. M. L. Russell and R. K. McCardell, Three Mile Island Unit 2 Core Geometry, *Nucl. Technol.*, 87(4): 865–874 (December 1989).
18. G. E. Korth, *Metallographic and Hardness Examinations of TMI-2 Lower Pressure Vessel Head Samples*, Report TMI V(92)EG01, OECD-NEA-TMI-2 Vessel Investigation Project, January 1992.

Insight Into the TMI-2 Core Material Relocation Through Examination of Instrument Tube Nozzles[a]

By L. A. Neimark[b]

Abstract: *The examination of instrument penetration tube nozzles removed from the lower head of the Three Mile Island Nuclear Station Unit 2 (TMI-2) reactor provided key information on the manner in which core debris relocated to and across the lower head. The examinations included visual inspections, gamma spectroscopy, metallography, microhardness measurements, and scanning electron microscopy. The examination results showed varying degrees of damage to the lower-head nozzles from ≈ 50% melt-off to no damage at all to nearby nozzles. The elevations at which nozzle damage occurred suggest that the lower elevations (near the lower head) were protected from molten fuel, apparently by an insulating layer of debris that had cooled and solidified when it reached the lower head. The pattern of nozzle damage suggests fuel movement toward the hot spot location in the vessel wall. Evidence was found for the existence of control assembly debris on the lower head before the massive relocation of fuel occurred.*

The 1979 accident at the Three Mile Island Nuclear Station Unit 2 (TMI-2) reactor resulted in the relocation of approximately 19 000 kg of molten core material to the lower head of the reactor vessel.[1] This material caused extensive damage to the instrument guide tubes and nozzles and was suspected of having caused significant metallurgical changes in the lower head itself. These changes and their effect on the margin to failure of the lower head became the focal point of an investigation cosponsored by the U.S. Nuclear Regulatory Commission (NRC) and the Organization for Economic Cooperation and Development (OECD). The TMI-2 Vessel Investigation Project (VIP) was formed to determine the metallurgical state of the vessel at the lower head and to assess the margin to failure of the vessel under the conditions existing during the accident. The material in this article was developed under the VIP.

Under the auspices of the VIP, MPR Associates, Inc., removed specimens of the reactor vessel in February 1990.[2] In addition to these specimens, 14 instrument nozzle segments and 2 segments of instrument guide tubes were retrieved for metallurgical evaluation. The purposes of this evaluation were to provide additional information on the thermal conditions on the lower head that would influence the margin to failure and to provide insight into the progression of the accident scenario, specifically the movement of the molten fuel across the lower head.

Six of the instrument nozzle segments were examined at the Illinois site of Argonne National Laboratory (ANL)[3] and eight were examined at the Idaho National Engineering Laboratory (INEL).[4] The examinations at the two laboratories were complementary in that both laboratories received segments from different areas of the lower head which were representative of the range of damage that occurred to all the nozzles. Thus, from the nozzles that were examined in detail at ANL and from complementary data from INEL, it was possible to construct a scenario for the movement of the fuel debris across the lower head and to even obtain insight into how and where the fuel debris impacted on the lower head.

The original scope of the nozzle examinations at both ANL and INEL was geared to provide information that would aid in evaluating the thermal conditions of the lower head and thus aid the analysis of the thermal–mechanical state of the vessel and establish its margin to failure. To this end, the objectives of the examination were to (1) estimate peak temperatures of the nozzles from their metallurgical end state; (2) determine the mechanisms, modes, and extent of nozzle degradation to evaluate possible damage to the lower head; (3) determine the nature and extent (axial and radial) of fuel–debris ingress into a nozzle; (4) determine the nature and degree of chemical and thermal interaction among fuel, debris, and nozzles; (5) determine thermal-related

[a]Work sponsored by the U.S. Nuclear Regulatory Commission under an agreement with the U.S. Department of Energy, Contract W-31-109-Eng-38.

[b]Argonne National Laboratory, Argonne, Illinois 60439.

metallurgical changes in the nozzles as a function of axial position to evaluate the axial temperature distribution and attempt to quantify temperatures near the vessel; and (6) determine the position and composition of debris adhering to nozzle surfaces to establish a "debris bed depth."

The nozzle segments received at ANL were from locations Dl0, E11, H5, H8, L6, and M9, indicated in the reactor grid plan shown in Fig. 1. These nozzle segments represented a range of thermal damage (i.e., melt-off and surface degradation) found in the 14 nozzles during the removal operations. Observation of the damage after removal of the core debris from the head revealed that nozzles in the area of E–H/7–9 were significantly more damaged than the nozzles around the periphery of the lower head. The degree of damage to individual nozzles would be indicative of the possible damage, or change in metallurgical condition, of the vessel close to the nozzle. Nozzle H8 was the most heavily damaged of those examined at ANL, having a length of only 70 mm and leaving a 51-mm-long segment, or stub, on the vessel. Nozzle L6, on the other hand, was 241 mm long and showed no outward damage. The other four nozzles exhibited either melt-off damage at different elevations (M9 and H5) or different degrees of surface damage (D10 and E11). Thus examination of these six nozzles provided sufficient information and insight to satisfy all the objectives of the examinations and provided insight into the movement of the molten fuel across the lower head.

In this article, we report the examination findings and show how they lead to the conclusions on fuel relocation and its qualitative significance to the integrity of the lower head.

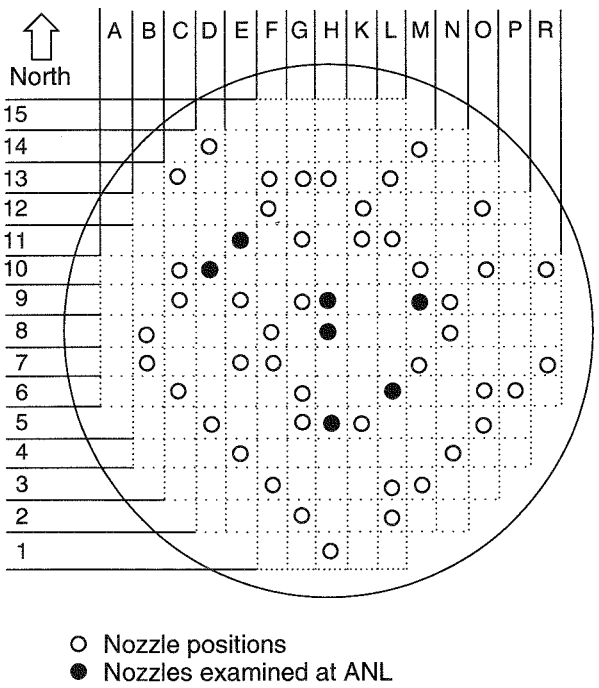

Fig. 1 Grid plan of TMI core showing positions of nozzles.

EXAMINATION METHODS

The examination methods used at ANL consisted of visual examination and macrophotography, axial gamma scanning for ^{137}Cs, macroexamination of cut surfaces, metallography, microhardness measurements, and scanning electron microscopy–energy-dispersive X-ray (SEM–EDX) analysis.

The nozzle segments were systematically sampled for detailed examination to obtain the desired data. Sectioned areas were based on the following attributes: (1) top and bottom locations, to obtain information on the hottest (sometimes molten) and coldest (nearest the vessel) temperature extremes in a nozzle; (2) fuel–nozzle interaction areas (nozzle degradation mechanism); (3) indications from gamma scans of fuel penetration into the nozzle; (4) obvious locations of debris on a nozzle; and (5) locations of surface cracking (nozzle degradation mechanism).

SIGNIFICANT FINDINGS

Pattern of Nozzle Damage

For the significance of the identified damage to be appreciated, the elevation of the damage to a particular nozzle above the bottom of the vessel must be considered. Figure 2 shows the relationships among the elevations of nozzle locations referenced to the lowest nozzle location at H8, and Table 1 provides the actual elevations for and segment lengths of the six ANL nozzles. These elevations are important to the understanding of how the molten debris moved on the lower head and caused the nozzle damage. Figure 3 shows the as-removed appearance of the six nozzles examined at ANL. Table 1 should be used to obtain a true comparison of the elevations at which nozzle damage occurred because the stub lengths remaining on the vessel were different for each nozzle. The tops of nozzles M9 and H5 clearly exhibited an appreciable amount of melting. The transition zone

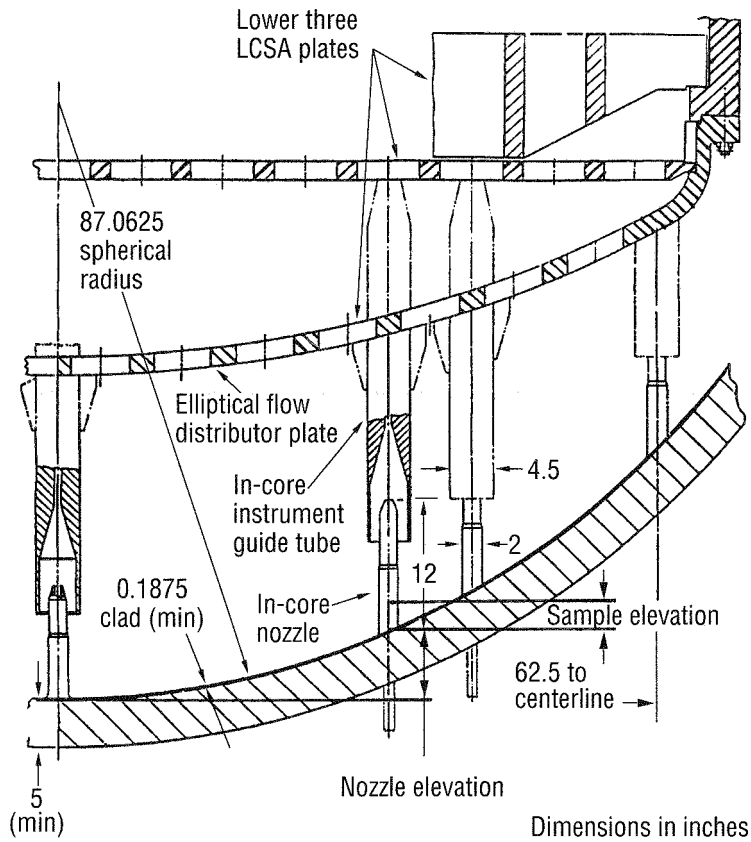

Fig. 2 Lower head area and in-core instrument guide tubes.

Table 1 Lengths, Elevations, and Fuel Penetration Depths of Nozzle Segments Examined at ANL

Nozzle	Elevation of nozzle base, mm	Segment length, mm	Stub length, mm	Elevation of top of segment,[a] mm	Fuel penetration elevation above nozzle base,[b] mm
M-9	119	254	26[c]	280	241
L-6	94	241	64[c]	305	75
H-5	107	146	0	146	89 max 117 min
H-8	0	70	51	121	<64
D-10	244	235	57[c]	292	55 max 184 min
E-11	221	225	77[c]	302	204

[a]Referenced to nozzle base.

[b]Based only on gamma scans.

[c]Calculated as the difference between 305 mm and the sum of the two known values. Measurements of stub lengths for D10 and E11 from photographs were not deemed sufficiently accurate because of angle of photo.

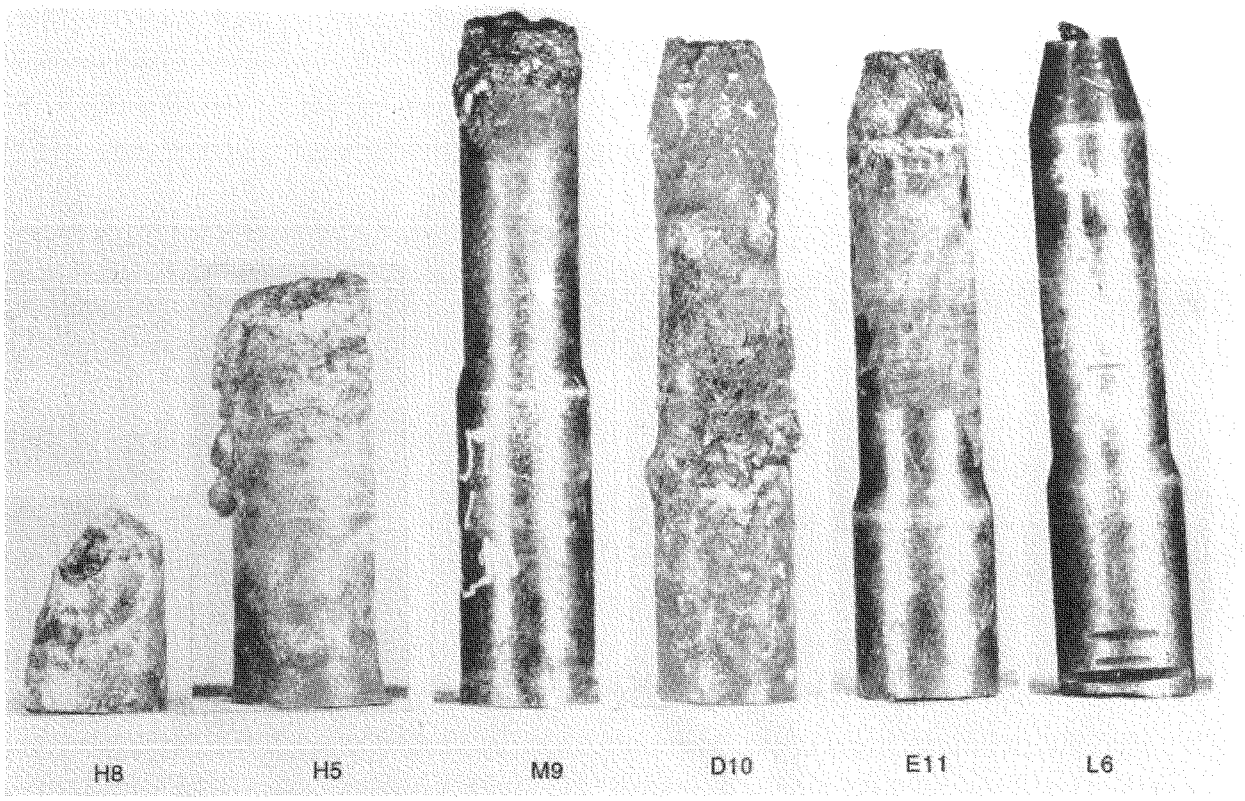

Fig. 3 As-removed appearance of six nozzles examined at ANL.

between the molten region and the unaffected lower part of the nozzles was relatively narrow on M9 and more extensive on the shorter H5. These transition zones were typically covered with a thin scale that was basically an iron oxide with entrapped shards of various core debris materials (Fig. 4); the lower areas of the nozzles were clean of adherent scale and showed little, if any, effects of being in contact with very hot core debris.

Significant fuel penetration into these molten nozzles was essentially limited to the melted and scaled elevations, i.e., the hot top of the nozzles. The material found in the top of nozzle M9 (Fig. 5) was a mixture of solidified fuel and nozzle remnants in a matrix of chromium oxide from the Inconel 600 nozzle material; this oxide was different from the iron-based oxide scale on the outside of the nozzles. It is believed that the ability of the fuel to penetrate downward into the nozzle was limited by the chromium oxide in which it was trapped (Cr_2O_3 melts at 1990 °C).

The H8 nozzle segment received at ANL was only the bottom portion of a longer postaccident segment, the top of which was broken off during the removal operations. The top surface of the bottom portion, shown in Fig. 3, 121 mm above the vessel surface, was smooth when compared with the melted regions of M9 and H5. Upon detailed examination by SEM–EDX analysis, it was found that this surface had reacted extensively with a molten iron-rich phase that contained ingots of silver–cadmium. These elements would have come from control assembly components that apparently melted early in the accident and were deposited on the lower head in advance of the major fuel flow at that location. Intergranular penetration of silver–cadmium was found in several nozzles and into the surface of the vessel cladding.[5]

In contrast to the melted condition of nozzles M9 and H5, nozzle L6 (almost midway between them on the lower head) showed no external damage at all. This indicates that the fuel movement in the lower head was not a unified flow but rather individual flows from various directions.

Although the surface of nozzle L6 was clean, the nozzle contained solidified fuel masses down to within 75 mm of its base, the deepest penetration into any

Fig. 4 Layer of debris on outer surface of nozzle D10 at the 82-mm elevation (magnification, 190×).

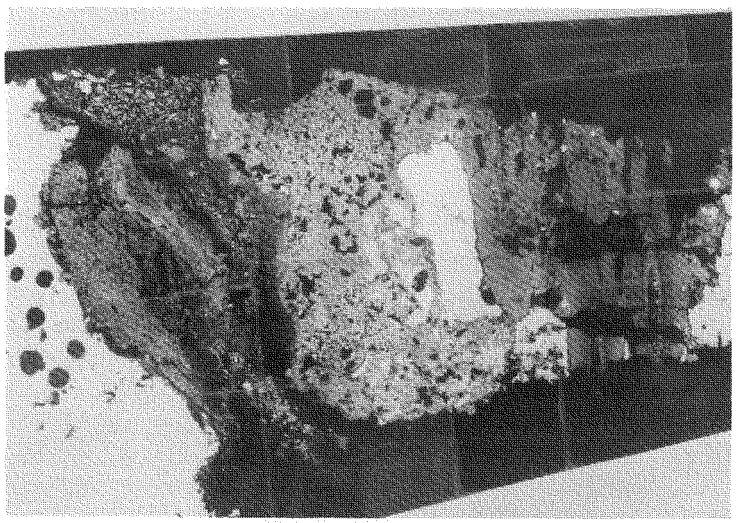

Fig. 5 Longitudinal section through top of nozzle M9 (magnification, 7×).

nozzle, 230 mm, from the apparent entry elevation. This deep penetration is attributed to the lack of fuel–nozzle interaction that would have formed a binding chromium oxide. Because both the nozzle and its overlapping guide tube were undamaged, the source of this fuel is not obvious: it appears to have been physically impossible for molten fuel to have traveled up under the guide tube and down into the nozzle without damaging either. It must be concluded that the fuel came down directly through the guide tube from somewhere up in the reactor.

Nozzle D10 was at the periphery of the lower head and appears to have been on the edge of the flow of molten fuel. One side of the nozzle was heavily encrusted along its entire height, whereas the other side, in a 180 ° arc, showed only the more common light surface scale. When it was sectioned, it was found that an unexplained

internal pressurization had pushed out the hot, crusted side of the nozzle and thus made it egg-shaped in cross section. The internal pressure created a crack in the outer surface of the nozzle and also collapsed the inner Inconel 600 tube of the instrument string. The body of the nozzle had undergone intergranular hot tearing, which apparently penetrated to the surface and formed the crack. The nonuniform damage indicates that these events occurred quickly with no time for heat transfer to the rest of the nozzle. This could be expected at the edge of a fuel flow coming to rest against the nozzle.

The last nozzle, E11, was damaged only at its tip, below which was a fairly extensive area of the iron-based scale. Melting was limited to the inner and outer surfaces of the tip, and rapid melting and solidification were indicated. Fuel penetration was relatively deep (compared with that in M9, which also had Inconel melting), apparently because the temperature at the top was too low to form chromium oxide, which most likely would have limited downward fuel movement. Instead, the material in the tip of the nozzle was in an iron-based oxide similar to that of the surface scales.

Two principal conclusions may be reached from the variable degradation of the instrument tube nozzles. First, considering that most of the nozzles on the lower head were covered with a hard, solidified layer of fuel debris but nozzles such as L6 sustained no outward damage from contacting this debris, it can be concluded that much of this debris acted as an insulator and protector of both the nozzles and the lower head. The absence of virtually any indication of degradation in the bottom parts of nozzles (even in those whose tops had melted) indicates that what was likely the first fuel debris to reach the lower head solidified relatively quickly and built up a significantly thick insulating layer. Once this layer had built up, the later material arriving on top of the solidified material melted off the tops of those nozzles which were exposed. The elevations at which these melt-offs occurred provide evidence for the thickness of the initial protective layer at various locations around the lower head. Thus the fact that the nozzles in the vessel hot spot area of E–F/7–9 were melted down the most indicates that only an initially thin insulating layer existed there, which apparently was the reason the hot spot formed where it did.

The second conclusion is that the movement of fuel debris across the lower head was not one massive, unidirectional flow but more likely a number of flows from various directions. This derives from the lower-head locations where specific nozzles melted off and the elevations at which they melted. The melt-off of M9, in the eastern side of the lower head at a relatively high elevation, indicates a thick initial debris layer, with subsequent hot fuel moving downward toward the reactor center atop this thick crust. Similarly, nozzles H5 and G5 were melted off atop a somewhat thinner initial crust, whereas nozzle L6 did not melt because it was initially totally covered with debris that had already solidified. These crust thicknesses are very likely indicative of the amount of molten core material that initially solidified on these locations, and indeed these locations correlate with the locations in the elliptical flow distributor through which debris is believed to have come. The initial debris from the major fuel relocation apparently impacted the lower head around the periphery, upward on the vessel curvature, and formed a cup-like debris mound that solidified rapidly. Debris flowing downward, lava like, atop initial crusts at M9 and H5 would effectively be moving toward the area of the short, melted-off nozzles where the vessel hot spot occurred.

Penetration of Materials Into Nozzles

The penetration of gamma-active materials downward into the nozzles was estimated from the ^{137}Cs gamma activity profiles; the results are summarized in Table 1. The gamma activity was assumed to be associated with fission products in the fuel, and therefore the results are reported as "fuel penetration." Metallic debris, essentially molten Inconel from the nozzle, was also found in the nozzles but not tabulated.

Although porous, ceramic-appearing material was seen in the as-cut transverse sections at elevations below the nozzle tops (e.g., in H8 and L6), there seemed to be difficulty in retaining this material during the subsequent sectioning operations to form metallographic mounts. This finding attests to the friable nature of the material. In most cases fuel material that was retained at the lower elevations exhibited two features. First, it appeared to be in the early stages of transformation to uranium-rich and zirconium-rich phases, which indicated relatively rapid cooling. Second, it contained iron, aluminum, and chromium in the grain boundaries, which indicated likely fluidity significantly below 2000 °C, which would aid the fuel's mobility to the elevation where it finally solidified.[6]

In nozzles M9 and H5, which melted off, the penetration was shallow, which indicates a quick melting and relatively rapid cooling, notwithstanding the phase transformations in the fuel areas. It is likely that the melting point of chromium oxide dominated the mobility

of this material before thermal equilibrium and lower melting eutectics could form. The phase transformation of the fuel would have occurred below 1990 °C while the solidified fuel was trapped in the insulating chromium oxide. In contrast, porous fuel was found at the base of the H8 nozzle segment, far below where the nozzle apparently had melted (i.e., in the part of the nozzle not received at ANL). This fuel may have entered the breach where the nozzle had interacted with liquid zirconium and at too low a temperature to form chromium oxide.

The fuel in the tops of nozzles D10 and E11 differed from that in nozzles M9 and H5 in that it was trapped in an iron-based rather than a chromium-based matrix. This reflects two probabilities. First, the Inconel did not readily give up its chromium to oxidation, probably because the temperature was too low. Second, the source of the fuel and the iron-based matrix was probably the same as that of the iron-based surface scales. That many of the fuel particles were shards and not solidified in situ masses indicates that the fuel flow in this region of the vessel was cooler than the flow that contacted nozzles M9, H5, and H8. This is consistent with a scenario that has the fuel flow coming to the vessel hot spot from the east and south and piling up on the far side against nozzles D10 and E11. (Note that the surface crust and major heating load was on only one side of D10.)

Presence of Control Assembly Materials

Four of the six nozzle segments examined at ANL were under control rod assemblies: M9, L6, H5, and H8. One, D10, was beneath an axial power-shaping rod that contained 914 mm of Ag–In–Cd clad in stainless steel. The last, H5, was beneath a burnable poison rod that contained Al_2O_3–B_4C pellets clad in Zircaloy. There is pervasive evidence from the ANL examinations that materials from assemblies containing Ag–In–Cd were deposited in some form, probably as solid particulates, on the lower head before the principal fuel flow occurred at 226 minutes. Unfortunately, there is no direct, unequivocal evidence that a bed of control rod debris existed on the lower head. Most, if not all, of such a bed of control rod debris would have remelted and possibly been consumed when it came in contact with even the initial, cooler, fuel that reached the lower head first. Therefore evidence for such a bed would now be, at best, on a microscopic scale and fortuitously derived.

The first evidence that the control materials were on the lower head before the fuel flow arrived was the finding of Ag–Cd nodules and In–Fe–Ni–Zr phases solidified in situ in the cracks of the vessel cladding of the E6 and G8 boat samples.[5] Second, the liquid that ablated nozzle H8 was overwhelmingly zirconium-rich and contained silver–cadmium masses. The zirconium-to-uranium ratio of approximately 8.5:1 was far in excess of the zirconium-to-uranium ratios found in fuel masses that were analyzed. This excess of zirconium would be from the Zircaloy shroud tubes in the control assemblies. Minimum depth of the zirconium-containing debris bed at this location would have been approximately 120 mm. Third, the findings of silver and silver–cadmium inclusions deep beneath the surfaces in most of the nozzles in a form of liquid-metal penetration indicate there was a layer of control materials either adhering to the surface ready to be melted when contacted by the hot fuel or there was a thick debris bed up against the nozzle that would yield the same result. That liquid silver–cadmium had penetrated the Inconel nozzles somewhat before nozzle melting occurred is supported by the apparently vapor-pressure-derived bubbles containing silver–cadmium deposits in the molten Inconel tops of some nozzles (see Fig. 5). Finally, the finding of a layer of 10-μm particles of silver–cadmium beneath a fuel debris scale on nozzle E11 indicates predeposition of control materials.

The significance of a bed of control material debris could be twofold. First, intergranular penetration of the vessel cladding by silver–cadmium may have played a role in the hot tearing of the cladding. Second, interaction of control material with nozzle material was at a low elevation, which may have allowed greater penetration of molten fuel into nozzle H8 than otherwise would have occurred. A third consideration, a potential insulating effect of the debris bed on the thermal impact to the vessel, was not supported by a heat transfer analysis performed at INEL.

EXAMINATION CONCLUSIONS

- The nature of the degradation of nozzles M9, H5, and H8 indicates that their melt-off was by liquid fuel approaching the nozzles at elevations of approximately 140 to 270 mm above the lower head. Surface scale on the nozzles below the melt-offs suggests that the liquid was atop a crust of solidified and partially solidified debris that had been cooled below its solidus, initially by the water in the lower head and finally by contact with the lower head.
- The flow of very hot material on the lower head followed multiple paths. The damage to nozzles M9, H5, and H8 suggests that flows occurred from the east and

south but apparently did not affect nozzle L6 because it had already been covered by cooler material that had reached the lower head first.

- The pattern of nozzle degradation and the assumed directions of fuel flow are consistent with a vessel hot spot at E–F/7–8, where there was apparently only a thin protective crust.
- The fuel debris in and on nozzles D10 and E11 and the one-sided degradation of D10 suggest that these nozzles were at the periphery of the fuel flow.
- Nozzle temperatures ranged from 1400 °C (melting) at 140 mm from the vessel at H5, down to approximately 1000 °C, based on a nickel–zirconium eutectic temperature of 961 °C at 64 mm from the vessel at H8.
- In addition to melting, nozzle degradation mechanisms were ablation by liquid zirconium, intergranular penetration by zirconium and silver–cadmium, chemical interaction with aluminum, chromium depletion caused by extensive oxidation, and internal pressurization that caused hot tearing and nozzle ballooning.
- The presence of significant quantities of zirconium and silver–cadmium on the vessel that interacted with the nozzles is attributed to the prior deposition at that location of control assembly material. The depth or nature of such a debris bed could not be confirmed, but the depth is estimated to have been at least 120 mm at the H8 location.
- Penetration of fuel debris downward into the nozzles was influenced by the temperature of the fuel at the time of entry; by the composition, and hence the fluidity, of the fuel; by the temperature of the nozzle and its ability to solidify the debris; and by the degree of interaction between the fuel and the molten nozzle to entrap the fuel in chromium oxide.

SIGNIFICANCE OF FINDINGS

Perhaps the most significant finding of the nozzle examinations and the examinations of the surfaces of the vessel samples was the lack of evidence of molten-fuel contact with the vessel surface. This would indicate that the temperature of the fuel debris that contacted the vessel surface had already dropped below the solidus temperature while the fuel moved through the water. The only evidence for molten material on the lower head was that for control rod constituents in both the nozzles and the vessel cladding. Much like volcanic lava flows entering the sea, an insulating crust was formed and kept the internal molten material contained and thus away from the vessel. The presence of water in the lower head, therefore, was paramount in mitigating the consequences of the accident. It follows that molten fuel entry into the lower plenum is not tantamount to failure of the lower head because of being contacted by molten fuel if water is present.

The fuel debris that eventually reached the lower head apparently took a circuitous path from its initial core location, and contact with reactor internals along the way likely extracted significant thermal energy.[7] Evidence was present for multiple pour locations through the elliptical flow distributor because of the peripheral path the fuel took as it was being guided in those directions from its initial reentry point through the baffle plate near the R7 location. Smaller, multiple pours onto the lower head apparently allowed greater heat transfer to the surrounding water and thereby allowed more rapid solidification of the material that became the initial insulating and protective crust on the lower head. Although computer codes are available for predicting the transfer of heat from fuel passing through water, the events on the TMI-2 lower head indicate the need for benchmarking the codes against situations such as those which apparently existed in TMI-2.

REFERENCES

1. D. Akers, S. M. Jensen, and B. K. Schuetz, *Companion Sample Examinations*, Report EGG-OECD-9810, April 1992.
2. Phase 4 Status Report, *Removal of Test Specimens from the TMI-2 Reactor Vessel Bottom Head*, Project Summary, Report MPR-1195, MPR Associates, Inc., October 1, 1990.
3. L. A. Neimark et al., *TMI-2 Instrument Nozzle Examinations at Argonne National Laboratory*, Report NUREG/CR-6185, March 1994.
4. D. Akers and B. K. Schuetz, *TMI-2 Nozzle Examinations Performed at the Idaho National Engineering Laboratory*, Report NUREG/CR-6198, March 1994.
5. D. Diercks and L. A. Neimark, Mechanical Properties and Examination of Cracking in TMI-2 Pressure Vessel Lower Head Material, in *Proceedings of the Achievements of the OECD Three Mile Island Vessel Investigation Project, Boston, Mass., October 20–22, 1993*, and *Results of Mechanical Tests and Supplementary Microstructural Examinations of the TMI-2 Lower Head Samples*, Report NUREG/CR-6187, April 1994.
6. R. V. Strain, L. A. Neimark, and J. E. Sanecki, Fuel Relocation Mechanisms Based on Microstructures of Debris, *Nucl. Technol.*, 87(1): 187-190 (August 1989).
7. J. R. Wolf et al., Lower Head Relocation Scenario, in *Proceedings of the Achievements of the OECD Three Mile Island Vessel Investigation Project, Boston, Mass., October 20–22, 1993*, and *TMI-2 Vessel Investigation Project Integration Report*, Report NUREG/CR-6197, March 1994.

Physical and Radiochemical Examinations of Debris from the TMI-2 Lower Head[a]

By D. W. Akers and B. K. Schuetz[b]

Abstract: *As part of the Three Mile Island Nuclear Station Unit 2 (TMI-2) Vessel Investigation Project, sponsored by the Organization for Economic Cooperation and Development, physical, metallurgical, and radiochemical examinations were performed on samples of previously molten material that had relocated to the lower plenum of the TMI-2 reactor during the accident on March 28, 1979. This article presents the results of those examinations and some limited analyses of these results. Principal conclusions of the examinations are that the bulk lower-head debris is homogeneous and composed primarily of* $(U,Zr)O_2$. *This molten material reached temperatures greater than 2600 °C and probably reached the lower head as a liquid or slurry at temperatures below the peak temperature. A debris bed composed of particulate debris was formed above a monolithic melt that solidified on the lower head.*

As part of the Vessel Investigation Project (VIP), companion samples were examined to (1) assess the physical and radiochemical properties of the debris adjacent to the vessel lower head, (2) assess the potential for interactions between the molten core materials and the lower head, and (3) provide information needed for the vessel margin-to-failure analysis effort.

This section summarizes results of the physical and radiochemical examinations of the companion samples and the analysis of these data. A more detailed description of companion sample examination results may be found in Ref. 1. This article also describes how the companion samples were acquired from the vessel lower head, their approximate location in the debris bed, and sample designations. The results are presented from examinations to characterize the physical characteristics of the companion sample debris and from examinations to determine radiochemical properties of the debris. Companion sample data are summarized for the margin-to-failure analyses. Last, major conclusions from the companion sample examinations are presented.

SAMPLE ACQUISITION

As part of the defueling efforts, all loose debris on the vessel lower head was removed, revealing a variable topography of solidified debris (the companion material). Results from probing examinations performed on February 15, 1989 (see Ref. 2), were used to create the topographical map of the debris height shown in Fig. 1. The contour lines in Fig. 1 represent the depth of the hard debris (i.e., the difference between the "hard stop" from the probe tests and the bowl-shaped lower head) rather than the surface contour of the hard layer. Figures 2 and 3 illustrate cross-sectional views through this hard layer at row 10 and row 12. As indicated in Fig. 1, the maximum depth of this hard layer was approximately 46 cm and

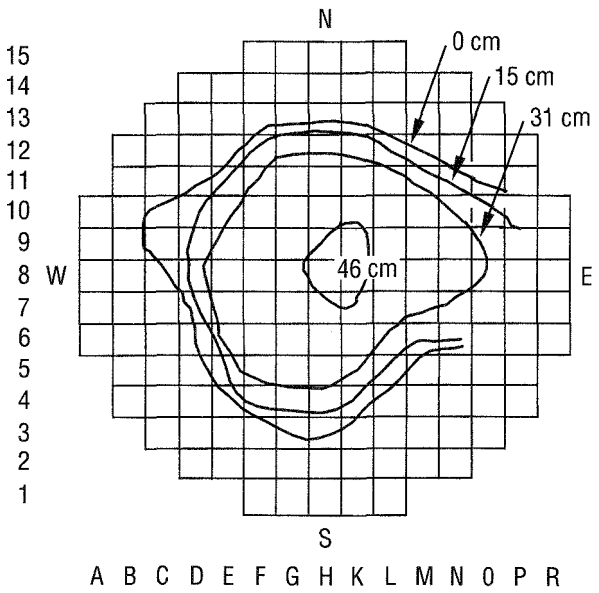

Fig. 1 Depth of hard layer of solidified debris. (Contour lines designate the distance between a "hard stop" from probe tests and the bowl-shaped lower head.)[2]

[a]This work was supported by the U.S. Nuclear Regulatory Commission in conjunction with the Organization for Economic Cooperation and Development through DOE Contract DE-AC07-76ID01570.

[b]Idaho National Engineering Laboratory, EG&G Idaho, Inc., P.O. Box 1625, Idaho Falls, ID 83415-3840.

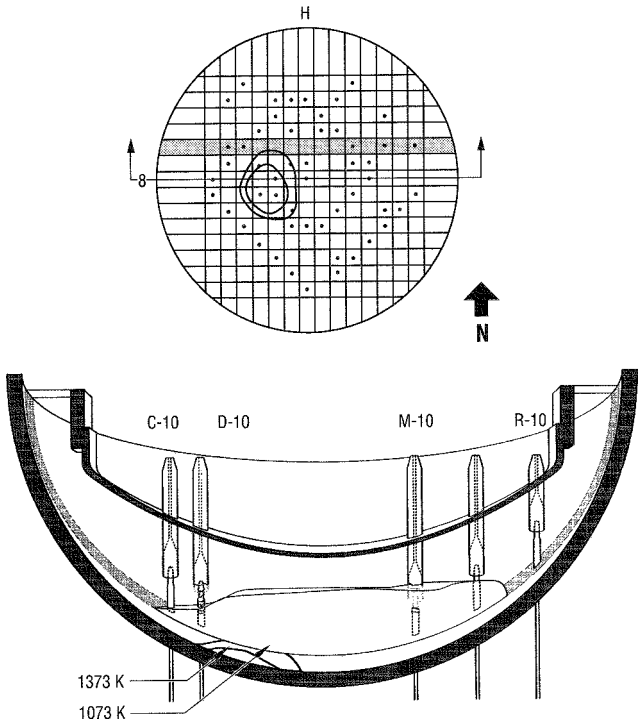

Fig. 2 TMI-2 lower-head cross section of hard debris, row 10. (In the top figure, the center of the vessel is at row 8, and the cross section shown below is highlighted.)

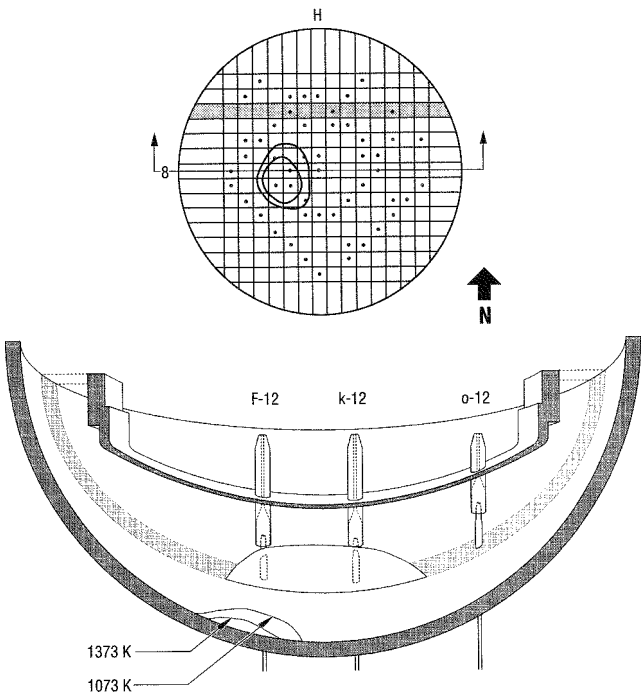

Fig. 3 TMI-2 lower-head cross section of hard debris, row 12.

was located within the central region of the core, near locations K-8 through K-10.

During the defueling process, it was discovered that the solidified layer was hard and monolithic (i.e., it could not be broken with normal defueling tools). This solidified layer was broken by a 136-kg (300-lb) slid hammer, which was dropped from an elevation of 6.1 m (20 ft). However, once the material was broken into pieces, there was virtually no adherence of the material to the lower head itself. Furthermore, the resulting pieces of debris appeared fairly uniform in composition (no metallic layer was observed).

As shown in Fig. 4, bulk companion samples were acquired from each of the four quadrants of the reactor vessel and are designated according to the quadrant from which they were taken: 1-9 for samples from the southeast quadrant, 1-10 for samples from the northwest quadrant, 1-11 for samples from the southwest quadrant, and 1-12 for samples from the northeast quadrant. Individual pieces of samples from each quadrant were further designated by a letter. For example, samples 1-11-C and 1-11-D both come from the southwest quadrant. Unfortunately, because the samples were removed during the bulk defueling process, it was impossible to determine the exact depth from which the samples were removed. As indicated in Table 1, much less debris was obtained from the northwest quadrant of the reactor vessel. During the removal of the loose layer in the northwest quadrant, almost all the hard layer was also removed. This left little debris still attached to the lower head when the companion samples were gathered. Hence examinations focused primarily on samples from the southeast, southwest, and northeast quadrants.

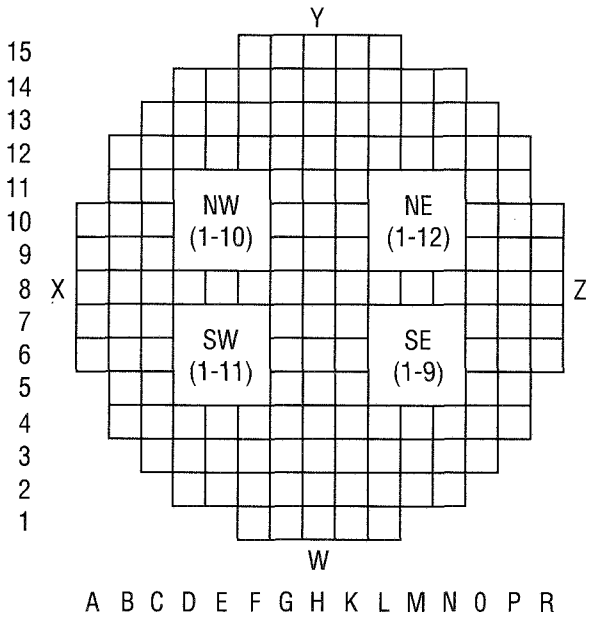

Fig. 4 Locations from which companion samples were taken. (Numbers are sample identification designations given by MPR Associates, Inc.)

Table 1 TMI-2 Bulk Sample Weights and Densities

Sample No.	Location (quadrant)	Weight, g	Density, g/cm^3
1-9	Southeast	2436	9.4
1-10	Northwest	0.5	6.9
1-11	Southwest	1214	8.6
1-12	Northeast	2700	8.2

PHYSICAL CHARACTERIZATION

Nondestructive examinations of the companion samples included visual examinations, photography, sample weights, bulk density, and individual particle densities. Figures 5 to 8 show the bulk companion samples from which individual particles were selected for examination. All companion samples were composed of large pieces of broken-up debris except companion sample 1-10 (see Fig. 6) from the northwest quadrant. This sample was composed of fine particulate debris and was not considered to be representative of the companion sample material. In retrospect, it is suspected that sample 1-10 was material that did not get removed during attempts to remove loose debris.

Eleven individual particle samples from the lower plenum were selected for destructive examinations. The examinations included optical metallography, scanning electron microscopy (SEM) with energy-dispersive and wavelength-dispersive X-ray spectroscopy, bulk elemental analysis, and radionuclide content. Of the 11 samples, 5 were from the southeast quadrant of the reactor vessel (samples 1-9-A, 1-9-B, 1-9-C, 1-9-F, and 1-9-G). Three samples (1-11-R, 1-11-C, and 1-11-D) were from the principal damage region in the southwest quadrant of the reactor vessel, and the remaining three samples (1-12-R, 1-12-C, and 1-12-D) were from the northeast quadrant of the reactor vessel head (see Figs. 2 and 3). These samples were sectioned and prepared for metallographic examination, after which representative samples were obtained for SEM/microprobe examinations and radiochemical analysis.

Fig. 5 Sample collected from the southeast quadrant (sample 1-9; total sample weight is 2 436 g).

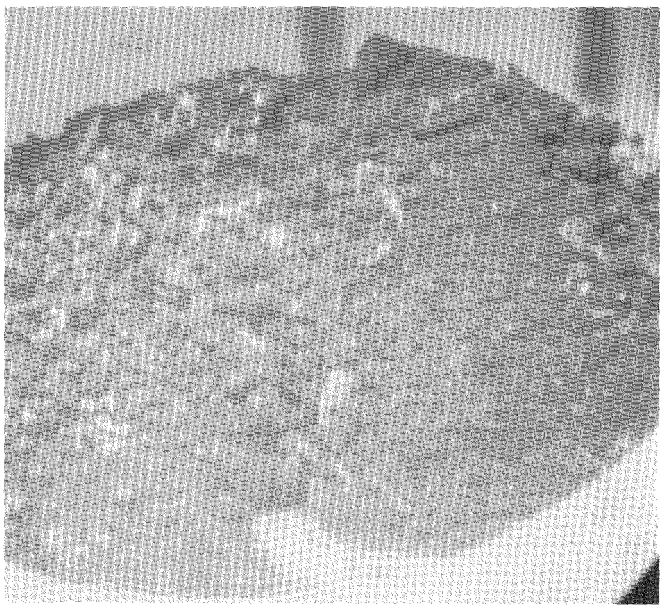

Fig. 6 Sample collected from the northwest quadrant (sample 1-10; total sample weight is 0.5 g).

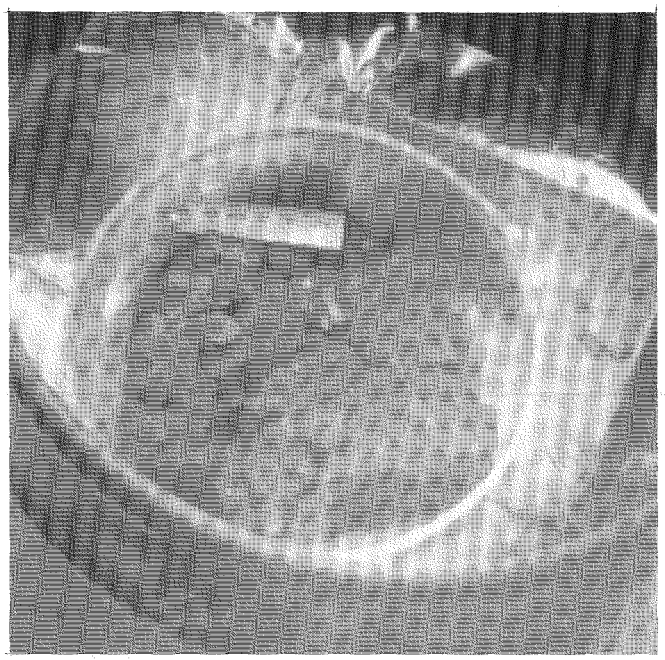

Fig. 7 Sample collected from the southwest quadrant (sample 1-11; total sample weight is 1 214 g).

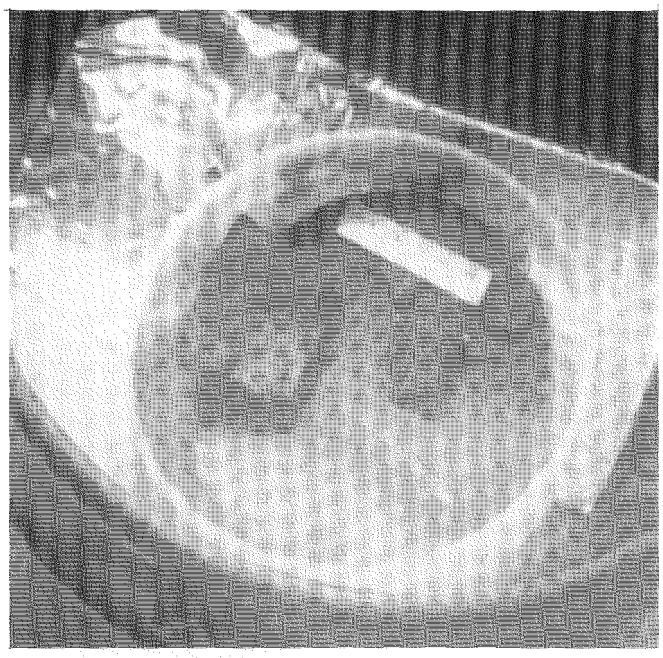

Fig. 8 Sample collected from the northeast quadrant (sample 1-12; total sample weight is 2 700 g).

Visual Examinations

On the basis of previous sample examinations, visual examinations suggested that the samples were composed primarily of previously molten ceramic material and possibly included small amounts of metallic material. The samples were generally dull grey, although some areas were yellow (lighter areas in Figs. 5 to 8). This material is probably hexavalent uranium, although no analyses were performed to confirm this.

Density Measurements

Density measurements were performed on entire companion samples from each quadrant and from individual pieces of companion samples from each quadrant using the standard immersion method. Table 1 lists the location, total weight, and density of the total companion sample from each quadrant. Densities ranged from 6.0 to 9.4 g/cm^3. A numerical average density for the companion samples is 8.7 ± 0.4 g/cm^3. The low density of the sample taken from the northwest quadrant was excluded from this average because of the small size of the sample and its noticeable difference in physical form. Table 2 shows the weight and density of individual particles from several quadrants. Densities of these samples ranged from 7.45 to 9.40 g/cm^3, with an average value of 8.4 ± 0.6 g/cm^3. The measured densities are consistent with samples composed primarily of $(U,Zr)O_2$ with a large proportion of UO_2. Examination of the elemental analysis results indicates that the composition of all samples is similar. Hence differences in sample density are primarily attributed to differences in debris porosity.

Table 2 TMI-2 Lower Plenum Individual Sample Weights and Densities

Sample No.	Weight, g	Density, g/cm^3
1-9-R	51.81	9.40
1-9-F	14.90	7.45
1-9-G	12.10	8.07
1-11-R	52.23	8.62
1-11-C	49.50	8.39
1-11-D	76.40	8.30
1-12-R	47.16	8.18
1-12-C	45.50	9.29
1-12-D	15.20	7.60

Porosity Data

Table 3 lists porosity data for individual particle samples from the three quadrants of the lower head where most of the debris was obtained. The porosity was determined with optical methods on polished metallographic specimens. The numerical average porosities of samples from the southeast, southwest, and northeast quadrants are 21 ± 7%, 18 ± 14%, and 17 ± 9%, respectively. These data can be misleading, however, because of several high values and the range of observed porosities. The average porosity for all samples is 18 ± 11%, which suggests a very broad range of porosities in the debris. The metallographic examination of these samples indicated no significant interconnected porosity.

Microstructure Examinations

Sample 1-11-R was sectioned to provide longitudinal and transverse cross sections labeled 1-11-R/L and 1-11-R/T. Figure 9 shows apparent connected pores in

Table 3 TMI-2 Lower Plenum Sample Porosities[a]

Sample No.	Porosity, %	Remarks
1-9-A	29.2	Holes/cracks
1-9-B1	10.8	Holes/cracks
1-9-B2	19.5	Holes/cracks
1-9-F	27.0	Holes/halftone[b]
1-9-G	17.3	Original macro
1-11-C	7.6	Holes/halftone
1-11-D-A	20.5	Original photo
1-11-R/L	21	Fine holes not resolved
1-11-R/T	7.0	Halftone
1-11-R/T	5.7	Large holes only
1-11-D-B	47.5	Mottled stringers of metal not included in porosity estimate
1-12-R	9.5	Halftone
1-12-R	19.8	Halftone
1-12-R	22.0	Original photo
1-12-C	5.7	Stringers of metal not included in porosity calculation
1-12-D	31.7	Original photo

[a]Reference 1 provides additional information related to the particular photographs from which porosity measurements were made.

[b]Halftones are report-quality photographs that may not contain the level of detail of the original photographs. Some smaller porosity may not be apparent from the optical analysis. Comparisons indicate that the difference in porosity between halftones and originals is 1 to 2%.

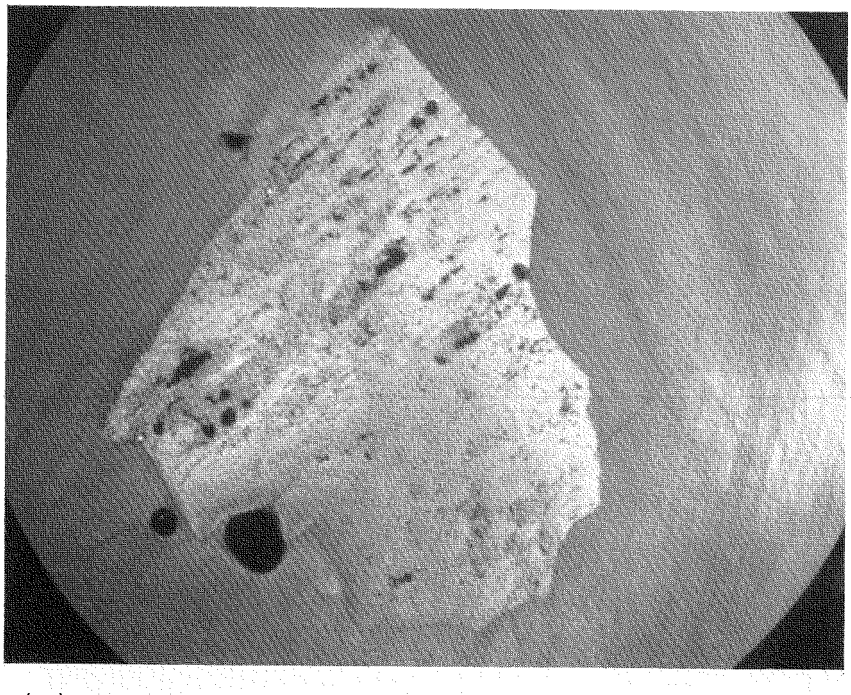

(a) 90m141 ×2.9

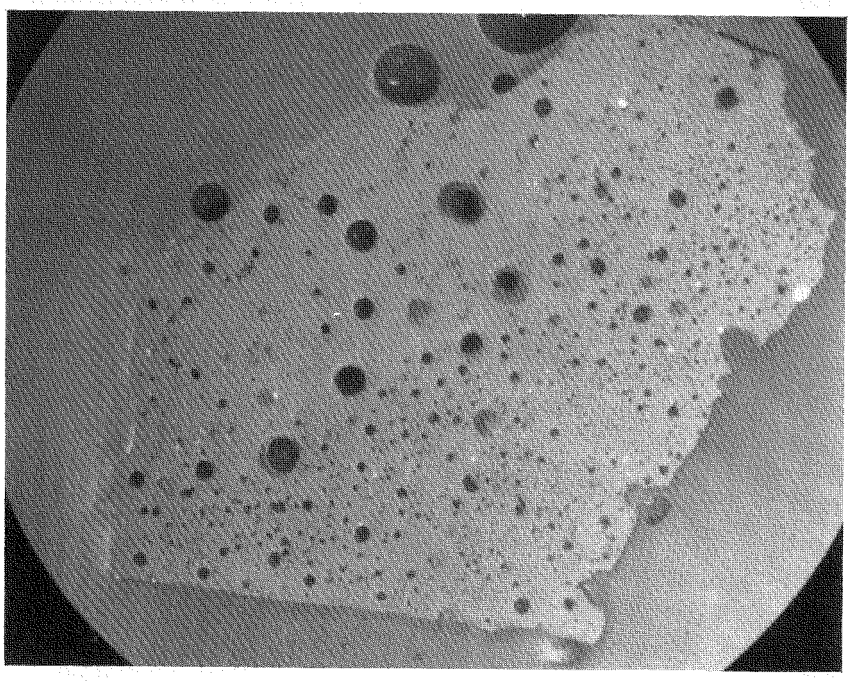

(b) 90m142 ×2.8

Fig. 9 Cross-sectional views of sample 1-11-R. (a) Longitudinal section (sample 1-11-R/L) (b) Transverse section (sample 1-11-R/T).

the longitudinal section of this sample. These interconnected pores were observed in many of the samples and may have been caused by the bubbling of steam or structural material vapors through the molten pool when the pool froze.[3] The physical examination of the lower head and the presence of the interconnected pores in the companion samples suggest that the molten pool cooled slowly enough to allow bubble coalescence to occur.

The morphology of the material surrounding the pores was discernible only on the scanning electron microscope. As indicated in Fig. 10, SEM examinations reveal that the material surrounding the pores within samples was composed of two phases: a light, uranium-rich $(U,Zr)O_2$ phase and a dark, zirconium-rich $(Zr,U)O_2$ phase. Away from the porous regions, the single-phase regions consisted of uranium-rich $(U, Zr)O_2$. UO_2–ZrO_2-phase diagrams indicate that the presence of two-phase $(U,Zr)O_2$ and $(Zr,O)_2$ structures corresponds to material that underwent a gradual cooldown rather than a rapid quench because of the time required for apparent visible phase separation to occur.

Composition Analyses

Analyses were performed for key elements in the principal components of the Three Mile Island Unit 2 (TMI-2) core. Table 4 lists the elemental composition of each of the core constituents (see Ref. 4). Through summing of the masses of each element within the core, an average composition of the TMI-2 core was estimated assuming that the core was homogeneously mixed (including the end fittings). These values are also listed in Table 4. Note that these average values include the oxygen content of the uranium but exclude the oxygen that might be present because of the oxidation of Zircaloy and structural materials.

In-depth SEM analyses were performed to characterize the composition of companion samples 1-11-R/T, 1-9-A, and 1-9-B, which appeared visibly to be representative of the debris bed. Energy-dispersive X-ray spectroscopy was performed, and dot maps were developed with wavelength-dispersive X-ray spectroscopy to assess the composition of specific phases within the samples. Dot maps were generated for the following core constituents: U, O, Zr, Ag, Al, Cd, Cr, Fe, In, Mn, Mo, Nb, Ni, Sn, and some fission products. Reference 1 includes a discussion of the regions examined and shows dot maps of the elements for which significant results were obtained.

Areas of interest that were examined include the edge of large pores, metallic inclusions or ingots, secondary

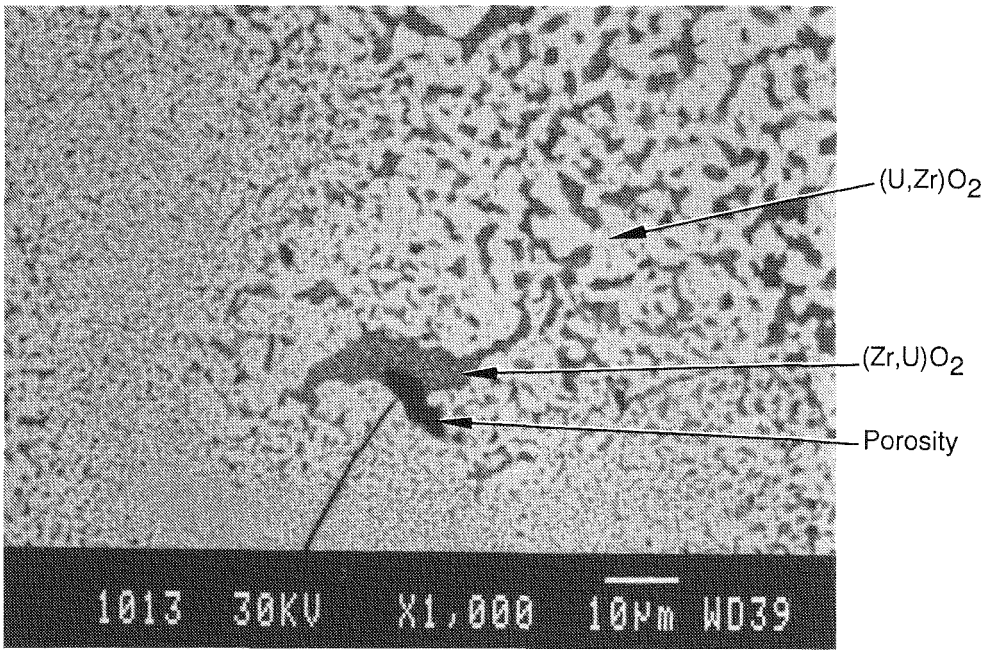

Fig. 10 SEM backscattered electron image of two-phase region (sample 1-9-A, Area 2).

Table 4 TMI-2 Reactor Core Composition[a]

Material weight	Elements	Wt%	Average core composition: Element	Average core composition: Composition, wt%
UO_2	U-235[a]	2.265	U	65.8
(94 029 kg)	U-238[a]	85.882	Zr	18.0
(531.9 kg)[b]	0	11.853	O	8.5
			Fe	3.0
Zircaloy-4	Zr[a]	97.907	Ag	1.8
(23 177 kg)	Sn[a]	1.60	Cr	1.0
(125 kg)[b]	Fe[a]	0.225	Ni	0.9
	Cr[a]	0.125	In	0.3
	O	0.095	Sn	0.3
			Al	0.2
Type 304				
stainless	Fe[a]	68.635	B	0.1
steel (676 kg)	Cr[a]	19.000	Cd	0.1
and unidentified	Ni[a]	9.000	Mn	0.8
stainless steel	Mn[a]	2.000	Nb	0.04
(3960 kg)	Si[a]	1.000		
(16.8 kg)[b]	N	0.130		
	C	0.080		
	Co	0.080		
Inconel-718	Ni[a]	51.900		
(1211 kg)	Cr[a]	19.000		
(6.8 kg)[b]	Fe[a]	18.000		
	Nb[a]	5.553		
	Mo[a]	3 000		
	Ti	0.800		
	Al[a]	0.600		
	Co	0.470		
	Si[a]	0.200		
	Mn[a]	0.200		
	N	0.130		
	Cu	0.100		
Ag–In–Cd	Ag[a]	80.0		
(2749 kg)	In[a]	15.0		
(43.6 kg)[b]	Cd[a]	5.0		
B_4C–Al_2O_3	Al[a]	34.33[c]		
(626 kg)	O	30.53[c]		
(0 kg)[b]	B[a]	27.50[a]		
	C	7.64[c]		
Gd_2O_3–UO_2	Gd[a]	10.27[c]		
(131.5 kg)	U[a]	77.72[c]		
(0 kg)[b]	O	12.01[c]		

[a]These are elements for which inductively coupled plasma analysis was performed.

[b]This value is the weight of material in a control rod fuel assembly.

[c]Representative compositions of these components were used.

phases, and pores without secondary phases. As previously discussed, each sample is composed of a homogeneous $(U,Zr)O_2$ matrix with relatively low concentrations of Al, Sb, and Sn, and a zirconium-rich secondary phase around pores and at grain boundaries.[a] Results from these examinations indicate that all the samples appear to consist primarily of previously molten $(U,Zr)O_2$. Droplets of metallic melt were found only in samples 1-11-R/L, 1-11-R/T, and 1-11-D-A (see Fig. 11). SEM/microprobe examinations indicate that these metallic melts are silver and indium. A secondary ceramic phase was also observed within the $(U,Zr)O_2$ matrix of sample 1-11-R/T (see Fig. 11). SEM/microprobe examinations of this ceramic phase indicate that it was composed primarily of chromium oxide.

Examination of the secondary phases around pores and in the matrix of the debris indicates that the secondary phases are composed primarily of $(Zr,U)O_2$ with greater amounts of iron and chromium present. The fact that there was time during the cooling process for the lower-temperature $(Zr,U)O_2$ phase to form and time for the iron and chromium to migrate to the secondary phases suggests that the molten pool remained at a relatively high temperature for a period of time.

RADIOCHEMICAL CHARACTERIZATION

Radiochemical analyses were performed on the companion samples to assess bulk composition and radionuclide content. Before the destructive analysis, the intact samples were analyzed through gamma spectroscopy to provide an initial estimate of the gamma-emitting radionuclide content. Then the samples were dissolved through the use of a pyrosulfate fusion technique in a closed system. Elemental analyses were performed on dissolved samples with the use of inductively coupled plasma spectroscopy techniques. Reference 5 contains a detailed description of the analysis methods used for the companion sample examinations.

Elemental Composition

Elemental analyses were performed for key elements in principal core components (see Table 4). Table 5 lists the average compositions of the companion samples from the three quadrants of the lower head for which examinations were performed. The average composition for each of the core constituents is repeated in Table 5 for comparison. Examination results indicate that the companion

[a]Aluminum is found in Inconel-718 that is used in spacer grid strips, tin is contained within Zircaloy that is found in fuel cladding and in other fuel assembly components, and Antimony-125 is a fission product from U-235 (see Table 4).

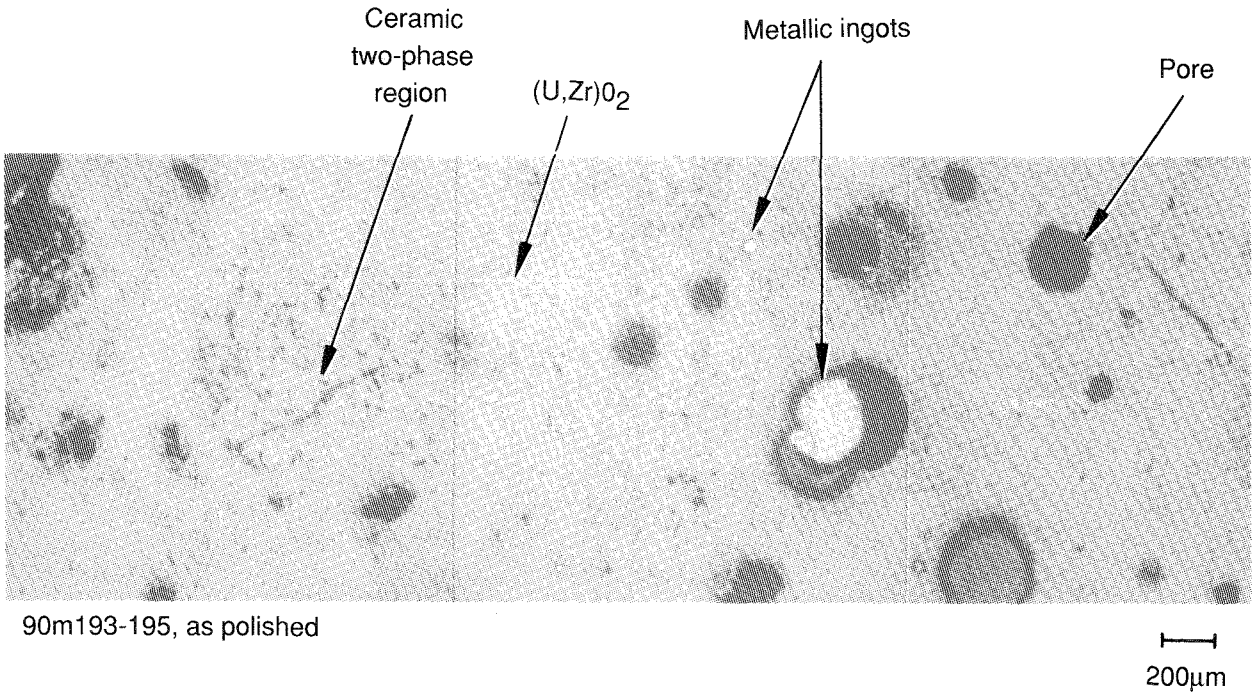

Fig. 11 Photocomposite of microstructure in sample 1-11-R/T.

material was relatively homogeneous on a macroscopic scale in all the areas examined.

The total amount of sample weight accounted for in this analysis is between 84 and 88 wt% of the total sample weight. Within the uncertainties of the analysis, the remaining material is accounted for by the oxidation of the uranium and zirconium present in the samples.

Comparison of the analysis results with the average composition of core constituents indicates that the fuel melt is composed almost entirely of the constituents of a fuel rod and that little contamination by other structural constituents occurred. It is interesting to note that a relatively high fraction of the indium within a fuel element was found in the companion samples.

Radionuclide Concentration and Decay Heat

The companion sample examination effort included analyses to determine the decay heat within the debris, which was required as input to the margin-to-failure calculational effort. The procedure used to determine the decay heat required that the radionuclide concentration within the debris be measured for selected species. These measured concentrations were compared with concentrations predicted in an ORIGEN2 calculation[6,7] to verify calculational results. Then other radionuclide concentrations contributing to the decay heat were obtained from the ORIGEN2 calculation, and calculations were performed to estimate the decay heat from the radionuclide concentration within the debris as a function of time. Results from major steps in this process to estimate the decay heat are presented in the following paragraphs.

Radionuclide Concentration. Dissolution techniques were used to measure the radionuclide content of the lower-head debris samples for several key radionuclides. Table 6 summarizes the normalized radionuclide retentions found in the companion samples. Radionuclide retention percentages reported in Table 6 are the ratios of measured retention to the retention predicted by an ORIGEN2 analysis for undamaged fuel.[7] A ratio of less than 1 indicates that the measured retention is less than the calculated value. Results are discussed here according to the volatility of the chemical group and element.

The high-volatility fission-product groups include the noble gases, halogens, alkali metals, and heavy chalcogens. From this group, measurements were made for ^{137}Cs. As indicated in Table 6, the volatile ^{137}Cs was

Table 5 Average Debris Composition by Quadrant[a] (wt%)

Element	Southeast (1-9)	Southwest (1-11)	Northeast (1-12)	Core average[b]
U	72.3	70.8	68.2	65.8
Zr	14.1	12.0	15.2	18.0
Sn	[c]	[c]	[c]	0.3
Ag	[c]	[c]	[c]	1.8
In	0.28	0.26	[c]	0.3
Al	[c]	[c]	[c]	0.2
Cr	0.33	0.26	0.52	1.0
Fe	0.74	0.53	0.93	3.0
Mn	0.030	0.026	0.028	0.8
Mo	[c]	[c]	[c]	[d]
Nb	[c]	[c]	[c]	0.04
Ni	0.099	0.081	0.10	0.9
Total	87.8[e]	84.3[e]	85.1[e]	92.14

[a]This table presents the average of the examination results obtained from the companion samples; however, because of the small number of samples examined, these data must be used with caution.

[b]This value is based on data in Table 4.

[c]Values are below the analytical detection limit. Detection limits differ for individual elements; however, a nominal value is approximately 0.1 wt%. The sample matrix may affect detection limits.

[d]Data were not available.

[e]This value is the total of measurable constituents. Oxygen content was not measured.

Table 6 Radionuclide Retention in the Debris Bed[a]

Radionuclide	Radionuclide retention, %		
	Southeast (1-9)	Southwest (1-11)	Northeast (1-12)
^{90}Sr	48	47	96
^{125}Sb	1.9	1.1	5.6
^{137}Cs	3.6	1.3	18
^{144}Ce	91	85	97
^{154}Eu	83	84	80

[a]Retention is calculated on the basis of the uranium content of the sample material as determined from the elemental analysis results. Results have been corrected for burnup and show a reduction of almost a factor of 2 in the inventory of ^{154}Eu and ^{125}Sb. Radionuclide concentration data are in Ref. 1.

measurable in all samples at retentions substantially lower than those predicted with ORIGEN2 for undamaged fuel. However, higher retentions (18%) were found in the northeast quadrant. It is not known why higher levels of this radionuclide, as well as medium- and low-volatile radionuclide concentrations, existed in the northeast region.

The medium-volatility fission products are from the metals, alkaline earths, some of the rare earths, and actinides. Radionuclides from these groups for which measurements were made are ^{125}Sb and ^{90}Sr. Strontium-90 is less volatile than ^{125}Sb, as discussed in Refs. 1 and 5, and is expected to be retained by the fuel to the greatest extent. However, the ^{90}Sr data shown in Table 6 range in retention from 48 to 96%, which indicates that this radionuclide was mobile and was not fixed in the fuel melt with the low-volatile radionuclides. The low retention of ^{125}Sb in the companion samples probably resulted from the partition of metallic antimony (unoxidized because of the high potential required to oxidize the element) from the oxidic uranium melt in the upper core region. As a consequence, the melt that relocated to the lower head was low in ^{125}Sb content. In previous core examinations, high concentrations of ^{125}Sb were found in metallic samples from the upper core region.[5]

The low-volatility fission products include elements from the noble metals, the remaining rare earths and actinides, tetravalents, and early transition elements. The radionuclides from this group that were measured are ^{154}Eu and ^{144}Ce. The concentrations of ^{144}Ce measured in the companion samples indicate that nearly all this radionuclide was retained. Considering the uncertainty in the ability to predict ^{154}Eu production, which for TMI-2 was verified through a burnup analysis, the data in Table 6 also indicate that most of this radionuclide was retained.

Decay Heat. Decay heat calculations were performed to estimate the heat generated within the hard layer of debris upon the lower head. Results from an ORIGEN2 analysis of the TMI-2 core were used to perform these calculations. An analysis model with 1239 fuel nodes was used to calculate burnup for the TMI-2 reactor core.[7] Results indicate that the burnup ranged from about 900 to 6000 MWd/MtU, and the core average was about 3200 MWd/MtU. A benchmark comparison was performed with the measured ^{144}Ce concentrations (an indicator of burnup) to determine the actual burnup of the debris on the lower head. This comparison indicated that the debris was at near-average burnup. The TMI-2 reactor core was operated for approximately 96 effective full-power days.

Although the average burnup of the TMI-2 core at the time of the accident was relatively low, previous calculations[8] indicate that the decay heat for a core that had been operated for a considerably longer period of time would not be significantly different for the time periods of concern during the reactor accident. As shown in Fig. 12, the difference in decay heat for a full burnup equilibrium core at 34 GWd/MtU and the decay heat for the TMI-2 core with an average burnup of 3.2 GWd/MtU is negligible for the first 1000 minutes after reactor scram. Although more volatile fission products would be present in higher burnup fuel than TMI-2, additional calculations[9] that include the effect of volatile release on debris decay heat indicate that the maximum increase in fission-product decay power for relocated fuel in a full burnup core would be less than 20% for time periods of concern during the reactor accident.

With the use of the methodology described in Ref. 10, radionuclide concentrations for other species contributing to debris decay heat were estimated with results from the ORIGEN2 TMI-2 calculation. On the basis of the radionuclide concentration results discussed previously, it was determined that some principal radionuclides should not be included in decay heat calculations. Specifically, the noble gases (primarily xenon and kryton) and the high volatiles (all cesiums and iodines) were removed from the decay heat calculations. These radionuclides were omitted because they would be expected to have volatilized and been released from the fuel before the molten material relocated to the lower head.

Representative specific decay heats were calculated at 224 minutes and at 600 minutes, which is representative of the later cooldown period. The decay heat produced from the selected radionuclide list is 0.13 W/g of debris at 224 minutes and 0.096 W/g of debris at 600 minutes after the accident. These data indicate that the decay heat production during any reactor transient in which the volatile radionuclides were released would be similar to that of TMI-2.

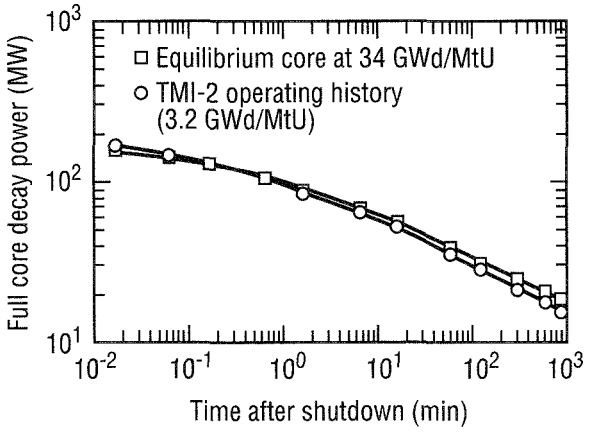

Fig. 12 Comparison of TMI-2 reactor core decay heat with a higher burnup at the core.

INPUT TO MARGIN-TO-FAILURE ANALYSIS

One of the objectives of the companion sample examinations was to obtain input for the margin-to-failure analyses. In some cases, companion sample data can be used directly as input to the margin-to-failure calculations; in other cases, additional information was required to obtain the desired margin-to-failure analysis input. This section summarizes results from the companion sample examinations that provide input to the margin-to-failure analysis effort.

Debris Composition

Radiochemical examination results indicated that the composition of the debris bed is similar for all samples with an average composition of approximately 70 wt% uranium, 13.75 wt% zirconium, and 13 wt% oxygen. This composition accounts for about 97 wt% of the debris.

On the basis of the metallography and SEM examination results, the extent of the oxidation of the companion samples can be considered to be almost complete with little or no unoxidized material present other than small quantities of materials that do not readily oxidize, such as silver.

Peak Debris Temperature at Relocation

Hofmann[11] addressed the range of temperatures that might be expected in a severe reactor accident and has shown that the lowest temperatures that might be expected in the dissolution of uranium by zirconium are on the order of 1760 °C, which is approximately 1000 °C below the melting point of UO_2 (approximately 2850 °C). However, the companion samples have compositions that are principally $(U,Zr)O_2$ (i.e., about 78 wt% UO_2 and 17 wt% ZrO_2) with some secondary $(Zr,U)O_2$ phases. Hofmann indicates that a well-mixed $(U,Zr)O_2$ solid solution, as shown by the metallography and SEM results, would be expected to be found in a peak temperature range between 2600 and 2850 °C. Consequently it is suggested that the peak temperature of the melt that relocated to the lower head was at least 2600 °C.

Debris Cooling Rate

Companion sample examinations provide insight into the debris cooling rate, which is based on the formation of secondary phases around pores and in the matrix material. These secondary phases contain apparent $(Zr,U)O_2$ phases with the presence of iron and chromium. The formation of these phases would require a finite cooldown period as opposed to an instantaneous quench to allow the phase separation to occur between the $(U,Zr)O_2$ and $(Zr,U)O_2$ phases. Bart[12] has suggested that a cooling time between 3 and 72 hours is needed to cause this type of phase separation.

Debris Decay Heat

On the basis of radionuclide concentrations measured within the companion sample debris, it is estimated that the decay heat within the debris at 224 minutes after shutdown is 0.18 W/g of uranium; and at 600 minutes after shutdown, it is 0.14 W/g of uranium. After conversion of these data to the known debris composition, the decay heat present is 0.13 W/g of debris at 244 minutes and 0.096 W/g of debris at 600 minutes.

SUMMARY AND CONCLUSIONS

Examinations were performed on samples from the hard, monolithic layer of debris near the lower head, which are referred to as companion samples. These examinations indicate that the companion samples were relatively homogeneous with relatively small variations in composition and density. The companion samples consisted primarily of previously molten $(U,Zr)O_2$ ceramic melt. Small amounts of metallic melt (<0.5%) were observed only in samples from the southwest quadrant.

The pores in some of the samples were interconnected and surrounded by microporosity and two-phase structures consisting of uranium-rich $(U,Zr)O_2$ and zirconium-rich $(Zr,U)O_2$. This interconnected porosity may result from gases percolating up through the melt, which suggests that the debris was molten while on the lower head and it remained molten for a sufficient period of time to allow bubble coalescence. The presence of two-phase $(U,Zr)O_2$ and $(Zr,U)O_2$ structures in areas of some samples indicates that these specimens were not rapidly quenched. However, the incomplete phase separation in these samples suggests that these specimens were not at high temperatures for an extended period of time.

Radiochemical analyses of the debris indicate that the debris was composed of approximately 70 wt% uranium, 13.75 wt% zirconium, and 13 wt% oxygen. This composition accounts for approximately 97 wt% of the debris. The remaining constituents are the elemental constituents of stainless steel and Inconel core components that probably melted during the relocation of debris to the lower head.

The examinations suggest that much of the high-volatile radionuclide content had volatilized out of the debris before the solidification of the molten debris and thus left primarily medium- and low-volatile components in the debris bed. The small amount of interconnected porosity and the nonreactive nature of the solidified ceramic indicate that leaching and other release mechanisms were insignificant. Decay heat analyses were performed to determine the amount of heat present in the debris bed at the time of relocation (224 minutes after shutdown) and at 600 minutes after reactor shutdown. Calculation results indicate that the retained heat in the lower debris bed was approximately 0.13 W/g of debris at 244 minutes after shutdown and 0.096 W/g of debris at 600 minutes after shutdown.

REFERENCES

1. D. W. Akers, S. M. Jensen, and B. K. Schuetz, *Companion Sample Examinations,* Report TMI V(92)EG10, OECD-NEA-TMI-2 Vessel Investigation Project, July 1992.
2. A. P. Kelsey, *Lower Head Debris Topography*, Report TMI-2 Technical Bulletin TB-89-02, February 27, 1989.
3. Private communication with L. A. Neimark, Argonne National Laboratory, May 13, 1992.
4. S. M. Jensen et al., *Examination of the TMI-2 Core Distinct Components,* Report GEND-INF-082, 1987.
5. D. W. Akers et al., *TMI-2 Core Bore Examinations,* Report GEND-INF-092, January 1990.
6. A. G. Croff, *ORIGEN2: A Revised and Updated Version of the Oak Ridge Isotope Generation and Depletion Code*, Report ORNL-5621, July 1980.
7. B. G. Schnitzler and J. B. Briggs, *TMI-2 Isotopic Inventory Calculations*, Report EGG-PBS-6798, August 1985.
8. T. R. England and W. B. Wilson, *TMI-2 Decay Power: LASL Fission-Product and Actinide Decay Power Calculations for the President's Commission on the Accident at Three Mile Island*, Report LA-8041-MS (Revised), March 1980.
9. B. G. Schnitzler, *Fission Product Decay Heat Power for Disrupted Fuel Regions*, Report BGS-08-93, internal INEL memo to J. R. Wolf, October 1, 1993.
10. C. S. Olsen et al., *Examinations of Debris from the Lower Head of the TMI-2 Reactor,* Report GEND-INF-084, January 1988.
11. P. Hofmann, J. L. Hagen, G. Schanz, and A. Skokan, Reactor Core Material Interactions at Very High Temperatures, *Nucl. Technol.*, 87(1) (August 1989).
12. G. Bart, TMI-2 Core Sample Evaluation at Paul Scherrer Institute, *TMI-2 Examination Results from the OECD-CSNI Program, Vol. 2*, Report EGG-OECD-9168, August 1990.

Results of Metallographic Examinations and Mechanical Tests of Pressure Vessel Samples from the TMI-2 Lower Head[a]

By D. R. Diercks[b] and G. E. Korth[c]

Abstract: *Fifteen prism-shaped steel samples were removed from the lower head of the damaged Three Mile Island Nuclear Station Unit 2 (TMI-2) reactor pressure vessel to assess the effects of approximately 19 metric tons of molten core debris that had relocated there during the 1979 loss-of-coolant accident. Metallographic examinations of the samples revealed that inside-surface temperatures of 800 to 1100 °C were attained during the accident in an elliptical "hot spot" approximately 1 × 0.8 m. Tensile, creep, and Charpy V-notch specimens were cut from the samples to assess the mechanical properties of the lower-head material at temperatures up to the peak accident temperature. These properties were used in a margin-to-failure analysis of the lower head.*

The Three Mile Island Nuclear Station Unit 2 (TMI-2) Vessel Investigation Project (VIP) is an international program conducted jointly by the U.S. Nuclear Regulatory Commission (NRC) and the Organization for Economic Cooperation and Development/Nuclear Energy Agency (OECD/NEA). The objectives of the overall program are to (1) determine a scenario for the relocation of molten core debris during the TMI-2 nuclear reactor loss-of-coolant accident in March 1979 and deduce the thermal history of the steel in the lower vessel head during the relocation event, (2) determine the mechanical properties of the lower head steel under the accident conditions, and (3) assess the integrity of the TMI-2 lower head under the accident conditions. Participants in the project include the United States, Japan, Belgium, Germany, Finland, France, Italy, Spain, Sweden, Switzerland, and the United Kingdom (U.K.).[1-14]

The relocation of approximately 19 000 kg of molten core debris onto the lower head of the reactor pressure vessel during the accident caused a considerable threat to the integrity of the pressure vessel. The lower head is fabricated of 136-mm-thick A 533, Grade B, Class 1 low-alloy steel base metal with a 5-mm-thick type 308L stainless steel inside cladding. The approximately 19 000 kg of molten debris had the potential to melt the lower head or cause it to fail by short-term creep under the tensile loadings present during the accident. That the lower head did not fail indicates that significant melting did not occur and that time at temperature was not sufficient to produce creep failure under the loadings that were present. The purpose of the present investigation is to determine the maximum temperature of the lower-head material during the accident and to measure the mechanical properties of that material under the accident conditions. These results were subsequently used in another phase of the TMI program to assess the integrity of the lower head during the accident.[13]

Fifteen prism-shaped samples, each approximately 152 to 178 mm long, 64 to 89 mm wide, and 64 to 76 mm deep, were recovered from the TMI-2 lower head during the first phase of the program (Fig. 1). The samples were cut from the inner surface of the lower head and typically extend through approximately half of the lower-head thickness. These 15 samples were subjected to detailed initial examinations and were then sectioned into metallographic and mechanical test specimens for further characterization (Fig. 2). The results of the initial sample examinations, metallographic studies, and mechanical tests are reported here. Results of the examinations of the lower-head samples before sectioning and of selected instrument nozzles from the lower head are reported elsewhere in Ref. 14.

METALLOGRAPHIC STUDIES

Following initial examinations at Argonne National Laboratory (ANL), metallographic specimens were cut

[a]Work supported by the Office of Nuclear Regulatory Research, U.S. Nuclear Regulatory Commission, and by the Organization for Economic Cooperation and Development/Nuclear Energy Agency.

[b]Energy Technology Division, Argonne National Laboratory, Argonne, IL 60439.

[c]Idaho National Engineering Laboratory, EG&G Idaho, Inc., Idaho Falls, ID 83415.

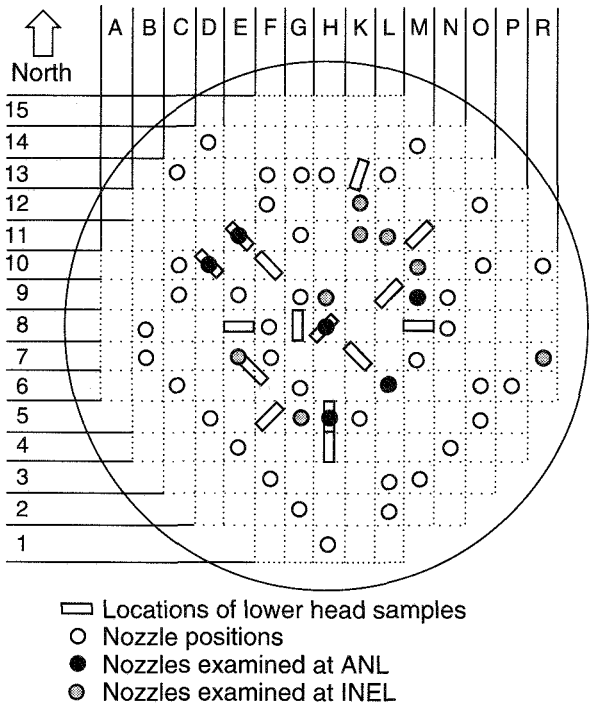

Fig. 1 Grid map of TMI core showing locations of lower-head samples and nozzles.

from the lower-head samples, decontaminated, and sent to the Idaho National Engineering Laboratory (INEL). These specimens were subjected to detailed characterization by optical metallography and hardness measurements to determine the maximum temperature attained at various lower-head locations during the accident. The ANL and participating OECD partner laboratories also conducted supplemental examinations.

Background Information

For corrosion protection, the A 533 B low-alloy steel TMI-2 lower head was clad on the inside with Type 308L austenitic stainless steel by a multiple-wire submerged arc welding process. The fabrication history of the vessel is summarized as follows: 136-mm (minimum) plate formed to shape by hot pressing, austenitized at 871 to 899 °C for 5.5 hours, brine quenched and tempered at 649 °C for 5.5 hours, clad on the inside with 5-mm-thick (minimum) ER308L stainless steel, and then stress-relieved at 607 °C for 50 hours.

Because the amount of material extracted from the TMI-2 vessel was limited, archive A 533 B steel was also obtained from the abandoned Midland reactor, which had never been put into service. The Midland reactor pressure vessel was of the same design and

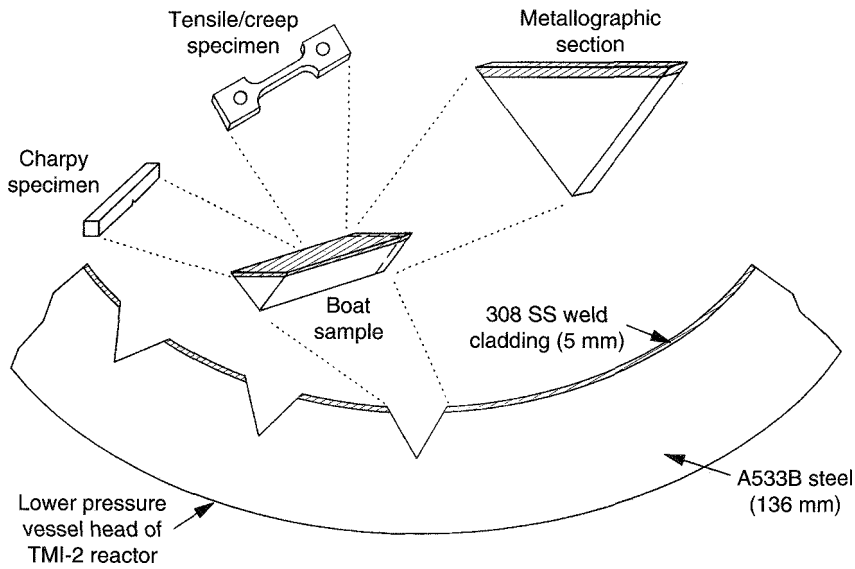

Fig. 2 Schematic diagram of source of TMI-2 metallographic and mechanical property samples.

vintage as the TMI-2 vessel, was built by the same contractor, and had a very similar fabrication history. The Midland material was plentiful and provided a valuable resource for studying properties and accident-simulated thermal response of lower-head material.

The cladding overlay and fabrication history left their "thermal signature" on the lower head. In some cases this as-fabricated condition was further altered thermally by the molten core debris that relocated during the accident. The typical as-fabricated condition (microstructure and hardness) found in the TMI-2 and Midland lower-head material is illustrated in Fig. 3 for sample H-5 from the TMI-2 lower head. A heat-affected zone (HAZ) of 7 to 12 mm is observed in the A 533 B steel directly adjacent to the stainless steel cladding. The first 2 to 3 mm of the HAZ is made up of enlarged, partially decarburized grains, and the remainder of this HAZ band consists of refined grains that reached temperatures above the ferrite-to-austenite transformation temperature of 727 °C from the welding operation and were then quenched because of the massive heat sink provided by the remaining material. Beyond the HAZ band, tempered bainite is uniformly observed throughout the remaining thickness. Any further thermal exposure greater than 727 °C during the accident would alter this as-fabricated structure and create a new thermal signature, which could be used to determine the thermal history caused by the accident.

The thermal histories of the lower-head samples were assessed by hardness profiles and microstructural examinations of the base metal, cladding, and interface regions. Typical hardness profiles were taken of the samples from the weld cladding to the bottom tip of the triangular cross sections through the lower-head samples. The microstructure was examined by standard optical metallographic practices or by scanning and transmission electron microscopy.

Hardness Measurements

The hardness profiles of most of the TMI-2 samples displayed the typical characteristic profile of as-fabricated material, as shown in Fig. 3, but the hardness profiles from samples E-6, E-8, F-10, and G-8 were markedly different from the other samples, as shown in Fig. 4. In these four samples the characteristic hardness profile through the HAZ band had risen sharply to much higher levels and was then sustained throughout the full sample depth. Heat-affected bands from the cladding were not evident in these four samples but were completely eliminated by the thermal effects of the accident.

Two other samples (H-8 and F-5) also showed anomalies in the hardness profiles. The hardness of H-8, measured in a longitudinal direction (parallel to the inside surface of the lower head) on several strips remaining after tensile specimens were cut, increased as the end closest to G-8 was approached. This observation indicates that the ferrite-to-austenite transformation temperature was reached on the end of H-8 nearest to G-8. The hardness profile of F-5, as measured by some of the participating laboratories, showed some deviation from the typical weld HAZ effects, which indicates that temperatures near this sample slightly exceeded the 727 °C threshold.

The final hardness of the TMI-2 samples not only strongly indicates that the A 533 B steel transformation temperature of 727 °C was exceeded during the accident but also indicates some bounds on the cooling rate back through the phase change. To achieve the same hardness values on standards as observed in samples E-6, E-8, F-10, and G-8, the cooling rate must have been 10 to 100 °C/min. Studies with the Midland material showed that if the cooling rate had been approximately 1 °C/min or less, the final hardness would have been approximately the same as that of the parent metal. If that had been the case, hardness measurements would not have been very helpful in determining the thermal history as a result of the accident; they would reveal only that the hardness peak from the HAZ band in the cladding was eliminated. However, the final hardness values for E-8, F-10, G-8, and E-6 are consistent with cooling rates ≥10 °C/min and peak temperatures above 800 °C. Therefore hardness values of the TMI-2 samples indicate (1) whether the material had exceeded the transformation temperature and (2) if it had, some bounds on the cooling rate. Hardness values are not conclusive as to the peak temperatures that may have been reached, even though some trends were observed by ANL and Saclay in France. From just the hardness measurements, it was concluded that F-5 and one end of H-8 slightly exceeded 727 °C and that E-6, E-8, F-10, and G-8 exceeded 830 °C. Examination of the microstructure, discussed in the following text, was used to assess peak temperatures after the initial screening was performed with hardness measurements.

Midland Archive Standards

Standards with known thermal histories were prepared from Midland archive material and later from actual as-fabricated TMI-2 material. These accident-simulated standards provided a means to compare a similar material, with a known thermal history, with

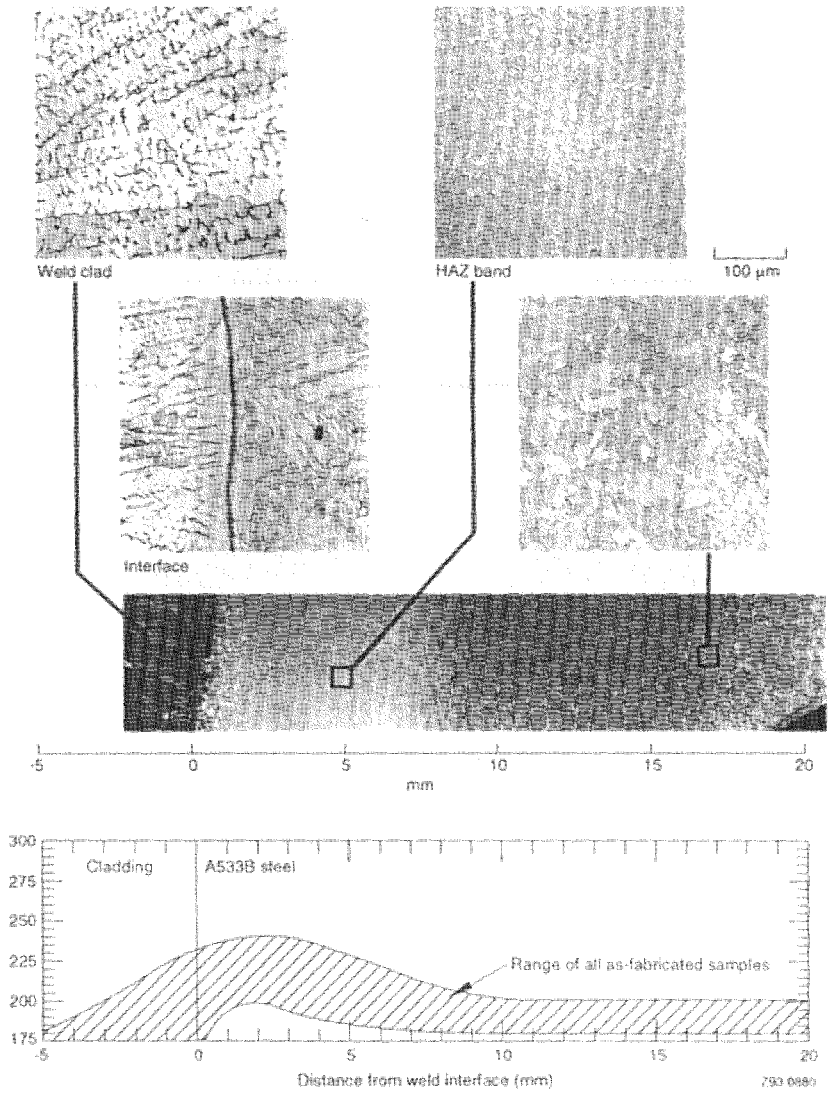

Fig. 3 Typical as-fabricated microstructure and hardness of TMI-2 lower-head material (from TMI-2 lower-head sample H-5).

TMI-2 material with an unknown thermal history. Initially, standards were prepared to determine the effect of cooling rate through the austenite-to-ferrite transition temperature range, which affects hardness. Several laboratories then prepared standards from Midland archive material with maximum temperatures that ranged from 700 to 1300 °C and with dwell times at peak temperatures of 1 minute to 2 hours. The heat-up rate was controlled at 40 °C/min, and the cooling rate following the dwell period was 1 to 100 °C/min. Finally, as unknown thermal histories were narrowed down, an additional set of standards was prepared from actual TMI-2 lower-head material determined to be in the as-fabricated condition. These small sections of TMI-2 material were heat-treated at 950, 1000, 1050, and 1100 °C for dwell times of 10, 30, and 100 minutes and provided the final basis for comparison to determine the thermal history of the lower head as a result of the accident.

As the standards were prepared and examined, various metallurgical observations revealed a stepwise process that could be used to determine the thermal histories of the TMI-2 samples. A diagram (Fig. 5) was constructed

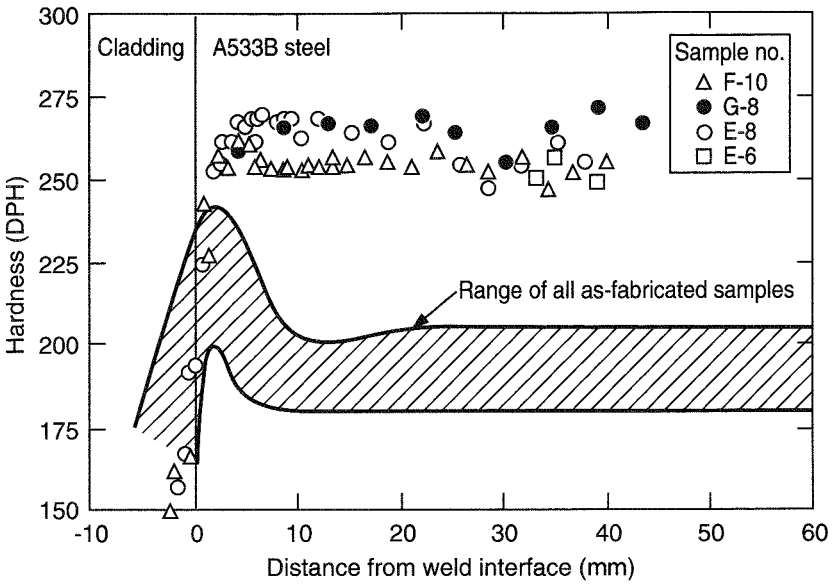

Fig. 4 Hardness profiles of samples F-10, G-8, E-8, and E-6 compared with as-fabricated samples.

to illustrate the metallurgical changes with time and temperature of the Midland and TMI-2 lower-head A 533 B steel with a 308L stainless cladding. Because the vessel was stress-relieved at 607 °C, after the cladding was in place, no thermal effects from the accident could be detected at or below this temperature; therefore the diagram shows metallurgical observations only for temperatures above this point. The lowest temperature indicator was the ferrite-to-austenite transformation, which starts at 727 °C and is complete by approximately 830 °C. Variations in the typical as-fabricated hardness profile will be evident when this threshold is exceeded. The next indicator is the dissolution or dissipation of a dark feathery band at the interface; this occurs between 800 and 925 °C, depending on time of exposure. The next indicator of increasing temperature is the appearance of small equiaxed grains, which formed in the A 533 B steel adjacent to the interface between 850 and 900 °C and disappeared between 1025 and 1100 °C as they were consumed by grain growth in the low-alloy steel. These equiaxed grains, which are not typical for a low-alloy steel, appear to be devoid of cementite, probably because of a loss of carbon into the stainless steel during the elevated temperature excursion associated with the accident. Grain growth in the A 533 B steel becomes significant above approximately 950 to 1075 °C, depending on the time involved.

The highest temperature indicator shown in Fig. 5 is the change in morphology of the δ-ferrite islands in the stainless steel cladding. In the approximate range of 975 to 1000 °C at 100 minutes or 1100 to 1125 °C at 10 minutes, the δ-ferrite islands begin to lose their slender branch-like morphology and become spherical in shape. This spheroidizing of the δ-ferrite islands is believed to be associated with the dissolution of $M_{23}C_6$ carbides that decorate the ferrite–austenite boundaries and stabilize their shape. When the carbides dissolve, the δ-ferrite becomes more spherical to minimize surface energy. There was also evidence that some of the δ-ferrite was consumed into the austenitic matrix after exposures above 1000 °C because there was a net loss of δ-ferrite after cooling. Researchers in Germany[7] and Spain[9] used magnetic measurement techniques to determine that δ-ferrite levels in the cladding of nonaffected samples were 4 to 5 vol % but only 1.4 vol % in E-8.

Microstructure of TMI-2 Samples

The microstructural indicators illustrated in Fig. 5 were used to further assess the thermal history of the four samples (E-6, E-8, F-10, and G-8) that clearly show thermal effects above the ferrite-to-austenite transformation temperature. Examinations of the microstructure showed that the dark feathery band had dissipated at the A 533 B steel–weld cladding interface in all four samples. Austenitic grain growth was evident in all four samples, with E-6 and E-8 showing the most pronounced effect. Sample F-10 revealed that a small remnant of the

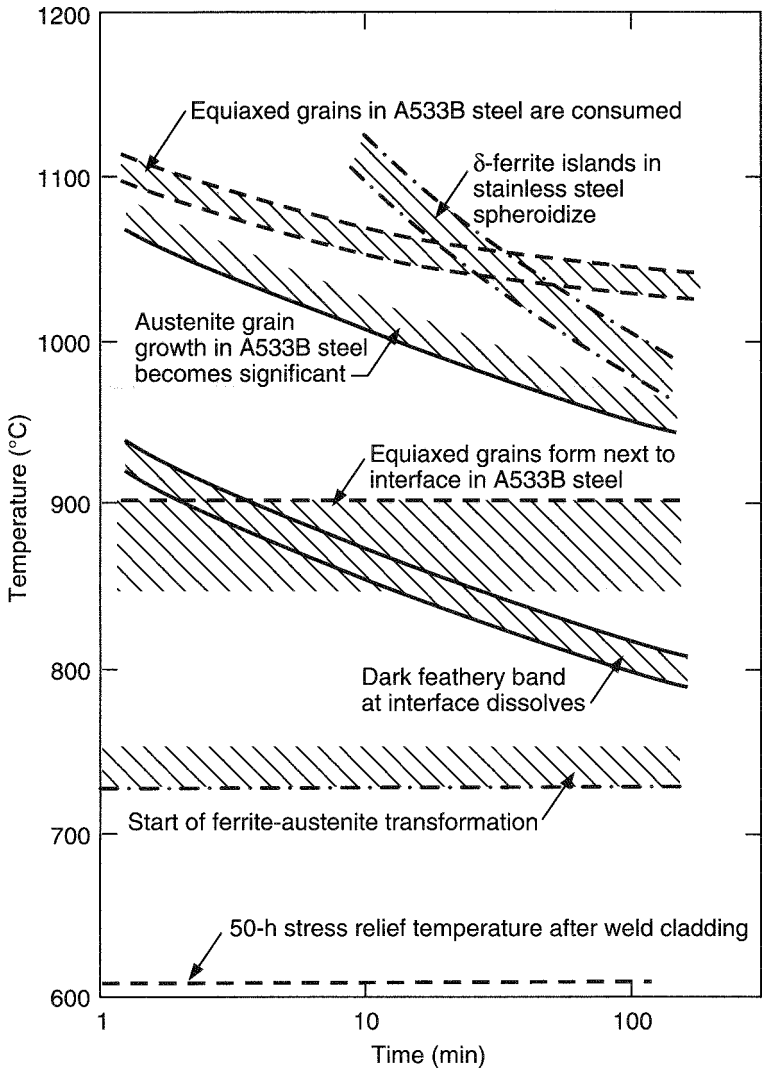

Fig. 5 Diagram of time–temperature observations of A 533, Grade B pressure-vessel steel clad with Type 308L stainless steel.

cementite-devoid equiaxed small ferrite grains was still present; none was evident in the other three samples. Spheroidization of the δ-ferrite islands in the cladding was not readily detected in F-10, was partially observed in G-8, and was fairly significant in E-6 and E-8. The preceding microstructural observations were supplemented by scanning electron microscopy of etched specimens and surface replicas and analytical transmission electron microscopy of thin foils and carbon extraction replicas.[2] By means of meticulous comparisons of these observations with the standards of known thermal history, INEL, the lead laboratory for metallurgical examinations, estimated peak temperatures and time at temperature within approximately 2.5 mm of the cladding–base metal interface as follows:

- E-6 and E-8: 1075 to 1100 °C for ~30 minutes
- F-10 and G-8: 1040 to 1060 °C for ~30 minutes

The results of examinations at ANL and some of the OECD partner laboratories of different sections of these same samples are consistent with the INEL conclusions. U.K. researchers showed evidence that M-11 also slightly exceeded the 727 °C transformation temperature near the surface, although this determination was not confirmed by five other laboratories that examined different sections of the M-11 boat sample. On the basis of the preceding

observations and conclusions, a thermal contour map of peak temperatures (Fig. 6) was constructed. The hardness profile and microstructure of one of the thermally altered samples, E-8, is shown in Fig. 7.

The temperature gradient through the thickness of the lower vessel head wall was estimated by two methods. First, because the high level of hardness of the four affected samples persisted to the full depth of the boat samples (50 mm from the inside surface or 45 mm from the cladding interface; see Fig. 4), it could be concluded that the temperature at that depth was greater than the 727 °C transformation temperature. Second, on the basis of the assumption from the microstructure comparisons that the thermal excursion on the lower head as a result of the accident was approximately 30 minutes, prior austenite grain size at the bottommost tip of the heat-affected samples was compared with prepared standards that were heat-treated for 30 minutes. This comparison indicated that the temperature 50 mm from the inside surface (45 mm from the stainless steel–low-alloy steel interface) was 50 to 150 °C lower than the peak temperatures determined previously for the region near the interface. By combining temperature gradient estimates from INEL, ANL, and Finland and assuming a linear relationship, the gradient was estimated to be 2 to 4 °C/mm.

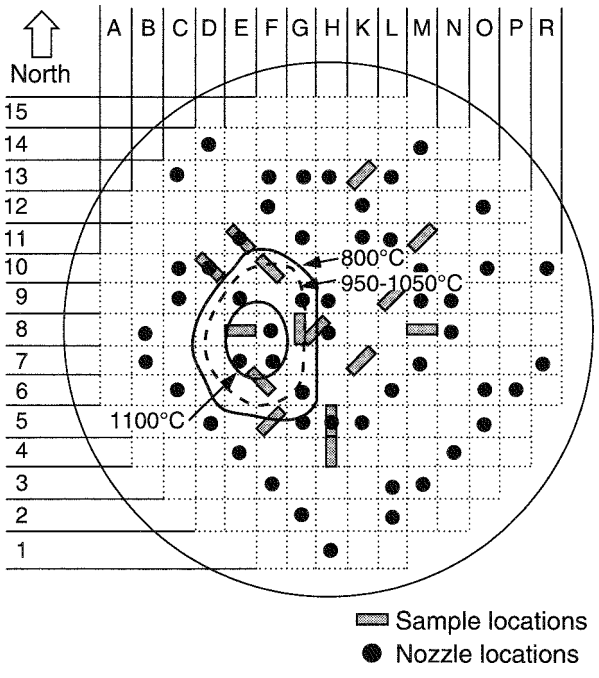

Fig. 6 Thermal contour map of peak temperature constructed as best estimate on the basis of results of metallographic examinations of boat samples.

MECHANICAL-PROPERTY TESTS

Test specimens were cut from the lower-head samples to determine the mechanical properties of this material under the accident conditions. The tests conducted included tensile tests at room temperature and 600 to 1200 °C, stress-rupture tests at 600 to 1200 °C, and impact tests over the temperature range from –20 to +300 °C. The results of these tests are summarized here; more complete information, including a tabulation of the data and the strain vs. time curves for the stress-rupture tests, can be found in Ref. 15.

The room-temperature tensile tests were conducted to obtain results that could be compared with literature data; the minimum temperature of 600 °C for the remaining tests reflects the judgment that (1) little or no damage would have occurred to those portions of the lower head for which the maximum temperature did not exceed this value and (2) failure was unlikely at these locations. The maximum temperature of 1200 °C for these tests lies slightly above the maximum lower-head temperature believed to have been attained during the accident.

The tests were conducted on specimens with various prior thermal histories that resulted from the accident. Because the number of specimens from the portion of the lower head that reached the highest temperature was limited, it was necessary, in some cases, to heat-treat low-damage specimens before testing to produce a corresponding microstructure. This treatment consisted of heating the specimen to 1000 °C, holding it at this temperature for 2 hours, and then cooling it to room temperature at about 10 to 50 °C/min. For specimens to be tested at 1000 °C or greater, this prior heat treatment was omitted because its effects would be negated by the thermal treatment imposed during testing.

Tensile Tests

The tensile tests were conducted in general accordance with American Society for Testing and Materials (ASTM) Standards E8 and E8M using a rectangular cross-section specimen that also complied with applicable standards of the Deutsches Institut für Normung. All elevated temperature tests were conducted in an argon or helium environment. The strain rate for the elastic portion of the loading was $\leq 5 \times 10^{-4}$ s^{-1}, and the strain rate during plastic loading was 4×10^{-4} s$^{-1} \pm 1 \times 10^{-4}$ s^{-1}.

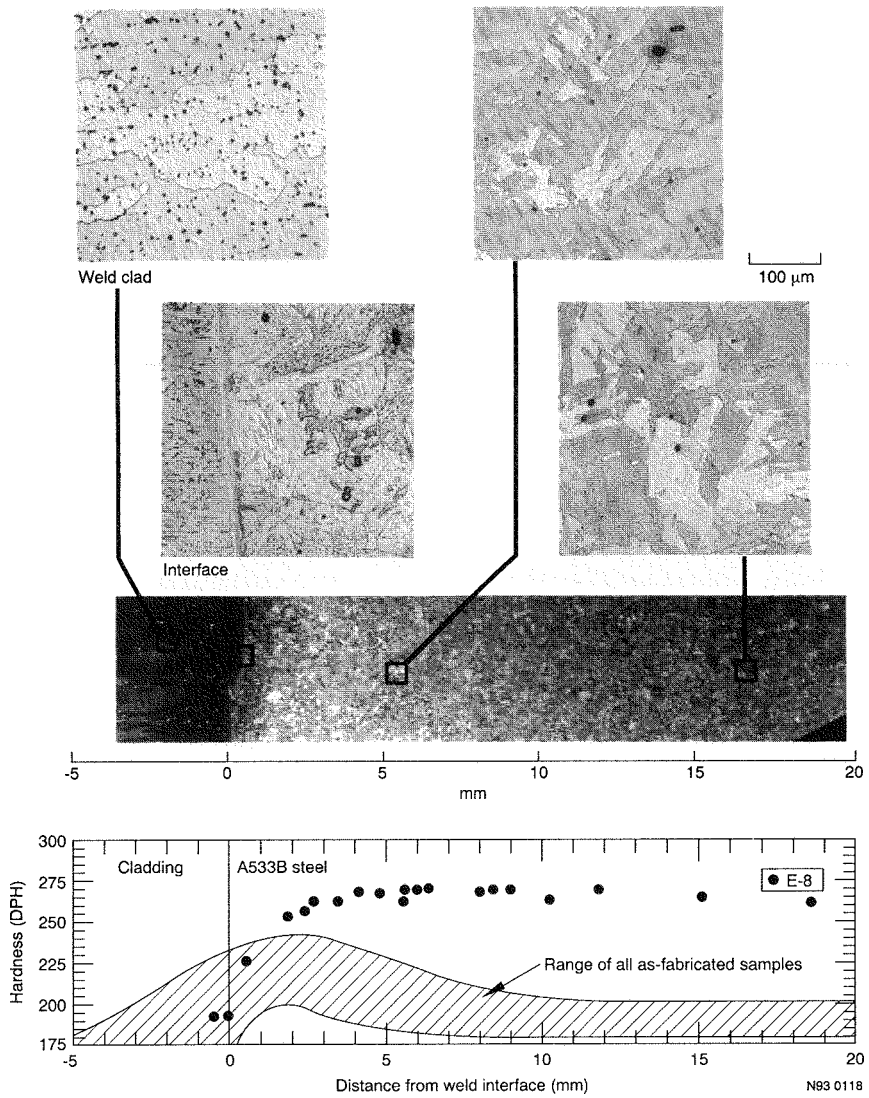

Fig. 7 Microstructure and hardness profile of sample E-8.

The reported yield strength values were obtained by the 0.2% offset method except where discontinuous yielding occurred; in these cases, the observed upper yield strength was reported.

The results of the tensile tests conducted on the lower-head base-metal specimens are shown in Fig. 8. These tests were carried out at ANL[3] as well as in Belgium,[4] France,[6] and Spain.[11] Also plotted in Fig. 8 are average values reported by the Japanese National Research Institute for Metals (NRIM) for five other heats of A 533, Grade B, Class 1 steel.[16] The NRIM data were obtained at a strain rate of 5×10^{-5} s^{-1} up to yield and 1.25×10^{-3} s^{-1} for the remainder of the test. The NRIM tensile strength data suggest a strain-aging effect between 100 and 300 °C, which resulted in a local tensile strength minimum at approximately 150 °C. Both the tensile and yield strengths of this alloy are strongly temperature dependent; the room-temperature tensile strength values are reduced by a factor of more than 2 at 600 °C and more than 10 at 900 °C.

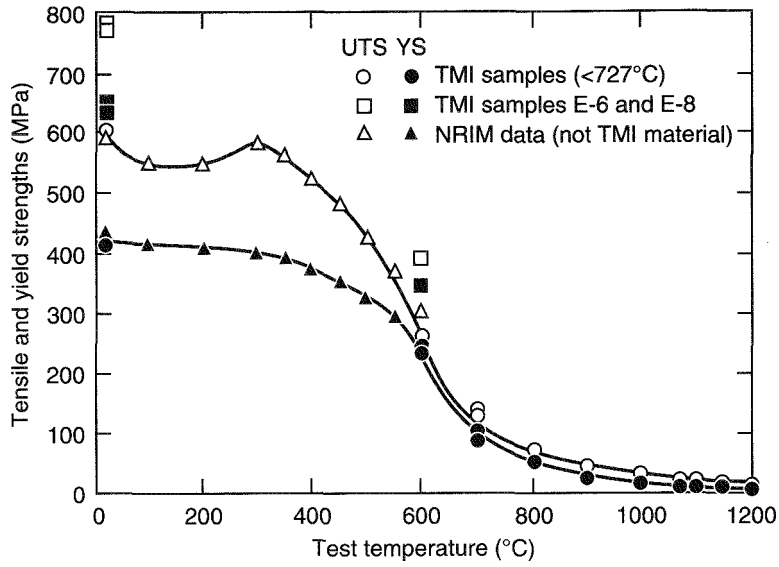

Fig. 8 Tensile and yield strengths of TMI-2 lower-head material. UTS, ultimate tensile strength; YS, yield strength.

The data for specimens taken from lower-head samples E-6 and E-8 are plotted separately in Fig. 8, and these data lie significantly above the best-fit curve to the remaining data. As discussed earlier, both of these samples were heated to maximum temperatures of about 1075 to 1100 °C during the accident, followed by a relatively rapid cooling at about 10 to 100 °C/min. The resulting hardening has produced significant increases in strength at both room temperature and 600 °C.

Stress-Rupture Tests

The stress-rupture tests used the same specimen design as the tensile tests, and testing was carried out in general accordance with ASTM Standard E139. These tests were carried out at ANL[3] and in Belgium,[4] France,[6] and Spain.[10] The resulting data for stress vs. time to failure are plotted in Fig. 9 along with a Manson–Haferd best fit (explained in the following text). The tests were conducted in an argon or helium environment except for those conducted in Belgium. All but one of the Belgian tests were conducted in a vacuum; a single test at 800 °C and 30 MPa was conducted in an argon environment.

Materials with slightly different thermal histories were tested at both 600 and 700 °C. At 600 °C, tests were conducted on specimens from sample K-13, for which the maximum temperature during the accident did not exceed 727 °C, as well as on specimens from sample F-5, for which the maximum temperature was apparently somewhat greater than 727 °C over a portion of the sample. No significant difference in time to failure is observed in Fig. 9. This lack of an effect may be attributed to the fact that the maximum temperature probably did not significantly exceed the transformation temperature of 727 °C in F-5, particularly in the bottom half of the sample, from which the creep test specimens were taken. Similarly, at 700 °C, specimens from sample M-11, for which the maximum temperature may have approached or slightly exceeded 727 °C, show no difference in behavior when compared with specimens from sample H-8, for which the maximum temperature remained below 727 °C.

Two time–temperature correlations were explored in an attempt to fit the base-metal creep data. The first of these was the Larson–Miller parameter L (Ref. 17), defined as

$$L = T[C + \log_{10}(t_f)]$$

where T is temperature in Kelvin, t_f is time to failure in hours, and C is a fitting constant. A least-squares analysis determined that the optimal value of C for the present

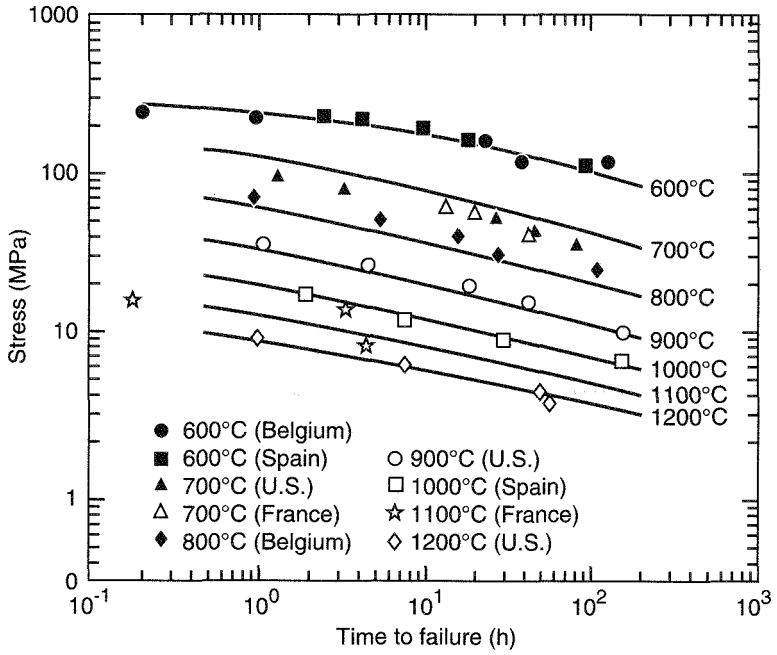

Fig. 9 Stress-rupture data with Manson–Haferd best fit.

data base was 12.5, and stress σ was related to the Larson–Miller parameter by the relation

$$\log_{10}(\sigma) = 4.3406 - 0.00018767 \cdot L \qquad (1)$$

where the applied stress σ is in MPa.

The ability of the Manson–Haferd time–temperature correlation[18] to fit the data was also evaluated. The Manson–Haferd parameter M has the form

$$M = \frac{\log_{10}(t_f) - t_a}{T - T_a}$$

where t_f is time to failure in helium, T is test temperature in Kelvin, and t_a and T_a are fitting constants. A least-squares analysis was again carried out, and the optimal values for t_a and T_a were found to be 7.57 and 520, respectively. Log(σ) was found to vary with the Manson–Haferd parameter M according to the relationship

$$\log_{10}(\sigma) = -0.80467 - 261.41 \cdot M - 5291.25 \cdot M^2 \qquad (2)$$

A comparison of the resulting best-fit curves with the actual σ vs. t_f data in Fig. 9 shows a reasonably good fit to the data. However, systematic departures from the actual data are noted in the 700 to 900 °C region. This problem may be associated in part with the ferrite-to-austenite phase transformation that occurs over the temperature regime from 727 to approximately 830 °C.

Impact Tests

The impact tests on the lower-head material were conducted in Italy[8] by using the procedure and conventional Charpy V-notch test specimen described in ASTM E23; the data are summarized in Fig. 10. The three groups of test specimens for which the maximum temperature did not exceed 727 °C (D-10, H-4, and E-11) show similar behavior, with an upper-shelf energy of approximately 170 J and a transition temperature of approximately 20 °C. However, the data from specimens of sample F-10, for which the maximum temperature was approximately 1040 to 1060 °C, stand in marked contrast. The F-10 material shows a significantly higher ductile-to-brittle transition temperature of approximately 70 °C as well as a lower upper-shelf energy of approximately 120 J. These differences reflect the reduced ductility and impact resistance that was produced in this material by the high temperatures and relatively rapid cooling associated with the accident.

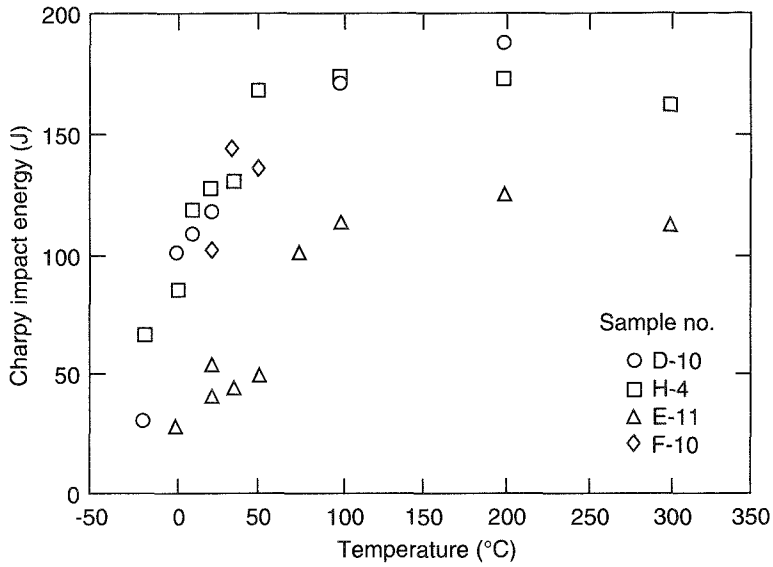

Fig. 10 Absorbed impact energy vs. test temperature.

SUMMARY AND CONCLUSIONS

The INEL, ANL, and the OECD partner laboratories have conducted microstructural characterization and mechanical property tests on material from 15 locations in the lower head of the pressure vessel of the TMI-2 nuclear reactor. The microstructural characterization was conducted by conventional optical metallography, hardness measurements, scanning electron microscopy of etched specimens and surface replicas, and analytical transmission electron microscopy of thin foils and carbon extraction replicas. The mechanical tests consisted of tensile tests at room temperature, tensile and creep tests at 600 to 1200 °C, and Charpy-impact tests at –20 to +300 °C. The specimens were taken from locations where the maximum temperature had not exceeded 727 °C during the accident and from locations where the maximum temperature had been as high as 1100 °C. The results of these investigations lead to the following conclusions:

1. An elliptical hot spot approximately 1 × 0.8 m on the inside surface of the lower pressure vessel head was heated to temperatures from approximately 800 to 1100 °C for approximately 30 minutes by relocated fuel debris.

2. The remainder of the lower head remained below 727 °C, but some areas may have been almost this temperature.

3. The temperature gradient through the thickness of the vessel wall was approximately 2 to 4 °C/mm.

4. The thermal excursion of the lower head was "quenched" (i.e., cooled at approximately 10 to 100 °C/min).

5. The results of tensile tests conducted on base-metal specimens for which the maximum temperature during the accident (T_{max}) did not exceed 727 °C agree well with literature data for A 533 B steel and show a dramatic drop in strength at temperatures above 600 °C.

6. Tensile specimens from samples for which T_{max} exceeded 727 °C showed significantly higher strengths at room temperature and 600 °C when compared with specimens for which the temperature did not exceed 727 °C.

7. Stress-rupture tests at 600 and 700 °C indicated no significant difference in behavior between base-metal specimens for which T_{max} was approximately 727 °C and those for which it was well below this value.

8. The stress-rupture data obtained from base-metal specimens were fit with both the Larson–Miller and Manson–Haferd time–temperature parameters.

9. Charpy V-notch impact tests conducted on lower-head base-metal material revealed a substantial difference between specimens from sample F-10, for which T_{max} was approximately 1040 to 1060 °C, and specimens from samples for which T_{max} was less than 727 °C. The F-10 material showed a significantly higher ductile-to-brittle transition temperature as well as a lower upper-shelf energy value.

ACKNOWLEDGMENTS

The authors gratefully acknowledge the support and direction provided by C. Z. Serpan, A. Rubin, E. Hackett, and M. Mayfield of the NRC. The financial support and significant technical contributions of the OECD partner laboratories participating in the TMI-2 Vessel Investigation Project Metallurgical Program are also gratefully acknowledged. The following persons at ANL contributed to the completion of this work: T. L. Shearer, D. O. Pushis, F. M. Basso, S. L. Phillips, J. A. Zic, W. Kettman, F. Pausche, J. E. Sanecki, A. G. Hins, W. F. Burke, and W. A. Moll. INEL contributors include G. L. Fletcher and D. V. Miley.

REFERENCES

1. J. R. Wolf, J. L. Rempe, L. A. Stickler, D. W. Akers, G. E. Korth, L. A. Neimark, and D. R. Diercks, *OECD-NEA-TMI-2 Vessel Investigation Project Integration Report,* Report TMI V(93) EG10, October 1993.
2. G. E. Korth, *Metallographic and Hardness Examinations of TMI-2 Lower Pressure Vessel Head Samples,* Report NUREG/CR-6194, March 1994.
3. D. R. Diercks and L. A. Neimark, *Results of Mechanical Tests and Supplementary Metallographic Examinations of the TMI-2 Lower Head Samples,* Report TMI V(93) AL02, June 1993.
4. W. Vandermeulen and W. Hendrix, *Examination Report of the Samples of the TMI-2 RPV Received by SCK/CEN (Belgium),* SCK/CEN, Mol, Belgium, March 1992.
5. Reijo Pelli, *Metallographic Examination of TMI-2 RPV Lower Head Sample E-8 and the Archive Material of Midland Reactor,* Report TMI V(92) SF01, VTT Technical Research Centre of Finland, Espoo, April 1992.
6. F. Le Naour, *CEA Contribution to the TMI-2 Vessel Material Investigation Project,* N.T. SRMA 92-1956, Centre d'Etudes de Saclay, France, May 1992.
7. H. Ruoff, K.-H. Katerbau, and D. Sturm, *Metallographic Examination of TMI-2 Lower Pressure Vessel Head Samples,* Report TMI V(91) D001, Staatliche Materialprüfungsanstalt, Stuttgart, Germany, September 1991.
8. P. P. Milella and F. Bigagli, *Charpy V Testing of Specimens of the TMI-2 Vessel Lower Head,* Report TMI V(92) I01, European Nuclear Energy Association, Rome, Italy, May 1992.
9. L. Pedrero and P. Veron, *Metallographic Investigation of TMI-2 Lower Pressure Vessel Head Samples,* Report TMI V(92) E002, Equipos Nucleares S. A., Maliaño, Spain, April 1992.
10. A. Ballesteros, *TMI-2 Vessel Investigation Project Creep Tests,* Report TMI V(92) E004, TECNATOM, Madrid, Spain, February 1992.
11. E. López Rincón, *Testing of Lower Head Specimens in Spain (Tensile Results),* Report TMI V(92) E001, CIAT, Madrid, Spain, May 1992.
12. J. M. Titchmarsh and R. Cooke, *AEA-Technology Examinations of TMI-VIP Lower Head Samples,* Report TMI V(91) UK2, AEA Technology, Harwell, U.K., September 1991.
13. L. A. Stickler, J. L. Rempe, S. A. Chavez, G. L. Thinnes, S. D. Snow, R. J. Witt, M. L. Corradini, and J. A. Kos, *Calculations to Estimate the Margin to Failure in the TMI-2 Vessel,* Report NUREG/CR-6196 (EGG-2733), March 1994.
14. L. A. Neimark, Insight Into the TMI-2 Core Material Relocation Through Examination of Instrument Tube Nozzles, *Nuclear Safety,* this issue.
15. D. R. Diercks and L. A. Neimark, *Results of Mechanical Tests and Supplementary Microstructural Examinations of the TMI-2 Lower Head Samples,* Report NUREG/CR-6187 (ANL-94/8), April 1994.
16. *Data Sheets* on *the Elevated-Temperature Properties of 1.3 Mn–0.5 Mo–0.5 Ni Steel Plates for Boilers and Other Pressure Vessels (SBV 2),* NRIM Creep Data Sheet No. 18B, National Research Institute for Metals, Tokyo, 1987.
17. F. R. Larson and J. Miller, *Trans. ASME,* 74: 765–771 (1952).
18. S. S. Manson, Design Considerations for Long Life at Elevated Temperatures, in *Proceedings of the International Conference on Creep, London, October 3, 1963,* pp. 1-27.

Margin-to-Failure Calculations for the TMI-2 Vessel[a]

By J. Rempe,[b] L. Stickler,[b] S. Chàvez,[b] G. Thinnes,[b] R. Witt,[c] and M. Corradini[c]

Abstract: *As part of the Three Mile Island Unit 2 (TMI-2) Vessel Investigation Project (VIP) sponsored by the Organization for Economic Cooperation and Development (OECD), margin-to-failure (MTF) calculations for mechanisms having the potential to threaten the integrity of the vessel lower head were performed to better understand events that occurred during the TMI-2 accident. Analyses considered four failure mechanisms: penetration tube rupture, penetration tube ejection, global vessel rupture, and localized vessel rupture. Calculational input was based on data from the TMI-2 VIP examinations of the vessel steel samples, penetration tube nozzles, and samples of the hard layer of debris found on the TMI-2 vessel lower head. Sensitivity studies were performed to investigate the uncertainties in key parameters for these analyses. Calculation results indicate that less margin existed for vessel failure mechanisms, rather than tube failure mechanisms, during the TMI-2 accident. In addition, calculations suggest that additional experimental data are needed to reduce uncertainties in models for predicting debris cooling and vessel failure.*

On March 28, 1979, the Three Mile Island Nuclear Station Unit 2 (TMI-2) pressurized-water reactor underwent a prolonged, small-break loss-of-coolant accident that severely damaged the reactor core. The postulated end-state conditions of the TMI-2 reactor vessel and core are shown in Fig. 1. As illustrated in this figure, at least 45% of the core melted. Video examinations after the accident indicate that approximately 19 000 kg of molten material relocated from the core region to the water-filled, lower head of the reactor vessel. Examinations indicate that relocated debris severely ablated several instrument tube penetrations inside the lower head, although instrument tubes appeared to be protected at the point where they were welded to the lower head. Instrument tubes outside the vessel and the vessel lower head, however, remained intact throughout the accident. Metallurgical examinations indicate that a localized region of the vessel, approximately 1 m by 0.8 m, reached temperatures between 1075 and 1100 °C during the accident; these examinations also indicate that vessel temperature away from the hot spot did not exceed 727 °C during the accident. However, these temperatures are well above the 538 °C maximum operating temperature limit considered in Case N-499 of the American Society of Mechanical Engineers (ASME) Boiler and Pressure Vessel Code.[1]

As part of the TMI-2 Vessel Investigation Project (VIP), margin-to-failure (MTF) analyses were performed to increase understanding of the events that occurred during the TMI-2 accident. Calculations were performed considering four vessel lower-head failure mechanisms: penetration tube rupture, penetration tube ejection, global vessel rupture, and localized vessel rupture. Although experimental data have validated many aspects of severe accident analyses models, no integral experimental data are available to validate entire models. Hence the data available from the TMI-2 VIP, previous TMI-2 research programs, and plant instrumentation provide a unique opportunity to assess uncertainties in severe accident analyses models.

This article summarizes models used in the MTF analysis effort. Significant results from these calculations are also presented. A more complete description of the analyses and results can be found in Ref. 2.

APPROACH

Figure 2 depicts the four failure mechanisms considered in these analyses. The tube rupture failure mechanism (part a of Fig. 2) may result from a combination of high pressure and elevated ex-vessel tube temperatures as the result of contact with debris that has traveled through the tube to ex-vessel locations. Failure of a penetration tube weld (part b of Fig. 2) could result from

[a]The U.S. Nuclear Regulatory Commission supported this work in conjunction with OECD, through DOE Contract DE-AC07-76IDO1570.

[b]Idaho National Engineering Laboratory, P.O. Box 1625, Idaho Falls, Idaho 83415-3840.

[c]University of Wisconsin, Madison, Department of Nuclear Engineering and Engineering Physics, 153 Engineering Research Building, 1500 Johnson Drive, Madison, Wisconsin 53706-1687.

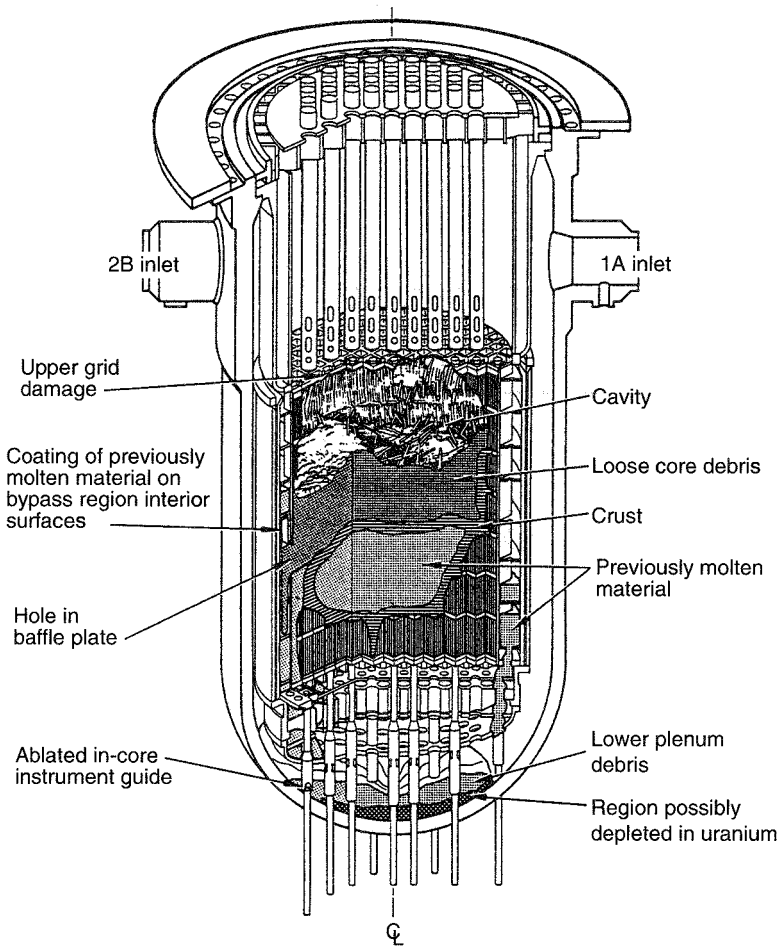

Fig. 1 Postulated TMI-2 end-state configuration.

debris melt attack and sustained heating from accumulated debris around the perimeter of a tube combined with reactor system pressure. Once the weld has failed, tube ejection is possible. Global vessel rupture (part c of Fig. 2) may be caused by elevated system pressure and/or the weight of debris on the lower head in conjunction with sustained heating from debris on the lower head. Localized vessel rupture (part d of Fig. 2) may be caused by thermal loads on the lower head as the result of nonuniform heat sources within the debris bed or a coherent jet of debris impinging directly onto the lower head in conjunction with mechanical loads caused by system pressure and debris weight.

As discussed previously, data from the TMI-2 VIP provide a unique opportunity to assess uncertainties in severe accident analysis tools. Little, if any, validation has been performed on methods used to predict melt–water interaction, molten pool behavior, cooling in debris that solidifies after relocation, and structural creep failure in a severe accident. Thus this calculational effort is useful not only because it provides insights into what failure mechanisms were plausible during the TMI-2 event and identifies the failure mode with the smallest margin during the TMI-2 event but also because it indicates areas where additional data are needed for severe accident modeling.

Calculations relied on VIP examination data from the TMI-2 instrument nozzles, the hard layer of debris found on the head (the "companion debris samples"), and the TMI-2 reactor vessel steel (the "vessel boat samples"). Metallurgical examination data were used to characterize peak vessel temperatures, the duration of

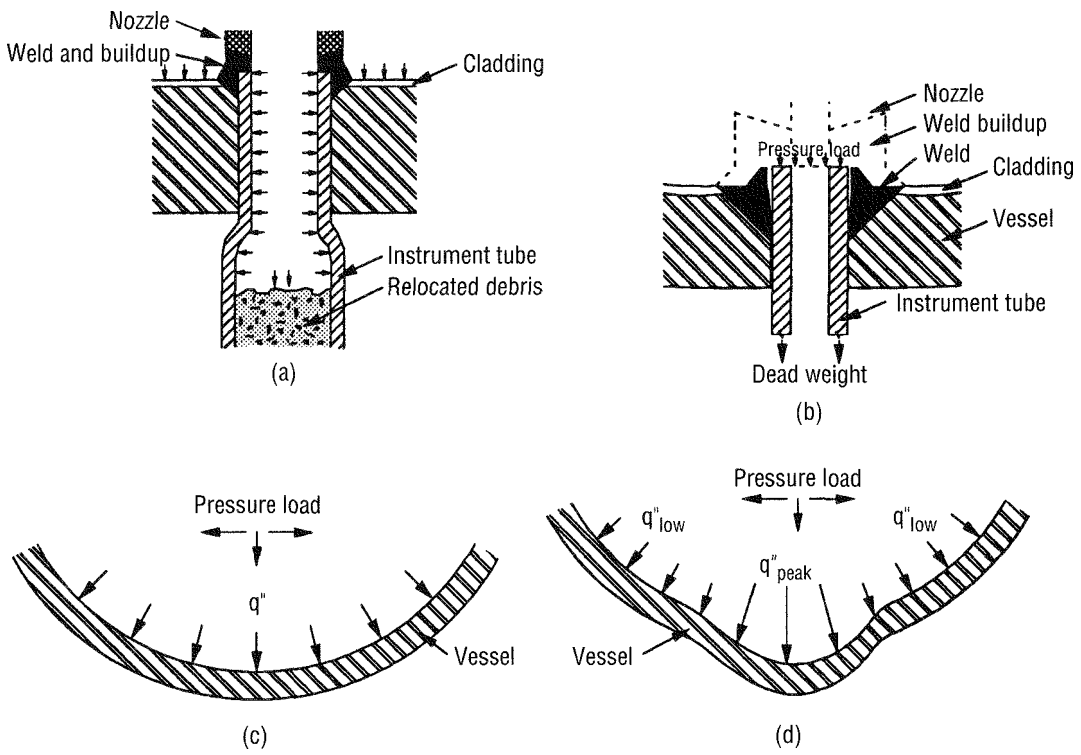

Fig. 2 Failure mechanisms considered in TMI-2 MTF analyses: (a) tube rupture, (b) weld failure–tube ejection, (c) global vessel failure, and (d) localized vessel failure.

peak temperatures, vessel cooling rates, and the end state of instrument nozzle weld material.[3,4] Data from examinations of companion debris samples were used to characterize such debris properties as decay heat and material composition.[5] Nozzle examination data were used to characterize the composition of melt attached to nozzles, elevations for nozzle ablation heights in the vessel, and melt penetration distances within nozzles.[6] Uncertainties for each data source are discussed in Ref. 2. Calculations included sensitivity studies to consider the range of input associated with uncertainties in data.

The potential for each failure mechanism to occur was evaluated on the basis of both ultimate strength and creep damage. Ultimate strength MTF was defined by

$$\text{MTF} = (1 - \text{effective stress/ultimate strength})\ 100\%$$

The TMI-2 Structural Mechanics Peer Review Group defined by consensus a separate stress-based MTF for creep failure.[7] The procedure includes converting multidimensional stress history to an effective stress (equivalent uniaxial stress) history and predicting time to failure for the converted stress and temperature histories using a time-damage model. When results from the initial scoping calculations suggested that a stress-based failure criterion may be too conservative for the prediction of failure, calculations were performed in which creep failure was defined as the point at which strain instability occurred (strain rate approaches infinity).[8]

The MTF calculations investigated an inconsistency between companion debris sample data, which suggest slow debris cooling, and vessel steel sample examination data, which imply relatively fast vessel cooling rates. When results primarily obtained from input based on companion debris sample data indicated that vessel failure would occur, irrespective of which failure criterion was selected, it was postulated that additional cooling (not currently modeled in severe accident analysis codes) occurred. A thermal analysis based on plant thermal hydraulic parameters measured or inferred from data measured during the accident [coolant temperature, reactor coolant system (RCS) pressure,

coolant flow rates entering and exiting the vessel, etc.] confirmed that more cooling than currently considered in severe accident analysis codes occurred during the period between debris relocation and vessel repressurization. Hence calculations were performed to quantify the magnitude of this cooling and possible debris configurations that could explain how this cooling could have occurred.

HIGHLIGHTS FROM MTF ANALYSIS RESULTS

Results from scoping calculations, which evaluate each of the failure mechanisms identified are reviewed in the following text. Results from thermal analyses, required as input for structural response calculations, are also discussed. Finally, results from calculations performed to assess sensitivity to debris cooling rates and different failure criteria are presented.

Melt Penetration–Ex-Vessel Tube Rupture

For ex-vessel tube rupture to occur, melt must travel through an ablated instrument tube to a distance that is below the vessel outer surface in part a of Fig. 2. Several models have been developed to predict the penetration distance of molten debris through vessel instrumentation nozzles. Although previous research was insufficient to select a model for predicting melt flow through light-water-reactor instrument tubes, melt penetration distances have been experimentally determined to be bounded by distances predicted by the bulk-freezing model and the conduction heat transfer model. The bulk-freezing model, first advanced by Ostensen and Jackson,[10,11] assumes that turbulent heat transfer governs melt solidification and penetration behavior. The conduction heat transfer model, first advanced by Epstein,[12,13] assumes that (as its name implies) conduction heat transfer governs melt solidification and penetration behavior.

Data from some TMI-2 instrument nozzles provide measurable distances for melt that traveled through in-vessel instrument structures during the TMI-2 accident. Longer nozzles containing melt with measurable penetration distances were used to select an appropriate model for estimating penetration distances; this model was then used to determine if melt could travel below the vessel lower head through shorter nozzles (see Fig. 3). Melt penetration distances predicted with a bulk-freezing model,[9] modified to consider heat loss from the melt to the tube and the coolant, were found to be consistent with distances measured in TMI-2 instrument nozzles. Distances predicted with a conduction model,[12,13] on the other hand, were found to be much longer (typically, several orders of magnitude longer) than melt penetration distances measured in TMI-2 instrument nozzles. Hence the modified bulk-freezing model was determined to be more appropriate for estimating the melt penetration distances observed in the TMI-2 nozzles.

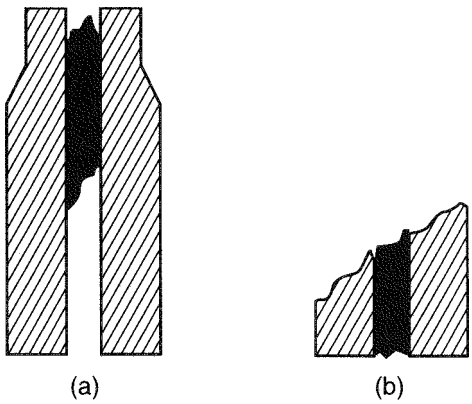

Fig. 3 Various configurations of melt observed in TMI-2 instrument nozzles: (a) nozzle stub containing melt with measurable penetration distance and (b) nozzle stub containing melt with unknown penetration distance.

Melt penetration distances predicted with the modified bulk-freezing model indicate that fuel containing molten debris would not travel through instrument tubes to locations below the lower head. Calculations bounded possible melt compositions, temperatures, and melt flow areas to maximize penetration distances. Furthermore, the nozzle stub height was assumed as 1.3 cm, which was the smallest ablated nozzle height observed in TMI-2 defueling efforts.[14] Although calculations indicate that it is possible for molten debris with highly metallic compositions to flow to ex-vessel tube locations, previous review of TMI-2 instrumentation data[15] suggests that metallic material quenched when it relocated to the lower head during the TMI-2 accident. Hence ex-vessel tube temperatures are not predicted to be higher than the RCS temperatures. Therefore ex-vessel tube rupture calculations were performed assuming that the tube temperatures were consistent with the vessel coolant temperatures.

A simple model comparing the pressure force on the tube and the tube's ultimate strength was used to evaluate ex-vessel tube rupture. As discussed previously, tube

temperatures for these analyses were assumed to equal the vessel coolant temperature. An upper bound on the coolant temperature was taken to be a representative saturation temperature (327 °C) corresponding to system pressures during the first 12 hours after the major relocation of fuel occurred; a lower-bound temperature was based on the minimum temperature (127 °C) measured in the cold legs during the transient. Although ultimate strength data for Inconel are limited,[9] data shown in Fig. 4 indicate that the ultimate strength for the TMI-2 Inconel instrument tubes is above 700 MPa for the temperatures of interest (127 to 327 °C). Because such temperatures were expected to result in very high MTFs, a conservatively high constant upper system pressure of 15 MPa was also applied in the tube rupture calculations. Thus calculations indicate that ultimate-strength MTF for tube temperatures of 127 and 327 °C are both above 95%. Times to creep rupture at these temperatures are estimated to be on the order of 10^{15} and 10^{29} hours. Hence ex-vessel tube rupture can effectively be eliminated as a potential failure mechanism for this accident.

Jet Impingement–Vessel Thermal Response

Calculations were performed to investigate melt relocation and the subsequent thermal loading to the vessel during the TMI-2 accident. Results from these calculations provide input to subsequent weld failure, global vessel failure, and localized failure analyses. Analytical models were applied to simulate the debris–vessel interaction to investigate the thermal response of the vessel during and after debris relocation. These models include phenomena such as breakup of melt relocating into and through the lower plenum water, growth of the debris pool and its associated top and bottom crusts, heat fluxes delivered to the vessel inner surface, and the resulting vessel temperature distribution. Because considerable uncertainty is associated with many input parameters for these models, studies were performed considering lower-bound, upper-bound, and best-estimate (or nominal) values for input parameters related to debris decay heat, debris relocation mass, and heat transfer from the debris and the vessel. Many of the input parameters for the thermal analysis were based on companion debris sample examination data (debris composition, decay heat levels, and "slow cooling" evidence).[5] Results from the thermal analyses were compared with results from vessel steel sample examinations (peak hot spot and global vessel temperatures, duration of peak hot spot temperatures, and cooling rate of vessel in the hot spot location).[4]

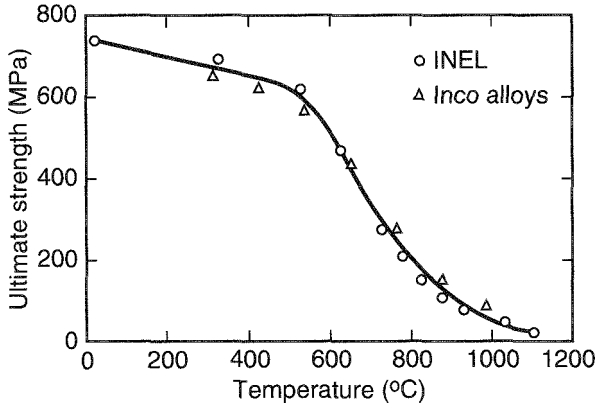

Fig. 4 Inconel-600 ultimate strength as a function of temperature.

The potential for melt to disperse and quench as it passes through the flow distributor plate and into the water-filled lower plenum was analyzed with the TEXAS fuel–coolant interaction (FCI) model.[16] TEXAS predicts the behavior of molten fuel interacting with water during the mixing and propagation phases of a molten FCI. As with many phenomena considered in severe accident analysis codes, considerable uncertainty may exist in TEXAS results because of limited data for validating FCI codes; however, various TEXAS sensitivity studies were used to address the impact of code modeling uncertainties. Sensitivity studies were also used to assess the impact of input data uncertainties. Posttest examination data and plant instrumentation data indicate that the major relocation of melt occurred within a 2-minute time period during the accident (224 to 226 minutes after reactor scram). Calculations considered total mass flow rates ranging from 300 to 1000 kg/s to address uncertainties in mass flow rates, although the duration of the jet pour was reduced to keep the total mass that relocated constant. Because melt may have drained from more than one of the holes in the elliptical flow distributor plate, analyses considered one and three jet cases. For all the cases, the system pressure was 10 MPa, which was the reactor vessel pressure during the time period when most debris relocation is postulated to have occurred. Jets were assumed to pour through coolant at saturated and subcooled conditions (the amount of subcooling was bounded by the temperatures measured in the RCS cold leg). The temperature of the melt at injection was assumed as 2630 °C, the liquidus temperature for the

composition of the melt identified in the companion sample examinations.[5]

Simulation results from the TEXAS fuel–coolant interaction model indicate that insignificant amounts of melt dispersal or "breakup" occur as melt relocates to the lower head. Maximum breakup was obtained for cases in which three jets were assumed to be present; however, even in these cases, less than 1% of the relocating material is estimated to break away from the jet and quench. When the breakup was predicted to be insignificant, the analyses of fuel relocation continued under the assumption that molten debris reached the lower plenum in a substantially liquid state, ultimately impinging on the vessel. Because vessel thermal response calculations indicate that the molten material that relocated to form the "hard layer" could, by itself, impose a thermal load resulting in temperatures that exceeded peak values estimated from metallurgical examinations and because there is uncertainty about when the additional rubble on top of the hard layer relocated, no further assessment of the impact of the rubble on vessel thermal response was performed.

A model was developed to estimate heat transfer to the vessel from jet impingement and natural convection in the molten pool.[17] The model assumes that one jet impinges at the center of the lower head and a crust forms on the lower head as soon as the melt contacts it. Heat is then transferred through the crust to the vessel at locations where the melt is in contact with the vessel. When the molten jet stops draining and surface agitation is reduced, a crust may form on pool upper and lower surfaces. An energy balance is used in the model to determine the size of the crusts and melt pool. A detailed description of this model may be found in Refs. 2 and 17.

Sensitivity calculations considered the vessel thermal response using various combinations of upper-bound, lower-bound, and best-estimate values for input parameters, such as debris-to-coolant heat transfer, debris decay heat, debris-to-vessel thermal contact, and heat removal from the vessel. Results from several sensitivity studies revealed a consistent vessel thermal response; namely, the thermal response can be divided into three time periods: (a) an initial localized temperature excursion over the time and location of jet impingement (typically lasts for about 1 minute); (b) a transient vessel heatup (typically lasts for about 1 hour); and (c) a quasi-steady vessel temperature distribution (typically lasts for several hours). Best-estimate input values used for a case with nominal input parameters resulted in global peak temperatures of more than 900 °C, which is inconsistent with metallurgical examination data. Only a case with lower-bound input assumptions results in temperature predictions that are, considering the uncertainty range associated with these predictions, consistent with metallurgical examination data; namely, that global vessel temperatures remain below values at which the material undergoes a transition from ferritic to austenitic steel (727 °C).

Results from jet impingement and vessel thermal response calculations indicate that the magnitude and duration of the hot spot temperatures estimated in TMI-2 vessel examinations could not have been caused by an impinging jet because peak temperatures during melt relocation are typically not predicted to be sustained for more than a few minutes (instead of the 30-minute duration indicated by vessel examinations). Hence it is postulated that hot spot temperatures occurred later in the scenario because of a sustained heat load from debris resting on the lower head. The limited area estimated to have experienced hot spot temperatures suggests that this region was subjected to a localized heat source, such as might occur with a nonhomogeneous debris bed or a localized region with better contact between the debris and the vessel.

Weld Failure–Tube Ejection

Before the performance of a tube ejection analysis, it must be established that the nozzle-to-vessel weld failed. Because it is not known if the hot spot temperatures occurred when the RCS was at high pressure, weld failure calculations were performed with the use of a simple model based on force equilibrium (see part b of Fig. 2) in which it was conservatively assumed that peak temperatures and pressures occurred simultaneously. Metallurgical evidence from TMI-2 examinations indicates that the Inconel penetration welds did not melt.[3] Hence peak temperatures inferred from metallurgical examinations of vessel specimens from the hot spot region (less than 1100 °C)[4] were assumed in these calculations. The maximum value of RCS pressure measured after melt relocation, 15 MPa, was assumed for system pressure in these calculations. Shear stress at the weld–tube interface was calculated, converted to effective stress, and used in the MTF calculations.

Results indicate that, even for these conservative assumptions, there was considerable margin in the weld's integrity. Nominal case calculations based on nominal input indicate that the ultimate-strength MTF is 60%. Lower- and upper-limit estimates of the ultimate-strength MTF were 54 and 65%, respectively. If the peak hot spot

temperature and a 15 MPa system pressure were both maintained constant, the time to creep failure is estimated as 7.2 hours with upper and lower estimates of 4.2 and 16.9 hours, respectively. The large ultimate-strength MTF and the long estimated time to creep failure are conservative for several reasons. One reason is that the analysis assumed a constant pressure of 15 MPa, whereas the peak temperatures may have occurred at a lower pressure. Furthermore, calculations assumed that the peak temperature remained constant when, in fact, the peak temperature was estimated to last for only 0.5 hour.[4] In addition, the load-bearing weld area was minimized by ignoring the weld buildup material above the stainless steel cladding and using a minimum weld depth into the vessel. Finally, the load was assumed to be carried solely by the weld, and none of the load was distributed to the tube support located beyond the tube bend outside the vessel. Because penetration weld integrity during the TMI-2 accident was predicted in this very conservative analysis, penetration tube ejection was ruled out as a possible failure mode.

Global Vessel Failure

Two models were used to assess vessel structural response. The first is a simpler, one-dimensional (1-D) model imposing global force equilibrium in spherical geometry, and the second is a more sophisticated, two-dimensional (2-D) model. The 1-D model was applied to provide an initial, rough estimate of failure times. Although this model was quicker and easier to apply, uncertainties associated with 2-D and stress redistribution effects required the more detailed 2-D model.

In the 1-D model, average radial and hoop components of stress are used to define effective stress, as formulated by Huddleston.[18] Creep damage is tracked as a function of stress and temperature at 20 equally spaced layers through the thickness of the vessel. Damage within a particular time interval and at a given location is defined on the basis of the effective stress and temperature through the use of a Larson–Miller Parameter (LMP).[19] The LMP is used to obtain a rupture time, t_r, under the stress and temperature conditions. Incremental damage, d, within a time increment, Δt, is defined as $d = \Delta t/t_r$. As the thermal transient proceeds, the accumulated damage is summed from the incremental damage. When the accumulated damage exceeds unity in a particular layer, that layer of the vessel is removed from the calculated load carrying capacity of the vessel. As discussed previously, MTF is defined as the difference between unity and the ratio of load to load-carrying-capacity. As more layers experience 100% damage, the load-carrying-capacity continues to diminish. Vessel failure is defined as the time when MTF becomes zero.

The 2-D model is an axisymmetric variation of a finite deformation shell theory described in Ref. 20, and the details of the adopted form of the method are described in Ref. 9. The shell theory allows for thermal, plastic, and creep as well as elastic strains but is not as general as an axisymmetric continuum model in that the radial stress is neglected, normal strains are assumed to vary linearly through thickness, and shear strains are assumed to vary parabolically through thickness. The assumed through-thickness behavior permits enforcement of vertical and horizontal force equilibrium and moment equilibrium through integrated force and moment resultants.

Implementation of the stress-based failure criterion in the 2-D model differs slightly from that used in the 1-D model. In the 2-D model, the vessel is divided in the radial direction into ligaments; ligament behavior is allowed to vary continuously in the meridional direction. Stress can vary in both the radial and meridional directions, whereas the simpler 1-D model uses average radial and hoop stresses. Incremental and accumulated damage are evaluated the same way for both models, but when a ligament becomes fully damaged in the 2-D model, it is "clipped," which means the stress state is set to zero and equilibrium necessitates redistribution of stresses to the remaining, intact ligaments. In this stress-based criterion, failure occurs when all the ligaments become fully damaged through thickness at any one location.

Figure 5 compares results from the 1-D model and the 2-D model for the vessel subjected to lower-bound heat fluxes. Parts a and b of Fig. 5 illustrate output from the 1-D model. These parts illustrate the phasing of vessel wall temperature, system pressure, the calculated MTF history, and the timing of vessel layer failure during the accident. As shown in part a of Fig. 5, MTF starts at 80%, reduces to approximately 45% at the 2-hour mark, and quickly drops to 0.0% afterward. Layers of the vessel start to fail after 2.0 hours, and all the layers have failed at 2.3 hours (part b of Fig. 5). Thus the 1-D model predicts failure in slightly less than 2.3 hours.

Part c of Fig. 5 illustrates accumulated damage as calculated from the 2-D model. Damage is defined in the 2-D model as the *average* of the damage evaluated at all integration points along the shell's meridian, so accumulated damage never exceeds unity. This definition is more appropriate for the 2-D model because the number of nodes is variable. As discussed previously, failure is defined in the 2-D model as the time when all

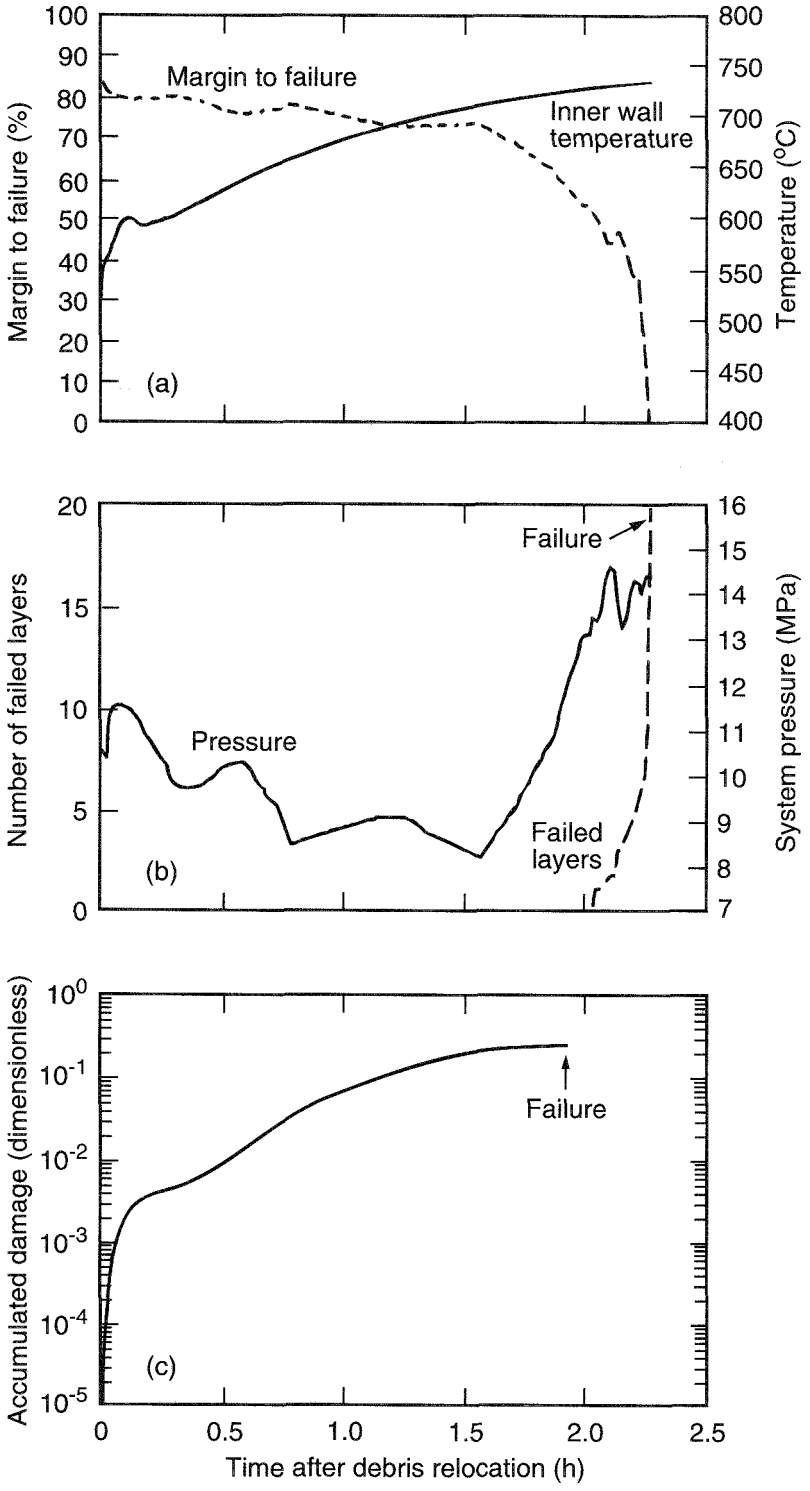

Fig. 5 Comparison of one- and two-dimensional model results for lower-bound case: (a) MTF (1-D model), (b) number of failed layers (1-D model), and (c) accumulated damage (2-D model).

the ligaments become fully damaged at any one location along the shell's meridian. The 2-D model predicts failure at approximately 1.9 hours.

Temperature distributions based on input from companion debris sample examination data (i.e., slow cooling of debris) resulted in calculations from both models predicting vessel failure. Although the inclusion of stress redistribution and 2-D effects in the 2-D model decreased failure predictions by approximately 0.4 hour, both models predict vessel failure at approximately 2 hours. Obviously, this did not occur. Hence it appears that global vessel temperatures must have decreased within 2 hours after core relocation. Hence it is postulated that additional debris cooling, not modeled in these initial calculations based on companion debris sample examination data, occurred within the first 2 hours after melt relocation.

Localized Vessel Failure

The potential for the vessel to experience a localized failure was also evaluated by application of an elevated heat flux over a localized region, which resulted in temperatures and temperature gradients consistent with metallurgical observations of the TMI-2 vessel steel samples.[4] The 2-D structural model used in the global vessel failure analyses was applied to calculate thermal, plastic, and creep strains when the vessel is subjected to a localized heat source.

To understand the relative roles of the hot spot temperature distribution and the global background temperature distribution outside the hot spot, two cases were considered: (a) hot spot temperatures imposed on top of global temperatures estimated for the lower-bound case (see discussion in Jet Impingement/Vessel Thermal Response) and (b) hot spot temperatures imposed on a vessel with cool background temperatures (327 °C inner surface, 277 °C outer surface). These two temperature distributions bounded possible background distributions inferred from vessel steel sample examinations. In these calculations, failure was predicted to occur in 1.5 hours for Case (a), and the vessel was predicted to survive for Case (b).

The effect of a hot spot was evaluated for a shell with a cool background [Case (b)] to confirm that the metallurgically estimated hot spot temperatures alone would not result in a localized vessel failure. Because metallographic examinations of vessel specimens outside the hot spot indicated only that the vessel did not reach the ferritic-to-austenitic transition temperature (approximately 727 °C), global vessel temperatures could have been considerably lower than this transition temperature. (Note that peak values predicted in the lower-bound temperature distribution were approximately equal to the transition temperature.) The initial temperature distribution from the lower-bound case was used to bound possible temperatures in this cooler case; that is, a linear temperature distribution through the thickness with a 327 °C inner surface and a 277 °C outer surface.

The structural response results for Case (b) are in Fig. 6, which shows damage rate vs. time. Note that for

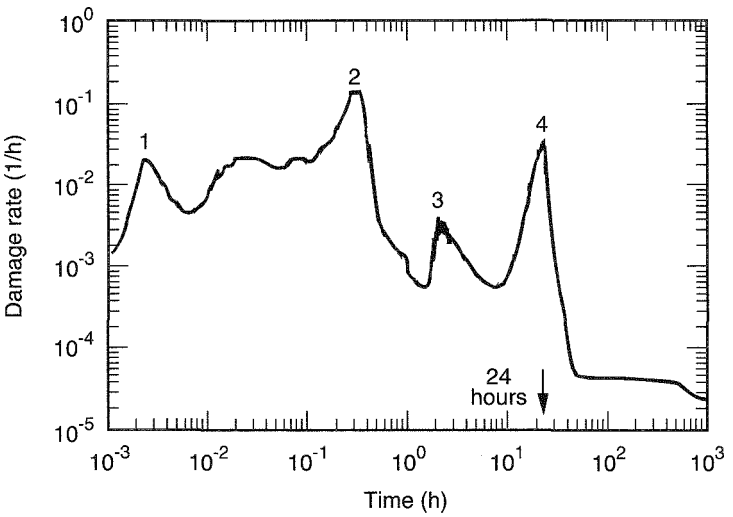

Fig. 6 Damage rate vs. time for localized failure analysis of hot spot temperatures on a cool background.

the 2-D structural model damage is defined in the 2-D model as the *average* of the damage evaluated at all integration points along the shell's meridian. Four important peaks, labeled 1 through 4 in Fig. 6, are in the damage rate.

The first peak (point 1 in Fig. 6), which occurs between 3 and 30 seconds, was associated with the thermal shock (i.e., the nodes on the inner surface experienced a relatively severe damage rate as they reached temperatures in excess of 1027 °C, yielding in compression as they expanded against the cooler shell). This severe damage rate was diminished as the temperature front moved into the interior wall of the vessel.

The second peak (point 2 in Fig. 6) occurs at just over 1000 seconds into the transient and represents the largest rate (0.1 h^{-1}) at any time during the transient. This state occurred when the temperature front had elevated the outer surface temperatures to levels of 527 to 577 °C. The outer surface material was supporting a large tensile stress (~250 MPa) and at this temperature experienced both a high damage rate and creep rate. The damage rate dissipated when the temperature front completely penetrated the shell and thus pushed the outer surface temperature above 727 °C, which reduced the temperature gradient and associated stresses.

At 1.6 hours into the TMI-2 transient, the system was repressurized, and the damage rate experiences a third peak (point 3 in Fig. 6), although of substantially lesser size than the transient heat-up peak. The fluctuations in the repressurization peak mirror the fluctuations in the TMI-2 pressure history associated with relief valve opening and reseating. Although the transient pressure fluctuations continued until 260 minutes after relocation, these calculations assumed a constant pressure for time periods greater than 180 minutes after relocation and thus caused the fluctuations to disappear from the damage rate plot after this time. Repressurization to 14.5 MPa at 2.1 hours also corresponds to the attainment of maximum temperatures in the shell, so the damage rate decreased shortly after repressurization as the shell cooled.

The final damage rate peak (point 4 in Fig. 6) occurs approximately 24 hours after the major melt relocation occurred and is associated with cooldown. During the heat-up and high-temperature periods, material near the inner surface of the vessel at its base experienced compressive stress and underwent negative creep strain under compressive load. As the vessel cooled, this material then contracted and experienced tension. As the material temperature dropped during the cooldown period, tensile stresses on the bottom inner surface exceeded +100 MPa and thus caused rapid damage accumulation and the damage rate peak at 24 hours, which is shown in Fig. 3.

The Structural Mechanics Peer Review Group[7] defined MTF for creep to be the difference between time to failure and the time at which pressure and temperature states are fixed at points of maximum damage rate. Hence the MTF for this case was evaluated by assuming constant temperature and pressure conditions for each of the peaks in Fig. 3 and predicting time to failure, as discussed in the Approach. The initial peak associated with the thermal shock (during melt relocation) was not relevant to the MTF analysis because only the material on the inner surface experienced elevated temperatures during the first 30 seconds of the transient. Hence MTF for this case is the minimum failure time estimated in MTF calculations for peaks 2, 3, and 4 in the damage rate curve. The minimum MTF was obtained by fixing the pressure and temperature conditions corresponding to peak 3. The MTF for this is estimated at 8 hours.

The cases examined in this localized vessel failure analysis indicate that background temperatures play a pivotal role in determining whether the vessel is predicted to survive. The vessel is predicted to fail when hot spot temperatures are superimposed on a global temperature distribution obtained with heat fluxes corresponding to lower-bound input assumptions; however, the vessel can survive local hot spots in the temperature range and of the duration inferred from TMI-2 metallurgical examinations, but the balance of the shell must remain cool.

Sensitivity to Debris Cooling and Failure Criterion

As noted previously, thermal analyses were performed on the basis of debris properties (decay heat levels, "slow cooling" evidence) from the companion debris sample examinations; however, thermal and structural calculational results combined with metallurgical examination results suggest the hypothesis that some form of cooling occurred that was not evident in the TMI-2 companion debris samples. In addition, analysis results suggest that the stress-based failure criterion that is used to predict failure may be too conservative. Analyses performed to investigate the effects of debris cooling and failure criterion on calculational results are discussed in the following text.

Changes in Debris Internal Energy After Relocation

Initial scoping calculation results suggest that some form of debris cooling occurred within the vessel after a

major relocation occurred (approximately 224 minutes) and before the vessel was repressurized (approximately 320 minutes). Through the application of some simplifying assumptions related to heat transfer within the vessel, equations for volume, mass, and energy conservation were used to obtain an order-of-magnitude estimate of the change in debris internal energy after debris relocation. Sources of coolant entering the vessel during the time period of interest include normal RCS makeup and high-pressure injection from the emergency core cooling system. Sources of coolant exiting the vessel during this time period include normal RCS letdown and coolant flowing out the open power-operated relief valve (PORV). These coolant flow rates and associated uncertainties were quantified with results from previous analyses of plant data.[21–24] The amount of decay heat input to the system was quantified with information in Ref. 25 to account for the reduction caused by volatile fission-product release.

Calculation results indicate that the debris internal energy decreased between relocation and vessel repressurization. Calculations considered upper and lower bounds for all the input parameters, such as coolant flow rates entering and exiting the vessel and debris decay heat levels. Hence results from these scoping calculations should be viewed as order-of-magnitude estimates; however, results indicate that a negative change in debris internal energy occurred for the time period of interest in all the cases considered and support the hypothesis that debris cooling occurred that was not evident in the TMI-2 companion debris samples. Although considerable uncertainty is associated with these results, scoping calculations suggest that the estimated decrease in debris internal energy is sufficient for all the debris that relocated to the lower head to solidify and experience a decrease in temperature ranging from 420 to 2250 °C.

Slow and Rapid Cooling Analysis

Although there are insufficient data from the companion debris samples to determine the exact mechanisms that caused the rapid cooling of the debris within the first 2 hours after relocation, two possible forms of cooling were investigated. The first form of cooling considered was a slow cooling mode in which channels or cracks in the debris allowed for infusion of water that cooled the debris near the channels but left interior portions hot. This slow cooling was investigated by analyzing cases with a hot spot temperature distribution superimposed on 25, 33, and 50% of the background heat fluxes obtained using nominal case input values. Results, summarized in part a of Fig. 7, indicate that the vessel would fail at 2.6 hours for a hot spot on a background equal to 50% of nominal case heat flux, but the vessel would survive on a background of 25% of nominal case heat flux. For the 33% of nominal case, results in part a of Fig. 7 indicate that the damage rate begins to rise during the repressurization period, which implies that failure is imminent. Depressurization 4 hours into the transient enables the vessel to survive a couple of hours longer, but ultimately the vessel is predicted to fail at 6.5 hours after melt relocation. These results indicate that, under slow cooling conditions and with a stress-based failure criterion, the vessel can survive a hot spot in the presence of background heat fluxes between 25 and 33% of nominal values.

The second form of cooling considered was a rapid cooling mode in which gaps or channels between the lower debris crust and the vessel allowed relatively high flow rates of coolant between the debris and the vessel. (These high flow rates rapidly cooled the vessel and outer portions of the debris but left interior portions of the debris relatively hot.) Analyses were performed to investigate the cooling needed to obtain vessel cooling rates consistent with the values observed in metallurgical examinations of specimens in the hot spot region, namely, that vessel specimens from the hot spot region underwent cooling rates between 10 and 100 °C/min in the ferritic-to-austenitic transition temperature region (727 to 827 °C) at approximately 30 minutes after the hot spot reached 1047 °C. Rapid cooling calculations were performed for cases of hot spot temperatures on 33 and 50% of nominal background heat fluxes. The heat sinks required to obtain these cooling rates were 25 and 125 kW/m^2, respectively. Under rapid cooling conditions, it is concluded that the structure must be close to failure before initiation of cooling for the vessel to subsequently fail. For these conditions, additional damage or strain accumulated during the cooldown period is minimal. The difference between cooling rates is exhibited in the timing and magnitude of damage peaks associated with cooldown. The faster cooling rate produces higher tensile stresses earlier in the transient, which results in an earlier and larger damage rate peak. Unlike the case illustrated in Fig. 6, however, the structure moves through this peak quickly, with little additional accumulated damage, and the damage rate then falls rapidly to a benign level. Simulations were also run for a hot spot on 75% of the nominal heat flux, but these simulations predict vessel failure in a little over 2 hours. Hence the vessel can survive a hot

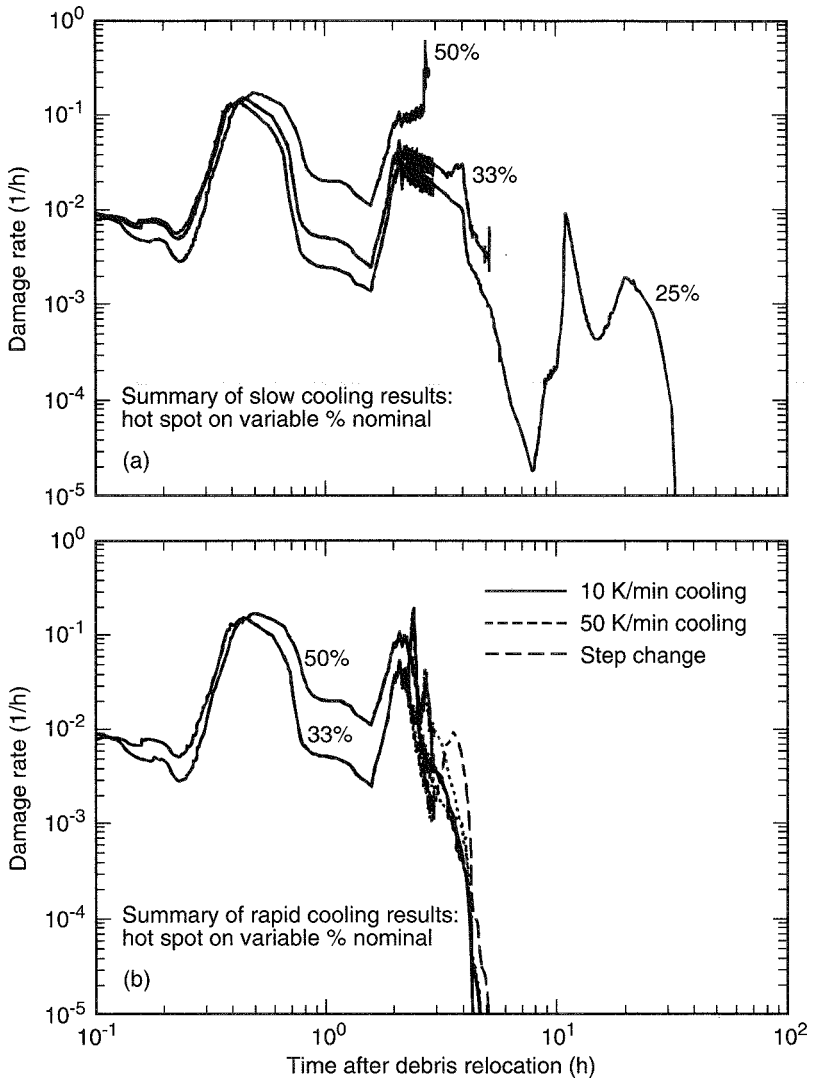

Fig. 7 Summary of slow and rapid cooling results obtained with a stress-based failure criterion: (a) slow cooling results and (b) rapid cooling results.

spot in the presence of background heat fluxes between 50 and 75% of the nominal case heat fluxes during the 30-minute time interval that hot spot temperatures are sustained and before the initiation of rapid cooling.

In summary, analyses indicate that both slow and rapid cooling occurred in some debris locations during the first 2 hours after melt relocation. If only a slow cooling mechanism were present, the vessel temperatures would not experience the rapid cooling rates observed in the metallurgical examinations. Furthermore, the vessel will not survive hot spot temperatures on the nominal case heat fluxes long enough to permit material to exist at elevated (>1050 °C) temperatures for the 30-minute time period estimated in metallurgical examinations. Thus analyses indicate that both slow and rapid cooling mechanisms must be considered to obtain results consistent with TMI-2 VIP examinations.

Configurations to Obtain Required Cooling Rates

Although there are insufficient data to quantitatively determine the exact cooling mechanisms required to obtain a vessel response consistent with metallurgical data, scoping calculations were performed to investigate

the potential for channels and gaps within the debris to cause this cooling (the presence of this cooling would allow consistency of the companion debris sample data, the vessel steel sample data, and the thermal and structural response analyses). Estimating the number and size of debris channels and the size of debris-to-vessel gaps requires many assumptions related to debris properties and heat transfer parameters. This large uncertainty in input parameters was treated by estimating upper and lower bounds for each parameter and obtaining results by propagating upper- and lower-bound estimates. Lower-bound geometric parameters for channels within the debris and between the debris and the vessel were selected to minimize heat transfer capabilities. As discussed previously, results indicate that both rapid and slow cooling mechanisms were needed to be consistent with metallurgical examination data. Therefore it is assumed that the simultaneous presence of cracks and gaps within the debris provides multiple pathways for steam release (e.g., water may travel down along the gap and boil up through cracks). To maximize the number of cooling cracks and the gap size required to cool the debris, the heat transfer from the debris to the coolant was minimized by assuming that the coolant traveling through these cracks and gaps remained in a liquid state and neglecting any enhanced heat removal associated with subcooled or saturated boiling of the coolant.

Results indicate that a relatively insignificant volume of channels within the TMI-2 debris bed (<1% of the debris volume) could have removed a sufficient amount of heat to preclude vessel failure. Calculations also indicate that coolant traveling through a relatively small gap (a value of 1 mm was assumed) between the debris and the vessel could cause the vessel cooling rates estimated by metallurgical examination data. Although companion debris sample examinations did not substantiate the hypothesis that portions of the debris cooled within the first 2 hours, the mass of the companion debris samples was small compared with the mass that relocated (<7 kg of the 19 000 kg that relocated were examined).

Sensitivity of Results to Failure Criterion

Vessel deformation and damage distributions obtained in the initial scoping calculations indicate that failure strains are quite modest (<10%). For these reasons, the Structural Mechanics Peer Review Group suggested that another set of structural simulations be performed with a failure criterion based upon mechanical instability.[8] Calculations were performed to investigate the influence of failure criterion on the amount of slow cooling needed to preclude vessel failure and the amount of rapid cooling needed to obtain cooling rates consistent with the cooling indicated by metallurgical examinations. The characteristic deformations used to define instability are the maximum hoop strain, u/r_0, located underneath the hot spot; the maximum vertical deflection, w, also located under the hot spot; and the maximum rotation of the shell meridian from its undeformed state, β, located somewhere in the cusped region of the undeformed shell.

In the slow cooling calculations, simulations were performed involving the hot spot on background heat flux distributions corresponding to 100, 75, 62.5, and 50% of the nominal case. Results for the 62.5 and 50% nominal cases are shown in part a of Fig. 8. For the 50% nominal case, the bulk of the vessel remains sufficiently stiff to restrain the hot spot region; consequently, tensile stresses in the hot spot region 4 hours after relocation are quite modest. When the system depressurizes at 4 hours, the vessel unloads elastically, and most of the vessel under the hot spot subsequently experiences compression. Under these conditions, the vessel creeps down in the hot spot region and u/r_0 decreases. Maximum values of w and β remain nearly constant.

Deflections for the case with 62.5% nominal are substantially greater than those for the case with 50%. When the vessel is less restrained, more tension exists, and no discernible decrease in hoop strain occurs when the pressure decreases. Once depressurization stops at 5.25 hours, the deformations again begin to increase. The increasing deflections near 6 hours for the 62.5% case suggest, however, that it is unlikely the vessel would survive upon complete repressurization to 16 MPa at 11 hours. It is concluded that, under slow cooling conditions and a deformation-based criterion, the vessel can survive a hot spot on a background heat flux between 50 and 62.5% of the nominal level.

In the rapid cooling calculations, simulations were performed for hot spots on background heat fluxes equal to 62.5, 75, and 80% of the nominal level. Results in part b of Fig. 8 indicate that the vessel easily survives rapid cooling from 62.5% of nominal, and all deformations asymptotically settle to benign values. When rapid cooling is initiated from hot spots on 75% of nominal, however, the vessel has already experienced substantial deformation before initiating cooling. The inspection of curves in part b of Fig. 8 indicates that during the cooling period the rotation β actually decreases but then begins to climb again once cooling is completed. The depressurization period between 4 and 11 hours greatly slows the rate of vessel deformation, but repressurization to 15 MPa at

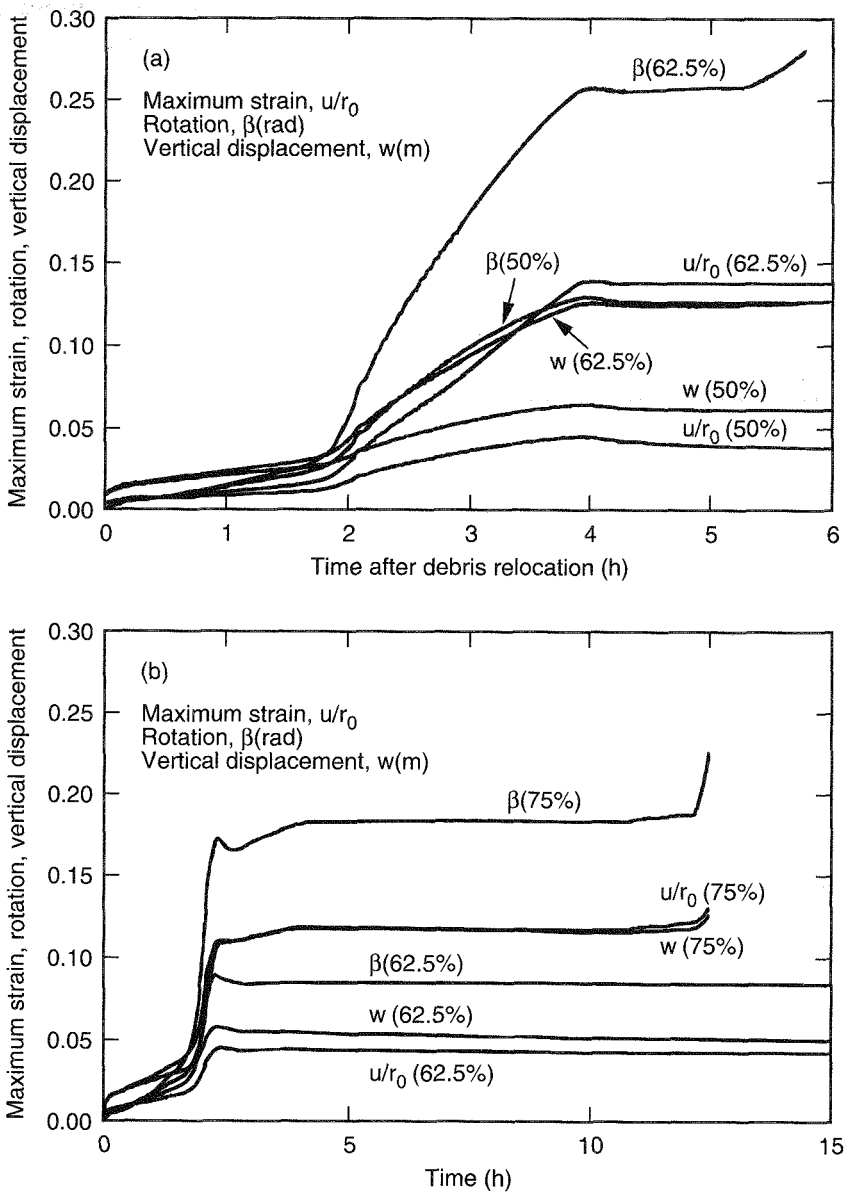

Fig. 8 Results obtained with a deformation-based criterion: (a) slow cooling results and (b) rapid cooling results.

11 hours causes the deformation to increase dramatically. It appears that under rapid cooling hot spots on 75 and 80% of nominal background heat fluxes cause failure in approximately 13 and 11 hours, respectively. Therefore it is concluded that, under rapid cooling conditions and the deformation-based criterion, the vessel can survive a hot spot on a background heat flux between 62.5 and 75% of nominal.

SUMMARY

Data available from the OECD-sponsored TMI-2 VIP, plant instrumentation during the accident, and previous TMI-2 research programs were used to estimate the MTF that existed in the vessel during the accident. These data also provided a unique opportunity to evaluate the predictive capability of severe accident analysis models for

which limited validation data exists. The MTF analysis effort of the VIP included calculations to consider four vessel lower-head failure mechanisms: penetration tube rupture, penetration tube ejection, global vessel rupture, and localized vessel rupture.

Analyses results indicate that tube rupture and tube ejection could be eliminated as potential failure mechanisms during the TMI-2 accident. Global vessel failure analyses suggest that significant debris cooling, not considered in severe accident analysis models, must have occurred within approximately 2 hours after debris relocation to the lower head. Analyses also indicate that additional data are needed to select an appropriate vessel failure criterion because the magnitude of cooling required to obtain vessel temperatures consistent with values inferred from vessel steel examinations was sensitive to the failure criterion used in structural response calculations. Although examinations of companion debris samples did not provide supporting evidence of this additional debris cooling, metallurgical examinations did provide evidence that this cooling occurred in the hot spot location. Localized vessel failure analyses indicate that it is possible for the vessel to withstand the hot spot temperatures for time periods inferred from VIP metallurgical examinations provided that the balance of the vessel is relatively cool. Although there are insufficient data to determine the exact mechanisms that caused the debris to cool, scoping calculation results indicate that a minimal volume of cooling channels within the debris and a minimal size gap between the debris and the vessel could supply the cooling needed to obtain vessel temperatures and cooling rates determined in metallurgical examinations.

REFERENCES

1. ASME, Use of SA-533 Grade B, Class 1 Plate and SA-508 Class 3 Forgings and Their Weldments for Limited Elevated Temperature Service, Sect. III, Division 1, Cases of ASME Boiler and Pressure Vessel Code, Case N-499, Approved December 16, 1991.
2. L. A. Stickler et al., *Calculations to Estimate the Margin to Failure in the TMI-2 Vessel*, Report NUREG/CR-6196 (EGG-2733) [TMI V(93) EG01], October 1993.
3. D. R. Diercks and L. A. Neimark, *Results of Mechanical Tests and Supplementary Microstructural Examinations of the TMI-2 Lower Head Samples*, Report NUREG/CR-6187 (ANL-94/8) [TMI V(93)AL02], June 1993.,
4. G. E. Korth, *Metallographic and Hardness Examinations of TMI-2 Lower Pressure Vessel Head Samples*, Report NUREG/CR-6194 (EGG-2731) [TMI V(92)EG01], January 1992..
5. D. W. Akers, S. M. Jensen, and B. K. Schuetz, *Companion Sample Examinations*, Report NUREG/CR-6195 (EGG-2732) [TMI V(92)EG10], July 1992.
6. L. A. Neimark, T. L. Shearer, A. Purohit, and A. G. Hins, *TMI-2 Instrument Nozzle Examinations at Argonne National Laboratory*, Report NUREG/CR-6185 (ANL-94/5) [OECD-NEA-TMI-2 V(93)AL01], February 1993.
7. J. Strosnider, *Summary Record of the TMI VIP Structural Mechanics Peer Review Group Meeting, Idaho Falls, Idaho, May 11, 1992*, TMI V(92) EG09, OECD-NEA-TMI-2 Vessel Investigation Project, July 20, 1992.
8. Y. R. Rashid, Summary of Comments on the Margin-to-Failure Report, Presentation at the 11th Programme Review Meeting of the OECD-NEA-TMI-2 Vessel Investigation Project, TMI V(93)MAN17.
9. J. L. Rempe, S. A. Chavez, and G. L. Thinnes, *Light Water Reactor Lower Head Failure Analysis*, Report NUREG/CR-5642 (EGG-2618), October 1993.
10. R. W. Ostensen and J. F. Jackson, Extended Fuel Motion Study, in *Reactor Development Program Progress Report*, Report ANL-RDP-18, pp. 7.4-7.7 July 1973.
11. R. W. Ostensen, R. E. Henry, J. F. Jackson, G. T. Goldfuss, W. H. Gunther, and N. E. Parker, Fuel Flow and Freezing in the Upper Subassembly Structure Following an LMFBR Disassembly, *Trans. Am. Nucl. Soc.*, 18: 214-215 (1974).
12. M. Epstein, Transient Freezing of Flowing Ceramic Fuel in a Steel Channel, *Nucl. Sci. Eng.*, 61(3): 310-323 (1976).
13. M. Epstein, Heat Conduction in the UO_2-Cladding Composite Body with Simultaneous Solidification and Melting, *Nucl. Sci. Eng.*, 51(1): 84-87 (May 1973).
14. Personal communication with Norman Cole, MPA Associates, Inc., Washington, D.C., October 1992.
15. H. Warren, *Interpretation of TMI-2 Instrument Data*, Report EPRI-NSAC-028, May 1982.
16. C. C. Chu, M. L. Corradini, J. Murphy, and J. Tang, *A Code Manual for TEXAS-II: One-Dimensional Transient Fluid Model for Fuel/Coolant Interaction Analysis*, Report UWRSR-39, July 1992.
17. J. A. Kos, Model of Fuel-Melt Quenching in the Lower Plenum of the RPV, M.S. Thesis, University of Wisconsin, Madison, Wisconsin, August 1992.
18. R. L. Huddleston, An Improved Multiaxial Creep-Rupture Strength Criterion, *Am. Soc. Mech. Eng., Pressure Vessel Technology*, 107: 421-429 (1985).
19. F. R. Larson and J. Miller, A Time–Temperature Relationship for Rupture and Creep Stress, *Trans. ASME*, 765-775 (July 1952).
20. S. Lin, T. Lin, and B. Mazelsky, Large Deflection of Axisymmetric Shell with Creep Strain, *J. Eng. Mech.*, 100: 79-94 (1974).
21. J. L. Anderson, *Recommended HPI Rates for the TMI-2 Analysis Exercise (0–300 Minutes)*, Report EGG-TMI-7833, EG&G Idaho, Inc., September 1987.
22. P. Kuan and E. L. Tolman, *Electromatic Relief Valve Flow and Primary System Hydrogen Storage During the TMI-2 Accident*, Report EGG-TMI-7703, EG&G Idaho, Inc., May 1987.
23. R. D. McCormick, J. L. Anderson, and D. W. Golden, *TMI-2 Data Summary Report*, Report EGG-TMI-7843, EG&G Idaho, Inc., September 1987.
24. Y. Nomura, *PORV Discharge Flow During the TMI-2 Accident*, Report EGG-TMI-7825, EG&G Idaho, Inc., July 1987.
25. B. G. Schnitzler, *Fission Product Decay Heat Modeling for Disrupted Fuel Regions (FDECAY)*, Report EGG-PHYS-5698, EG&G Idaho, Inc., December 1981.

U.S. Nuclear Regulatory Commission Information and Analyses

1993 Accident Sequence Precursor (ASP) Program Results

L. N. Vanden Heuvel,[a] J. W. Cletcher,[a] D. A. Copinger,[a]
J. W. Minarick,[b] B. W. Dolan,[b] and P. D. O'Reilley[c]

[*Editor's Note:* **This new section, which makes its first appearance in issue 35(2) of *Nuclear Safety* and which is intended to be a regular feature of this journal, will carry analyses and other information reports originating with the U.S. Nuclear Regulatory Commission's Office for the Analysis and Evaluation of Operational Data (NRC/AEOD). The articles in this section differ from the other material in this journal in that they are provided to *Nuclear Safety* by AEOD in finished form and therefore undergo neither the peer review process nor the text editing process to which the papers in all other sections of the journal are subjected. The material in this new section is selected solely by NRC/AEOD.**]

INTRODUCTION

The Accident Sequence Precursor (ASP) Program involves the systematic review and evaluation of operational events that have occurred at light water reactors (LWRs). The ASP Program identifies and categorizes precursors to potential severe core damage accident sequences. The results of the ASP Program are published in the Annual ASP Program Precursor Report. The most recent report, which contains the precursors for 1993, is NUREG/CR-4674, Volumes 19 and 20, *Precursors to Potential Severe Core Damage Accidents: 1993, A Status Report,*[1,2] published in September 1994. Licensee Event Reports (LIRAS) submitted by licensees serve as the chief source of operational experience data for the ASP Program. The requirements for LIRAS are described in NUREG-1022, *Licensee Event Report System. Description of System and Guidelines for Reporting.*[3] Attached are an overview of the ASP review and evaluation process, taken from Section 2 of Ref.1, and a summary of the results for 1993, which is Section 3 of the same document. Further details about the ASP Program and the 1993 precursors may be found in Refs. 1 and 2.

SELECTION CRITERIA AND QUANTIFICATION

Accident Sequence Precursor Selection Criteria

The Accident Sequence Precursor (ASP) Program is concerned with the identification and documentation of operational events that have involved portions of core damage sequences and with the estimation of associated frequencies and probabilities.

Identification of precursors requires the review of operational events for instances in which plant functions that provide protection against core damage have been challenged or compromised. On the basis of previous experience with reactor plant operational events, it is known that most operational events can be directly or indirectly associated with three initiators: trip [which includes loss of main feedwater (LOFW) within its sequences], loss of offsite power (LOOP), and small-break loss-of-coolant accident (LOCA). These three initiators are primarily associated with loss of core cooling. The ASP Program

[a]Oak Ridge National Laboratory.
[b]Science Applications International Corporation.
[c]U.S. Nuclear Regulatory Commission.

staff members examine Licensee Event Reports (LIRAS) to determine the impact that operational events have on potential core damage sequences.

Precursors

This section describes the steps used to identify events for quantification. Figure 1 illustrates this process.

A computerized search of the SCSS data base at the Nuclear Operations Analysis Center (NOAC) of the Oak Ridge National Laboratory was conducted to identify LIRAS that met minimum selection criteria for precursors. This computerized search identified LIRAS potentially involving failures in plant systems that provide protective functions for the plant and core damage-related initiating events. On the basis of a review of the 1984–1987 precursor evaluations, this computerized search successfully identifies almost all precursors within a subset of approximately one-third to one-half of all LIRAS.

LIRAS were also selected for review if an Augmented Inspection Team (AIT) or Incident Investigation Team (IIT) report was written regarding the event. The Nuclear Regulatory Commission (NRC) may designate other events for inclusion in the review process.

After the ASP computer search, those events selected underwent two independent reviews by different NOAC staff members. Each LER was reviewed to determine whether the reported event should be examined in greater detail. This initial review was a bounding review meant to capture events that in any way appeared to deserve detailed review and to eliminate events that were clearly unimportant. This process involved eliminating events that satisfied predefined criteria for rejection and accepting all others as potentially significant and requiring analysis. Events also were eliminated from further review if they had little impact on core damage sequences or provided little new information on the risk impacts of plant operation; for example, single failures in redundant systems, uncomplicated reactor trips, and LOFW events.

LIRAS were eliminated from further consideration as precursors if they involved, at most, only one of the following:

- A component failure with no loss of redundancy
- A loss of redundancy in only one system
- A seismic design or qualification error
- An environmental design or qualification error
- A structural degradation
- An event that occurred prior to initial criticality
- A design error discovered by reanalysis
- An event impact bounded by a reactor trip or LOFW
- An event with no appreciable impact on safety systems
- An event involving only post core-damage impacts

Events identified for further consideration typically included the following:

- Unexpected core damage initiators (LOOP and small-break LOCA)
- All events in which reactor trip was demanded and a safety-related component failed
- All support system failures, including failures in cooling water systems, instrument air, instrumentation and control, and electric power systems
- Any event in which two or more failures occurred
- Any event or operating condition that was not predicted or that proceeded differently from the plant design basis
- Any event that, on the basis of the reviewers' experience, could have resulted in or significantly affected a chain of events leading to potential severe core damage

Events determined to be potentially significant as a result of this initial review were then subjected to a thorough, detailed analysis. This extensive analysis was intended to identify those events considered to be precursors to potential severe core damage accidents, either because of an initiating event or because of failures that could have affected the course of postulated off-normal events or accidents. These detailed reviews were not limited to the LIRAS; they also used final safety analysis reports (FSARS) and their amendments, individual plant examinations (IPEs), and other information available at NOAC and from the NRC, related to the event of interest.

The detailed review of each event considered the immediate impact of an initiating event or the potential impact of the equipment failures or operator errors on readiness of systems in the plant for mitigation of off-normal and accident conditions. In the review of each selected event, three general scenarios (involving both the actual event and postulated additional failures) were considered.

1. If the event or failure was immediately detectable and occurred while the plant was at power, then the event was evaluated according to the likelihood that it and the ensuing plant response could lead to severe core damage.

2. If the event or failure had no immediate effect on plant operation (i.e., if no initiating event occurred), then the review considered whether the plant would require the failed items for mitigation of potential severe core

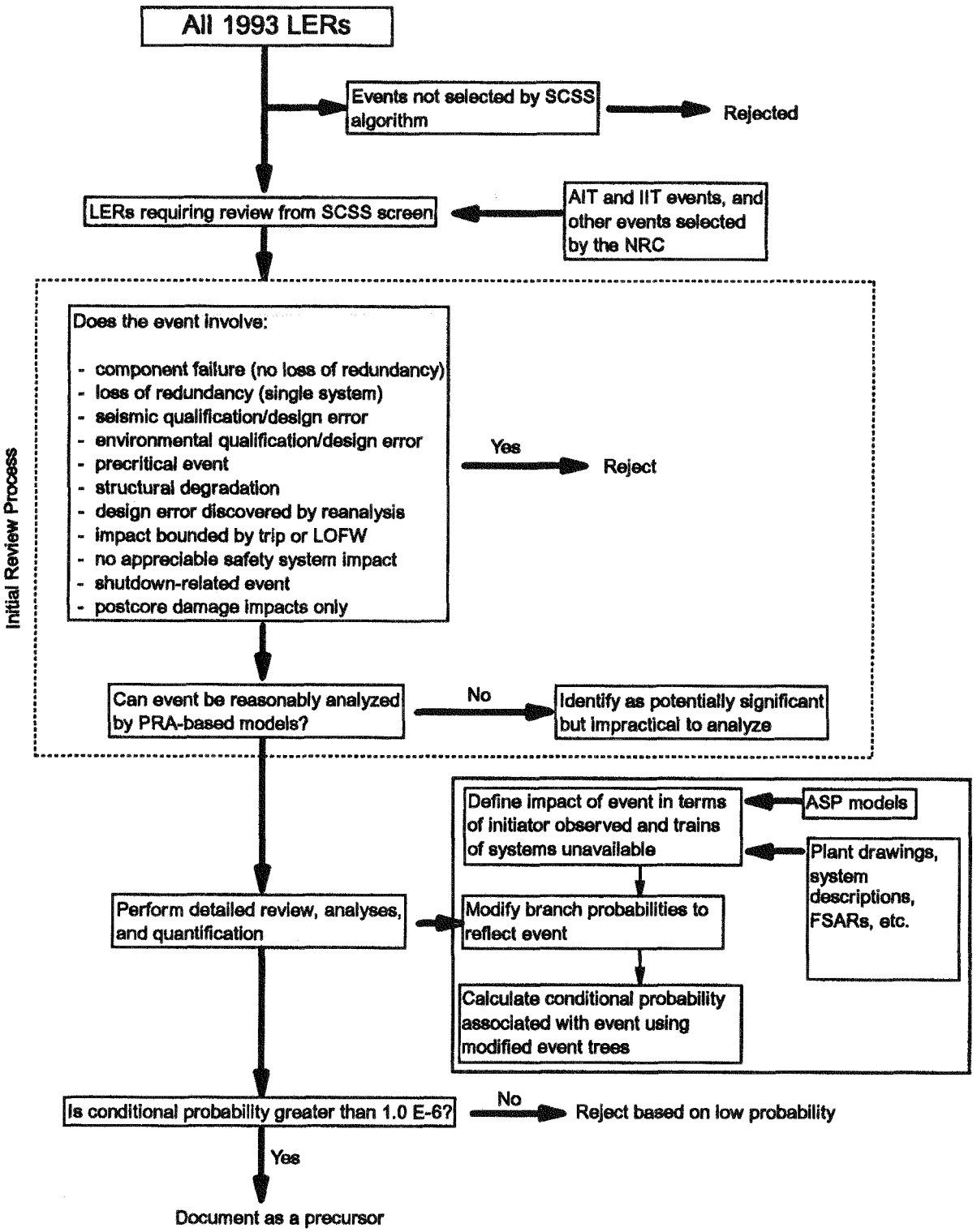

Fig. 1 The Advanced Precursor Program analysis process.

damage sequences should a postulated initiating event occur during the failure period.

3. If the event or failure occurred while the plant was not at power, then the event was first assessed to determine whether it could have occurred while at power or at hot shutdown immediately following power operation. If the event could only occur at cold shutdown or refueling shutdown, then its impact on continued decay heat removal during shutdown was assessed.

For each actual occurrence or postulated initiating event associated with an operational event reported in an LER, the sequence of operation of various mitigating systems required to prevent core damage was considered. Events were selected and documented as precursors to potential severe core damage accidents (accident sequence precursors) if the conditional probability of subsequent core damage was at least 1.0×10^{-6}. Events of low significance are thus excluded, which allows attention to be focused on the more important events.

This approach is consistent with the approach used to define 1987–1992 precursors but differs from that of earlier ASP reports, which addressed all events meeting the precursor selection criteria regardless of conditional core damage probability. Although review of LIRAS identified by this process is expected to identify almost all precursors, it is possible that a few precursors exist within the set of unreviewed LIRAS. Some potential precursors that would have been found if all 1993 LIRAS had been reviewed may not have been identified, Because of this, it should not be assumed that the set of 1988–1993 precursors is consistent with precursors identified in 1984–1987.

Sixteen operational events with conditional probabilities of subsequent severe core damage $\geq 1.0 \times 10^{-6}$ were identified as accident sequence precursors.

Containment-Related Events

In addition to accident sequence precursors, events involving loss of containment functions, such as containment cooling, containment spray, containment isolation (direct paths to the environment only), or hydrogen control, identified in the review of 1993 LIRAS, are documented in Appendix B of Ref. 1. No such events were identified in 1993.

"Interesting" Events

Other events that provided insight into unusual failure modes with the potential to compromise continued core cooling but that were determined not to be precursors were also identified. These are documented as "interesting" events in Appendix C of Ref. 1.

Potentially Significant Events Considered Impractical to Analyze

In some cases events are impractical to analyze because of the lack of information or inability to model the event reasonably within a probabilistic risk assessment (PRA) framework, considering the level of detail typically available in PRA models and the resources available to the ASP Program.

Several LIRAS identified as potentially significant were considered impractical to analyze. It is thought that such events are capable of impacting core damage sequences; however, the events usually involve component degradations in which the extent of the degradation could not be determined or the impact of the degradation on plant response could not be ascertained.

For many events classified as impractical to analyze, an assumption that the affected component or function was unavailable over a 1-year period (as would be done using a bounding analysis) would result in the conclusion that a very significant condition existed. This conclusion would not be supported by the specifics of the event as reported in the LER or by the limited engineering evaluation performed in the ASP Program. Brief descriptions of events considered impractical to analyze are provided in Appendix D of Ref. 1.

RESULTS

This section summarizes results of the review and evaluation of 1993 operational events. The primary result of the ASP Program is the identification of operational events with conditional core damage probabilities of $\geq 1.0 \times 10^{-6}$ that satisfy at least one of the four precursor selection criteria: (1) a core damage initiator requiring safety system response, (2) the failure of a system required to mitigate the consequences of a core damage initiator, (3) degradation of more than one system required for mitigation, or (4) a trip or loss of feedwater with a degraded mitigating system. Sixteen such events identified for 1993 are documented in Appendix A of Ref. 1.

Direct comparison of results with those of earlier years is not possible without substantial effort to reconcile analysis differences. Additional equipment and procedures (beyond those addressed in the ASP models

described in Appendix A of Volume 17 of NUREG 1022 were incorporated into the analysis of 1992 and 1993 events. The models used in the analysis of 1988–1993 events differ from those used in 1984–1987 analyses. Starting in 1988, the project team evaluated only a portion of the LIRAS (as described in the Section "Precursors"). Before 1988, all LIRAS were reviewed by members of the project team. Because of the differences in analysis methods, only limited observations are provided here. The 1986 precursor report[4] carries a discussion of observations for 1984–1986 results and the 1987 through 1991 reports[5–9] for the results for those years.

TABULATION OF PRECURSOR EVENTS

The 1993 accident sequence precursor events are listed in Tables 1 to 4. The following information is included in each table:

- Docket/LER number associated with the event (Event Identifier)
- Name of the plant where the event occurred (Plant)
- A brief description of the event (Description)
- Conditional probability of potential core damage associated with the event [p(cd)]
- Date(s) of the event (Event Date)

Table 1 Precursors Involving Unavailabilities Sorted by Plant

Plant	Event Identifier	Description	Plant Type	Event Date	p(cd)	TRANS[a]
Arkansas Nuclear One, Unit 1	313/93-003	Both trains of recirculation inoperable for 14 h	PWR	9/30/93	5.1×10^{-5}	UNAVAIL
Beaver Valley 2	412/93-012	Failure of both EDG load sequencers	PWR	10/4/93–10/6/93	2.1×10^{-6}	UNAVAIL
Catawba 1 and 2	413/93-002	Essential service water potentially unavailable during dual unit LOOP	PWR	2/25/93	1.5×10^{-4}	UNAVAIL
Haddam Neck	213/93-S01,[b] 213/93-006, 213/93-007	Degradation of MCC-5, pressurizer PORV, and both emergency diesel generators	PWR	6/27/93	6.5×10^{-5}	UNAVAIL
Quad Cities 2	265/93-010, 265/93-012	Degradation of both emergency diesel generators	BWR	4/22/93	6.0×10^{-5}	UNAVAIL
South Texas Project, Unit 1	498/93-005, 498/93-007	Unavailability of one EDG and the turbine driven AFW pump	PWR	12/29/92–1/22/93	1.2×10^{-5}	UNAVAIL
Three Mile Island 1	289/93-002	Both RHR heat exchangers unavailable	PWR	1/29/93	3.1×10^{-6}	UNAVAIL

[a]UNAVAIL, system(s) unavailable.
[b]AIT Report 213/93-80.

Table 2 Precursors Involving Initiating Events Sorted by Plant

Plant	Event Identifier	Description	Plant Type	Event Date	p(cd)	TRANS[a]
Beaver Valley 1	334/93-013	Dual-unit loss-of-offsite power	PWR	10/12/93	5.5×10^{-5}	LOOP
Cook 2	316/93-007	Reactor trip with degraded AFW	PWR	8/2/93	2.4×10^{-6}	TRIP
LaSalle 1	373/93-015	Scram and loss-of-offsite power	BWR	9/14/93	1.3×10^{-4}	LOOP
McGuire 2	370/93-008	Loss-of-offsite power and failure of an MSIV to close	PWR	12/27/93	9.3×10^{-5}	LOOP
North Anna 2	339/93-002	AFW disabled after reactor trip	PWR	4/16/93	1.1×10^{-6}	TRIP
Palo Verde 2	529/93-001	Steam generator tube rupture	PWR	3/14/93	4.7×10^{-5}	SGTR
Perry	440/93-011, 440/93-010	Clogged suppression pool strainers	BWR	3/26/93	1.2×10^{-4}	TRIP
Pilgrim	293/93-004	Weather-induced LOOP, vessel pressure/temperature limits violated	BWR	3/13/93	4.6×10^{-6}	LOOP

[a]LOOP, loss of offsite power; SGTR, steam generator tube rupture; TRIP, reactor trip.

Table 3 Precursors Involving Unavailabilities Sorted by Conditional Core Damage Probability

p(cd)	Plant	Plant Type	Event Identifier	Description	Event Date	TRANS[a]
1.5×10^{-4}	Catawba 1 and 2	PWR	413/93-002	Essential service water potentially unavailable during dual-unit LOOP	2/25/93	UNAVAIL
6.5×10^{-5}	Haddam Neck	PWR	213/93-S01,[b] 213/93-006, 213/93-007	Degradation of MCC-5, pressurizer PORV, and both emergency diesel generators	6/27/93	UNAVAIL
6.0×10^{-5}	Quad Cities 2	BWR	265/93-010, 265/93-012	Degradation of both emergency diesel generators	4/22/93	UNAVAIL
5.1×10^{-5}	Arkansas Nuclear One, Unit 1	PWR	313/93-003	Both trains of recirculation inoperable for 14 hours	9/30/93	UNAVAIL
1.2×10^{-5}	South Texas Project, Unit 1	PWR	498/93-005, 498/93-007	Unavailability of one EDG and the turbine-driven AFW pump	12/29/92–1/22/93	UNAVAIL
3.1×10^{-6}	Three Mile Island 1	PWR	289/93-002	Both RHR heat exchangers unavailable	1/29/93	UNAVAIL
2.1×10^{-6}	Beaver Valley 2	PWR	412/93-012	Failure of both EDG load sequencers	10/4/93–10/6/93	UNAVAIL

[a]UNAVAIL, system(s) unavailable.
[b]AIT Report 213/93-80.

Table 4 Precursors Involving Initiating Events Sorted by Conditional Core Damage Probability

p(cd)	Plant	Plant Type	Event Identifier	Description	Event Date	TRANS[a]
1.3×10^{-1}	LaSalle 1	BWR	373/93-015	Scram and loss-of-offsite power	9/14/93	LOOP
1.2×10^{-1}	Perry	BWR	440/93-011, 440/93-010	Clogged suppression pool strainers	3/26/93	TRIP
9.3×10^{-5}	McGuire 2	PWR	370/93-008	Loss-of-offsite power and failure of an MSIV to close	12/27/93	LOOP
5.5×10^{-5}	Beaver Valley 1	PWR	334/93-013	Dual unit loss-of-offsite power	10/12/93	LOOP
4.7×10^{-5}	Palo Verde 2	PWR	529/93-001	Steam generator tube rupture	3/14/93	SGTR
4.6×10^{-6}	Pilgrim	BWR	293/93-004	Weather-induced LOOP, vessel pressure–temperature limits violated	3/13/93	LOOP
2.4×10^{-6}	Cook 2	PWR	316/93-007	Reactor trip with degraded AFW	8/2/93	TRIP
1.1×10^{-6}	North Anna 2	PWR	339/93-002	AFW disabled after reactor trip	4/16/93	TRIP

[a]LOOP, loss-of-offsite power; SGTR, steam generator tube rupture; TRIP, reactor trip.

• Plant type (Plant Type)
• Initiator associated with the event or unavailability if no initiator was involved (TRANS)

The tables are sorted as follows:

• Table 1: Precursors involving unavailabilities sorted by plant
• Table 2: Precursors involving initiating events sorted by plant
• Table 3: Precursors involving unavailabilities sorted by conditional core damage probability
• Table 4: Precursors involving initiating events sorted by conditional core damage probability
• Table 5: Event initiator or unavailability abbreviations

Containment-Related Events

No containment-related events were found for 1993. This event category includes losses of containment function, such as containment cooling, containment spray, containment isolation (direct paths to the environment only), or hydrogen control.

"Interesting" Events

One "interesting" event was found for 1993 and is documented in Appendix C of Ref. 1. This event category includes events that were not selected as precursors but that provided insight into unusual failure modes with the potential to compromise continued core cooling.

Potentially Significant Events That Were Impractical to Analyze

Nineteen potentially significant events were considered impractical to analyze for 1993. This event category typically includes events that are impractical to analyze because of the lack of information or the inability to model the event reasonably within a probabilistic risk assessment framework, considering the level of detail typically available in probabilistic risk analysis models. These potentially significant events are documented in Appendix D of Ref. 1.

Table 5 Event Initiator or Unavailability Abbreviations

Abbreviation	Definition
LOFW	Loss of feedwater
LOOP	Loss-of-offsite power
LOCA	Loss-of-coolant accident
LSDC	Loss of shutdown cooling
MSLB	Main steam-line break
SGTR	Steam generator tube rupture
TRIP	Reactor trip
UNAVAIL	System(s) unavailable
UNIQ	Unique sequence

IMPORTANT PRECURSORS

Four precursors with conditional core damage probabilities of $\geq 10^{-4}$ were identified for 1993. Events with such conditional probabilities have traditionally been considered significant in the ASP Program. For 1993, these events, in alphabetical order, include the following:

Catawba Units 1 and 2 (LER 413/93-002)

On February 25, 1993, with Catawba 1 at 100% power and Catawba 2 in refueling shutdown, three of the four essential service water (ESW) pump discharge valves failed to open during a surveillance test. It was later determined that the torque switch settings (TSSs) for all four of the ESW pump discharge valves were improperly set.

In 1989, the "open" torque switch settings (TSSs) for 56 butterfly valves were to be set to the maximum value to address problems with opening these valves under high differential pressure. The four ESW pump discharge valves were included in these 56 valves. The "open" TSSs for the Unit 1 ESW pump discharge valves were set to the maximum value (3.0). However, the "open" TSSs for the Unit 2 valves were incorrectly left at 1.5. The "close" TSS was adjusted to the maximum value instead.

In August 1992 the Unit 1 ESW pump discharge valves were set up per Generic Letter (GL) 89-10 criteria.[10] This resulted in the "open" TSSs being reduced from the maximum value of 3.0 to 2.0. The Unit 2 valves were not reset to the GL 89-10 criteria at the time of the event.

Following the failure of the B train valves on February 25, 1993, the licensee realized that the TSSs for the Unit 2 ESW valves had been mistakenly reversed in 1989. The TSSs for the Unit 2 valves were changed to the maximum setting. The discharge valves for the Unit 1 pumps were set to 20 degrees open. Following these changes, all valves were successfully opened against maximum differential pressure.

The licensee conducted a study of the history of TSSs for the ESW valves and discovered that (1) ESW pump

1A was affected between August 1992 and February 1993, (2) ESW pump 1B was affected between November 1985 and July 1989 and between August 1992 and February 1993, and (3) ESW pump 2B was affected between November 1985 and February 1993. As a result, from August 1992 through February 1993, three of the four ESW pump discharge valves (1A, 1B, and 2B) were unable to open against full differential pressure.

With three of the four valves unable to open under full differential pressure conditions, the failure of the ESW pump associated with the operable valve would result in a loss of ESW to both Catawba units.

The event was modeled as a potential failure of the "2A" ESW pump to run. Following the failure of ESW pump 2A, two mitigation strategies were considered possible. The first involves the recovery of one ESW pump before an RCP seal LOCA (50 min). Recovery of the one ESW pump would supply sufficient cooling water for both units if a LOCA did not occur on either unit. A LOCA concurrent with a trip of the running ESW pump was considered unlikely. Even if a LOCA did occur, once the first ESW pump was running, the second could be started from the control room because the discharge valves would not have to open against full differential pressure. Once ESW is recovered, systems cooled by ESW would become operable. The other recovery strategy involves placing the safe shutdown facility (SSF) in service to provide RCP seal cooling and starting the turbine-driven AFW pump to provide secondary-side heat removal. This would allow the plant to achieve a hot shutdown condition even without the recovery of the ESW system.

The conditional probability of core damage estimated for this event is 1.2×10^{-4}. The dominant core damage sequence involves a failure of the running ESW pump, failure to recover ESW within 50 min, and failure of the SSF. A second important core damage sequence involves a failure of the operating ESW pump, failure to recover ESW within 50 min, successful SSF operation, and failure of the turbine-driven AFW pump for secondary-side heat removal.

This event was considered to be two precursor events because it affected both Catawba 1 and 2.

LaSalle 1 (LER 373/93-015)

LaSalle 1 was operating at 100% power on September 14, 1993, when a fault occurred in the buswork associated with the system auxiliary transformer (SAT). The resulting electrical system perturbations caused the loss of one main feed pump and a reactor scram on low vessel level. Reactor makeup after the scram was initially supplied by the motor-driven reactor feed pump, but the vessel overfilled, which resulted in feed pump and main turbine–generator trips. Once the main generator separated from the grid, the unit auxiliary transformer was deenergized and the plant experienced a LOOP. The emergency diesel generators (EDGs) started and loaded to supply the emergency buses. The high-pressure core spray (HPCS) diesel also started. Safety relief valves (SRVs) were operated to reduce pressure by relieving steam to the suppression pool. Suppression pool cooling (SPC) was initiated and reactor core isolation cooling (RCIC) was aligned for vessel makeup. After about 75 minutes, offsite a-c power was restored to Unit 1 by connecting Unit 1 buses to Unit 2. Late in the event, one SRV failed to operate on demand. When reactor pressure decreased to 500 psig, the low-pressure core spray (LPCS) system was aligned to provide makeup, and the reactor was then placed in shutdown cooling (SDC).

The conditional probability of subsequent core damage for this event is estimated to be 1.3×10^{-4}. The dominant core damage sequence involves the plant-centered LOOP, a postulated failure of emergency power, successful reactor shutdown, and postulated failure to recover emergency power before battery depletion.

Perry (LER 440/93-010)

When the Perry suppression pool was inspected in May 1992, an accumulation of dirt and debris was noticed on the suction strainers for residual heat removal (RHR) trains A and B. Strainer cleaning was scheduled for a later date because RHR system performance was considered acceptable on the basis of surveillance testing.

The suppression pool strainers were inspected again and cleaned during a maintenance outage in January 1993. RHR train A and B suction strainers were found to be deformed, with the area of the strainer surface between internal stiffeners partially collapsed inward in the direction of system flow. It was determined that the strainers were deformed by excessive differential pressure caused by strainer fouling during normal pump operation. Review of a videotape taken during the May 1992 inspection revealed evidence of deformation that had not been noticed at the time of the taping. The containment side of the suppression pool was inspected and cleaned in February 1993, and the deformed strainers were replaced.

On March 26, 1993, the reactor was scrammed following the rupture of a 30-in. service water (SW) line.

Condenser vacuum was lost after the loss of SW, which required closure of the main steam isolation valves. The RCIC system was used for pressure vessel makeup, and both trains of the RHR system were started for SPC. After shutdown cooling was established using RHR train A, RHR train B continued to provide SPC for an additional 5 h. Then RCIC was secured and the control-rod-drive (CRD) system was used for level control. The A CRD pump experienced minor cavitation as the result of suction.

Approximately 1.7 million gallons was discharged through the SW break. About 5% of the total leakage entered numerous plant buildings, accumulating in the lowest level of the auxiliary building and control complex, where safety-related equipment is located. Although no safety-related equipment was impacted by the flood, water entered multiple plant buildings that would normally be considered independent structures in an internal flooding analysis.

If SW had not been secured, continued flooding of the auxiliary building and control complex could have resulted in damage to emergency core cooling (ECC) components. During the actual event, the HPCS pump motor was wetted by water dripping from a ceiling hatch plug; however, the pump was not damaged. The lack of detailed information concerning equipment locations and flood pathways prevented consideration of potential flooding effects in the analysis; however, sensitivity analysis was performed to bound the potential effects of the flood.

On April 14, 1993, all emergency core cooling system (ECCS) strainers were inspected. The RHR train B strainer was fouled and deformed in a manner similar to that observed during the January 1993 inspection. The remaining strainers showed no signs of fouling. Without disturbing the debris on the strainer, a test run of RHR pump B was performed. The pump running suction pressure decreased to 0 psig after operating for 8 h, and the pump was secured. The pump suction strainer was then inspected. The debris from the strainer was analyzed, and it was determined that the debris contained fibrous material and corrosion products. The predominant fibrous material was glass fiber from roughing filter material used in the drywell air cooler system. The RHR strainer provided a structural framework for a uniform covering of the fibrous material, which, in turn, acted as a filter for suspended solids that would have otherwise passed through the strainer.

The licensee inspected and cleaned the containment and the suppression pool following the discovery of the clogged strainers and did not identify large quantities of the fibrous material. On the basis of this, the licensee concluded that there was no chronic degradation of the properly installed filter media. Instead, the licensee concluded that the fibrous material entered the suppression pool as intact pieces as a result of installation or maintenance activities (the roughing filters are normally replaced before startup from refueling outages). These pieces subsequently broke down to fibers once they were in the suppression pool. The actual time when the material entered the suppression pool could not be determined.

Excessive differential pressure across the RHR strainers from debris accumulation would cause the SPC to fail and could result in failure of the LPCI if it were required to operate for long periods of time. The event was modeled as an unavailability of RHR/SPC following (1) postulated initiators in the 1-year period before discovery of the clogged strainers and (2) the reactor trip following the SW pipe rupture on March 26, 1993.

The conditional core damage probability estimated for this event is 1.2×10^{-4}. The dominant core damage sequence involves a scram with PCS and feed water (FW) unavailable following the SW pipe rupture, HPCS success, failure of long-term decay heat removal via the RHR system, and failure to vent the containment. The results of the sensitivity analysis to address potential flooding effects indicate that potential flooding effects do not significantly contribute to the overall event. If the HPCS pump motor had been damaged by the water that dripped from the ceiling hatch, the estimated core damage probability could have been substantially greater than the 1.2×10^{-4} estimated for the event.

NUMBER OF PRECURSORS IDENTIFIED

Sixteen precursors with probability of core damage [p(cd)] $\geq 10^{-6}$ affecting 16 units were identified in 1993. The distribution of precursors as a function of conditional probability is shown in Table 6. The distribution of 1988–1992 precursors is also shown for comparison purposes.

As described previously, differences in the ASP models and the analysis methods from year to year preclude a direct comparison between the number of events identified for different calendar years. In particular, the conditional core damage probabilities estimated for the 1992 and 1993 events are lower for equivalent events in earlier years because supplemental and plant-specific mitigating systems beyond those included in the ASP models were incorporated into the analyses.

Table 6 Number of Precursors

Year	$10^{-3} \leq p(cd) < 1$	$10^{-4} \leq p(cd) < 10^{-3}$	$10^{-5} \leq p(cd) < 10^{-4}$	$10^{-6} \leq p(cd) < 10^{-5}$	Total number of precursors
1988	0	7	14	11	32
1989	0	7	11	12	30
1990	0	6	11	11	28
1991	1	27	8	6	27
1992	0	7	7	13	27
1993	0	4	7	5	16

INSIGHTS

Likely Sequences

Precursors with conditional probabilities of $\geq 10^{-4}$ that were identified for 1993 were reviewed to determine the most likely core damage sequences associated with each event. These sequences include the observed plant state plus additional postulated failures required for core damage. For the events that occurred or could have occurred at power and with core damage probabilities of $\geq 10^{-4}$, the following dominant core damage sequences were identified:

Pressurized water reactors (PWRs)—based on two events (the one Catawba event that affects both units)

- Failure of the running ESW pump, failure to recover ESW within 50 minutes, and failure of the safe shutdown facility.

Boiling Water Reactors (BWRs—based on two events

- Plant-centered LOOP with failure of emergency power that is not recovered before battery depletion.
- Transient with FW and PCS unavailable, failure of long-term decay heat removal, and failure to vent containment.

Observations

A review of the analyses for all 16 precursors for 1993 revealed the following trends and patterns across the different analyses:

- As can be seen in Tables 3 and 4, two of the four precursors with p(cd) $>10^{-4}$ selected for 1993 are PWR events. For all 1993 precursors, 12 were associated with PWRs and 4 with BWRs.
- A number of the events involved problems with electrical systems. LOOP events occurred at four plants. These four events had conditional core damage probabilities that ranged from 1.3×10^{-4} to 4.6×10^{-6}. The range in the conditional core damage probabilities for these events is primarily due to the type and number of mitigating systems incorporated into the models beyond the normal ASP models. For example, in the Pilgrim LOOP (LER 293/93-004) with a conditional core damage probability of 4.6×10^{-6}, the inclusion of a blackout diesel generator and an offsite power line that is used only after EDG failure resulted in a significant decrease in the conditional core damage probability from the base ASP value.

Three of the precursors associated with unavailabilities involved the degradation or unavailability of electrical equipment: (1) the degradation of the bus transfer scheme for motor control center 5 and the EDGs at Haddam Neck, (2) the degradation of the emergency load sequencers at Beaver Valley 2, and (3) the loss of the diesel generator cooling water pumps at Quad Cities Unit 2.

- The precursors are evenly divided between unavailabilities and initiators. The distribution of the events by conditional core damage probability in the two categories is roughly the same (see Table 7).
- Seven of the eight precursors associated with unavailabilities occurred at PWRs. The precursors associated with the initiating events were roughly evenly divided between the PWRs (5 events) and BWRs (3 events).
- Twelve of the sixteen events (75%) occurred at multiunit sites. This is about the same as the percentage of units at multiunit sites (71%). Only one of the precursor events affected both units at a dual-unit site.

A review of the ASP reports for 1990–1993 indicates the following trends and patterns:

- Long-term unavailabilities and LOOP initiators typically dominate the events with the highest conditional core damage probabilities.

Table 7 Number of Precursors

Event Category	$10^{-4} \leq p(cd) < 10^{-3}$	$10^{-5} \leq p(cd) < 10^{-4}$	$10^{-6} \leq p(cd) < 10^{-5}$	Total
Unavailabilities	2	4	2	8
Initiators	2	3	3	8

• The events with the highest conditional core damage probabilities are dominated by PWRs.

• The number of precursors identified for 1993 is lower than that for previous years. This decrease is due in part to the differences in the ASP models for 1993. In particular, the conditional core damage probabilities estimated for the 1993 events are lower than equivalent events in earlier years because of consideration of supplemental and plant-specific mitigating systems beyond those modeled in the ASP models. A number of events that would have met the precursor criteria for prior years were rejected on low probability following the incorporation of additional mitigating systems.

REFERENCES

1. L. N. Vanden Heuvel, J. W. Cletcher, D. A. Copinger, J. W. Minarick, and B. W. Dolan, *Precursors to Potential Severe Core Damage Accidents: 1993—A Status Report,* Main Report and Appendixes A–D, NUREG/CR-4674 (ORNL/NOAC-232), Vol. 19, September 1994.
2. L. N. Vanden Heuvel, J. W. Cletcher, D. A. Copinger, J. W. Minarick, and B. W. Dolan, *Precursors to Potential Severe Core Damage Accidents: 1993—A Status Report,* Appendixes E and F, NUREG/CR-4674 (ORNL/NOAC-232), Vol. 20, September 1994.
3. Nuclear Regulatory Commission, *Licensee Event Report System. Description of System and Guidelines for Reporting (Second Draft Revision for Comment),* NUREG-1022, 182 pp., February 1994.
4. J. W. Minarick, J. D. Harris, P. N. Austin, J. W. Cletcher, and E. W. Hagen, *Precursors to Severe Core Accidents: 1986—A Status Report,* NUREG/CR-4674 (ORNL/NOAC-232), Main Report and Appendices A through C, Vol. 5; Appendices D through F, Vol. 6, May 1988.
5. J. W. Minarick, J. D. Harris, J. W. Cletcher, P. N. Austin, and A. A. Blake, *Precursors to Severe Core Accidents: 1987—A Status Report,* NUREG/CR-4674 (ORNL/NOAC-232), Main Report and Appendix A, Vol. 7; Appendices B through D, Vol. 8, July 1989.
6. J. W. Minarick, J. W. Cletcher, and A. A. Blake, *Precursors to Severe Core Accidents: 1988—A Status Report,* NUREG/CR-4674 (ORNL/NOAC-232), Main Report and Appendix A, Vol. 9; Appendices B and C, Vol. 10, February 1990.
7. J. W. Minarick, J. W. Cletcher, D. A. Copinger, and B. W. Dolan, *Precursors to Severe Core Accidents: 1989—A Status Report,* NUREG/CR-4674 (ORNL/NOAC-232), Main Report and Appendix A, Vol. 11; Appendices B and C, Vol. 12, August 1990.
8. J. W. Minarick, J. W. Cletcher, D. A. Copinger, and B. W. Dolan, *Precursors to Severe Core Accidents: 1990—A Status Report,* NUREG/CR-4674 (ORNL/NOAC-232), Main Report and Appendix A, Vol. 13; Appendices B and C, Vol. 14, August 1991.
9. J. W. Minarick, J. W. Cletcher, D. A. Copinger, and B. W. Dolan, *Precursors to Severe Core Accidents: 1990—A Status Report,* NUREG/CR-4674 (ORNL/NOAC-232), Main Report and Appendix A, Vol. 15; Appendices B, C, and D, Vol. 16, September 1992.
10. Nuclear Regulatory Commission, Generic Letter 89-10 (GL-89-10), Supplement 6, *Safety-Related Motor-Operated Valve Testing and Surveillance. Information on Schedule and Grouping and Staff Responses to Additional Public Questions,* 23 pp., March 1994.

Recent Developments

Edited by E. G. Silver

Reports, Standards, and Safety Guides

By D. S. Queener

This article contains four lists of various documents relevant to nuclear safety as compiled by the editor. These lists are: (1) reactor operations-related reports of U.S. origin, (2) other books and reports, (3) regulatory guides, and (4) nuclear standards. Each list contains the documents in its category which were published (or became available) during the April 1994 through September 1994 reporting period covered by this issue of *Nuclear Safety*. The availability and cost of the documents are noted in most instances.

OPERATIONS REPORTS

This category is listed separately because of the increasing interest in the safety implications of information obtainable from both normal and off-normal operating experience with licensed power reactors. The reports fall into several categories shown, with information about the availability of the reports given where possible. The NRC reports are available from the Nuclear Regulatory Commission (NRC) Public Document Room, 2120 L Street, NW, Washington, DC 20555.

NRC Office of Nuclear Reactor Regulation

The NRC Office of Nuclear Reactor Regulation (NRR) issues reports regarding operating experience at licensed reactors. These reports, previously published by the NRC Office of Inspection and Enforcement (IE), fall into two categories of urgency: (1) NRC Bulletins and Generic Letters, which require remedial actions and/or responses from affected licensees, and(2) NRC Information Notices and Administrative Letters, which are for general information and do not require any response from the licensee. The Administrative Letters are relatively new generic communications issued by the NRC which were previously distributed under the generic letter category. They contain information of an administrative or informational nature. No specific action is required in response to these Administrative Letters.

NRC Information Notices

NRC IN 90-68, Suppl. 1 *Stress Corrosion Cracking of Reactor Coolant Pump Bolts,* April 14, 1994, 5 pages.

NRC IN 92-51, Suppl. 1 *Misapplication and Inadequate Testing of Molded-Case Circuit Breakers,* April 12, 1994, 10 pages.

NRC IN 94-28 *Potential Problems with Fire-Barrier Penetration Seals,* April 5, 1994, 5 pages.

NRC IN 94-29 *Charging Pump Trip During a Loss-of-Coolant Event Caused by Low Suction Pressure,* April 11, 1994, 4 pages.

NRC IN 94-30 *Leaking Shutdown Cooling Isolation Valves at Cooper Nuclear Station,* April 12, 1994, 3 pages plus two pages of attachments.

NRC IN 94-31 *Potential Failure of Wilco, Lexan-Type HN-4-L Fire Hoze Nozzles,* April 14, 1994, 2 pages.

NRC IN 94-32 *Revised Seismic Hazard Estimates,* April 29, 1994, 3 pages plus 4 pages of attachments.

NRC IN 94-33 *Capacitor Failures in Westinghouse Eagle 21 Plant Protection Systems,* May 9, 1994, 3 pages plus 2 pages of attachments.

NRC IN 94-34 *Thermo-Lag 330-660 Flexi-Blanket Ampacity Derating Concerns,* May 13, 1994, 3 pages plus 4 pages of attachments.

NRC IN 94-35 *NIOSH Respirator User Notices, "Inadvertent Separation of the Mask-Mounted Regulatory (MMR) from the Facepiece on the Mine Safety Appliances (MSA) Com-*

pany MMR Self-Contained Breathing Apparatus (SCBA) and Status Update," May 16, 1994, 2 pages plus 5 pages of attachments.

NRC IN 94-36 *Undetected Accumulation of Gas in Reactor Coolant System,* May 24, 1994, 4 pages plus 2 pages of attachments.

NRC IN 94-37 *Misadministration Caused by a Bent Interstitial Needle During Brachytherapy Procedure,* May 27, 1994, 2 pages plus one-page attachment.

NRC IN 94-38 *Results of a Special NRC Inspection at Dresden Nuclear Power Station Unit 1 Following a Rupture of Service Water Inside Containment,* May 27, 1994, 4 pages plus 3 pages of attachments.

NRC IN 94-39 *Identified Problems in Gamma Steriotactic Radiosurgery,* May 31, 1994, 4 pages plus 3 pages of attachments.

NRC IN 94-40 *Failure of a Rod Control Cluster Assembly to Fully Insert Following a Reactor Trip at Braidwood Unit 2,* May 26, 1994, 3 pages plus 2 pages of attachments.

NRC IN 94-41 *Problems with General Electric Type CR124 Overload Relay Ambient Compensation,* June 7, 1994, 3 pages plus 2 pages of attachments.

NRC IN 94-42 *Cracking in the Lower Region of the Core Shroud in Boiling-Water Reactors,* June 7, 1994, 3 pages plus 3 pages of attachments. (Supplement 1 issued July 19, 1994.)

NRC IN 94-43 *Determination of Primary-to-Secondary Steam Generator Leak Rate,* June 10, 1994, 4 pages plus 2 pages of attachments.

NRC IN 94-44 *Main Steam Isolation Valve Failure to Close on Demand Because of Inadequate Maintenance and Testing,* June 16, 1994, 3 pages plus 4 pages of attachments.

NRC IN 94-45 *Potential Common-Mode Failure Mechanism for Large Vertical Pumps,* June 17, 1994, 3 pages plus 4 pages of attachments.

NRC IN 94-46 *Nonconservative Reactor Coolant System Leakage Calculation,* June 20, 1994, 3 pages plus 3 pages of attachments.

NRC IN 94-47 *Accuracy of Information Provided to NRC During the Licensing Process,* June 21, 1994, 3 pages plus 3 pages of attachments.

NRC IN 94-48 *Snubber Lubricant Degradation in High-Temperature Environments,* June 30, 1994, 3 pages plus 4 pages of attachments.

NRC IN 94-49 *Failure of Torque Switch Roll Pins,* July 6, 1994, 4 pages plus 3 pages of attachments.

NRC IN 94-50 *Failure of General Electric Contactors to Pull in at the Required Voltage,* July 14, 1994, 3 pages plus 2 pages of attachments.

NRC IN 94-51 *Inappropriate Greasing of Double Shielded Motor Bearings,* July 15, 1994, 2 pages plus 2 pages of attachments.

NRC IN 94-52 *Inadvertent Containment Spray and Reactor Vessel Draindown at Millstone Unit 1,* 3 pages plus 3 pages of attachments.

NRC IN 94-53 *Hydrogen Gas Burn Inside Pressurizer During Welding,* July 18, 1994, 3 pages plus 2 pages of attachments.

NRC IN 94-54 *Failures of General Electric Magne-Blast Circuit Breakers to Latch Closed,* August 1, 1994, 4 pages plus 4 pages of attachments.

NRC IN 94-55 *Problems with Copes–Vulcan Pressurizer Power-Operated Relief Valves,* August 4, 1994, 4 pages plus 2 pages of attachments.

NRC IN 94-56 *Inaccuracy of Safety Valve Set Pressure Determinations Using Assist Devices,* August 11, 1994, 3 pages plus 2 pages of attachments.

NRC IN 94-57 *Debris in Containment and the Residual Heat Removal System,* August 12, 1994, 4 pages plus 2 pages of attachments.

NRC IN 94-58 *Reactor Coolant Pump Lube Oil Fire,* August 16, 1994, 3 pages plus 2 pages of attachments.

NRC IN 94-59 *Accelerated Dealloying of Cast Aluminum–Bronze Valves Caused by Microbiologically Induced Corrosion,* August 17, 1994, 3 pages plus 2 pages of attachments.

NRC IN 94-60 *Potential Overpressurization of Main Steam System,* August 22, 1994, 2 pages plus 11 pages of attachments.

NRC IN 94-61 *Corrosion of William Powell Gate Valve Disc Holders,* August 25, 1994, 3 pages plus 2 pages of attachments.

NRC IN 94-62 *Operational Experience on Steam Generator Tube Leaks and Tube Ruptures,* August 30, 1994, 5 pages.

NRC IN 94-63 *Boric Acid Corrosion of Charging Pump Casing Caused by Cladding Cracks,* August 30, 1994, 5 pages.

NRC IN 94-64 *Reactivity Insertion Transient and Accident Limits for High Burnup Fuel,* August 31, 1994, 3 pages plus 4 pages of attachments.

NRC IN 94-65 *Potential Errors in Manual Brachytherapy Dose Calculations Generated Using a Computerized Treatment Planning System,* September 12, 1994.

NRC IN 94-66 *Overspeed of Turbine-Driven Pumps Caused by Governor Valve Stem Binding,* September 19, 1994, 4 pages plus 2 pages of attachments.

NRC IN 94-67 *Problems with Henry Pratt Motor-Operated Butterfly Valves,* September 26, 1994, 2 pages plus 3 pages of attachments.

NRC IN 94-68 *Safety-Related Equipment Failures Caused by Faulted Indicating Lamps,* September 27, 1994, 3 pages plus 2 pages of attachments.

NRC IN 94-69 *Potential Inadequacies in the Prediction of Torque Requirements for and Torque Output of Motor-Operated Butterfly Valves,* September 28, 1994, 4 pages plus 2 pages of attachments.

NRC IN 94-70 *Issues Associated with Use of Strontium-89 and Other Beta Emitting Radiopharmaceuticals,* September 29, 1994, 5 pages plus 2 pages of attachments.

NRC Administrative Letters

NRC AL 94-04 *Change of the NRC Operations Center Commercial Telephone & Facsimile Numbers,* April 11, 1994, 2 pages plus 3 pages of attachments.

NRC AL 94-05 *Notification Concerning Changes to 10 CFR Part 55,* April 25, 1994, 2 pages plus 7 pages of attachments.

NRC AL 94-06 *Visits by Members of the Public to Nuclear Power Plants,* April 27, 1994, 2 pages plus 2 pages of attachments.

NRC AL 94-07 *Distribution of Site-Specific and State Emergency Planning Information,* May 6, 1994, 2 pages plus 3 pages of attachments.

NRC AL 94-08 *Consolidation of the NRC Region IV and Region V Offices,* July 13, 1994, 2 pages plus 3 pages of attachments.

NRC AL 94-09 *Changes to the "Mandatory Guidelines for Federal Workplace Drug Testing Programs,"* August 4, 1994, 1 page plus 2 pages of attachments.

NRC AL 94-10 *Distribution of NUREG-1478, "Non-Power Reactor Operator Licensing Examiner Standards,"* August 17, 1994, 2 pages plus 3 pages of attachments.

NRC AL 94-11 *Request for Voluntary Comment on the Pilot Program for NRC Recognition of Good Performance by Nuclear Power Plants,* September 7, 1994, 3 pages plus 8 pages of attachments.

NRC AL 94-12 *Operator Licensing National Examination Schedule,* September 12, 1994, 3 pages plus 4 pages of attachments.

NRC AL 94-14 *Distribution of Supplement to NUREG-1021, "Operator Licensing Examiner Standards,"* September 22, 1994, 2 pages plus 2 pages of attachments.

Other Operations Reports

These are other reports issued by various organizations in the United States dealing with power-reactor operations activities. Most of the NRC publications (NUREG series documents) can be ordered from the Superintendent of Documents, U.S. Government Printing Office (GPO), P.O. Box 37082, Washington, DC 20013. NRC draft copies of reports are available free of charge by writing the NRC Office of Administration (ADM), Distribution and Mail Services Section, Washington, DC 20555. A number of these reports can also be obtained from the NRC Public Document Room (PDR). Specify the report number when ordering. Telephone orders can be made by contacting the PDR at (202) 634-3273.

Many other reports prepared by U.S. Government laboratories and contractor organizations are available from the U.S. Department of Commerce, Technology Administration, National Technical Information Service, Springfield, VA 22161, and/or DOE Office of Scientific and Technical Information (OSTI), P.O. Box 62, Oak Ridge, TN 37831. Reports available through one or more of these organizations are designated with the appropriate information (i.e., GPO, PDR, NTIS, and OSTI) in parentheses at the end of the listing, followed by the price, when available.

NUREG-1416 *Operational Experience and Maintenance Programs of Transamerica Delaval Inc., Diesel Generators,* J. Rajan, May 1994, 42 pages (GPO).

NUREG/CR-6093 *An Analysis of Operational Experience During Low Power and Shutdown and a Plan for Addressing Human Reliability Assessment Issues,* M. Barriere and W. Luckas, Brookhaven National Lab., NY, June 1994, 200 pages (GPO).

NUREG/CR-6160 *Summary of Important Results and SCDAP/RELAP5 Analysis for OECD LOFT Experiment LP-FP-2,* E. W. Coryell and D. W. Akers, EG&G Idaho Inc., ID, April 1994, 165 pages (GPO).

NUREG/CR-6252 *Lessons Learned from the Three Mile Island-Unit 2 Advisory Panel,* D. Lach et al., Pacific Northwest Lab., WA, August 1994, 45 pages (GPO).

NRC Office for Analysis and Evaluation of Operational Data

The NRC Office for Analysis and Evaluation of Operational Data (AEOD) is responsible for the review and assessment of commercial nuclear power plant operating experience. AEOD publishes a number of reports, including case studies, special studies, engineering evaluations, and technical reviews. Individual copies of these reports may be obtained from the NRC Public Document Room (PDR).

AEOD/S94-02 *Turbine-Generator Overspeed Protection Systems at U.S. Light-Water Reactors,* H. L. Ornstein, September 30, 1994, 80 pages.

AEOD/T94-02 *Review of Mispositioned Equipment Events,* S. Israel, May 1994, 25 pages.

DOE- and NRC-Related Items

NUREG-1145 *U.S. Nuclear Regulatory Commission 1993 Annual Report,* 306 pages, September 1994 (GPO).

NUREG-1470 *Financial Statement for Fiscal Year 1993,* 110 pages, August 1994.

NUREG-1484 *Final Environmental Impact Statement for the Construction and Operation of Claiborne Enrichment Center, Homer, Louisiana,* August 1994, 800 pages (GPO).

NUREG-1488 *Revised Livermore Seismic Hazard Estimates for Sixty-Nine Nuclear Power Plant Sites East of the Rocky Mountains. Final Report,* April 1994, 108 pages (GPO).

NUREG/CR-5726 *Review of the Diablo Canyon Probabilistic Risk Assessment,* G. E. Bozoki et al., Brookhaven National Lab., NY, August 1994 (GPO).

NUREG/CR-6143, Vol. 4 *Evaluation of Potential Severe Accidents During Low Power and Shutdown Operations at Grand Gulf, Unit 1. Analysis of Core Damage Frequency from Internally Induced Flooding Events for Plant Operational State 5 During a Refueling Outage,* V. Dandini et al., Future Resources Associates Inc., CA, July 1994 (GPO).

NUREG/CR-6143, Vol. 5 *Evaluation of Potential Severe Accidents During Low Power and Shutdown Operations at Grand Gulf, Unit 1. Analysis of Core Damage Frequency from Seismic Events for Plant Operational State 5 During a Refueling Outage,* R. J. Budnitz et al., Future Resources Associates Inc., CA, August 1994 (GPO).

NUREG/CR-6144, Vol. 5 *Evaluation of Potential Severe Accidents During Low Power and Shutdown Operations at Surry, Unit 1. Analysis of Core Damage Frequency from Seismic Events During Mid-Loop Operations,* R. J. Budnitz et al., Future Resources Associates Inc., CA, August 1994 (GPO).

NUREG/CR-6181 *A Pilot Application of Risk-Based Methods to Establish In-Service Inspection Priorities for Nuclear Components at Surry Unit 1 Nuclear Power Station,* T. Vo, Pacific Northwest Lab., WA, August 1994, 60 pages (GPO).

NUREG/CR-6181 *Review of the Diablo Canyon Probabilistic Risk Assessment,* G. E. Bozoki et al., Brookhaven National Lab., NY, August 1994 (GPO).

Other Items

ORAU 94/F-10 *Committee on Interagency Radiation Research and Policy Coordination (CIRRPC), 10th Anniversary Report,* June 1994, 40 pages (NTIS).

ENS (European Nuclear Society) World Yearbook 1994 + Britain, Journal of ENS, No. 7/8, July/August 1994, 100 pages (Nuclear Europe Worldscan, P.O. Box 5032, CH-3001 Berne, Switzerland).

Utility Data Institute (UDI) 1993 Report on Power Plant Operating and Maintenance Expenses, UDI, Washington, DC, 1994 (UDI, 1200 G Street, NW, Suite 250, Washington, DC 20005).

U.S. Nuclear Plant Statistics During 1993, UDI, 1200 G Street NW, Suite 250, Washington, DC, June 8, 1994 (UDI).

REGULATORY GUIDES

To expedite the role and function of the NRC, its Office of Nuclear Regulatory Research prepares and maintains a file of Regulatory Guides that define much of the basis for the licensing of nuclear facilities. These Regulatory Guides are divided into 10 divisions as shown in Table 1.

Table 1 Regulatory Guides

Division 1	Power Reactor Guides
Division 2	Research and Test Reactor Guides
Division 3	Fuels and Materials Facilities Guides
Division 4	Environmental and Siting Guides
Division 5	Materials and Plant Protection Guides
Division 6	Product Guides
Division 7	Transportation Guides
Division 8	Occupational Health Guides
Division 9	Antitrust and Financial Review Guides
Division 10	General Guides

Single copies of the draft guides may be obtained from NRC Distribution Section, Division of Information Support Services, Washington, DC 20555. Draft guides are issued free (for comment) and licensees receive both draft and final copies free; others can purchase single copies of active guides by contacting the U.S. Government Printing Office (GPO), Superintendent of Documents, P.O. Box 37082, Washington, DC 20013. Costs vary according to length of the guide. Of course, draft and active copies will be available from the NRC Public Document Room, 1717 H Street, NW, Washington, DC, for inspection and copying for a fee.

Revisions in these rates will be announced as appropriate. Subscription requests should be sent to the National Technical Information Service, Subscription Department, Springfield, VA 22161. Any questions or comments about the sale of regulatory guides should be directed to Chief, Document Management Branch, Division of Technical Information and Document Control, Nuclear Regulatory Commission, Washington, DC 20555.

Actions pertaining to specific guides (such as issuance of new guides, issuance for comment, or withdrawal), which occurred during the reporting period, are listed below.

Division 1 Power Reactor Guides

1.118 (Draft revision 3, for comment) *Periodic Testing of Electric Power and Protection Systems,* September 1994.

Division 3 Fuels and Materials Facilities Guides

3.068 *Nuclear Criticality Safety Training,* April 1994.

Division 5 Materials and Plant Protection Guides

5.052 (Draft revision 3) *Standard Format and Content of Licensee Physical Protection Plan for Strategic Special Nuclear Material at Fixed Sites (Other Than Nuclear Power Plants),* April 1994.

Division 6 Product Guides

6.002 (Draft, for comment) *Establishing QA Programs for Manufacturing and Distribution of Sealed Sources and Devices Containing Byproduct Material,* May 1994.

NUCLEAR STANDARDS

Standards pertaining to nuclear materials and facilities are prepared by many technical societies and organizations in the United States, including the Department of Energy (DOE) (NE Standards). When standards prepared by a technical society are submitted to the American National Standards Institute (ANSI) for consideration as an American National Standard, they are assigned ANSI standard numbers, although they may also contain the identification of the originating organization and be sold by that organization as well as by ANSI. We have undertaken to list here the most significant nuclear standards actions taken by organizations from April 1994 through September 1994. Actions listed include issuance for comments, approval by the ANSI Board of Standards Review (ANSI-BSR), and publication of the approved standard. Persons interested in obtaining copies of the standards should write to the issuing organizations.

American National Standards Institute

ANSI does not prepare standards; it is devoted to approving and disseminating standards prepared by technical organizations. However, it does publish standards, and such standards can be ordered from ANSI, Attention: Sales Department, 1430 Broadway, New York, NY 10018. Frequently, ANSI is an alternate source for standards also available from the preparing organization.

ANSI N15.36-1994 (New standard, approved by ANSI/BSR) *Nuclear Materials—Nondestructive Assay Measurement Control and Assurance.*

American Nuclear Society

Standards prepared by ANS can be obtained from ANS, Attention: Marilyn D. Weber, 555 North Kensington Avenue, LaGrange Park, IL 60525.

ANSI/ANS 3.1-1993 (Published) *Selection, Qualification, and Training of Personnel for Nuclear Power Plants,* $70.00.

ANSI/ANS 3.8.5-1992 (Published) *Criteria for Emergency Radiological Field Monitoring, Sampling, and Analysis,* $55.00.

ANSI/ANS 5.1-1993 [Revision of ANSI/ANS 5.1-1979(r1985), approved by ANSI/BSR] *Decay Heat Power in Light Water Reactors.*

ANSI/ANS 15.11-1993 (Published) *Radiation Protection at Research Reactor Facilities,* $80.00.

ANSI/ANS 56.8-1994 (Revision of ANSI/ANS 56.8-1987, approved by ANSI/BSR) *Containment System Leakage Testing Requirements.*

ANSI/ANS 58.8-1994 (revision of ANSI/ANS 58.8-1984, approved by ANSI/BSR) *Time Response Design Criteria for Safety-Related Operator Actions.*

BSR/ANS-3.4 [Revision of ANSI/ANS-3.4-1983(R1988), for comment] *Medical Certification and Monitoring of Personnel Requiring Operator Licenses for Nuclear Power Plants,* $7.50.

BSR/ANS 3.8.6 (New standard, for comment) *Criteria for Conduct of Offsite Radiological Assessment for Emergency Response for Nuclear Power Plants,* $7.50.

BSR/ANS 15.8 [Revision of ANSI/ANS 15.81975(R1986), for comment] *Quality Assurance Program Requirements for Research Reactors,* $7.50.

BSR/ANS 50.1 (Revision and consolidation of ANSI/ANS 51.1-1993 and ANSI/ANS 52.1-1983, for comment) *Nuclear Safety Design Criteria for Light Water Reactors,* $15.00.

BSR/ANS 59.52 (New standard, for comment) *Lubricating Oil Systems for Emergency Diesel Generators for Light Water Reactors,* $10.00.

American Society of Mechanical Engineers

Standards prepared by ASME can be obtained from ASME, Attention: R. D. Palumbo, 345 East 47th Street, New York, NY 10017.

ANSI/ASME QME-1-1994 (Revision and redesignation of ANSI B16.41-1983, approved by ANSI/BSR) *Section QV Functional Qualification Requirements for Active Valve Assemblies for Nuclear Power Plants.*

Institute of Electrical and Electronics Engineers

Standards prepared by IEEE can be obtained from IEEE, Attention: M. Lynch, 345 East 47th Street, New York, NY 10017.

ANSI/IEEE 334-1994 (New standard, approved by ANSI/BSR) *Standard for Qualifying Continuous Duty Class IE Motors for Nuclear Power Generating Stations.*

ANSI/IEEE 535-1986 (R1994, reaffirmation of ANSI/IEEE 535-1986, approved by ANSI/BSR) *Standard Qualification of Class 1E Lead Storage Batteries for Nuclear Power Generating Stations.*

BSR/IEEE 334 (New standard, for comment) *Qualifying Continuous Duty Class 1E Motors for Nuclear Power Generating Stations,* $27.00.

BSR/IEEE 535-1986 (Reaffirmation of ANSI/IEEE 535-1986, for comment) *Standard Qualification of Class 1E Lead Storage Batteries for Nuclear Power Generating Stations,* $49.50.

International Standards

This section includes publications for any of the three types of international standards:

—IEC standards (International Electrotechnical Commission)

—ISO standards (International Standards Organization)

—KTA standards [Kerntechnischer Ausschuss (Nuclear Technology Commission)].

Standards originating from the IEC and ISO can be obtained from the American National Standards Institute (ANSI), International Sales Department, 1430 Broadway, New York, NY 10018.

The KTA standards are developed and approved by the Nuclear Safety Standards Commission (KTA). The KTA, formerly a component of the Gesellschaft für Reaktorsicherheit (GRS), is now integrated in the Federal Office for Radiation Protection (Bundesamt für Strahlenschutz BfS) in Salzgitter, Germany. Copies of these standards can be ordered from Dr. T. Kalinowski, KTA-Geschäftsstelle, Postfach 10 01 49, 3320 Salzgitter 1, Germany. These standards are in German and, unless otherwise noted, an English translation is available from the KTA.

Prices for the international standards are shown in German currency (DM). The IEC and ISO standards are included in this issue.

IEC

IEC 951-5:1994 (Published) *Nuclear Power Plants—Radiation Monitoring Equipment for Accident and Post-Accident Conditions—Part 5: Radioactivity of Air in Light Water Nuclear Power Plants,* $62.00.

IEC 1301:1994 (Published) *Nuclear Instrumentation—Guidelines for Selection of Metrologically Supported Nuclear Radiation Spectrometry Systems,* $55.00.

IEC 1306:1994 (Published) *Nuclear Instrumentation—Microprocessor-Based Nuclear Radiation Measuring Devices,* $119.00.

ISO

ISO 10979:1994 (Published) *Identification of Fuel Assemblies for Nuclear Power Reactors,* $26.00.

Proposed Rule Changes as of June 30, 1994[a,b]

(Changes Since the Previous Issue of *Nuclear Safety* Are Indicated by Shaded Areas)

Number of part to be changed	Date published for comment	Date comment period expired	Date published; date effective	Topic or proposed effect	Current action and/or comment, *Federal Register* volumes and page numbers
5 CFR 48 10 CFR 0			4-13-94; 7-12-94	Supplemental standards of ethical conduct for employees of the NRC	Final rule in 59:71 (17457)
10 CFR 1	2-24-92	3-6-92		Special review of NRC regulations	Published for comment in 57:36 (6299)
10 CFR 1	6-19-92	8-18-92; 9-30-92		Review of reactor licensee reporting requirements	Published for comment in 57:119 (27394); comment period extended in 57:153 (34886)
10 CFR 1 10 CFR 21 10 CFR 30 10 CFR 32 10 CFR 50			2-7-94; 2-7-94	Minor clarifying amendments	Final rule in 59:25 (5519)
10 CFR 1 10 CFR 20 10 CFR 30 10 CFR 40 10 CFR 55 10 CFR 70 10 CFR 73			4-13-94; 4-4-94	Consolidation of NRC Region V Office with the Region IV Office	Final rule in 59:71 (17464)
10 CFR 2	12-23-92	3-8-93		Availability of official records	Published for comment in 57:247 (61013)
10 CFR 2 10 CFR 72	6-3-93	8-17-93; 10-1-93		Interim storage of spent fuel in an independent spent fuel storage installation; site-specific license to a qualified applicant	Published for comment in 58:105 (31478); comment period extended in 58:176 (48004)
10 CFR 2	9-29-93	11-15-93		Informal hearing procedures for materials licensing adjudications	Published for comment in 58:187 (50858); final rule in 59:107 (29187)
10 CFR 2	5-11-94	6-10-94		Summary reports on the status of petitions for rulemaking; frequency	Published for comment in 59:90 (24371)
10 CFR 12	8-2-93	9-1-93	5-5-94; 6-6-94	Equal Access to Justice Act: implementation	Published for comment in 58:146 (41061); final rule in 59:86 (23119)
10 CFR 19, 20, 21, 30, 36, 40, 51, 70, 170	12-4-90	3-4-91		Licenses and radiation safety requirements for large irradiators	Published for comment in 55:233 (50008)

(Table continues on the next page.)

Proposed Rule Changes as of June 30, 1994 (Continued)

Number of part to be changed	Date published for comment	Date comment period expired	Date published; date effective	Topic or proposed effect	Current action and/or comment, *Federal Register* volumes and page numbers
10 CFR 19 10 CFR 20	2-3-94	4-4-94		Radiation protection requirements; amended definitions and criteria	Published for comment in 59:23 (5132)
10 CFR 19, 20, 21, 26, 51, 70, 71, 73, 74, 76, 95	2-11-94	4-12-94		Certification of gaseous diffusion plants	Published for comment in 59:29 (6792)
10 CFR 20	2-25-94	5-26-94		Disposal of radioactive material by release into sanitary sewer systems	Advanced notice of proposed rulemaking published in 59:38 (9146)
10 CFR 20 10 CFR 61	4-21-92	7-20-92		Low-level waste shipment manifest information and reporting	Published for comment in 57:77 (14500)
10 CFR 20	6-18-93	8-15-93; 9-20-93		Radiological criteria for decommissioning of NRC-licensed facilities; generic environmental impact statement (GEIS) for rulemaking, notice of intent to prepare a GEIS and to conduct a scoping process	Published for comment in 58:116 (33570); comment period extended in 58:154 (42882)
10 CFR 20 10 CFR 34			12-22-93; 1-1-94	Standards for protection against radiation; removal of expired material	Final rule in 58:244 (67657); correction in 59:9 (1900)
10 CFR 20	2-2-94	3-11-94		Radiological criteria for decommissioning of NRC-licensed facilities; enhanced participatory rulemaking, availability of the staff's draft of the rule	Published for comment in 59:22 (4868)
10 CFR 20, 21, 30, 35, 40, 50, 70, 72, 73			3-25-94; 5-31-94	NRC Operations Center commercial telephone number change	Final rule in 59:58 (14085)
10 CFR 20 10 CFR 35	6-15-94	8-29-94		Criteria for the release of patients administered radioactive material	Published for comment in 59:114 (30724)
10 CFR 26	3-24-93	6-22-93	1-5-94; 1-1-94	Modification of Fitness-for-Duty Program requirements	Published for comment in 58:55 (15810); final rule in 59:3 (502)
10 CFR 26	5-11-94	9-9-94		Consideration of changes to fitness-for-duty (FFD) requirements	Published for comment in 59:90 (24373)
10 CFR 30 10 CFR 40 10 CFR 70	2-20-92	4-30-92		Proposed method for regulating major materials licenses; availability of NUREG report	Published for comment in 57:34 (6077)

Proposed Rule Changes as of June 30, 1994 (Continued)

Number of part to be changed	Date published for comment	Date comment period expired	Date published; date effective	Topic or proposed effect	Current action and/or comment, *Federal Register* volumes and page numbers
10 CFR 30, 40, 50, 70, 72	1-11-93	3-29-93	12-29-93; 1-28-94	Self-guarantee as an additional financial assurance mechanism	Published for comment in 58:6 (3515); final rule in 58:248 (68726); corrections in 59:8 (1618)
10 CFR 30 10 CFR 40 10 CFR 70 10 CFR 72	1-13-93	3-29-93		Timeliness in decommissioning of materials facilities	Published for comment in 58:8 (4099)
10 CFR 30 10 CFR 40 10 CFR 50 10 CFR 70 10 CFR 72	2-2-93	4-5-93		Procedures and criteria for on-site storage of low-level radioactive waste	Published for comment in 58:20 (6730); withdrawn in 59:78 (19147)
10 CFR 30 10 CFR 32 10 CFR 35	6-17-93	10-15-93		Preparation, transfer for commercial distribution, and use of byproduct material for medical use	Published for comment in 58:115 (33396)
10 CFR 30 10 CFR 40 10 CFR 70 10 CFR 72	6-22-94	9-20-94		Clarification of decommissioning funding requirements	Published for comment in 59:119 (32138)
10 CFR 31 10 CFR 32	12-27-91	3-12-92		Requirements for the possession of industrial devices containing byproduct material	Published for comment in 56:248 (67011)
10 CFR 31 10 CFR 32	11-27-92	3-29-93		Requirements concerning the accessible air gap for generally licensed devices	Published for comment in 57:229 (56287)
10 CFR 34 10 CFR 150	2-28-94	5-31-94		Licenses for radiography and radiation safety requirements for radiographic operations	Published for comment in 59:39 (9429)
10 CFR 40	10-28-92	1-26-93		Licensing of source material	Published for comment in 57:209 (48749)
10 CFR 40 10 CFR 72 10 CFR 74 10 CFR 75 10 CFR 150	1-26-93	4-26-93		Licensee submittal of data in computer-readable form	Published for comment in 58:15 (6098)
10 CFR 40	11-3-93	12-17-93	6-1-94; 7-1-94	Uranium mill tailings regulations; conforming NRC requirements to EPA standards	Published for comment in 58:211 (58657); final rule in 59:104 (28220)

(Table continues on the next page.)

Proposed Rule Changes as of June 30, 1994 (Continued)

Number of part to be changed	Date published for comment	Date comment period expired	Date published; date effective	Topic or proposed effect	Current action and/or comment, *Federal Register* volumes and page numbers
10 CFR 50	9-28-92	12-28-92		Acceptability of plant performance for severe accidents; scope of consideration in safety regulations	Published for comment in 57:188 (44513)
10 CFR 50 10 CFR 52 10 CFR 100	10-20-92	2-17-93; 3-24-93; 6-1-93		Reactor site criteria, including seismic and earthquake engineering criteria for nuclear power plants and proposed denial of petition for rulemaking from Free Environment, Inc., et al.	Published for comment in 57:203 (47802); comment period extended in 58:2 (271); extended again in 58:57 (16377)
10 CFR 50	6-28-93	9-13-93		Production and utilization facilities; emergency planning and preparedness-exercise requirements	Published for comment in 58:122 (34539)
10 CFR 50	6-30-93	9-13-93	3-4-94; 4-4-94	Notification of spent fuel management and funding plans by licensees of prematurely shut down power reactors	Published for comment in 58:124 (34947); final rule in 59:43 (10267)
10 CFR 50	1-7-94	3-23-94; 4-25-94		Codes and standards for nuclear power plants; subsection IWE and subsection IWL	Published for comment in 59:5 (979); comment period extended in 59:59 (4373)
10 CFR 50			3-25-94; 6-23-94	Emergency planning and preparedness exercise requirements for nuclear power plants	Final rule in 59:58 (14087)
10 CFR 51	9-17-91	12-16-91; 3-16-92		Environmental review for renewal of operating licenses	Published for comment in 56:180 (47016); comment period extended in 56:228 (59898)
10 CFR 52	11-3-93	1-3-94		Rulemakings to grant standard design certification for evolutionary light water reactor designs	Advance notice of proposed rulemaking published in 58:211 (58664)
10 CFR 52	6-10-94	7-9-94	12-30-93; 1-22-93	Combined licenses; conforming amendments; response to post-promulgation comment	Post-adoption comment published in 58:249 (69220); supplementary post-promulgation comment period provided in 59:111 (29965)
10 CFR 55	5-20-93	7-19-93		Operator's licenses	Published for comment in 58:96 (29366)

Proposed Rule Changes as of June 30, 1994 (Continued)

Number of part to be changed	Date published for comment	Date comment period expired	Date published; date effective	Topic or proposed effect	Current action and/or comment, *Federal Register* volumes and page numbers
10 CFR 55			2-9-94; 3-11-94	Renewal of licenses and requalification requirements for licensed operators	Final rule in 59:27 (5934)
10 CFR 60	7-9-93	10-7-93		Disposal of high-level radioactive wastes in geologic repositories; investigation and evaluation of potentially adverse conditions	Published for comment in 58:130 (36902)
10 CFR 72	5-24-93	8-9-93; 11-9-93		Emergency planning licensing requirements for independent spent fuel facilities (ISFSI) and monitored retrievable storage facilities (MRS)	Published for comment in 58:98 (29795); comment period extended in 55:166 (45463)
10 CFR 72	9-14-93	11-29-93		Notification of events at independent spent fuel storage installations and the Monitored Retrievable Storage installation	Published for comment in 58:176 (48004)
10 CFR 72	6-2-94	8-16-94		List of approved spent fuel storage casks: addition	Published for comment in 59:105 (28496)
10 CFR 73	10-6-93	12-20-93		Annual physical fitness performance training for tactical response team members, armed response personnel, and guards at Category 1 licensees	Published for comment in 58:192 (52035)
10 CFR 73	11-4-93	1-3-94		Protection against malevolent use of vehicles at nuclear power plants	Published for comment in 58:212 (58804); correction in 58:217 (59965)
10 CFR 73			1-6-94; 2-7-94	Fingerprint cards: change in user fee	Final rule in 59:4 (661)
10 CFR 110	2-7-90 4-28-92	3-9-90 7-13-92		Import and export of radioactive wastes	Advance notice of proposed rulemaking for comment in 55:26 (4181); corrections in 55:57 (10786); published for comment in 57:82 (17859)
10 CFR 110	3-17-93	4-16-93		Specific licensing of exports of certain alpha-emitting radionuclides and byproduct material	Published for comment in 58:50 (14344)
10 CFR 170 10 CFR 171	4-19-93	7-19-93		NRC fee policy; request for public comment	Published for comment in 58:73 (21116)
10 CFR 170 10 CFR 171	5-10-94	6-9-94		Revision of fee schedules; 100% fee recovery, FY 1994	Published for comment in 59:89 (24065)

(Table continues on the next page.)

Proposed Rule Changes as of June 30, 1994 (Continued)

Number of part to be changed	Date published for comment	Date comment period expired	Date published; date effective	Topic or proposed effect	Current action and/or comment, *Federal Register* volumes and page numbers
10 CFR 171	9-29-93	10-29-93	3-17-94; 4-18-94	Restoration of the generic exemption from annual fees for non-profit educational institutions	Published for comment in 58:187 (50859); final rule in 59:52 (12539)
10 CFR 171			5-19-94; 5-19-94	Establishment of revised FY 1991 and FY 1992 annual fee surcharge	Final rule in 59:96 (26097)
48 CFR 20	10-2-89	12-1-89		Acquisition regulation (NRCAR)	Published for comment in 54:189 (40420); corrections in 58:43 (12988)

[a]NRC petitions for rule making are not included here, but quarterly listings of such petitions can be obtained by writing to Division of Rules and Records, Office of Administration, U.S. Nuclear Regulatory Commission, Washington, DC 20555. Quarterly listings of the status of proposed rules are also available from the same address.

[b]Proposed rules for which the comment period expired more than 2 years prior to the start of the period currently covered without any subsequent action are dropped from this table. Effective rules are removed from this listing in the issue after their effective date is announced.

The Authors

Consideration of Postaccident Consequences in the Determination of Safety Objectives for Future Nuclear Power Plants in France

Daniel Quéniart is the Director for Safety for the Protection and Nuclear Safety Institute (IPSN). The IPSN is an organisation that conducts research and expertise in all fields of nuclear safety as well as protection of man and the environment; in particular, it has the specific mission of providing the Nuclear Installations Safety Directorate, the French safety authority, with technical support. He is a graduate of the Ecole Polytechnique, the foremost French engineering school, and a senior engineer of the French "corps des mines." Most of his career has been devoted to the safety of nuclear facilities. He is currently a member of national and international consultative bodies and was recently asked to participate in the work of the International Atomic Energy Agency's International Nuclear Safety Advisory Group (INSAG). Current address: Protection and Nuclear Safety Institute, CEA-CE/FAR, B.P. No. 6, 92265 Fontenay-Aux-Roses, Cedex, France.

Annie Sugier is the Director of Protection at the IPSN (Institute for Protection and Nuclear Safety). The task of the IPSN is to carry out research and expert evaluations in all fields of study necessary for the control of risks. She was educated in Physics and Chimistry at the University of Orsay in France. Her professional background is mainly in radioactive waste management and decommissioning of nuclear plants. One of her main contributions to this area of activity was the launching of the dismantling of Marcoule gaz-graphite reactors (G2G3). In the field of radioprotection, she has been directly involved in the process of revision of the Basic Safety Standards at the international and national level as a member of the european expert group on radioprotection (article 31 group), a member of the OECD/CRPPH committee on radioprotection, and a leader of the French delegation at the AIEA technical committee for the establishment of the Basic Safety Standards. Furthermore, she is a member of the International Commission on Radiological Protection (ICRP) Committee 4 on Application of the System of radioprotection. She has been elected president of the French Society of Radiation Protection. Current address: Protection and Nuclear Safety Institute, CEA-CE/FAR, B.P. No. 6, 92265 Fontenay-Aux-Roses, Cedex, France.

Jacques Lochard is Director of CEPN (Nuclear Protection Evaluation Center), a nonprofit organization, founded in 1976, for research and consulting in the area of optimisation of radiological protection and comparative assessment of health and environmental risks associated with energy systems. He was educated in Economics at the University of Besançon-France (B.S.) and Paris-Pantheon-Sorbonne (M.S.). His main contribution in radiation protection has been in the development of methodologies and implementation tools in the field of optimisation of radiological protection. He has written numerous articles in scientific journals and proceedings of international conferences covering both the theoretical and practical aspects of optimisation. He is currently the Secretary of the French Society of Radiation Protection (SFRP) and is also widely involved in the international radiation protection scene: Member of the Executive Council of the International Radiation Protection Association (IRPA), Member of the Committee on Radiation Protection and Public Health (CRPPH) of the Nuclear Energy Agency of the OECD and Secretary of Committee 3 of the International Commission on Radiological Protection (ICRP). Current address: Nuclear Protection Evaluation Centre, Route du Panorama, B.P. No. 6, 92263, Fontenay-Aux-Roses, Cedex, France.

Nuclear Safety Research: The Phebus FP Severe Accident Experimental Program

Peter von der Hardt (Technical University Darmstadt, Germany 1961), Head of the In-Pile Test Division, is delegated by the European Commission (EC), Joint Research Centre, Safety Technology Institute, to Cadarache, France, as Assistant Phebus FP Programme Manager. Previous EC assignments were to Ispra, Italy; Petten, The Netherlands; and Mol, Belgium. His main interests concern nuclear materials and operation and utilization programs of research reactors. He has authored 82 publications and has given about 30 university and seminar lectures. Current address: Commission of the European Communities.

Alan V. Jones (Ph.D., University of Leeds, U.K., 1975), Head of the Source Term Analysis Section, Safety Technology Institute, European Commission (EC) Joint Research Centre at Ispra, Italy, has been involved in light-water-reactor safety research since 1988. Currently, his main activities are the interpretation of Phebus FP results, analytical support to future Phebus tests, and the development of "ESTER," a European integrated severe accident code. He has authored 64 journal and conference papers. Current address: Commission of the European Communities.

Catherine Lecomte (Ingénieur des Mines, Ecole Polytechnique, Paris, France, 1977) is Head of the Accident Evaluation Service, SEAC, at the Institute for Nuclear Protection and Safety (IPSN) at Fontenay-aux-Roses, France. Her present fields of interest include reactor safety studies and the underlying experimental and analytical programs. Current address: Institut de Protection et de Sûreté Nucléaire.

Alain Tattegrain (Ecole Superieure d'Electricité, Paris, France, 1958) is Deputy Head of the Safety Research Department, DRS, Institute for Nuclear Protection and Safety, Cadarache, France. He has been Phebus FP Programme Leader since 1988 and has managed in-pile severe-accident experiments (CABRI, SCARABEE, SURA, PHEBUS-LOCA and -CSD) during the past 20 years. Current address: Institut de Protection et de Sûreté Nucléaire.

Containment Performance Analysis of the Advanced Neutron Source Reactor at the Oak Ridge National Laboratory

S. H. Kim, R. P. Taleyarkhan, and V. Georgevich: Current address: Engineering Technology Division, Oak Ridge National Laboratory, Oak Ridge, TN 37831-8057.

Assessment of Fission Product Deposits in the Reactor Coolant System: The DEVAP Program

Gilles Le Marois is a research engineer in the Fuel Behaviour Studies Branch at the Grenoble Nuclear Research Centre. In 1976 he received the diploma of Doctor in Chemistry. He has been involved previously in reprocessing, waste corrosion research, and in-pile programs. He has specialized in the operation and interpretation of fission product behavior experiments since 1982. Current address: Commissariat à l'Energie Atomique, DTP/SECC, Centre d'Etudes Nucleaires de Grenoble, 17, Avenue des Martyrs, 38054 Grenoble Cedex 9, France.

Michel Megnin is a member of the research staff in the Fuel Behaviour Studies Branch at the Grenoble Nuclear Research Centre. He participated in isotopic separation research and has been involved in the design and operation of fission product experiments since 1989. Current address: Commissariat à l'Energie Atomique, DTP/SECC, Centre d'Etudes Nucleaires de Grenoble, 17, Avenue des Martyrs, 38054 Grenoble Cedex 9, France.

Effects of Normal Aging on Calibration and Response Time of Nuclear Plant Resistance Temperature Detectors and Pressure Sensors

H. M. Hashemian is president of Analysis and Measurement Services Corporation of Knoxville, Tennessee. His company specializes in testing the performance of nuclear plant instrumentation and performing high-technology research for the Federal Government. He received the M.S. degree in nuclear engineering from The University of Tennessee and is a Fellow of the Instrument Society of America. He has had more than 15 years of experience in nuclear power plant instrumentation and has authored or coauthored nearly 100 technical papers and reports, including 6 NUREG/CR reports for the U.S. Nuclear Regulatory Commission. Current address: Analysis and Measurement Services Corporation, AMS 9111 Cross Park Drive, Knoxville, TN 37923.

Defense in Depth Against the Hydrogen Risk—A European Research Program

Fabio Fineschi received a degree in nuclear engineering from the University of Pisa (Italy) in 1971 and is now Associate Professor of Nuclear Plant Control and Operation. He is the leader of the research group that, since 1976, has been performing theoretical and experimental studies on hydrogen diffusion and explosion in nuclear plants at the Department of Nuclear and Mechanical Constructions of the University of Pisa. He

has been cooperating on this problem with the European Nuclear Energy Association (ENEA) (the Atomic Energy Authority in Italy), ENEL (the national utility in Italy), the Commission of the European Communities (CEC) (he has been the coordinator of the CEC Hydrogen Project since 1992), and the International Atomic Energy Agency (IAEA) (he is cooperating to write an IAEA document on the mitigation of the hydrogen risks). Current address: Dipartimento di costruzioni meccaniche e nucleari, via Diotisalvi 2, 56126 Pisa, Italia.

Technical Note: A Preliminary Analysis of the Risks to Hong Kong Resulting from Potential Accidents of Daya Bay Nuclear Power Plant

Z. Shi and *X. Wei*. Current address: Institute of Nuclear Energy Technology, Tsinghua University, Beijing 100084, People's Republic of China.

Three Mile Island—New Findings 15 Years After the Accident

Alan M. Rubin is a Section Leader in the Accident Evaluation Branch in the Office of Research of the Nuclear Regulatory Commission (NRC). He has over 15 years of engineering experience in the nuclear power field in both private industry and the NRC and was the project manager for the Three Mile Island Vessel Investigation Project. He received the B.S. degree in mechanical engineering from Rutgers University in 1966 and the M.S. and Ph.D. degrees, also in mechanical engineering, from the University of Pennsylvania in 1967 and 1971, respectively. Current address: Office of Nuclear Regulatory Research, U.S. NRC, Mail Stop T10-K8, Washington, DC 20555.

Eric S. Beckjord received the A.B. degree in physics from Harvard College in 1951, the M.S. degree in electrical engineering from Massachusetts Institute of Technology (MIT) in 1956, and the M.B.A. degree from the University of Chicago in 1984. He was a development engineer for the General Electric Company Atomic Power Equipment Department (1956–1963); Engineering Manager for Westinghouse Nuclear Energy Divisions (1963–1975); Director, Division of Reactor Development and Demonstration of the Energy Research and Development Administration and the Department of Energy (1976–1979); Deputy Director of Argonne National Laboratory (1980–1984); Visiting Professor, MIT Nuclear Engineering Department (1984–1986); and Director, Office of Research, Nuclear Regulatory Commission (NRC) (1986–present). Current address: Office of Nuclear Regulatory Research, U.S. NRC, Mail Stop T10-F12, Washington, DC 20555.

Relocation of Molten Material to the TMI-2 Lower Head

James R. Wolf is Manager of the Nuclear Fuels and Materials Unit of EG&G Idaho, Inc. He has been involved in the Three Mile Island Nuclear Station Unit-2 Vessel Inspection Program (VIP) since 1991 and currently serves as the EG&G Idaho, Inc., VIP Program Manager. He has been involved in many different aspects of reactor safety, including severe accident research, experimental thermal hydraulics, and two-phase flow instrumentation development. He received his M.S. degree in 1972 and his Ph.D. degree in physics from American University, Washington, D.C., in 1975. Current address: Idaho National Engineering Laboratory, EG&G Idaho, Inc., P.O. Box 1625, Idaho Falls, ID 83415-3840.

Douglas W. Akers is the technical leader of Radiological Physics Technical Area of the Advanced Nuclear Energy Projects Department of Lockheed Idaho Technologies Company. Akers, who holds a B.A. in chemistry from Idaho State University and an M.S. in chemistry from the University of Idaho, has 18 years of diversified experience in radiological assessment, characterization of commercial and DOE nuclear facilities, and radiation measurements. He has been involved in the examination and analysis of results from Three Mile Island Nuclear Station Unit 2 since shortly after the accident and was most recently involved in the reactor core and the lower-head examination program. He is currently involved in Nuclear Regulatory Commission programs addressing radiological issues and the evaluation of low-level waste characterization practices and in the development of radiation detectors for specialized applications. Current address: Idaho National Engineering Laboratory, EG&G Idaho, Inc., P.O. Box 1625, Idaho Falls, ID 83415-3840.

Lawrence A. Neimark is a senior metallurgist and the manager of the Irradiation Performance Section and the Alpha–Gamma Hot Cell Facility, Energy Technology Division, at the Argonne National Laboratory (ANL) in Argonne, Illinois. He received the B.S. degree in 1956

and the M.S. degree in 1958 in metallurgy from the University of Minnesota and joined ANL in 1958. He assumed his current management positions in 1967, and significant activities have been in the development of metallic, oxide, and carbide fuels for liquid-metal fast breeder reactors; characterization of light-water reactor UO_2 fuel; development of U_3Si_x fuel for reduced enrichment reactors; off-normal behavior of UAl_x fuels; characterization of debris from Three Mile Island Nuclear Station Unit 2; and the behavior of fission products with respect to fuel/cladding and fuel/fission-product interactions. He has authored or coauthored more than 100 publications on nuclear fuel performance. He is a Fellow of the American Nuclear Society. Current address: Argonne National Laboratory, Argonne, IL 60439.

Insight Into the TMI-2 Core Material Relocation Through Examination of Instrument Tube Nozzles

Lawrence A. Neimark is a senior metallurgist and the manager of the Irradiation Performance Section and the Alpha–Gamma Hot Cell Facility, Energy Technology Division, at the Argonne National Laboratory (ANL) in Argonne, Illinois. He received the B.S. degree in 1956 and the M.S. degree in 1958 in metallurgy from the University of Minnesota and joined ANL in 1958. He assumed his current management positions in 1967, and significant activities have been in the development of metallic, oxide, and carbide fuels for liquid-metal fast breeder reactors; characterization of light-water reactor UO_2 fuel; development of U_3Si_x fuel for reduced enrichment reactors; off-normal behavior of UAl_x fuels; characterization of debris from Three Mile Island Nuclear Station Unit 2; and the behavior of fission products with respect to fuel/cladding and fuel/fission-product interactions. He has authored or coauthored more than 100 publications on nuclear fuel performance. He is a Fellow of the American Nuclear Society. Current address: Argonne National Laboratory, Argonne, IL 60439.

Physical and Radiochemical Examinations of Debris from the TMI-2 Lower Head

Douglas W. Akers is the technical leader of Radiological Physics Technical Area of the Advanced Nuclear Energy Projects Department of Lockheed Idaho Technologies Company. Akers, who holds a B.A. in chemistry from Idaho State University and an M.S. in chemistry from the University of Idaho, has 18 years of diversified experience in radiological assessment, characterization of commercial and DOE nuclear facilities, and radiation measurements. He has been involved in the examination and analysis of results from Three Mile Island Nuclear Station Unit 2 since shortly after the accident and was most recently involved in the reactor core and the lower-head examination program. He is currently involved in Nuclear Regulatory Commission programs addressing radiological issues and the evaluation of low-level waste characterization practices and in the development of radiation detectors for specialized applications. Current address: Idaho National Engineering Laboratory, EG&G Idaho, Inc., P.O. Box 1625, Idaho Falls, ID 83415-3840.

Brian K. Schuetz is a scientist with the Radioanalytical Chemistry Section at the Idaho National Engineering Laboratory. He holds a B.S. in chemistry from Idaho State University. He was involved in the examination of the reactor vessel lower head of Three Mile Island Nuclear Station Unit 2 and in the performance of nuclear material measurements. He is currently involved in the spectrometric alpha analysis of environmental and low-level radioactive samples and in the treatment and remediation of low-level mixed waste. Current address: Idaho National Engineering Laboratory, EG&G Idaho, Inc., P.O. Box 1625, Idaho Falls, ID 83415-3840.

Results of Metallographic Examinations and Mechanical Tests of Pressure Vessel Samples from the TMI-2 Lower Head

Dwight R. Diercks is manager of the Mechanics of Materials Section in the Energy Technology Division of Argonne National Laboratory. He has 25 years of research experience in the areas of mechanical testing, failure analysis, and physical metallurgy in both breeder and light-water nuclear reactor technologies as well as nonnuclear energy-related programs. In addition to his work on the examination and testing of material from the Three Mile Island Nuclear Station Unit 2 (TMI-2) pressure vessel, he has recently been involved in reviewing

materials aging issues in advanced reactor designs and in studies on pressurized-water-reactor steam generator tubing degradation. He holds undergraduate and graduate degrees in metallurgical engineering from the University of Illinois at Urbana-Champaign having completed his Ph.D. studies in 1971. Current address: Energy Technology Division, Argonne National Laboratory, Argonne, IL 60439.

Gary Korth has been associated with the Idaho National Engineering Laboratory for the past 26 years and currently holds the position of principal scientist. He received the B.S. degree in mechanical engineering in 1963 and the Ph.D. degree in metallurgy in 1968, both at the University of Utah. He holds three U.S. patents and an IR-100 award. He has over 50 publications in refereed technical journals and conference proceedings of various subjects dealing with mechanical properties and microstructure correlations. For over 15 years he was associated with the Liquid-Metal Fast Breeder Program in the generating of design data of irradiated and unirradiated structural materials for elevated temperature service. Current address: Idaho National Engineering Laboratory, P.O. Box 1625, Idaho Falls, ID 83415-2218.

Margin-to-Failure Calculations for the TMI-2 Vessel

Joy L. Rempe is a Senior Engineering Specialist at the Idaho National Engineering Laboratory. She was principal investigator and performed thermal analysis for the Three Mile Island Unit 2 Margin-to-Failure Analysis Effort and the U.S. Nuclear Regulatory Commission-sponsored Light-Water Reactor Vessel Lower Head Failure Analysis Program. She graduated from the University of Missouri in 1981 with a B.S. degree in nuclear engineering and received an M.S. degree in 1983 and a Ph.D. degree in 1986 in nuclear engineering from Massachusetts Institute of Technology. Her current research interests are in the areas of thermal analysis and fission product transport. Current address: Idaho National Engineering Laboratory, P.O. Box 1625, Idaho Falls, ID 83415.

Lisa Stickler is a Senior Engineer at the Idaho National Engineering Laboratory in the Advanced Nuclear Analysis Technologies Department. Her research interests are in the fields of computational heat transfer and fluid flow. Current projects include analysis of advanced reactor designs. She received her B.S. and M.S. degrees in mechanical engineering from the University of Missouri. Current address: Idaho National Engineering Laboratory, P.O. Box 1625, Idaho Falls, ID 83415.

Susan Chàvez is a Senior Engineering Specialist at the Idaho National Engineering Laboratory. She is a structural analyst with interests in high-temperature material behavior, computational fracture mechanics, and acoustics in solids. She received her B.S. degree in civil engineering from the University of New Mexico in Albuquerque, her M.S. degree in mechanical engineering at the University of California in Berkeley, and her Ph.D. degree in mechanical engineering from the University of Idaho in Moscow. Current address: Idaho National Engineering Laboratory, P.O. Box 1625, Idaho Falls, ID 83415.

Gary Thinnes is a Science and Engineering Manager at the Idaho National Engineering Laboratory. He graduated from the University of Nebraska with B.S. and M.S. degrees in civil engineering and has 19 years of experience in the field of stress analysis of nuclear reactor systems. He performed the initial structural calculations of the Three Mile Island-Unit 2 (TMI-2) reactor vessel lower head prior to the TMI-2 Vessel Investigation Project's (VIP's) beginning, mapping vessel head stress scenarios for postulated accidents. He has provided structural analysis support for the TMI-2 VIP and for the U.S. Nuclear Regulatory Commission's Light-Water-Reactor Lower Head Failure Analysis Program. Current address: Idaho National Engineering Laboratory, P.O. Box 1625, Idaho Falls, ID 83415.

Robert J. Witt is an Associate Professor of Nuclear Engineering and Engineering Physics at the University of Wisconsin-Madison. His research interests are in the area of computational methods in fluid and solid mechanics with specific interests in severe reactor accidents and advanced reactor systems. He received his B.S. degree in mechanical engineering from the University of California-Davis and his M.S. and Ph.D. degrees in nuclear engineering from Massachusetts Institute of Technology. Current address: University of Wisconsin, 147 ERB, 1500 Johnson Dr., Madison, WI 53706-1687.

Michael Corradini is a professor of nuclear engineering and engineering physics at the University of Wisconsin-Madison. He received the Ph.D. degree from the Massachusetts Institute of Technology in 1978. His research interests include nuclear and industrial safety, multiphase flow, and heat transfer. His current research focuses on vapor explosion phenomena, jet spray

dynamics, and chemical reactions in multiphase systems. He is a Fellow of the American Nuclear Society and was the recipient of the 1990 Young Members Engineering Achievement Award. His other achievements and activities include Advisor/Consultant to the Presidential Commission on Three Mile Island, 1979; the NSF Presidential Young Investigator's Award, 1984; member of the Radioactive Waste Review Board Technical Advisory Council for the State of Wisconsin; consultant to the Nuclear Regulatory Commission (NRC) Advisory Committee on Reactor Safeguards for Class-9 Accidents; Vice-Chairman of the NRC Steam Explosion Expert Review Group; and Chairman of the NRC NUREG-1150 Containment Event-Tree Review Group, 1985. Current address: University of Wisconsin, 205 ERB, 1500 Johnson Dr., Madison, WI 53706-1687.

1993 Accident Sequence Precursor (ASP) Program Results

L. N. Vanden Heuvel, J. W. Cletcher, and D. A. Copinger, Current address: Oak Ridge National Laboratory.

J. W. Minarick and B. W. Dolan, Current address: Science Applications International Corporation.

P. D. O'Reilley, Current address: U.S. Nuclear Regulatory Commission.

1995 INTERNATIONAL INCINERATION CONFERENCE

Seattle, Washington, May 8–12, 1995

The 1995 International Incineration Conference is sponsored by the University of California, Irvine (UCI), with participation of the American Society of Mechanical Engineers, the U.S. Environmental Protection Agency, DOE, the Health Physics Society, the American Nuclear Society, the American Institute of Chemical Engineers, the Air & Waste Management Association, and the Coalition for Responsible Waste Incineration. The conference will offer invited and contributed papers on topics of current interest to waste management professionals. Technical and scientific advances will be discussed by experts from the international community involved with thermal treatment technologies for the management of special waste streams: radioactive, hazardous chemical, mixed, munitions and pharmaceutical wastes.

A pre-conference Incineration Basics Course will include classes on both theory and practice. An Advanced Tutorials Course will offer subjects of interest to professionals with three or more years of incineration experience.

Topics to be discussed include combustion research and recent advances in combustion technologies, behavior of organics and non-metals during thermal treatment, behavior of metals during thermal treatment, innovative and emerging thermal treatment technologies for specific waste streams, radioactive, hazardous chemical, mixed, munitions and pharmaceutical wastes, innovative and emerging emissions control systems technologies, innovative and emerging emissions monitoring systems, performance at environmental restoration and remedial action sites, demonstrated thermal treatment experience for specific waste streams (e.g., radioactive, hazardous chemical, mixed, munitions and pharmaceutical wastes, trial burn protocols and results, system design, modification, and startup experience, emissions control and monitoring systems performance, application of quality control procedures to support compliance and operational reliability, waste sampling and characterization considerations, multi-pathway risks from incinerator emissions and operations, materials handling systems for reliable operation, status of regulatory programs and their impacts, demonstrating compliance (operations and maintenance, training, data management and reporting, etc.), DOE's Waste Management Environmental Restoration, and Decontamination and Decommissioning Programs, DoD waste management and environmental restoration programs, ash chemistry/treatment/and disposal, waste minimization/source reduction/segregation/resource recovery, siting and public acceptance, and risk assessment, management and communication.

For further information, contact Ms. Lori Baranow, UC-Irvine, Office of Environment, Health & Safety, Irvine, CA 92717-2725, Phone: (714) 824-7006, FAX: (714) 824-8539.

Reviewers of *Nuclear Safety*, Volume 35

The technical quality of a journal depends not only on the competence and efforts of its authors and editorial staff but also, to a major extent, on the dedication of its corps of peer reviewers. We wish to acknowledge gratefully the many technical experts whose voluntary and unrewarded reviews of proposed *Nuclear Safety* articles have been indispensable in the selection of articles and in the revision of articles to prepare them for publication.

We list below all the names of those who reviewed articles for publication in Vol. 35, whether the articles were used or not. Since it is our policy not to reveal the reviewers' identities to the authors, all reviewers are listed in alphabetical order together with their affiliations.

This list does not include, though we are most grateful to them also, the names of the DOE and NRC staff members who review all *Nuclear Safety* articles to ensure that the policies and positions of their agencies are not misstated or distorted.

Beahm, E. C., Oak Ridge National Laboratory, Oak Ridge, Tenn.
Beck, D. F., Sandia National Laboratories, Waimea, Kauai, Hawaii

Campbell, D. O., Consultant, Oak Ridge, Tenn.
Canonico, D. A. (2), ABB CE Power Products Manufacturing, Chattanooga, Tenn.
Chakraborty, S., Swiss Federal Nuclear Safety Inspectorate, Switzerland
Cheverton, R. D., Oak Ridge National Laboratory, Oak Ridge, Tenn.
Chexal, B., Electric Power Research Institute, Palo Alto, Calif.
Cho, D. H., Argonne National Laboratory, Argonne, Ill.
Clark, R., Oak Ridge National Laboratory, Oak Ridge, Tenn.
Corradini, M. L., University of Wisconsin, Madison, Wis.
Correia, R. P., U.S. Nuclear Regulatory Commission, Washington, D.C.

Davis, F. J., Sandia National Laboratories, Albuquerque, N.M.
Dickson, P. W., Westinghouse Savannah River Company, Aiken, S.C.
Durant, W. S., Westinghouse Savannah River Company, Aiken, S.C.

Eidam, G. (2), Consultant, Richland, Wash.
Eltawila, Farouk, U.S. Nuclear Regulatory Commission, Washington, D.C.

Finelli, G., NASA Langley Research Center, Hampton, Va.
Fontana, M., Oak Ridge National Laboratory, Oak Ridge, Tenn.
Forsberg, C. W., Oak Ridge National Laboratory, Oak Ridge, Tenn.

Georgevich, G. (2), Oak Ridge National Laboratory, Oak Ridge, Tenn.
Gerhart, S., NSF, Washington, D.C.

Heames, T. J., Science Applications International Corporation, Albuquerque, N.M.
Hodge, S. A., Oak Ridge National Laboratory, Oak Ridge, Tenn.
Hyder, M. L., Westinghouse Savannah River Company, Aiken, S.C.

Jansen, J. M., Science Applications International Corporation, Oak Ridge, Tenn.

Kerlin, T. W., The University of Tennessee, Knoxville, Tenn.
Kmetyk, L. N., Sandia National Laboratories, Albuquerque, N.M.
Kohn, W. E., Oak Ridge National Laboratory, Oak Ridge, Tenn.
Kress, T. S. (4), Oak Ridge National Laboratory, Oak Ridge, Tenn.
Kryter, R. C., Oak Ridge National Laboratory, Oak Ridge, Tenn.
Kuczera, B., Projekt Nukleare Sicherheitsforschung, Karlsruhe, Germany

Lindemer, T. B. (2), Oak Ridge National Laboratory, Oak Ridge, Tenn.
Lorenz, R. A., Oak Ridge National Laboratory, Oak Ridge, Tenn.

Minarick, J. (2), Science Applications International Corporation, Oak Ridge, Tenn.
Muhlheim, M. D., Oak Ridge National Laboratory, Oak Ridge, Tenn.
Munro, J., Oak Ridge National Laboratory, Oak Ridge, Tenn.
Murphy, G. A., Oak Ridge National Laboratory, Oak Ridge, Tenn.

Nanstad, R. K., Oak Ridge National Laboratory, Oak Ridge, Tenn.
Nelson, L. D., University of Wisconsin, Madison, Wis.

Osborne, M. F., Oak Ridge National Laboratory, Oak Ridge, Tenn.

Pal Kalra, S., Electric Power Research Institute, Palo Alto, Calif.
Parker, G. W. (2), Oak Ridge National Laboratory, Oak Ridge, Tenn.
Powers, D. A. (4), Sandia National Laboratories, Albuquerque, N.M.

Rehn, D. L., Duke Power Company, York, S.C.

Shepard, R. L., Oak Ridge National Laboratory, Oak Ridge, Tenn.
Simonson, S. A., Massachusetts Institute of Technology, Cambridge, Mass.
Specter, H., New York Power Authority, White Plains, N.Y.

Tennery, V. J. (2), Oak Ridge National Laboratory, Oak Ridge, Tenn.

Valenti, S. (2), Oak Ridge National Laboratory, Oak Ridge, Tenn.
Vanden Heuvel, L. N., Oak Ridge National Laboratory, Oak Ridge, Tenn.
von der Hardt, P., Joint Research Centre, France

Weir, J. R., Jr., Oak Ridge National Laboratory, Oak Ridge, Tenn.
White, J. D., Oak Ridge National Laboratory, Oak Ridge, Tenn.
Williams, H. L., Tennessee Valley Authority, Chattanooga, Tenn.
Wilson, R., Harvard University, Cambridge, Mass.
Wright, R. W. (2), U.S. Nuclear Regulatory Commission, Washington, D.C.

Yoder, R. E., Science Applications International Corporation, Germantown, Md.

Zentner, M. D., Consultant, Kennewick, Wash.

FIFTH INTERNATIONAL CONTROLS AND INSTRUMENTATION CONFERENCE

La Jolla, California, June 19–21, 1995

The Electric Power Research Institute (EPRI) and the Power Industry Division (POWID) of the Instrument Society of America (ISA) are sponsoring the Fifth International joint ISA POWID/EPRI Controls and Instrumentation Conference at the Sheraton Grande Torrey Pines in La Jolla, Calif. The conference will provide a forum to discuss new and/or innovative techniques in the design and use of instrumentation and control (I&C) systems for improved productivity in power generation. The theme of the conference is "Challenging Competition Through Advanced Controls and Instrumentation."

For further information, contact Meetings Department, Instrument Society of America, P.O. Box 12277, Research Triangle Park, NC 27709, Phone: (919) 549-8411, FAX: (919) 549-8288.

ANS INTERNATIONAL TOPICAL MEETING ON SAFETY OF OPERATING REACTORS

Seattle, Washington, September 17–20, 1995

Industry, government, and international representatives will share technical information and experience on performance standards for operating nuclear reactors. Safety and technical experts from around the world will present information on effective approaches developing within the nuclear industry to ensure safe and productive operations.

Topics to be covered include Performance Indicators for Evaluating Reactor Safety; Operating Experience Feedback—Lessons Learned; Safety Culture; Plant Maintenance—The Maintenance Rule, Its Impact on Safety; Performance/Risk-Based Regulation; Regulatory Burden Reductions; Application of Risk Technology to Operating Plants; Operator Training for Response to Severe Accidents; Optimizing the Engineering Change Process for Nuclear Power Plants; Fire Protection at Nuclear Power Plants; Natural Events Impacts; IPEEE Results (Fire and Seismic); Technical Specification Improvement; Reactor Safety and Public Perception; Safety and Pressure Vessel Integrity; Power Oscillation Events; Research and Development in Reactor Safety; Safety Aspects of Mixed Oxide Fuels; Safety of Advanced Thermal Reactors; Shutdown Risk Management; Human Factors and Operating Safety; Safety of Eastern European and Former Soviet Reactors; Quality Assurance Approaches to Enhance Operating Plant Safety; Issues of Management-Prioritization and Resolution of Safety Concerns; Cost Beneficial Safety Initiatives.

For further information, contact Dr. G. Don Bouchey, Technical Program Chair, Safety of Operating Reactors, Box 182, 101B Wellsian Way, Richland, WA 99352, Phone: (509) 783-1446, FAX: (509) 735-4664.

FIFTH INTERNATIONAL CONFERENCE ON NUCLEAR CRITICALITY SAFETY

Albuquerque, New Mexico, September 17–22, 1995

This conference, co-sponsored by the American Nuclear Society and the Nuclear Energy Agency (NEA) of the European Community (OECD), will cover the following areas: Status of National Programs, Experiments, Standards, Facilities; Criticality Safety Data, Training Guides, Data Bases, Handbooks, International Standards; Case Studies and Applications: Facility Assessment, Decontamination and Decommissioning, Waste Issues; New Developments in Computational Methods; Validation of Codes and Data Libraries; Experimental Results and Analysis; Accident Analyses and Criticality Alarms.

For further information, contact R. Douglas O'Dell, ESH-6, MS F691, P.O. Box 1663, Los Alamos National Laboratory, Los Alamos, NM 87545, Phone: (505) 667-4614, FAX: (505) 665-4970, E-mail: rdo@lanl.gov.

INTERNATIONAL CONFERENCE ON PROBABILISTIC SAFETY ASSESSMENT METHODOLOGY AND APPLICATIONS

Seoul, Korea, November 26–30, 1995

Probabilistic Safety Assessment (PSA) continues to play an important role in enhancing the safety of nuclear power plants during the course of operation and maintenance. Implementation of PSA in the nuclear industry has changed the regulatory environment, and its techniques are being extended to other engineering fields. This meeting will provide a working forum to present recent developments and new ideas in this expanding area of PSA. While the primary focus of the meeting will be placed on the application of PSA to nuclear engineering, participants are also encouraged from other disciplines like environmental and non-nuclear industrial applications. Other related topics may include severe accident research and management.

This conference is the fifth in a series of similar meetings and is jointly sponsored by the Korea Atomic Energy Research Institute (KAERI) and the Japan Atomic Energy Research Institute (JAERI) as well as the American Nuclear Society (ANS).

Subject Categories include: PSA methods and applications, risk communication, expert opinion elicitation, PSA for decision/policy making, external events analysis, managerial factors in PSA, CANDU reactor PSA, uncertainty/sensitivity/importance analysis, advanced reactor PSA, public acceptance, PSA and NPP design/operation/maintenance, risk-based regulation, refinement of PSA technology, organizational factors, environmental application of PSA, safety cultures, industrial application of PSA, international cooperation, human factors, aging of systems and components, software reliability, severe accident analysis, structural reliability, accident management, consequence assessment, and other related topics.

For further information, contact Dr. Chang K. Park, Director, Integrated Nuclear Safety Assessment, Korea Atomic Energy Research Institute, P.O. Box 105, Yusung, Taejon, 305-600, KOREA, Phone: 42-868-2662, FAX: 42-861-2574.

(Continues from page ii)

melt-down, it is obviously of great importance to severe accident safety analysis to determine how the relocation of much of the core to the bottom head occurred and how it affected that structure. One wants to know what temperature and pressure history the lower head was subjected to and the remaining margin to failure.

The six articles in the special section of this issue discuss these questions in detail. Although the lower head did not fail at TMI-2, of course, evidence of a short-lived "hot spot" at a temperature above 700 °C suggests that creep failure might have been a possibility if the vessel pressure had been higher and the hot-spot duration longer.

I would like to express my appreciation to Eric Beckjord and Alan Rubin of the Nuclear Regulatory Commission for coordinating the preparation of these six papers in a time frame suitable for publishing them all in this one issue, which greatly strengthens their impact and usefulness to the reader.

It is gratifying that now, fifteen years after the accident, there are still lessons being learned from analyzing the event with consequent benefits to the future safety of nuclear power plants.

Dr. Ernest G. Silver, *Editor-in-Chief*

SUBSCRIPTIONS

To order this useful journal for one year, cite *Nuclear Safety* (NUSA) and send your check for $14 a year ($17.50 foreign) or provide your VISA or MasterCard number and expiration date to Superintendent of Documents, P.O. Box 371954, Pittsburgh, PA 15250-7954. Telephone credit card orders can be made from 8:00 a.m. to 4:00 p.m. eastern time, at (202) 512-1800. Fax order can be made 24 hours a day at (202) 512-2250.

FUTURE ARTICLES

THE CHERNOBYL ACCIDENT

The State of the Chernobyl Sarcophagus and Nuclear Fuel Located Within It, *A. R. Sich*

GENERAL SAFETY

Nuclear Power Safety in Central and Eastern Europe, *R. Wilson*

Issues Related to the Safety of Nuclear Power Reactors, *S. Chakraborty*

On the Definition of Common Cause Failures, *H. Paula*

Role of Experimental Measurements in Criticality Technology, *R. E. Malenfant*

Elements of a Nuclear Criticality Safety Program, *C. M. Hopper*

Technology and Competence in Criticality Safety, *R. E. Wilson*

ACCIDENT ANALYSIS

Modeling and Analysis of Core Debris Recriticality During Hypothetical Severe Accidents in the Advanced Neutron Source Reactor, *S. H. Kim, V. Georgevich, D. B. Simpson, C. O. Slater, and R. P. Taleyarkhan*

Ignitability of Hydrogen/Oxygen/Diluent Mixture in Simulated CANDU Cover Gas Atmospheres, *R. K. Kumar and G. W. Koroll*

Coupled RELAP5 and CONTAIN Accident Analyses Using PVM, *K. A. Smith, A. J. Baratta, and G. E. Robinson*

CONTROL AND INSTRUMENTATION

Application of Fuzzy Logic in Nuclear Reactor Control—Part I: An Assessment of the State of the Art, *N. K. Alang-Rashid, A. Sharif Heger, and M. Jamshidi*

ENVIRONMENTAL EFFECTS

The Atmospheric Dispersion and the Radiological Consequences of Normal Airborne Effluents from Nuclear Power Plants, *D. Fang, C. Sun, and L. Yang*

Calculation of Distribution Coefficients for Radionuclides in Soils and Sediments, *I. Puigdomenech and U. Bergstrom*